

**Cellular Pathology and Apoptosis in Experimental
and Human Acute and Chronic Compressive
Myelopathy**

ROWENA ELIZABETH ANNE NEWCOMBE

M.B.B.S. B.Med Sci. (Hons.)

**Discipline of Pathology, School of Medical Sciences
University of Adelaide**

June 2010

**A thesis submitted in partial fulfilment of the requirements for the
degree of Doctor of Philosophy**

REFERENCES

- Abe Y, Yamamoto T, Sugiyama Y, Watanabe T et al. "Anoikis" of oligodendrocytes induced by Wallerian degeneration: ultrastructural observations. *J Neurotrauma*. 2004;21(1):119-24.
- Ackery A, Robins S, Fehlings MG. Inhibition of Fas-mediated apoptosis through administration of soluble Fas receptor improves functional outcome and reduces posttraumatic axonal degeneration after acute spinal cord injury. *J Neurotrauma*. 2006;23(5):604-16.
- Adams MA, McNally DS, Dolan P. 'Stress' distributions inside intervertebral discs: the effects of age and degeneration. *J Bone Joint Surg Br*.1996;78(6):965-72.
- Adams RD, Victor M. Diseases of the spinal cord, peripheral nerve and muscle. In: Adams RD, Victor M, eds. Principles of neurology. 5th ed. New York:McGraw-Hill, Health Professions Division.1993:1100-1.
- Agrawal SK, Fehlings MG. Mechanisms of secondary injury to spinal cord axons in vitro: role of Na(+)-K(+)-ATPase, the Na(+)-H(+) exchanger, and the Na(+)-Ca(2+) exchanger. *J Neurosci*.1996;16(2):545-52.
- Akdemir O, Berksoy I, Karaoglan A, Barut S, Bilguvar et al. Therapeutic efficacy of Ac-DMQD-CHO, a caspase 3 inhibitor, for rat spinal cord injury. *J Clin Neurosci*.2008;15(6):672-8.
- Aleman CI, Mas RM, Rodeiro I, Noa M et al. Reference database of the main physiological parameters in Sprague-Dawley rats from 6-32 months. *Lab Animals*.1998;32:457-66.
- Allen JW, Eldadah BA, Huang X, et al. Multiple caspases are involved in beta-amyloid-induced neuronal apoptosis. *J Neurosci Res*.2001;65:45-53.
- American Spinal Injury Association/International Medical Society of Paraplegia. International Standards for Neurological and Functional Classification of Spinal Cord Injury Patients. Chicago, Ill: American Spinal Injury Association.2001.
- Anderson CW, Lees-Miller SP. The nuclear serine/threonine protein kinase DNA-PK. *Crit Rev Eukaryot Gene Expr*.1992;2:283-314.
- Anderson CW, Carter TH. The DNA-activated protein kinase-DNA-PK. *Curr Top Microbiol Immunol*.1996;217:91-111.
- Andersen JK. Oxidative stress in neurodegeneration: a cause or consequence? *Nat Med*.2004;10Suppl:S18-25.
- Angeletti PU, Levi-Montalcini R, Caramia F. Ultrastructural changes in sympathetic neurons of newborn and adult mice treated with nerve growth factor. *J. Ultrastruct. Res*.1971;36:24-36.

Annunziato L, Amoroso S, Pannaccioine A, Cataldi M, Pignataro G, D'Alessio A, Sirabella R, Secondo A, Sibaud L, DrRenzo GF. Apoptosis induced in neuronal cells by oxidative stress: role played by caspases and intracellular calcium ions. *Toxicol Lett.*2003;139(2-3):125-33.

Austin JW, Fehlings MG. Molecular mechanisms of Fas-mediated cell death in oligodendrocytes. *J Neurotrauma.*2008;25(5):411-26.

Ayala-Grosso C, Ng G, Roy S, Robertson GS. Caspase-cleaved amyloid precursor protein in Alzheimer's disease. *Brain Pathol.*2002;12(4):430-41.

Bach F, Agerlin N, Sorensen JB, Rasmussen TB, Dombernowsky P, Sorensen PR, Hansen HH. Metastatic spinal cord compression secondary to lung cancer. *J Clin Oncol.*1992;10(11):1781-7.

Backe HA, Betz RR, Mesgarzadeh M, Beck T, Clancy M. Post-traumatic spinal cord cysts evaluated by magnetic resonance imaging. *Paraplegia.*1991;29:607-612.

Balentine JD. Pathology of experimental spinal cord trauma II. Ultrastructure of axons and myelin. *Lab Investigation.*1978;39:254-266.

Baleriaux DL. Spinal cord tumours. *Eur Radiol.*1999;9(7):1252-8.

Baptiste DC, Fehlings MG. Pathophysiology of cervical myelopathy. *Spine J.*2006;6(6Suppl):190S-197S.

Baretton GB, Diebold JD, Christoforis G, Vogt M, Muller C, Dopfer K, Schneiderbanger K, Schmidt M, Lohrs U. Apoptosis and immunohistochemical Bcl-2 expression in colorectal adenomas and carcinomas: Aspects of carcinogenesis and prognostic significance. *Cancer.*1998;77(2):255-64.

Barger SW, Mattson MP. Induction of neuroprotective kappa B-dependent transcription by secreted forms of the Alzheimer's beta-amyloid precursor. *Brain Res Mol Brain Res.*1996;40(1):116-26.

Barnes NY, Li L, Yoshikawa K, et al. Increased production of amyloid precursor protein provides a substrate for caspase-3 in dying motoneurons. *J Neurosci.*1998;18(15):5869-80.

Barres BA, Jacobson MD, Schmid R, Sendtner M, Raff MC. Does oligodendrocyte survival depend on axons? *Curr. Biol.*1993;3:489-97.

Barros Filho TE, Molina AE. Analysis of the sensitivity and reproducibility of the Basso, Beattie, Bresnahan (BBB) scale in Wister rats. *Clinis (Sao Paulo).*2008;63(1):103-8.

Basso DM, Beattie MS, Bresnahan JC. A sensitive and reliable locomotion rating scale for open field testing in rats. *J. Neurotrauma.*1995;12:1-21.

Basso DM, Beattie MS, Bresnahan JC. Graded histological and locomotor outcomes after spinal cord contusion using the NYU weight-drop device versus transaction. *Exp Neurol.*1996;139:244-56.

- Beattie MS, Farooqui AA, Bresnahan JC. A review of current evidence for apoptosis after spinal cord injury. *J Neurotrauma*.2000;17(10):915-25.
- Beattie MS, Hermann GE, Rogers RC, Bresnahan JC. Cell death in models of spinal cord injury. *Prog Brain Res*.2002;137:37-47.
- Bedbrook GM. Are Cervical Spine Fractures Ever Unstable? *J. West. Pac. Orthop. Assoc*.1969;6:7.
- Bernardi P, Scorrano L, Colonna R, Petronilli V, Di Lisa F. Mitochondria and cell death. Mechanistic aspects and methodological issues. *Eur J Biochem*.1999;265(2):847.
- Bertrand E, Brouillet E, Caille I, Bouillot C, Cole GM et al. A short cytoplasmic domain of the amyloid precursor protein induces apoptosis in vitro and in vivo. *Mol Cell Neurosci*.2001;18(5):503-11.
- Bibel M, Barde YA. Neurotrophins: key regulators of cell fate and cell shape in the vertebrate nervous system. *Genes Dev*.2000;14(23):2919-37.
- Black P, Markowitz, RS, Damianov I, Finkelstein SD, Kushner H et al. Models of spinal cord injury: Part 3. Dynamic load technique. *Neurosurg*.1988;1(Pt1):51-60.
- Blankenberg FG. In vivo detection of apoptosis. *J Nuc Med*.2008;49Suppl2:81S-95.
- Blumbergs PC, Scott G, Manavis J, et al. Staining of amyloid precursor protein to study axonal damage in mild head injury. *Lancet*.1994;344:1055-56.
- Blumbergs PC, Scott G, Manavis J, et al. Topography of axonal injury as defined by amyloid precursor protein and the sector scoring method in mild and severe closed head injury. *J Neurotrauma*.1995;12:565-572.
- Blumbergs PC. Changing concepts of diffuse axonal injury. *J Clin Neurosci*.1998;5(2):123-4.
- Bock WJ. Surgery of spinal tumours. *Zentralbl Neurochir*.1991;52(4):185-96.
- Bonicalzi ME, Haince JF, Droit A, Poirier GG. Regulation of poly(ADP-ribose) metabolism by poly(ADP-ribose) glycohydrolase: where and when? *Cell Mol Life Sci*.2005;62(7-8):739-50.
- Bozzali M, Wrabetz L. Axonal signals and oligodendrocytes differentiation. *Neurochem Res*.2004;29(5):979-88.
- Bracken MB. Treatment of acute spinal cord injury with methylprednisolone: results of a multicenter randomized clinical trial. *J Neurotrauma*.1991;8 Suppl 1:S47-50;discussion S51-2.
- Bracken MB, Shepard MJ, Collins WF, Holford TR, Young W, Baskin DS, Eisenberg HM, Flamm E, Leo-Summers L, Maroon J, et al., A randomized, controlled trial of methylprednisolone or naloxone in the treatment of acute spinal cord injury. Results of the Second National Acute Spinal Cord Injury Study. *N Engl J Med*.1990;322(20):1405-11.

- Bradl M, Lassmann H. Oligodendrocytes biology and pathology. *Acta Neuropathol.*2010;119(1):37-53.
- Brain WR, Northfield DWC, Wilkinson M. The neurological manifestations of cervical spondylosis. *Brain.*1952;75:187-225.
- Brambilla R, Bracchi-Ricard V, Hu WH, Frydel B, Bramwell A, et al. Inhibition of astroglial nuclear factor kappaB reduces inflammation and improves functional recovery after spinal cord injury. *J Exp Med.*2005;202(1):145-56.
- Breasted JH. The Edwin Smith surgical papyrus, in Wilkins RH (Ed): *Neurosurgical classics*. Rolling Meadows, IL:AANS.1992:1-5.
- Brodbelt AR, Stoodley MA, Watling AM, Tu J, Burke S, Jones NR. Altered subarachnoid space compliance and fluid flow in an animal model of posttraumatic syringomyelia. *Spine.*2003;28(20):E413-9.
- Buki A, Okonkwo DO, Wang KK, et al. Cytochrome C Release and Caspase Activation in Traumatic Axonal Injury. *J Neurosci.*2000;20(8):2825-2834.
- Burkle A. Poly(ADP-ribose). The most elaborate metabolite of NAD⁺. *FEBS J.*2005;272(18):4576-89.
- Buss A, Brook GA, Kakulas B, Martin D, Franzen R et al. Gradual loss of myelin and formation of an astrocytic scar during Wallerian degeneration in the human spinal cord. *Brain.*2004;127(Pt1):34-44.
- Cailliet R. Committee on Continuing Education in Neurosurgery, Dunsker, S., B. (ed.) 1981. *Cervical Spondylotic Myelopathy: Pathogenesis and Pathophysiology. And: Systemic Disease and the Cervical Disc. And: Inflammation and Infections of the Cervical Disc Which Predispose to Degeneration* (Hess, E., V.) In; Cervical Spondylosis. Raven Press, New York.1980:119-134.
- Carroll AM, Brackenridge P. Post-traumatic syringomyelia: A review of cases presenting in a regional spinal injuries unit in the North East of England over a 5 years period. *Spine.*2005;30(10):1206-1210.
- Casha S, Yu WR, Fehlings MG. Oligodendroglial apoptosis occurs along degenerating axons and is associated with FAS and p75 expression following spinal cord injury in the rat. *Neurosci.*2001;103(1):203-18.
- Casha S, Yu WR, Fehlings MG. Fas deficiency reduces apoptosis, spares axons and improves function after spinal cord injury. *Exp Neurol.*2005;196(2):390-400.
- Cayli SR, Kocak A, Yilmaz U, Tekiner A, Erbil M, Oztuck C, Batcioglu K, Yologlu S. Effect of combined treatment with melatonin and methyprednisolone on neurological recovery after experimental spinal cord injury. *Eur Spine J.*2004;13(8):724-32.
- Cecconi F, Alvarez-Bolado G, Meyer BI, Roth KA, Gruss P. Apaf1(CED-4 homolog) regulates programmed cell death in mammalian development. *Cell.*1998;94(6):727-37.

Chang P, Jacobson MK, Mitchison J. Poly(ADP-ribose) is required for spindle assembly and structure. *Letters to Nature Nature*.2004;432:645-649.

Chapman JR, Dettori J, Norvell D. Spinal classifications and severity measures. AOS Spine International, Switzerland.2005:317-355.

Chen IH, Vasavada A, Panjabi MM, Kinematics of the cervical spine canal: changes with sagittal plane loads. *J Spinal Disord*.1994;7:93-101.

Chen M, Zsengeller Z, Xiao CY, Szabo C. Mitochondrial-to-nuclear translocation of apoptosis-inducing factor in cardiac myocytes during oxidant stress: potential role of poly(ADP-ribose) polymerase-1. *Cardiovasc Res*.2004;63(4):682-8.

Chen X-H, Siman R, Iwata A et al. Long-term accumulation of amyloid-beta, beta-secretase, presenilin-1, and caspase-3 in damaged axons following brain trauma. *Am J Pathol*.2004;165(2):357-71.

Cher LM. Cancer and the nervous system. *Med J Aust*.2001;175(5):277-82.

Cheung MM, Li DT, Hui ES, Fan S, Ding AY, Hu Y, Wu EX. In vivo diffusion tensor imaging of chronic compression in rat model. *Conf Proc IEEE Eng Med Biol Soc*.2009;1:2715-8.

Chiarugi A. Poly(ADP-ribosyl)ation and stroke. *Pharmacol Res*.2005;52(1):15-24.

Chiba-Falek O, Kowalak JA, Smulson ME, Nussbaum RL. Regulation of alpha-synuclein expression by poly(ADP ribose) polymerase-1 (PARP-1) binding to the NACP-Rep1 polymorphic site upstream of the SNCA gene. *Am J Hum Genet*.2005;76(3):478-92.

Choo AM, Liu J, Dvorak M, Tetzlaff W, Oxland TR. Secondary pathology following contusion, dislocation, and distraction spinal cord injuries. *Exp Neurol*.2008;212(2):490-506.

Chowdhury I, Tharakan B, Bhat GK. Current concepts in apoptosis: The physiological suicide program revisited. *Cell Mol Biol Lett*.2006;11(4):506-25.

Cipriani G, Rapizzi E, Vannacci A, Rizzuto R, Moroni F, Chiarugi A. Nuclear poly(ADP-ribose) polymerase-1 rapidly triggers mitochondrial dysfunction. *J Biol Chem*.2005;280(17):17227-34.

Clarkson AN, Sutherland BA, Appleton I. The biology and pathology of hypoxia-ischemia:an update. *Arch Immunol Ther Exp (Warsz)*.2005;53(3):213-25.

Cohen-Gadol AA, Spencer DD, Krauss WE. The development of techniques for resection of spinal cord tumors by Harvey W. Cushing. *J Neurosurg. Spine*.2005;2(1):92-7.

Coleman M. Axon degeneration mechanisms:commonality amid diversity. *Nature Neurosci Rev*.2005;6:889.

Coleman M, Perry V. Axon pathology in neurological disease: a neglected therapeutic target. *Trends Neurosci*.2002;25(10):532.

Coleman WP, Benzel D, Cahill DW, Ducker T, Geisler F et al. A critical appraisal of the reporting of the National Acute Spinal Cord Injury Studies (II and III) of methylprednisolone in acute spinal cord injury. *J Spinal Disord.*2000;13(3):185-99.

Coria F, Moreno A, Torres A, Ahmad I, Ghiso. Distribution of Alzheimer's disease amyloid protein precursor in normal human and rat nervous system. *Neuropathol Appl Neurobiol.*1992;18(1):27-35.

Courtine G, Bunge MB, Fawcett JW, Grossman RG et al. Can experiments in nonhuman primates expedite the translation of treatments for spinal cord injury in humans? *Nature Medicine.*2007;13:561-66.

Cripps R. Spinal Cord Injury, Australia, 2006-07. Injury research and statistics series no. 48, Published 2009.

Crowe MJ, Bresnahan JC, Shuman SL, Masters JN, Crowe MS. Apoptosis and delayed degeneration after spinal cord injury in rats and monkeys. *Nature Medicine.*1997;3(1):73-76.

D'Amours D, Desnoyers S, D'Silva I, Poirier GG. Poly(ADP-ribosyl)ation reactions in the regulation of nuclear functions. *Biochem J.*1999;342(Pt 2):249-68.

Dasari VR, Veeravalli KK, Tsung AJ, Gondi CS, Gujrati M, Dinh D, Rao JS. Neuronal apoptosis inhibited by cord blood stem cells after spinal cord injury. *J Neurotrauma.*2009;26(11):2057-69.

Daugas E, Nocky D, Ravagnan L, Loeffler M, Susin SA et al. Apoptosis-inducing factor (AIF): a ubiquitous mitochondrial oxidoreductase involved in apoptosis. *FEBS Lett.*2000;476(3):118-23.

De Forge D, Nymakr J, Lemaine E, Gardner S, Hunt M, Martel L, Curran D, Barbeau H. Effect of 4-aminopyridine on gait in ambulatory spinal cord injuries: a double-blind, placebo-controlled, crossover trial. *Spinal Cord.*2004;42(12):674-85.

Deftereos SN, Kechagias EA, Panagopoulos G, Seretis A, Orphanidis G, Antiniou E, Georgakoulias N, Karageorgou CE. Localisation of cervical spinal cord compression by TMS and MRI. *Funct Neurol.*2009;24(2):99-105.

Degli Esposti M, Dive C. Mitochondrial membrane permeabilisation by Bax/Bak. *Biochem Biophys Res Commun.*2003;304(3):455-61.

Dezawa M, Adachi-Usami E. Role of schwann cells in retinal ganglion cell axon regeneration. *Prog Retin Eye Res.*2000;19(2):171-204.

Di Giovanni S, Knobloch SM, Brandoli C, Aden SA, Hoffman EP, Faden AI. Gene profiling in spinal cord injury shows role of cell cycle in neuronal death. *Ann Neurol.*2003;53(4):454-68.

Di Lorenzo N, Cacciola F. Adult syringomyelia. Classification, pathogenesis and therapeutic approaches. *J Neurosurg Sci.*2005;49(3):65-72.

- Dimer, J, Glassman M, Raque G, et. al. The Influence of Spinal Canal Narrowing and Timing of Decompression on Neurologic Recover After Spinal Cord Contusion in a Rat Model. *Spine*.24(16):1623–1633.
- Ding Y, Kastin AJ, Pan W. Neural plasticity after spinal cord injury. *Curr Pharm Des*.2005;11(11):1441-50.
- Dong Y, Holly LT, Albistequi-Dubois R, Yan X, Marehbian J, Newton JM, Dobkin BH. Compensatory cerebral adaptations before and evolving changes after surgical decompression in cervical spondylotic myelopathy. *Neurosurg Spine*.2008;9(6):538-51.
- Donnelly DJ, Popovich PG. Inflammation and its role in neuroprotection, axonal regeneration and functional recovery after spinal cord injury. *Exp Neurol*.2008;209:378-88.
- Dumont C, Durrbach A, Bidere N, Rouleau M, Kroemer G, Bernard G, Hirsch F, Charpentier B, Susin SA, Senik A. Caspase-independent commitment phase to apoptosis in activated blood T lymphocytes: reversibility at low apoptotic insult. *Blood*.2000;96:1030-1038.
- Durkacz BW, Omidiji O, Gray DA, Shall S. (ADP-ribose)n participates in DNA excision repair. *Nature*.1980;283(5747):593-6.
- Durrant DH, True JM: Myelopathy, Radiculopathy, and Peripheral Entrapment Syndromes. Boca Raton, Florida: CRC Press.2002.
- Duvall E, Wyllie AH, Morris RG. Macrophage recognition of cells undergoing programmed cell death (apoptosis). *Immunology*.1985;56(2):351-8.
- Ealey PA, Henderson B, Loveridge N. A quantitative study of peroxidase activity in unfixed tissue sections of the guinea-pig thyroid gland. *Histochem J*.1984;16(2):111-22.
- Ekshyyan O, Aw TY. Apoptosis: a key in neurodegenerative disorders. *Curr Neurovasc Res*.2004;1(4):355-71.
- Elliot NS, Lockerby DA, Brodbelt AR. The pathogenesis of syringomyelia: a re-evaluation of the elastic-jump hypothesis. *J Biomech Eng*.2009;131(4):044503.
- Emery E, Aldana P, Bunge MB, et al. Apoptosis after traumatic human spinal cord injury. *J Neurosurg*.1998; 89:911-920.
- Epstein BS. Degenerative Changes. In: The Spine: A Radiological Text and Atlas. Lea & Febiger.1976, pp377-418.
- Epstein JA, Epstein BS, Lavine LS, Carras R, Rosenthal AD. Degenerative lumbar spondylolisthesis with an intact neural arch (pseudospondylolisthesis). *J Neurosurg*.1976;44:139–147.
- Erhardt P, Tomaselli KJ, Cooper GM. Identification of the MDM2 oncoprotein as a substrate for CPP32-like apoptotic proteases. *J Biol Chem*.1997;272(24):15049-52.

Faden AI, Chan PH, Longar S. Alterations in lipid metabolism, Na⁺,K⁺-ATPase activity, and tissue water content of spinal cord following experimental traumatic injury. *J Neurochem.*1987;48(6):1809-16.

Fawcett JW, Curt A, Steeves JD, Coleman WP, Tuszynski MH et al. Guidelines for the conduct of clinical trials for spinal cord injury as developed by the ICCP panel: spontaneous recovery after spinal cord injury and statistical power needed for therapeutic clinical trials. *Spinal cord.*2007;45:190-205.

Fehlings MG. Editorial: recommendations regarding the use of methylprednisolone in acute spinal cord injury: making sense out of the controversy. *Spine.*2001;26(24 Suppl):S56-7.

Fehlings MG, Perrin RG. The timing of surgical intervention in the treatment of spinal cord injury: a systematic review of recent clinical evidence. *Spine.*2006;31(11 Suppl):S28-35.

Fehlings MG, Skaf G, An HS. A review of the pathophysiology of cervical spondylotic myelopathy with insights for potential novel mechanisms drawn from traumatic spinal cord injury. *Spine.*1998;23(24):2730-37.

Fehlings MG, Tator CH. The relationships among the severity of spinal cord injury, residual neurological function, axon counts, and counts of retrogradely labelled neurons after experimental spinal cord injury. *Exp Neurol.*1995;132:220-28.

Ferguson AR, Christensen RN, Gensel JC et al. Cell death after spinal cord injury is exacerbated by rapid TNF α -induced trafficking of GluR2-lacking AMPARs to the plasma membrane. *J Neurosci.*2008;28(44):11391-11400.

Ferreira A, Caceres A, Kosik KS. Intraneuronal compartments of the amyloid precursor protein. *J Neurosci.*1993;13(7):3112-23.

Ferri KF, Kroemer G. Mitochondria – the suicide organelles. *Bioessays.*2001;23(2):111-5.

Finn JT, Weil M, Archer F, Siman R, Srinivasan A, Raff MC. Evidence that Wallerian degeneration and localized axon degeneration induced by local neurotrophin deprivation do not involve caspases. *J Neurosci.*2000;20(4):1333-41.

Finnie NJ, Gottlieb TM, Blunt T, Jeggo PA, Jackson SP. DNA-dependent protein kinase activity is absent in xrs-6 cells: implications for site-specific recombination and DNA double-strand break repair. *Proc. Natl. Acad. Sci. USA.*1995;92: 320-324.

Fischbein N, Dillon WP, Cobbs C, Weinstein PR. The “Presyrinx” state: A reversible myelopathic condition that may precede syringomyelia. *Am. J. Neurorad.*1999;20:7-20.

Fitch MT, Silver J. CNS injury, glial scars, and inflammation: Inhibitory extracellular matrices and regeneration failure. *Exp Neurol.*2008;209:294-301.

Fleming JC, Norenberg MD, Ramsay DA, Dekaban GA, Marcillo AE, Saenz AD, Pasquale-Styles M, Dietrich WD, Weaver LC. The cellular inflammatory response in human spinal cords after injury. *Brain.*2006;129(12):3249-3269.

- Frampton AE, Eynon CA. High dose methylprednisolone in the immediate management of acute, blunt spinal cord injury: What is the current practice in emergency departments, spinal units, and neurosurgical units in the UK? *Emerg Med J.*2006;23(7):550-3.
- Freeman TB, Martinez CR. Radiological evaluation of cervical spondylotic disease: limitation of magnetic resonance imaging for diagnosis and preoperative assessment. *Perspect Neurol Surg.*1992;3:34-6.
- Friedlander, RM. Apoptosis and caspases in neurodegenerative diseases. *New Eng J Med.*2003;348:1365-75.
- Frisen J, Haegerstrand A, Fried K, Piehl F, Culheim S, Risling M. Adhesive/repulsive properties in the injured spinal cord: relation to myelin phagocytosis by invading macrophages. *Exp Neurol.*1994;129(2):183-93.
- Fukui M, Chiba K, Kawakami M, et al. Japanese Orthopaedic Association cervical myelopathy evaluation questionnaire (JOACMEQ): Part 2. Endorsement of the alternative item. *J. Orthop. Sci.*2007;12(3):241-8.
- Genovese T, Mazzon E, Muia C, Patel NS, Threadgill MD, Bramanti P, De Sarro A, Thiernemann C, Cuzzocrea S. Inhibitors of poly(ADP-ribose) polymerase modulate signal transduction pathways and secondary damage in experimental spinal cord trauma. *J Pharmacol Exp Ther.*2005;312(2):449-57.
- Gentleman SM, Nash MJ, Sweeting CJ, Graham DI, Roberts GW. Amyloid precursor protein as a marker for axonal injury after head injury. *Neurosci. Lett.*1993;160:139-144.
- Gentry JJ, Rutkoski NJ, Burke TL, Carter BD. A functional interaction between the p75 neurotrophin receptor interacting factors, TRAF6 and NRIF. *J Biol Chem.*2004;279(16):16646-56.
- Gervais FG, Xu D, Robertson GS, et al. Involvement of caspases in proteolytic cleavage of Alzheimer's amyloid-beta precursor protein and amyloidogenic A beta peptide formation. *Cell.*1999;97:395-406.
- Golde TE, Estus S, Usiak M, Younkin LH, Younkin SG. Expression of beta amyloid protein precursor mRNAs: recognition of a novel alternatively spliced form and quantitation in Alzheimer's disease using PCR. *Neuron.*1990;4(2):253-67.
- Golstein P. Controlling cell death. *Science.*1997;275:1081-1082.
- Gorji A, Zahn PK, Pogatzki EM, Speckmann EJ. Spinal and cortical spreading depression enhance spinal cord activity. *Neurobiol Dis.*2004;15(1):70-9.
- Gottlieb RA. Mitochondria: execution central. *FEBS Lett.*2000;482:6-12.
- Graham DI, Gentleman SM, Lynch A, et al. Distribution of beta-amyloid protein in the brain following severe head injury. *Neuropathol Appl Neurobiol.*1995;21:27-34.
- Greitz D. Unraveling the riddle of syringomyelia. *Neursurg Rev.*2006;29(4):251-63.

- Grossman SD, Rosenberg LJ, Wrathall JR. Temporal-spatial pattern of acute neuronal and glial loss after spinal cord contusion. *Exp Neurol*.2001;168(2):273-82.
- Gruner JA. A monitored contusion model of spinal cord injury in the rat. *J Neurotrauma*.1992;9(2):123-6.
- Gschwind M, Huber G. Detection of apoptotic or necrotic death in neuronal cells M, B ans MA from Neuropmethods Vols 29: Apoptosis techniques and protocols and: J Porier Humana Press Inc.1997.
- Guder E, Hill S, Kandziora F, Schnake KJ. Partial nucleotomy of the ovine disc as an in vivo model for disc degeneration. *Z Orthop Unfall*.2009;147(1):52-8.
- Guo Z, Cupples LA, Jurz A, et al. head injury and the risk of AD in the MIRAGE study. *Neurology*.2000;54:316-23.
- Ha HC, Hester LD, Snyder SH. Poly(ADP-ribose) polymerase-1 dependence of stress-induced transcription factors and associated gene expression in glia. *Proc Natl Acad Sci U.S.A*.2002;99(5):3270-5.
- Haass C, Selkoe DJ. Cellular processing of beta-amyloid precursor protein and the genesis of amyloid beta-peptide. *Cell*.1993;75(6):1039-42.
- Hagg T, Oudega M. Degenerative and spontaneous regenerative processes after spinal cord injury. *J Neurotrauma*.2006;23(3-4):264-80.
- Hakem R, Hakem A, Duncan GS, Henderson JT, Woo M, et al. Differential requirement for caspase 9 in apoptotic pathways in vivo. *Cell*.1998;94(3):339-52.
- Harkey HL, Al-Mefty O, Marawi I, Peeler DF, Haines DE, Alexander LF. Experimental chronic compressive myelopathy: effects of decompression. *J Neurosurg*.1995;83(2):336-341.
- Harrington KD. Metastatic disease of the spine. *J Bone Joint Surg (Am)*.1986;68A:1110-1115.
- Hart RA, Boriani S, Biagini R, Currier B, Weinstein JN. A system for surgical staging and management of spine tumors. A clinical outcome study of giant cell tumors of the spine. *Spine (PHila Pa 1976)*.1997;22(15):1773-82.
- Hashizume Y, Iijima S, Kishimoto H, Yanagi T. Pathology of spinal cord lesions cause by ossification of the posterior longitudinal ligament. *Acta Neuropathol (Berl)*.1984;63:123-30.
- Hausmann ON. Post-traumatic inflammation following spinal cord injury. *Spinal Cord*.2003;41:369-378.
- Hayashi H, Okada K, Hamada M, Tada K, Ueno R. Etiologic factors of myelopathy: a radiographic evaluation of the aging changes in the cervical spine. *Clin Orthop Relat Res*.1987;214:200-9.

- Hayashi H, Okada K, Hashimoto J, Tada K, Ueno R. Cervical spondylotic myelopathy in the aged patient: A radiographic evaluation of the aging changes in the cervical spine and etiologic factors of myelopathy. *Spine*.1988;13(6):618-625.
- Henderson F, Geddes J, Vaccaro A, Woodard E, Berry K, Benzel E. Stretch-associated injury in cervical spondylotic myelopathy: New concept and review. *Neurosurg*.2005;56(5):1101-13.
- Hida K, Iwasaki Y, Imamura H, Abe H. Posttraumatic syringomyelia: Its characteristic magnetic resonance imaging findings and surgical management. *Neurosurgery*.1994;35:886-891.
- Hidaka C, Khan SN, Farmer JC, Sandhu HS. Gene therapy for spinal applications. *Orthop Clin North Am*.2002;33(2):439-46.
- Hisatomi T, Sakamoto T, Murata T, Yamanaka I, Oshima Y, Hata Y, Ishibashi T, Inomata J, Susin S, Kroemer G. Relocalization of apoptosis-inducing factor in photoreceptor apoptosis induced by retinal detachment in vivo. *Am J Pathol*.2001;158:1271-78.
- Holly LT, Johnson JP, Masciopinto JE, Batzdorf U. Treatment of posttraumatic syringomyelia with extradural decompressive surgery. *Neurosurg Focus*.2000; 8:E8.
- Holly LT, Batzdorf U. Syringomyelia associated with intradural arachnoid cysts. *J Neurosurg Spine*.2006;5(2):111-6.
- Holt S, Yates PO. Cervical spondylosis and nerve root lesions. Incidence at routine necropsy. *J Bone Joint Surg Br*.1966;48(3):407-23.
- Hong SJ, Dawson TM, Dawson VL. Nuclear and mitochondrial conversations in cell death: PARP-1 and AIF signaling. *Trends Pharmacol Sci*.2004;25(5):259-64.
- Hotchkiss RS, Strasser A, McDunn JE, Swanson PE. Cell death. *NEJM*.2009;361(16):1570-83.
- Horsburgh K, Cole GM., Yang F, et al. Beta-amyloid (A_{beta})₄₂(43), a_{beta}42, a_{beta}40 and apoE immunostaining of plaques in fatal head injury. *Neuropathol Appl Neurobiol*.2000;26:124-32.
- Hortobagyi T, Gorlach C, Benyo Z, Lacza Z, Hortobagyi S, Wahl M, Harkany T. Inhibition of neuronal nitric oxide synthase-mediated activation of poly(ADP-ribose) polymerase in traumatic brain injury: neuroprotection by 3-aminobenzamide. *Neuroscience*.2003;121(4):983-90.
- Houten JK, Cooper PR. Laminectomy and posterior cervical plating for multilevel cervical spondylotic myelopathy and ossification of the posterior longitudinal ligament: effects on cervical alignment, spinal cord compression and neurological outcome. *Neurosurgery*.2003;52(5):1081-7.
- Huang Z, Huang PL, Panahian N, Dalkara T, Fishman MC, Moskowitz MA. Effects of cerebral ischemia in mice deficient in neuronal nitric oxide synthase. *Science*.1994;265(5180):1883-5.

- Hukuda S, Ogata M, Katsuura A. Experimental study on acute aggravating factors of cervical spondylotic myelopathy. *Spine*.1988;13(1):15-20.
- Hurlbert RJ. Strategies of medical intervention in the management of acute spinal cord injury. *Spine*.2006;31(11 Suppl):S16-21;discussion S36.
- Husband DJ, Grant KA, Romaniuk CS. MRI in the diagnosis and treatment of suspected malignant spinal cord compression. *Br J Radiol*.2001;74(877):15-23.
- Iadecola C, Zhang F, Casey R, Nagayama M, Ross ME. Delayed reduction of ischemia brain injury and neurological deficits in mice lacking the inducible nitric oxide synthase gene. *J Neurosci*.1997;17(23):9157-64.
- Ishise J, Rosenbluth J. Nodal and paranodal structural changes in frog optic nerve during early Wallerian degeneration. *J Neurocytol*.1986;15(5):657-70.
- Iskandar BJ, Quigley M, Haughton VM. Foramen magnum cerebrospinal fluid flow characteristics in children with Chiari I malformation before and after craniocervical decompression. *J Neurosurg*.2004;101(2 Suppl):169-78.
- Iwata A, Chen XH, McIntosh TK, Browne KD, Smith DH. Long-term accumulation of amyloid-beta in axons following brain trauma without persistent upregulation of amyloid precursor protein genes. *J Neuropathol Exp Neurol*.2002;61(12):1056-68.
- Jafari S, Maxwell W, Neilson M, Graham D. Axonal cytoskeletal changes after non-disruptive axonal injury. *J Neurocytol*.1997;26:207-221.
- Jin R, Rock J, Jin JY, Janakiraman N, Kim JH, Movsas B, Ryu S. Single fraction spine radiosurgery for myeloma epidural spinal cord compression. *J Exp Ther Oncol*.2009;8(1):35-41.
- Johnson M, Carey F, McMillan RN. Alternative pathways of arachidonate metabolism: prostaglandins, thromboxane and leucotrienes, *Essays Biochem*.1983;19:40-141.
- Johnson MD, Kinoshita Y, Xiang H, Ghatan S, Morrison RS. Contribution of caspase activation to neuronal cell death declines with neuronal maturation. *J Neurosci*.1999;19:2996-3006.
- Jumah KB, Nyame PK. Relationship between load carrying on the head and cervical spondylosis in Ghanaians. *West Afr J Med*.1994;13(3):181-2.
- Kaar GF, N'Dow JM, Bashir SH. Cervical spondylotic myelopathy with syringomyelia. *Br J Neurosurg*.1996;10:413-415.
- Kakulas, BA, Taylor, JR. Pathology of injuries of the vertebral column and spinal cord. In: Frankel HL (eds) *Handbook of clinical neurology*, Elsevier Science Publishers, Amsterdam.1992: 21-51.
- Kakulas BA. The applied neuropathology of human spinal cord injury, *Spinal Cord*.1999;37:79-88.

- Kalfas IH. Image-guided spinal navigation: application to spinal metastases. *Neurosurg Focus*.2001;11(6):e5.
- Kamada S, Kikkawa U, Tsujimoto Y, Hunter T. Nuclear translocation of caspase-3 is dependent on its proteolytic activation and recognition of substrate-like protein. *J Biol. Chem*.2005;280(2):857-60.
- Kanno H, Ozawa H, Sekiguchi A, Itoi E. The role of autophagy in spinal cord injury. *Autophagy*.2009;5(3):390-2.
- Kasahara K, Nakagawa T, Kubota T. Neuronal loss and expression of neurotrophic factors in a model of rat chronic compressive spinal cord injury. *Spine*.2006 Aug 15;31(18):2059-66.
- Keirstead HS, Blakemore WF. The role of oligodendrocytes and oligodendrocyte progenitors in CNS remyelination. *Adv Exp Med Biol*.1999;468:183-97.
- Kerr JF, Wyllie AH, Currie AR. Apoptosis: a basic phenomenon with wide-ranging implications in tissue kinetics. *Br J Cancer*.1972;26(4):239-57.
- Kerr JFR. Definition of Apoptosis and Overview of its Incidence. In: Programmed Cell Death: The Cellular and Molecular Biology of Apoptosis. Lavin, M., Watters, D. (Eds) Harwood Academic Publishers, Switzerland.1993:1-19.
- Kerschensteiner M, Schwab ME, Lichtman JW, Misgelt T. In vivo imaging of axonal degeneration and regeneration in the injured spinal cord. *Nat Med*.2005;11(5):572-7.
- Kim DH, Vaccaro AR, Henderson FC, Benzel EC. Molecular biology of cervical myelopathy and spinal cord injury: role of oligodendrocyte apoptosis. *Spine J*.2003;3:510-19.
- Kim JH, Loy DN, Liang HF, Trinkaus K, Schmidt RE, Song SK. Noninvasive diffusion tensor imaging of evolving white matter pathology in a mouse model of acute spinal cord injury. *Magn Reson Med*.2007;58(2):253-60.
- Kim MY, Zhang T, Kraus WL. Poly(ADP-ribosyl)ation by PARP-1: 'PAR-laying' NAD⁺ into a nuclear signal. *Genes Dev*.2005;19(17):1951-67.
- Kim P, Haisa T, Kawamoto T. Delayed myelopathy induced by chronic compression in the rat spinal cord. *Ann Neurol*.2000;55(4):503-11.
- Knoeller SM, Seifried C. Historical perspective: history of spinal surgery. *Spine (Phila Pa 1976)*.2000;25(21):2838-43.
- Koeller KK, Rosenblum RS, Morrison AL. Neoplasms of the spinal cord and filum terminale: radiologic-pathologic correlation. *Radiographics*.2000;20(6):1721-49.
- Kofler J, Otsuka T, Zhang Z, Noppens R, Grafe MR, et al. Differential effect of PARP-2 deletion on brain injury after focal and global ischemia. *J Cereb Blood Flow Metab*.2006;26(1):135-41.

- Koh DW, Dawson TM, Dawson VL. Mediation of cell death by poly(ADP-ribose) polymerase-1. *Pharmacol Res.*2005;52(1):5-14.
- Komjati K, Besson VC, Szabo C. Poly(ADP-ribosyl)ation enzyme-1 as a target for neuroprotection in acute central nervous system injury. *Curr Drug Targets CNS Neurol Disord.*2005;(2):9-94.
- Komjati K, Besson VC, Szabo C. Poly (adp-ribose) polymerase inhibitors as potential therapeutic agents in stroke and neurotrauma. *Curr Drug Targets CNS Neurol Disord.*2005;4(2):179-94.
- Konno S, Yabuki S, Sato K, Olmarker K, Kikuchi S. A model for acute, chronic, and delayed graded compression of the dog cauda equina. Presentation of the gross, microscopic, and vascular anatomy of the dog cauda equina and accuracy in pressure transmission of the compression model. *Spine.*1995;20(24):2758-64.
- Koyanagi I, Iwasaki Y, Hida K, Houkin K. Clinical features and pathomechanisms of syringomyelia associated with spinal arachnoiditis. *Surg Neurol.*2005;63(4):350-5.
- Kozlowski P, Raj D, Liu J, Lam C, Yung AC, Tetlass. Characterizing white matter damage in rat spinal cord with quantitative MRI and histology. *J Neurotrauma.*2008;25(6):653-76.
- Krantic S, Mechawar N, Reix S, Quirion R. Apoptosis-inducing factor: a matter of neuron life and death. *Prog Neurobiol.*2007;81(3):179-96.
- Kroemer G, Galluzzi L, Vandenabeele P, Abrams J, Alnemri J et al. Classification of cell death: recommendations of the Nomenclature Committee on Cell Death. *Cell Death Differ.*2009;16(1):3-11.
- Krysko DV, Vanden Berghe T, D'Herde K, Vandenabeel P. Apoptosis and necrosis: detection, discrimination and phagocytosis. *Methods.*2008;44:205-21.
- Kuida K, Haydar TF, Kuan C, Gu, Y, Taya C, Karasuyama, H, Su MSS, Rakic P, Plavell RA. Reduced apoptosis and cytochrome-c mediated caspase activation in mice lacking caspase 9. *Cell.*1998;94:325-337.
- Kumar VG, Rea GL, Mervis LJ, McGregor JM. Cervical spondylotic myelopathy: functional and radiographic long-term outcome after laminectomy and posterior fusion. *Neurosurgery.*1999;44:771-8.
- Kutsyi MP, Kuznetsova EA, Gaziev AI. Involvement of proteases in apoptosis. *Biochemistry (Mosc).*1999;64(2):115-26.
- Lankiewicz S, Marc Luetjens C, Truc Bui N, Krohn AJ, Poppe M, Cole GM, Saido TC, Prehn JH. Activation of calpain I converts excitotoxic neuron death into a caspase-independent cell death. *J Biol Chem.*2000;275:17064-71.
- Levi AD, Green BA, Wang MY, Dietrich WD, Brindle T, et al. Clinical application of modest hypothermia after spinal cord injury. *J Neurotrauma.*2009;26(3):407-15.

- Levin S, Bucci TJ, Cohen SM, Fix AS, Hardisty JF, LeGrand EK, Maronpot RR, Trump BF. The nomenclature of cell death: recommendations of an ad hoc committee of the Society of Toxicologic Pathology. *Toxicol Pathol.*1999; 27:484-490.
- Levine D. Pathogenesis of cervical spondylotic myelopathy. *J Neurol Neurosurg Psychiatry.*1997;62:334-40.
- Li GL, Farooque M, Holtz A, Olsson Y. Changes of beta-amyloid precursor protein after compression trauma to the rat spinal cord: an experimental study in the rat using immunohistochemistry. *J Neurotrauma.*1995;12(3):269-77.
- Li Y, Field PM, Raisman G. Death of oligodendrocytes and microglia phagocytosis of myelin precede immigration of Schwann cells into the spinal cord. *J Neurocytol.*1999;28:417-27.
- Liepinsh E, Ilag LL, Otting G, Ibanez CF. NMR structure of the death domain of p75 neurotrophin receptor. *EMBO J.*1997;16:4999–5005.
- Little JW, Harris RM, Sohlberg RC. Locomotor recovery following subtotal spinal cord lesions in a rat model. *Neurosci Lett.*1988;87(1-2):189-94.
- Liu D, Ling Z, Wen J, Liu J. The role of reactive nitrogen species in secondary spinal cord injury: formation of nitric oxide, peroxynitrite, and nitrated protein. *J Neurochem.*2000;75(5):2144-54.
- Liu XZ, Xu XM, Hu R, Du C et al., Neuronal and glial apoptosis after traumatic spinal cord injury. *J Neurosci.*1997;17(14):5395-406.
- Loblaw DA, Perry J, Chambers A, Laperriere NJ. Systematic review of the diagnosis and management of malignant extradural spinal cord compression: the Cancer Care Ontario Practice Guidelines Initiative's Neuro-Oncology Disease Site Group. *J Clin Oncol.*2005;23:2028-37.
- Locke S, Brauer M. Response of the rat liver in situ to bromobenzene: in vivo proton MRI and ³¹P MRS studies. *Toxicol Appl Pharmacol.*1991;110:416–28.
- Lonskaya I, Potaman VN, Luda SS, Oussatcheva EA, Lyubchenko YL, Soldatenkov VA. Regulation of poly(ADP-ribose) polymerase-1 by DNA structure-specific binding. *J. Biol. Chem.*2005;280(17):17076-17083.
- Lorenzo HK, Susin SA, Penninger J, Kroemer G. Apoptosis inducing factor (AIF): a phylogenetically old, caspase-independent effector of cell death. *Cell Death Differ.*1999;6(6):516-24.
- Lou J, Lenke LG, Xu F, O'Brien M. In vivo Bcl-2 oncogene neuronal expression in the rat spinal cord. *Spine.*1998;23:517-523.
- Love S. Oxidative stress in brain ischemia. *Brain Pathol.*1999;9(1):119-31.
- Loy DN, Kim JH, Xie M, Schmidt RE, Trinkaus K, Song SK. Diffusion tensor imaging predicts hyperacute spinal cord injury severity. *J Neurotrauma.*2007;24(6):979-90.

- Lu J, Ashwell KW, Waite P. Advances in secondary spinal cord injury: role of apoptosis. *Spine*.2000;25(14):1859-66.
- McDonald JW, Liu XZ, Qu Y. Transplanted embryonic stem cells survive, differentiate, and promote recovery in injured rat spinal cord. *Nat Med*.1999;(5):1410-12.
- McIlwain DL, Hoke VB. The role of the cytoskeleton in cell body enlargement, increased nuclear eccentricity and chromatolysis in axotomized spinal motor neurons. *BMC Neurosci*.2005;6(1):19.
- Mack TG, Reiner M, Beirowski B, Mi W, Emanuelli M et al. Wallerian degeneration of injured axons is delayed by Ube4b/Nmnat chimeric gene. *Nature Neurosci*.2001;4:1199-1206.
- Majno G, Joris I. Apoptosis, oncosis and necrosis. An overview of cell death. *Am J Pathol*.1995;146:3-15.
- Malanga M, Althaus FR. The role of poly(ADP-ribose) in the DNA damage signaling network. *Biochem Cell Biol*.2005;83(3):354-64.
- Mate MJ, Ortiz-Lombardia M, Boitel B, Haouz A, Tello D, Susin SA, Penninger J, Kroemer G, Alzari PM. The crystal structure of the mouse apoptosis-inducing factor AIF. *Nature Struc. Biol*.2002;9(6):442-446.
- Matsushita K, Wu Y, Qiu J, Lang-Lazdunski L, Hirt L, et al. Fas receptor and neuronal cell death after spinal cord ischemia. *J Neurosci*.2000;20(18):6879-87.
- Mattson MP, Partin J, Begley JG. Amyloid beta-peptide induces apoptosis-related events in synapses and dendrites. *Brain Res*.1998;807(1-2):167-76.
- Matz PG, Anderson PA, Holly LT et al., Joint section on disorders of the spine and peripheral nerves of the American Association of Neurological Surgeons and Congress of Neurological Surgeons. The natural history of cervical spondylotic myelopathy. *J Neurosurg Spine*.2009;11(2):104-11.
- Maxwell W, Kosanlavit R, Graham D. Structural change in the internodal axolemma after stretch injury to the guinea pig optic nerve. *Neuropath.Appl.Neurobiol*.1997;23:165.
- Metz GA, Merkler D, Dietz V, Schwab ME, Fouad K. Efficient testing of motor function in spinal cord injured rats. *Brain Res*.2000;883:165-177.
- Migheli A, Attanasio A, Schiffer D. Ultrastructural detection of DNA strand breaks in apoptotic neural cells by in situ end-labelling techniques. *J Pathol*.1995;176(1):27-35.
- Mihara H, Ohnari K, Hachiya M, Kondo S, Yamada K. Cervical myelopathy caused by C3-C4 spondylosis in elderly patients: a radiographic analysis of pathogenesis. *Spine*.2000;25:796-800.

Mikami Y, Okano H, Sakaguchi M, Nakamura M, Shimazaki T et al. Implantation of dendritic cells in injured adult spinal cord results in activation of endogenous neural stem/progenitor cells leading to de novo neurogenesis and functional recovery. *J Neurosci Res.*2004;76:453-465.

Milhorat TH. Classification of syringomyelia. *Neurosurg Focus.*2000;8:1-6.

Milward EA, Papadopoulos R, Fuller SJ, et al. The amyloid precursor of Alzheimer's disease is a mediator of the effects of nerve growth factor on neurite outgrowth. *Neuron.*1992;9(1):129-37.

Miramar MD, Costantini P, Ravagnan L, Saraiva LM, Haouzi D, et al. NADH oxidase activity of mitochondrial apoptosis-inducing factor. *J Biol Chem.*2001;276(19):16391-8.

Miyakoshi N, Shimada Y, Suzuki T, Hongo M, Itoi E. Magnetic resonance imaging of spinal involvement by hematopoietic malignancies requiring surgical decompression. *J Orthop Sci.*2003;8(2):207-12.

Molica S, Mannella A, Dattilo A, Levato D, Iuliano F, Peta A, Consarino C, Magro S. Differential expression of Bcl-2 oncoprotein and Fas antigen on normal peripheral blood and leukemic bone marrow cells. A flow cytometric analysis. *Haematologica.*1996;81(4):302-9.

Morishita Y, Naito M, Hymanson H, Miyazaki M, Wu G, Wang JC. The relationship between the cervical spinal canal diameter and the pathological changes in the cervical spine. *Eur Spine J.*2009;18(6):877-83.

Mountz JD, Wu J, Cheng J, Zhou T., Autoimmune disease. A problem of defective apoptosis. *Arthritis Rheum.*1994;37(10):1415-20.

Moya KL, Benowitz LI, Schneider GE, Allinquant B. The amyloid precursor protein is developmentally regulated and correlated with synaptogenesis. *Dev Biol.*1994;161(2):597-603.

Muhle C, Metzner J, Weinert D. Kinematic MR imaging in surgical management of cervical disc disease, spondylosis and spondylotic myelopathy. *Acta Radiol.*1999;40(2):146-153.

Muppidi JR, Tschopp J, Siegel RM. Life and death decisions: secondary complexes and lipid rafts in TNF receptor family signal transduction. *Immunity.*2004;21(4):461-5.

Muresan Z and Muresan V. A phosphorylated, carboxy-terminal fragment of beta-amyloid precursor protein localizes to the splicing factor compartment. *Hum Mol Gen.*2004;13:475-88.

Murphy MP, Hickman LJ, Eckman CB, et al. Gamma-secretase, evidence for multiple proteolytic activities and influence of membrane positioning of substrate on generation of amyloid beta peptides of varying length. *J Biol Chem.*1999;274:11914-23.

Mut M, Schiff D, Shaffrey ME. Metastasis to nervous system: spinal epidural and intramedullary metastases. *J Neurooncol.*2005;75(1):43-56.

- Muthukumar N, Venkatesh G, Thiruppathy S. Arrested hydrocephalus and the presyrinx state. Case report. *J Neurosurg*.2005;103(5 Suppl):466-70.
- Nagata M, Ueda T, Komiya A, Suzuki H, Akakura K, Ischihara M, Tobe T, Ichikawa T, Igarashi T, Ito H. Treatment and prognosis of patients with paraplegia or quadriplegia because of metastatic spinal cord compression in prostate cancer. *Prostate Cancer Prostatic Dis*.2003;6(2):169-73.
- Nahn TQ, Liles C, Schwartz SM. Physiological functions of caspases beyond cell death. *Am J Path*.2006;169(3):729-37.
- Nakajima H, Uchida K, Kobayashi S, Inukai T, Horiuchi Y et al. Rescue of rat anterior horn neurons after spinal cord injury by retrograde transfection of adenovirus vector carrying brain-derived neurotrophic factor gene. *J Neurotrauma*.2007.24:703-712.
- Nakano R. Apoptosis: gene-directed cell death. An overview. *Horm Res*.1997;48Suppl(3):2-4.
- Nash HH, Borke RC, Anders JJ. Ensheathing cells and methylprednisolone promote axonal regeneration and functional recovery in the lesioned adult rat spinal cord. *J Neurosci*.2002;22(16):7111-20.
- Nashmi R, Fehlings MG. Changes in axonal physiology and morphology after chronic compressive injury of the rat thoracic spinal cord. *Neurosci*.2001;104(1):235-51.
- Neugebauer E, Lefering R, Noth J. New perspectives in neurotrauma research. *Restor Neurol Neurosci*.1999;14(2-3):83-84.
- Newcombe RLG. Neurotrauma in Collision Sports in Australia. Proceedings of 1994 International Conference in Recent Advances in Neurotraumatology, World Federation of Neurosurgical Societies.1994;2:315-324.
- Newton EJ. Syringomyelia as a manifestation of defective fourth ventricular drainage. *Ann R Coll Surg Engl*.1969;44(4):194-213.
- Nilsen H, et al. Nuclear and mitochondrial uracil-DNA glycosylases are generated by alternative splicing and transcription from different positions in the UNG gene. *Nuc Acids Res*.1997;25(4):4750-4755.
- Nishimura I, Uetsuki T, Kuwako K, Hara T, Kawakami T et al. Cell death induced by a caspase-cleaved transmembrane fragment of the Alzheimer amyloid precursor protein. *Cell Death Differ*.2002;9(2):199-208.
- Nomura H, Tator CH, Shoicet MS. Bioengineered strategies for spinal cord repair. *J Neurotrauma*.2006;23:496-507.
- Novikova LN, Novikov LN, Kellerth JO. Differential effects of neurotrophins on neuronal survival and axonal regeneration after spinal cord injury in adult rats. *J Comp Neurol*.2002;452(3):255-63.
- O'Brien V. Viruses and apoptosis. *J Gen Virol*.1998;79:1833-45.

- Okano H, Sakaguchi M, Ohki K, Suzuki N, Sawamoto K. Regeneration of the central nervous system using endogenous repair mechanisms. *J Neurochem.*2007;102-1459-1465.
- Onyango IG, Tuttle JB, Bennett JP Jr. Activation of p38 and N-acetylcystein-sensitive c-Jun NH₂-terminal kinase signalling cascades is required for induction of apoptosis in Parkinson's disease cybrids. *Mol Cell Neurosci.*2005;28(3):452-61.
- Orr RD, Zdeblick TA. Cervical myelopathy: Approaches to surgical treatment. *Clin.Orthop.Rel.Res.*1999;359:58-66.
- Otera H, et al., Export of mitochondrial AIF in response to proapoptotic stimuli depends on processing at the intermembrane space. *EMBO J.*2005;24:1375-86.
- Oudega M, Vargas CG, Weber AB, Kleitman N, Bunge MB. Long-term effects of methylprednisolone following transection of adult rat spinal cord. *Eur J Neurosci.*1999;11(7):2453-64.
- Ousman SS, David S. MIP-1 α , MCP-1, GM-CSF, and TNF- α Control the Immune Cell Response That Mediates Rapid Phagocytosis of Myelin from the Adult Mouse Spinal Cord. *J Neurosci.*2001; 21(13):4649-4656.
- Ozawa H, Wu Z, Tanaka Y, Kokubun S. Morphologic change and astrocyte response to unilateral spinal cord compression in rabbits. *J Neurotrauma.*2004;21(7):944-55.
- Panickar KS, Norenburg MD. Astrocytes in cerebral ischemic injury: morphological and general considerations. *Glia.*2005;50(4):287-98.
- Park E, Velumian AA, Fehlings MG. The role of excitotoxicity in secondary mechanisms of spinal cord injury: a review with an emphasis on the implications for white matter degeneration. *J Neurotrauma.*2004;21:754-74.
- Park SA, Shaked GM, Bredesen DE, Koo EH. Mechanism of cytotoxicity mediated by the C31 fragment of the amyloid precursor protein. *Biochem Biophys Res Commun.*2009;388(2):450-5.
- Patwardhan RV, Hadley MN. History of surgery for ruptured disk. *Neurosurg Clin N Am.*2001;12:173-179.
- Penning L. Some aspects of plain radiography of the cervical spine in chronic myelopathy. *Neurology.*1962;12:513-9.
- Perrin RG. Metastatic tumors of the axial spine. *Curr Opin Oncol.*1992;4(3):525-32.
- Pettus EH, Povlishock JT. Characterisation of a distinct set of intra-axonal ultrastructural changes associated with traumatically induced alteration in axolemmal permeability. *Brain Res.*1996;722:1-11.
- Plassman BL, Havlik RJ, Steffens DC, et al. Documented head injury in early adulthood and risk of alzheimer's disease and other dementias. *Neurology.*2000;55:1158-66.

- Poon PC, Gupta D, Shoichet MS, Tator CH. Clip compression model is useful for thoracic spinal cord injuries: histologic and functional correlates. *Spine (Phila Pa 1976)*.2007;32(25):2853-9.
- Popovich PG, Guan Z, McGaughy V, Fisher L, Hickey WF, Basso DM. The neuropathological and behavioural consequences of intraspinal microglial/macrophage activation. *J Neuropathol Exp Neurol*.2002;61(7):623-33.
- Povlishock JT. Traumatically induced axonal injury: pathogenesis and pathobiological implications. *Brain Pathol*.1992 Jan;2(1):1-12.
- Preciado DA, Sebring LA, Adams GL. Treatment of patients with spinal metastases from head and neck neoplasms. *Arch Otolaryngol Head Neck Surg*.2002;128:539-43.
- Profyris C, Cheema SS, Zang D, Azari MF, Boyle K, Petratos S. Degenerative and regenerative mechanisms governing spinal cord injury. *Neurobiol.Dis*.2004;15:415-36.
- Purnell MR, Whish WJ. Novel inhibitors of poly(ADP-ribose) synthetase. *Biochem J*.1980;185(3):775-7.
- Rabizadeh S, Bredesen DE. Ten years on: mediation of cell death by the common neurotrophin receptor p75(NTR). *Cytokine Growth Factor Rev*.2003;14(3-4):225-39.
- Raff MC, Whitmore AV, Finn JT. Axonal self destruction and neurodegeneration. *Science*.2002;296:868-71.
- Raj P. Intervertebral disc: anatomy-physiology-pathophysiology-treatment. *Pain Pract*.2008;8(1):18-44.
- Rao R. Neck pain, cervical radiculopathy, and cervical myelopathy: pathophysiology, natural history, clinical evaluation. *J Bone Joint Surg Am*.2002;84-A:1872-81.
- Reis AJ. New surgical approach for late complications from spinal cord injury. *BMC Surg*.2006;6:12.
- Robertson GS, Crocker SJ, Nicholson DW, Schulz JB. Neuroprotection by the inhibition of apoptosis. *Brain Pathol*.2000;10(2):283-92.
- Robins SL, Fehlings MG. Models of experimental spinal cord injury: Translational relevance and impact. *Drug Discovery Today: Disease Models*.2008;5(1):5-11.
- Roth KA. Caspases, apoptosis, and Alzheimer disease: causation, correlation, and confusion. *J Neuropathol Exp Neurol*.2001;60(9):829-38.
- Rowland D. 'An ageing population: emergence of a new stage of life?', The transformation of Australia's population: 1970-2030, eds Khoo, S and McDonald, P, UNSW Press, Sydney.2003:239-265.
- Saraste A, Pulkki K. Morphologic and biochemical hallmarks of apoptosis. *Cardiovasc. Res*.2000;45:528-537.

- Saunders RL. Corpectomy for cervical spondylotic myelopathy. In: Menezes AH, Sonntag VK, eds. Principles of spinal surgery. New York: McGraw-Hill Companies, Health Professions Division.1996:559-69.
- Savill J, Dransfield I, Hogg N, Haslett C. Vitronectin receptor-mediated phagocytosis of cell undergoing apoptosis. *Nature*.1990;343(6254):170-3.
- Schaller B, Mindermann T, Gratz O. Treatment of syringomyelia after posttraumatic paraparesis or tetraparesis. *J Spinal Disord*.1999;12(6):485-8.
- Schick U, Marquardt G, Lorenz R. Intradural and extradural spinal metastases. *Neurosurg Rev*.2001;24(1):1-5; discussion 6-7.
- Schmit B, Cole M. Quantification of morphological changes in the spinal cord in chronic spinal cord injury using magnetic resonance imaging. *Conf Proc IEEE Eng Med Biol Soc*.2004;6:4425-8.
- Schnell L, Fearn S, Klassen H, Schwab ME, Perry VH. Acute inflammatory responses to mechanical lesions in the CNS: differences between brain and spinal cord. *Eur J Neurosci*.1999;11(10):3648-58.
- Schubert W, Prior R, Weidemann A, et al. Localization of Alzheimer beta A4 amyloid precursor protein at central and peripheral synaptic sites. *Brain Res*.1991;563(1-2):184-94.
- Selznick LA, Holtzman DM, Han BH, Gokden M, Srinivasan AN et al. In situ immunodetection of neuronal caspase-3 activation in Alzheimer disease. *J Neuropathol Exp Neurol*.1999;58(9):1020-6.
- Sharma HS. New perspectives for the treatment options in spinal cord injury. *Expert Opin Pharmacother*.2008;9(16):2773-800.
- Sheetz MP, Pfister KK, Nulinski JC, Cotman CW. Mechanisms of trafficking in axons and dendrites: Implications for development and neurodegeneration. *Prog Neurobiol*.1998;55(6):577-94.
- Sheng H, Wang H, Homi HM, et al. A No-Laminectomy Spinal Cord Compression Injury Model in Mice *Journal of Neurotrauma*.2004;21(5):595-603.
- Sheriff FE, Bridges LR, Sivaloganathan S. Early detection of axonal injury after head trauma using immunocytochemistry for β -amyloid precursor protein. *Acta Neuropathol*.1994;87:55-62.
- Shimizu H, Kakita A, Takahashi H. Spinal cord tau pathology in cervical spondylotic myelopathy. *Acta Neuropathol*.2008;115(2):185-92.
- Shinomiya K, Mutoh N, Furuya K. Study of experimental cervical spondylotic myelopathy. *Spine*.1992;17(10 Suppl):S383-7.
- Short D. Is the role of steroids in acute spinal cord injury now resolved? *Curr Opin Neurol*.2001;14(6):759-63.

- Shuman SL, Bresnahan JC, Beattie MS. Apoptosis of microglia and oligodendrocytes after spinal cord contusion in rats. *J Neurosci Res.*1997;50:798-808.
- Siddall, P.J., Xu, C.L. and Cousins, M.J. Allodynia following traumatic spinal cord injury in the rat, *Neuroreport.*1995;6:1241-1244.
- Siegmund D, Mauri D, Peters N, Juo P, Thome M, Reighwein M, Blenis J, Scheurich P, Tschopp J, Wajant H. Fas-associated death domain protein (FADD) and caspase-8 mediate up-regulation of c-Fos by Fas ligand and tumour necrosis factor-related apoptosis-inducing ligand (TRAIL) via a FLICE inhibitory protein (FLIP)-regulated pathway. *J Biol Chem.*2001;276(35):32585-90.
- Simonin F, Hofferer L, Panzeter PL, Muller S, de Murcia G, Althaus FR. The carboxyl-terminal domain of human poly(ADP-ribose) polymerase. Overproduction in *Escherichia coli*, large scale purification, and characterization. *J Biol Chem.*1993;268:13454-61.
- Simonin F, Poch O, Delarue M, deMurcia G. Identification of potential active-site residues in the human poly(ADP-ribose) polymerase. *J Biol Chem.*1993;268(12):852935.
- Simonovich M, Barbiro-Michaely E, Mavevsky A. A real-time monitoring of mitochondrial NADH and microcirculatory blood flow in the spinal cord. *Spine.*2008;33(23):2495-502.
- Sinha S, Anderson JP, Barbour R, et al. Purification and cloning of amyloid precursor protein beta-secretase from human brain. *Nature.*1999;402:537-540.
- Skaper SD. Poly(ADP-ribosyl)ation enzyme-1 as a target for neuroprotection in acute central nervous system injury. *Curr Drug Targets CNS Neurol Disord.*2003;2(5):279-91.
- Smith C, Anderton BH. Dorothy Russell Memorial Lecture. The molecular pathology of Alzheimer's disease: are we any closer to understanding the neurodegenerative process? *Neuropathol Appl Neurobiol.*1994;20(4):322-38.
- Smith DH, Chen XH, Nonaka M, et al. Accumulation of amyloid beta and tau and the formation of neurofilament inclusions following diffuse brain injury in the pig. *J Neuropathol Exp Neurol.*1999;58:982-992.
- Smith DH, Chen XH, Iwata A, Graham DI. Amyloid beta accumulation in axons after traumatic brain injury in humans. *J Neurosurg.*2003;98(5):1072-7.
- Song KJ, Choi BW, Kim GH, Kim YS, Song JH. The Relationship between Spinal Stenosis and Neurological Outcome in Traumatic Cervical Spine Injury: An Analysis using Pavlov's Ratio, Spinal Cord Area, and Spinal Canal Area. *Clin. Orthop. Surg.*2009;1(1):11-8.
- Soriano S, Lu DC, Chandra S, Pietrzik CU, Koo EH. The amyloidogenic pathway of amyloid precursor protein (APP) is independent of its cleavage by caspases. *J Biol Chem.*2001;276(31):29045-50.
- Sroga JM, Jones TB, Kigerl KA, McGaughy VM, Popovich PG. Rats and mice exhibit distinct inflammatory reactions after spinal cord injury. *J Comp Neur.*2003;462:223-40.

Stavridis SI, Dehghani F, Korf HW, Hailer NP. Cocultures of rat sensorimotor cortex and spinal cord slices to investigate corticospinal tract sprouting. *Spine*.2009;34(23):2494-99.

Stevens A, Lowe J. Pathology: illustrated review in color. Second Ed. Mosby.2000.

Stone JR, Singleton RH, Povlishock JT. Antibodies to the C-terminus of the beta-amyloid precursor protein (APP): a site specific marker for the detection of traumatic axonal injury. *Brain Res*.2000;871(2):288-302.

Stone JR, Okonkwo DO, Singleton RH, Mutlu LK, Helm GA, Povlishock JT. Caspase-3-mediated cleavage of amyloid precursor protein and formation of amyloid- β peptide in traumatic axonal injury. *J Neurotrauma*.2002;19(5):601-614.

Suri A, Chhabra RP, Mehta VS, Gaikwad S, Pandey RM. Effect of intramedullary signal changes on the surgical outcome of patients with cervical spondylotic myelopathy. *Spine J*.2003;3(1):33-45.

Susin SA, Zamzami N, Larochette N, Dallaporta B, Marzo I, Brenner C, Hirsch T, Petit PX, Geuskens M, Kroemer G. A cytofluorometric assay of nuclear apoptosis induced in a cell-free system: application to ceramide-induced apoptosis. *Exp Cell Res*.1997;236(2):397-403.

Susin SA, Lorenzo HK, Zamzami N, Marzo I, Snow BE, et al. Molecular characterisation of mitochondrial apoptosis-inducing factor. *Nature*.1999;397(6718):387, 389.

Szabo C. Cardioprotective effects of poly(ADP-ribose) polymerase inhibition. *Pharmacol Res*.2005;52(1):34-43.

Takagi T, Takayasu M, Mizuno M, Yoshimotor M, Yoshida J. Caspase activation in neuronal and glial apoptosis following spinal cord injury in mice. *Neurologia medico-chirurgica*.2003;43(1):20-30.

Takahashi Y, Narusawa K, Shimizu K, Hijioka A, Nakamura T. Enlargement of cervical spinal cord correlates with improvement of motor function in upper extremities after laminoplasty for cervical myelopathy. *J Spinal Disord Tech*.2006;19(3):194-8.

Takenouchi T, Setoquchi T, Yone K, Komiya S. Expression of apoptosis signal-regulating kinase 1 in mouse spinal cord under chronic mechanical compression: possible involvement of the stress-activated mitogen-activated protein kinase pathways in spinal cord cell apoptosis. *Spine*.2008;33(18):1943-50.

Takui I, Kiyomitsu O, Hitoshi T, Hideaki E, Fisahiro I. Cervical Spondylotic Myelopathy: Clinicopathologic Study on the Progression Pattern and Thin Myelinated Fibers of the Lesions of Seven Patients Examined During Complete Autopsy. *Spine*.1996;21(7):827-33.

Tanaka S, Takehashi M, Iida S, Kitajima T, Kamanaka Y, Stedeford T, Banasik M, Ueda K. Mitochondrial impairment induced by poly(ADP-ribose) polymerase-1 activation in cortical neurons after oxygen and glucose deprivation. *J Neurochem*.2005;95(1):179-90.

Taoka Y, Okajima K, Uchiba M, Murakami K et al. Role of neutrophils in spinal cord injury in the rat. *Neuroscience*.79:1177-1182.

- Tarlov IM. Acute spinal cord compression paralysis. *J Neurosurg.*1972;36(1):10-20.
- Tate BA, Mathews PM. Targeting the role of the endosome in the pathophysiology of Alzheimer's disease: a strategy for treatment. *Sci Aging Knowledge Environ.*2006;(10):re2.
- Tator CH. Review of treatment trials in human spinal cord injury: issues, difficulties, and recommendations. *Neurosurgery.*2006;59(5):957-82.
- Tesco G, Koh YH, Tanzi RE. Caspase Activation Increases Beta-amyloid Generation Independently of Caspase Cleavage of the Beta-amyloid Precursor Protein (APP). *J Biol Chem.*2003;278(46):46074-80.
- Traill Z, Richards MA, Moore NR. Magnetic Resonance Imaging of metastatic bone disease. *Clin Orthop.*1995;(312):76-88.
- Tripathi R, McTigue DM. Prominent oligodendrocyte genesis along the border of spinal contusion lesions. *Glia.*2007;55(7):698-711.
- Tsai J, Grutzendler J, Duff K, Gan WB. Fibrillar amyloid deposition leads to local synaptic abnormalities and breakage of neuronal branches. *Nature Neurosci.*2004;7:1181-83.
- Tsutsumi S, Ueta T, Shiba K, Yamamoto S, Takagishi K. Effects of the Second National Acute Spinal Cord Injury Study of high-dose methylprednisolone therapy on acute cervical spinal cord injury-results in spinal injuries center. *Spine.*2006;31(26):2992-6.
- Uetani M, Hashmi R, Hayashi K. Malignant and benign compression fractures: differentiation and diagnostic pitfalls on MRI. *Clin Radiol.*2004;59(2):124-31.
- Vahsen N, Cande C, Dupaigne P, Giordanetto F, Kroemer RT, et al. Physical interaction of apoptosis-inducing factor with DNA and RNA. *Oncogene.*2006;25(12):1763-74.
- Van Wijk SJ, Hageman GJ. Poly(ADP-ribose) polymerase-1 mediated caspase-independent cell death after ischemia/reperfusion. *Free Radic Biol Med.*2005;39(1):81-90.
- Vaquero J, Zurita M, Oya S, Aguayo C, Bonilla C. Early administration of methylprednisolone decreases apoptotic cell death after spinal cord injury. *Histol Histopathol.*2006;21(10):1091-102.
- Vargas ME, Barres BA. Why is Wallerian degeneration in the CNS so slow? *Annual Rev Neurosci.*2007;30:153-179.
- Ventureyra EC, Aziz HA, Vassilyadi M. The role of cine flow MRI in children with Chiari I malformation. *Childs Nerv Syst.*2003;19(2):109-13.
- Verhagen AM, Ekert PG, Pakusch M, Silke J, Connolly LM et al. Identification of DIABLO, a mammalian protein that promotes apoptosis by binding to and antagonizing IAP proteins. *Cell.*2000;102(1):43-53.
- Virag L. Structure and function of poly(ADP-ribose) polymerase-1: role in oxidative stress-related pathologies. *Curr Vasc Pharmacol.*2005;3(3):209-14.

- Von Euler M, Seiger A, Sundstrom E. Clip compression injury in the spinal cord: A correlative study of neurological and morphological alterations. *Exp Neurol*.1997;145(2):502-10.
- Wada E, Yonenobu K, Suzuki S, Kanazawa A, Ochi T. Can intramedullary signal change on magnetic resonance imaging predict surgical outcome in cervical spondylotic myelopathy? *Spine*.1999;24(5):455-61.
- Wada S, Yone K, Ishidou Y, Nagamine T, Nakahara S, Niiyama T, Sakou T. Apoptosis following spinal cord injury in rats and preventative effect of N-methyl-D-aspartate receptor antagonist.*J Neurosurg*.1999;91(1 Suppl):98-104.
- Wajant H, Pfizenmaier K, Scheurich P. Tumor necrosis factor signalling. *Cell Death Differ*.2003;10(1):45-65.
- Walid MS, Zaytseva NV. Upper cervical spine injuries in elderly patients. *Aust Fam Physician*.2009;38(1-2):43-5.
- Walshe F. Compression and Injuries of the Spinal Cord. In: *Disease of the Nervous System: Described for Practitioners and Students*. E & S Livingstone, Edinburgh and London.1970:236-49.
- Warden P, Bamber NI, Li H, Esposito A, Ahmad KA, Hsu CY, Xu XM. Delayed glial cell death following wallerian degeneration in white matter tracts after spinal cord dorsal column cordotomy in adult rats. *Exp Neurol*.2001;168(2):213-24.
- Watson C, Paxinos G, Kayalioglu G. The spinal cord. Elsevier Ltd.2009.
- Weidemann A, Konig G, Bunke D. Identification, biogenesis and localization of precursor of Alzheimer's disease A4 amyloid protein. *Cell*.1989;57:115-126.
- Weidemann A, Palinga K, Rrwang D, et al. Proteolytic processing of the Alzheimer's disease amyloid precursor protein within its cytoplasmic domain by caspase-like proteases, *J Biol Chem*.1999;274:5823-29.
- Wieseler-Frank J, Jekich BM, Mahoney JH, Bland ST, Maier SF, Watkins LR. A novel immune-to-CNS communication pathway: Cells of the meninges surrounding the spinal cord CSF space produce proinflammatory cytokines in response to an inflammatory stimulus. *Brain Behav Immun*.2007;21(5):711-8.
- Williams LR,Varon S, Peterson GM, Wictorin K, Fischer W, Bjorklund A, et al. Continuous infusion of nerve growth factor prevents basal forebrain neuronal death after fimbria fornix transection. *Proc. Natl. Acad Sci. U.S.A*.1986;83:9231–9235.
- Wingrave JM, Schaecher KE, Sribnick EA, Wilford GG, Ray SK, et al. Early induction of secondary injury factors causing activation of calpain and mitochondria-mediated neuronal apoptosis following spinal cord injury in rats. *J Neurosci Res*.2003;73(1):95-104.
- Wong JK, Sharp K, Steward O. A straight alley version of the BBB locomotor scale. *Exp Neurol*.2009;217(2):417-20.

Woo M, Hakem R, Soengas MS, Ducan GS, Shahinian A, Kagi D, Hakem A, McCurrach M, Khoo W, Kaufman SA et al. Essential contribution of caspase 3/CPP32 to apoptosis and its associated nuclear changes. *Genes Dev.*1998;12:806-819.

Xu K, Chen QX, Li FC, Chen WS, Lin M, Wu QH. Spinal cord decompression reduces rat cell apoptosis secondary to spinal cord injury. *J Zhejiang Univ Sci B.*2009;10(3):180-7.

Xu P, Gong WM, Li Y, Zhang K, Yin DZ, Jia TH. Destructive pathological changes in the rat spinal cord due to chronic mechanical compression. Laboratory investigation. *J Neurosurg Spine.*2008;8(3):279-85.

Xu R, Garces-Ambrossi GL, McGirt MJ, Witham TF, Wolinsky JP, Bydon A, Gokasian ZL, Sciubba DM. Thoracic vertebrectomy and spinal reconstruction via anterior, posterior, or combined approaches: clinical outcomes in 91 consecutive patients with metastatic spinal tumors. *J Neurosurg Spine.*2009;11(3):272-84.

Yamaura I, Yone K, Nakahara S, Nagamine T, Baba H, Uchida K, Komiya S. Mechanism of destructive pathologic changes in the spinal cord under chronic mechanical compression. *Spine.*2002;27(1):21-6.

Yang L, Blumbergs PC, Jones NR, Manavis J, Sarvestani GT, Ghabriel MN. Early expression and cellular localization of proinflammatory cytokines interleukin-1beta, interleukin-6, and tumor necrosis factor-alpha in human traumatic spinal cord injury. *Spine (Phila Pa 1976).*2004;29(9):966-71.

Yong C, Arnold PM, Zoubine MN, Citron BA, Watanabe I, Berman NE, Festoff BW. Apoptosis in cellular compartments of rat spinal cord after severe contusion injury. *J Neurotrauma.*1998;15(7):459-72.

Yoshida H, Okada Y, Maruiwa H, Fukuda K, Nakamura M, Chiba K, Toyama Y. Synaptic blockade plays a major role in the neural disturbance of experimental spinal cord compression. *J Neurotrauma.*2003;20(12):1365-76.

Young W. NASCIS. National Acute Spinal Cord Injury Study. *J Neurotrauma.*1990;7(3):113-4.

Young WF. Cervical Spondylotic Myelopathy: A common cause of spinal cord dysfunction in older persons. *Am Fam Physician.*2000; 62(5):1064-70, 1073.

Yu WR, Baptiste DC, Liu T, Odrobina E, Stanisz GJ, Fehlings MG. Molecular mechanisms of spinal cord dysfunction and cell death in the spinal hyperostotic mouse: implications for the pathophysiology of human cervical spondylotic myelopathy. *Neurobiol Dis.*2009;33(2):149-63.

Yuan J, Yankner BA. Apoptosis in the nervous system. *Nature.*2000;407:802-809

Zamzami N, Kroemer G. The mitochondrion in apoptosis: How Pandora's box opens. *Nat Rev Mol Cell Biol.*2001;2:67-71.

Zeidman SM, Ducker TB. Cervical disk diseases: part 1. Treatment options and outcomes. *Neurosurgery Quarterly.*1992;2:116-43.

- Zhang C, Goto N, Suzuki M, Zhou M. Microscopic morphometry of the spinal cord with cervical spondylotic myelopathy. *Neuropathology*.2007;16(4):239-245.
- Zhang X, Chen J, Graham SH, Du L, Kochanek PM, Draviam R, Guo F, Nathaniel PD, Szabo C, Watkins SC et al. Intranuclear localization of apoptosis-inducing factor (AIF) and large scale dna fragmentation after traumatic brain injury in rats and in neuronal cultures exposed to peroynitrite. *J Neurochem*.2002;82:181-191.
- Zhang Y, Le Blanc AC. Microinjections to study the specific role of proapoptotic proteins in neurons. *Neuromethods*.2002;37:83-106.
- Zhang Z, Krebs CJ, Guth L. Experimental analysis of progressive necrosis after spinal cord trauma in the rat: etiological role of the inflammatory response. *Exp Neurol*.1997;143(1):141-52.
- Zheng TS, Schlosser SF, Dao T, Hingorani R, Crispe IM, Boyer JL, Flavell RA. Caspase-3 controls both cytoplasmic and nuclear events associated with Fas-mediated apoptosis in vivo. *Proc Natl Acad Sci U S A*.1998;95(23):13618-23.
- Zhivotovsky B, Samali A, Gahm A, Orrenius S. Caspases: their intracellular localization and translocation during apoptosis. *Cell Death Differ*.1999;6(7):644-51.
- Zileli M, Kiliçer C, Ersahin Y, Cagli S.. Primary Tumors of the Cervical Spine: A Retrospective Review of 35 Surgically Managed Cases. *In The Spine Journal*.2007;7(2):165-173.
- Zurita M, Vaquero J, Oya S, Morales C. Effects of dexamethasone on apoptosis-related cell death after spinal cord injury. *J Neurosurg*.2002;96:83-9.

APPENDIX – INDIVIDUAL HUMAN CASES

CASE 1

Clinical summary A 77 year-old male with quadriplegia following a cervical spine operation occurring 8 years prior to death from ischaemic heart disease.

On macroscopic examination there was an old fusion at C5-6. An anterior disc bar extending 8mm rostral-caudal, 3mm A-P and 20mm side to side was found at C3-4. At C4-5, there was focal wasting associated with the disc bar, and wasting of C6-C7 over 20mm corresponding to the level of fusion.

On microscopic examination the posterior cord was distorted and atrophied at C4-5. There was demyelination, subtotal loss of anterior horn cells and arachnoid fibrosis at this level. There was ascending tract degeneration of the posterior columns above. C6 segment showed severe old cystic necrosis in the dorsal and anterolateral region of the cord. Below the site of compression there was descending corticospinal tract degeneration.

Pathology – brain

1. Old plaques jaunes in both temporal lobes, left much worse than right.
2. Hydrocephalus, probably compensated aqueductal stenosis.

Pathology – spine and spinal cord

1. C3-4 disc bar.
2. C5-6 fusion (status post operative).
3. Compression myelopathy with focal cord wasting at both these levels.

Haematoxylin and Eosin

Macroscopic findings C2 (N21), C4 (N24, N25) were macroscopically normal. At C3 (N22) there was a well-defined loss of tissue in the lateral white matter however this appears to be artefact. The C4/5 (N26), C5 (N27, N28) C5/6 (N29) segments show a compressed or atrophied spinal cord and pallor of the posterolateral region. At C6 (N30, N31) there is mild wasting evident on the posterior aspect and continuing pallor of the cord. At C6/7 (N32, N33) and C7 (N34) there is significant wasting and a clearly defined loss of tissue can be seen in one posterior column and in the opposite lateral column. In C7 (N35) the cystic change extends from the lateral into the anterior spinal cord unilaterally. In segments C7/8 and C8 (N36, N37) the shape is normal and there is visible pallor of the grey matter. T1 (N40) segment was macroscopically normal.

Microscopic findings At segments C2 (N21), C3 (C22) and C4 (N24, N25) there is oedema as well as mild break-down of tissue within the posterolateral white matter which may be artefact. Sections N21-N24, and C4/5 (N26) show a decrease in AHC numbers on one side. At C2 (N21) there are two neurons displaying red cell change. Section N25 shows no AHC loss. In C3/4 (N23) and C4 (N24) there are occasional neurons showing the features of red cell change such as eosinophilia, shrinkage, nuclear pyknosis and loss of Nissl substance consistent with hypoxic or ischaemic damage. C4-5 (N27), C5 (N28) show a bilateral subtotal loss of AHCs. In N27 there is peripheral vacuolation and macrophages present in the posterior nerve root extending into the posterior horn. In N28 there is vacuolation throughout the cord and significant loss of tissue in both posterior columns as well as the posterior horn. The lateral corticospinal tracts appear unaffected. Macrophages are scattered through these areas. In C5/6 (N29), C6 (N30, 31) there is complete cystic cavitation of the posterior horn and lateral white matter on one side. Vacuolation and is seen throughout the spinal cord and many macrophages exist in the grey matter. In sections N29 (C5/6) and N30 (C6) the anterior horn cells appear spared but there is a subtotal loss of AHCs in N31 (C6) and N32 (C6/7). There are clusters of mononuclear cells of a morphology consistent with lymphocytes. At C6/7 (N33), C7 (N34, N35) there is severe, cystic cavitation and destruction of the lateral cord on one side. In section N35 there is also a loss of the anterior white matter. There is a subtotal loss of AHCs in these sections and congestion of vessels. C7/8 (N36) shows a complete loss of AHCs on one side and subtotal loss on the other. There is extensive cystic change of the grey matter and also affecting the medial white matter. Many tissue macrophages are seen in these necrotic areas and there is a general engorgement of vessels. T1 (N40) and C8 (N37) showed a unilateral loss of anterior horn cells. There is lateral vacuolation and disruption of the white matter but in places this is not distinguishable from artefact. No axonal swellings were observed.

Weil On Weil staining there was unilateral decreased staining of the lateral corticospinal tract below the lesion and of the posterior columns and lateral spinothalamic tracts above the lesion consistent with demyelination and Wallerian degeneration.

Immunohistochemical results

CASE 1 – Compression C3/4 – Immunological positivity (+) in glial, axonal or neuronal profiles:

Level	APP	Casp-3	DNA-PKcs	PARP	Bcl-2	Fas	Casp-9	TUNEL	Amy-33	CMAP	AIF
C2	-	-	+	+	-	-	-	+	+	+	+
C3	-	-	+	+	-	-	-	+	+	+	+
C4	-	-	+	+	-	-	-	+	+	+	+
C4/5	-	-	+	+	-	-	-	+	+	+	+
C5	-	-	+	+	-	-	-	-	+	+	+
C5/6	-	-	+	-	-	-	-	-	+	+	+
C6	-	-	+	+	-	-	-	+	+	+	+
C6/7	-	-	+	+	-	-	-	+	+	+	+
C7	-	-	+	+	-	-	-	+	-	+	+
C7/8	-	-	+	+	-	-	-	+	+	+	+
C8	-	-	+	+	-	-	-	+	+	+	+
T1	-	-	+	+	-	-	-	+	+	+	+

* Shaded rows represent the site of compression

APP Non-specific immunopositivity was present in segments C4-C8 (N23-N36).

Active caspase-3 Immunopositive cytoplasmic profiles were more numerous surrounding cystic areas and were morphologically suggestive of macrophages and lymphocytes. Non-specific, small foci of immunopositivity were seen within the neuropil.

DNA-PKcs Immunopositive nuclear and cytoplasmic profiles were more numerous surrounding areas of cystic degeneration and were morphologically suggestive of macrophages and lymphocytes. DNA-PKcs positive glial profiles were rare at the site of compression but were more numerous above and below the lesion, present in all sections except N30 (C6). These cells were most often seen in the subpial region where there is increased background and therefore may not be truly positive. Rare, immunopositive neuronal nuclei were found in C6 (N31) and C6/7 (N33) however the degree of tissue destruction near such cells may have contributed to a false result.

PARP Immunopositivity was found within the white matter at all levels except C5/6 (N29) and C6 (N30). Immunopositive nuclear and cytoplasmic profiles were more numerous surrounding areas of cystic degeneration and were morphologically suggestive of macrophages and lymphocytes. PARP

positive glial profiles were present in small numbers at the site of compression C4 (N23, N24) but were more numerous above and below the lesion at levels N21, 22, N25, N37 and N40, scattered throughout the white matter. Sections that were immunonegative for the PARP antibody corresponded to levels where necrosis and wasting were a feature at C4/5 (N26) to C7/8 (N36). Negative in neurons and axons.

Bcl-2 Immunopositive cytoplasmic profiles were seen surrounding cystic areas and were morphologically suggestive of macrophages and lymphocytes.

FAS Occasional cytoplasmic immunoreactivity to FAS was seen on the periphery of the spinal cord in C2 (N21) however this was in a region of increased background and likely therefore to be artefact. Non-specific staining, rare profiles recognised to be macrophages were seen in segment C6 (N31) and C6/7 (N32).

Caspase-9 Non-specific cytoplasmic immunostaining was seen in regions of cystic degeneration in cells whose morphology was consistent with lymphocytes.

TUNEL Occasional glial immunopositivity was found in segments C2 (N21), C3 (N22) and C3/4 (N23). Below the lesion at C7/8 (N36), C8 (N37) and T1 (N40) more numerous immunopositivity was present within nuclei, the morphology suggestive of glia. Immunopositive anterior horn cells were present in C2 (N21)-C4/5 (N26), C6 (N30)-C6/7 (N33) and C7 (N35)-T1 (N40). In 7 of these 12 sections there was also neuronal staining within the posterior horn (N22, 30, 31, 33, 35, 36, 37).

CMAP Immunopositivity was seen in glia, neurons, the majority of axons both small and large, and in ependymal cells. The degree of background staining negates the specificity of this marker at the dilution used.

Amy-33 amyloid beta Neuronal immunoreactivity was seen in all sections except C7 (N34) where no neuronal profiles were identified due to tissue necrosis. Rare axonal immunopositive profiles were present and non-specific staining in some sections. There was no glial immunoreactivity.

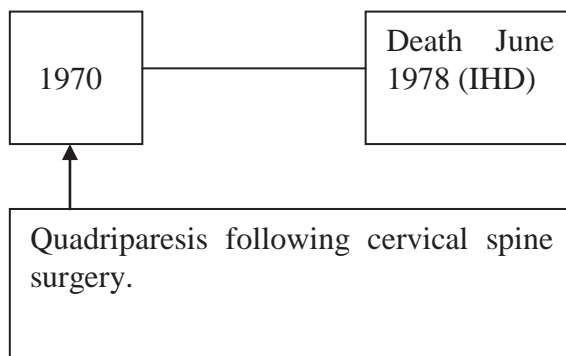
University of Melbourne amyloid-beta Negative.

DAKO amyloid-beta Negative.

AIF Glia cytoplasmic immunopositivity was present throughout the white matter, and neuronal immunopositivity in the grey, above (C2-N21, C3-N22, C3/4-N23) and below the lesion (C5/6-

N29, C8-N37, T1-N40). At C7 (N34, N35), C7/8 (N36) there was subtotal necrosis of the posterolateral cord, however glial immunoreactivity and neuronal immunoreactivity was present in preserved regions. A similar pattern of staining was present at C5 (N28), C6 (N30, N31) and C6/7 (N32, 33) however the degree of tissue necrosis / cystic necrosis was less than at C7, C8. In section N24 at the site of compression, C4, there were fewer immunopositive glial profiles throughout the white matter. Neuronal staining was present in more than ten neurons on one side and four on the other. A greater number of immunopositive glia were found in section N25 of C4 as well as neuronal immunoreactivity in both anterior horns. There was no immunopositivity within axonal profiles. At C4/5 (N26, N27) immunopositive glia were seen throughout the white matter and neuronal immunopositivity on both sides.

Timeline of clinical progression



Spatial Distribution of Staining – Case 1

Case: 1
Amy-33

Levels:

- a) One level above site - C2
- b) At the site of compression - C4
- c) Two levels below site - C8

a)



b)



c)



Case: 1
Haematoxylin and eosin

Levels:

- a) One level above site - C2
- b) At the site of compression - C4
- c) Two levels below site - C8

a)



b)



c)

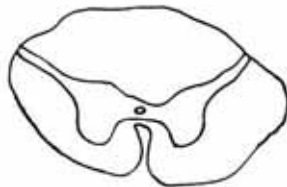


Case: 1
APP

Levels:

- a) One level above site - C2
- b) At the site of compression - C4
- c) Two levels below site - C8

a)



b)



c)

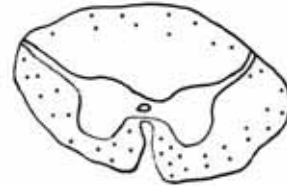


Case: 1
DNA-PKcs

Levels:

- a) One level above site - C2
- b) At the site of compression - C4
- c) Two levels below site - C8

a)



b)



c)



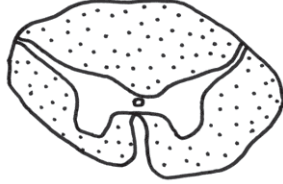
Spatial Distribution of Staining – Case 1

Case: 1
PARP

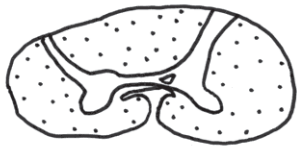
Levels:

- a) One level above site - C2
- b) At the site of compression - C4
- c) Two levels below site - C8

a)



b)



c)

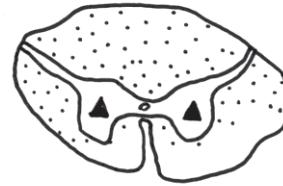


Case: 1
TUNEL

Levels:

- a) One level above site - C2
- b) At the site of compression - C4
- c) Two levels below site - C8

a)



b)



c)



Case: 1
AIF 1

Levels:

- a) One level above site - C2
- b) At the site of compression - C4
- c) Two levels below site - C8

a)



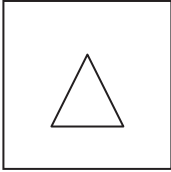
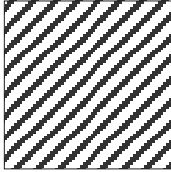

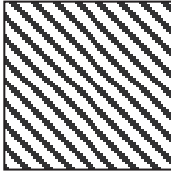
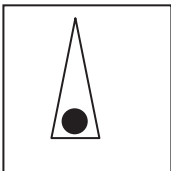
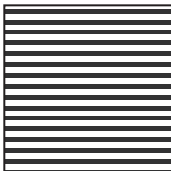
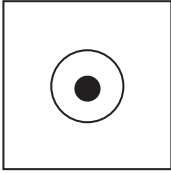

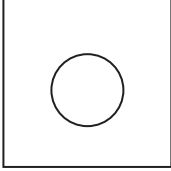
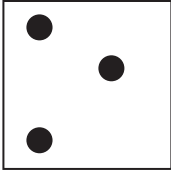

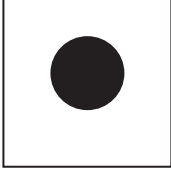
b)



c)



Key – Spatial distribution of staining for cross-sectional diagrams.

	Anterior horn cell loss		Cystic necrosis
	Central chromatolysis		Tissue necrosis
	Neuronal ischaemic change		Neoplasm
	Glial cell loss		Syrinx
	Axonal swellings / retraction bulbs		
	Immunopositive glia		
	Immunopositive neurons		
	Immunopositive axonal swellings / retraction bulbs		

Summary of immunohistochemistry Case 1

<p>Glia: DNA-PKcs, PARP, TUNEL, AIF, CMAP Axons: CMAP Neurons: TUNEL, AIF, Amy-33, CMAP</p>	<p>C2</p>	<p>H&E: oedema Weil: pallor posterior column</p>
<p>Glia: DNA-PKcs, PARP, TUNEL, AIF, CMAP Axons: CMAP Neurons: TUNEL, AIF, Amy-33, CMAP</p>	<p>C3</p>	<p>H&E: oedema, red cell change Weil: pallor posterior column</p>
<p>Glia: DNA-PKcs, PARP, TUNEL, AIF, CMAP Axons: CMAP Neurons: TUNEL, AIF, Amy-33, CMAP</p>	<p>C4</p>	<p>H&E: atrophy, pallor posterolateral cord, oedema, loss AHCs, red cell change, vacuolation subpial, macrophages</p>
<p>Glia: DNA-PKcs, AIF, CMAP Axons: CMAP Neurons: TUNEL, AIF, Amy-33, CMAP</p>	<p>C5</p>	<p>H&E: atrophy, pallor posterolateral cord, loss AHCs, vacuolation throughout, lateral cystic change, macrophages</p>
<p>Glia: AIF, CMAP Axons: CMAP Neurons: TUNEL, AIF, Amy-33, CMAP</p>	<p>C6</p>	<p>H&E: atrophy, pallor posterolateral cord, posterolateral cystic change, macrophages, loss AHCs Weil: pallor lateral corticospinal tract</p>
<p>Glia: DNA-PKcs, PARP, TUNEL, AIF, CMAP Axons: CMAP Neurons: TUNEL, AIF, CMAP</p>	<p>C7</p>	<p>H&E: atrophy, cystic change all regions, loss AHCs, cystic change, congestion Weil: pallor lateral corticospinal tract</p>
<p>Glia: DNA-PKcs, PARP, TUNEL, AIF, CMAP Axons: CMAP Neurons: TUNEL, AIF, Amy-33, CMAP</p>	<p>C8</p>	<p>H&E: loss AHCs, macrophages, congestion Weil: pallor lateral corticospinal tract</p>
<p>Glia: DNA-PKcs, PARP, TUNEL, AIF, CMAP Axons: CMAP Neurons: TUNEL, AIF, Amy-33, CMAP</p>	<p>T1</p>	<p>H&E: loss AHCs, vacuolation Weil: pallor lateral corticospinal tract</p>

Conclusion On postmortem examination a single anterior disc bar was found to impinge onto the spinal cord and there was associated wasting. Evidence of ongoing cord compression and chronic inflammation is seen on microscopic examination of the spinal cord with cystic degeneration, vacuolation, arachnoid fibrosis and the presence of macrophage invasion. In the intact areas of white and grey matter surrounding the cyst there was immunopositivity to caspase-3, DNA-PKcs, PARP, Fas, Bcl-2 and caspase-9. In addition there was loss of both neurons and glia. Significant numbers of anterior horn cells and neurons of the posterior horn were immunopositive for the TUNEL marker. Neuronal immunopositivity using Amy-33 marker of amyloid-beta was also a feature. In areas of the white matter where glia was still present, nuclear immunopositivity to PARP, DNA-PKcs and TUNEL was seen which indicate that nuclear DNA damage is a likely feature of the pathology. Furthermore, these regions of immunopositivity appear to be correlated with Wallerian degeneration and may indicate a preferential loss of oligodendrocytes. AIF immunopositivity was seen in profiles consistent with both oligodendrocytes and astrocytes. Glial immunopositivity was homogeneously spread throughout the white matter and reduced at the site of compression. Neuronal immunopositivity was consistently present. Staining in glia and neurons was only seen within the cytoplasm.

CASE 2

Clinical summary A 64 year-old male who died from acute haemorrhagic ulceration of the duodenum on a background of recurrent septicaemia secondary to pyelonephritis. Initial presentation was 14 years prior to death. There was a past history of ischaemic stroke resulting in left arm and left leg weakness for 2 weeks, which improved partially. He then had a sudden onset of right arm and right leg weakness associated with bending forward to pick up an object. 3 months later he developed neurological symptoms with reported numbness of all limbs, increasing difficulty in walking and a shuffling gait. There was no significant neck pain and only occasional occipital discomfort. Bending the head forwards produced paraesthesias in his arms and legs. He developed severe spastic quadriparesis with moderate weakness of the left arm and left leg and was diagnosed with cervical spondylosis. 3 years after the onset of symptoms he underwent a laminectomy operation at C3-C7.

On autopsy examination, the morphology of the cord suggested unrelieved chronic compression. Cystic necrosis and wasting were maximal at C5 segment. Only remnants of the cord parenchyma were found and adhesions of cord and dura occurred posteriorly. The evidence of severe, ongoing compression at the level of C5 was consistent with the macroscopic findings of an osteophytic nodule projecting from the level of the disc separating C4/C5.

Microscopy confirmed great deformity and loss of normal architecture. The pia mater was especially thickened and contained neuritic sprouts, which suggest the development of aberrant regeneration. Degeneration of ascending sensory tracts was seen at C4/C5 and of the descending corticospinal tracts at C6-T1 spinal cord segments consistent with the extent of damage to C5 segment. Subtotal loss of anterior horn cells existed from C3-C8, maximal at C5.

Pathology – brain

1. Cerebral lacunes.
2. Cervical spondylosis.

Pathology – spine and spinal cord

1. Osteophytosis of the vertebral column.

Haematoxylin and Eosin

Macroscopic findings On post-mortem examination there was severe osteophytosis of the lumbosacral cord with numerous osteophytic bars projecting into the neural canal. Sohmorl's nodes

were evident at many levels of the vertebral column. There was an osteophytic nodule at the level of the intervertebral disc separating C4 and C5 vertebral bodies with projection backwards into the neural canal. The cervical canal appeared smaller than usual. Dense fibrous scarring was present on the right side of the cervical region involving the dural sleeves of the existing spinal nerve roots. On opening the dural sac there was marked wasting of the spinal cord at C5 and C6 segmental level.

C2 (N2) and C4 (N3) have a macroscopically normal oval shape. Compression or atrophy is evident in spinal cord segments C5 (N4-N6), and C6 (N7) severe on one side, particularly in the corticospinal tract. The posterolateral spinal cord is pale staining in each of the above segments from C2-C6. C8 (N8) appears normal.

Microscopic findings C2 (N2) – There is subtotal loss of anterior horn cells more severe on one side and mild loss on the other. The white matter parenchyma is intact although there are decreased numbers of glia in the posterior cord and lateral corticospinal tract. Remaining glia have a morphology suggestive of oligodendrocytes. At C4 (N3) and C5(N4-N6) the cord appears compressed, particularly on one side. There is subtotal loss of AHCs more severe on the compressed side. There is cystic cavitation within the posterior column extending to the lateral corticospinal tracts. Mononuclear cells suggestive of lymphocytes are present within this region loosely distributed within the neuropil rather than as perivascular cuffing. There are no visible macrophages. There are decreased numbers of glia in the posterolateral cord and many areas of oedema dispersed throughout the white matter. Corpora amylacea are also seen. The vessel walls appear thickened and many of the walls are pale staining possibly due to the age of the archival material or due to hyaline sclerosis. However, in some walls there was segmental eosinophilic hyaline degeneration. At segment C6 (N7) there is a mild loss of AHCs with no cystic necrosis. The white matter is largely intact with some areas of vacuolation. The cord is deformed on one side indicating compression. At C8 (N8) there is vacuolation and a loss of AHCs. C8 (N8) shows pallor and loss of glia in both corticospinal tracts.

Weil Segments C2 (N2)- C8 (N8) are pale suggesting demyelination at these levels. There is no loss of myelin in the anterior corticospinal tract at any segment. At C2 (N2), C4 (N3), C5 (N4-6) and C6 (N7) there is a loss of myelin within the posterior columns.

Immunohistochemical results

CASE 2 – Compression C4/5 – Immunological positivity (+) in glial, axonal or neuronal profiles:

Level	APP	Casp-3	DNA- PKcs	PARP	Bcl-2	Fas	Casp-9	TUNEL	Amy-33	CMAP	AIF
C2	-	-	+	+	-	-	-	+	+	+	+
C4	-	-	+	+	-	-	-	+	-	+	+
C5	-	-	-	+	-	-	-	+	+	+	+
C6	-	-	-	+	-	-	-	+	+	+	+
C8	-	-	+	+	-	-	-	+	+	+	+

* Shaded rows represent the site of compression

APP There was no glial or neuronal immunopositivity using the APP antibody. Nonspecific immunopositivity was occasionally seen in the white matter of C5 (N4-6).

Active caspase-3 There was nonspecific immunopositivity of nuclei and smaller, unidentified structures in the posterolateral white matter at C4 (N3) and C5 (N4-6) along the border of necrotic areas. Neurons and axons were negative.

DNA-PKcs At the site of compression C5 (N4-6) occasional nuclear immunoreactivity was found near or surrounding necrotic regions. These cellular profiles were nonspecific and may have been lymphocytic. At segments C2 (N2) and C4 (N3) many immunopositive glia were homogeneously dispersed throughout the white matter. Occasional immunopositive glia were seen in segments C8 (N8). One immunopositive neuronal nucleus was seen in the anterior horn at C2 (N2). Axons were negative.

PARP Immunopositivity to PARP antibody in the nuclei of glia was seen in all segments throughout the white matter. Of these immunopositive cells, many profiles were present surrounding necrotic areas at C5 (N5 and N6). Cytoplasmic profiles were not clearly identified although the density, size and oval shape of many immunopositive nuclei suggest that these cells are oligodendrocytes. C6 (N7) showed rare PARP immunopositivity within the nucleolus of anterior horn neurons. Negative in axons.

Bcl-2 Neurons and axons were negative. There was occasional nonspecific cytoplasmic immunopositivity on the border of necrotic areas.

FAS Neurons and axons were negative. There was occasional nonspecific cytoplasmic immunopositivity on the border of necrotic areas.

Caspase-9 Neurons and axons were negative. There was occasional nonspecific cytoplasmic immunopositivity on the border of necrotic areas.

TUNEL Immunopositive glial profiles more numerous towards the deep white matter were visible above and below the lesion at C2 (N2) and C8 (N8)- T1 (N9). Occasional positive nuclear glial staining was found at C4 (N3) and C6 (N7). There was no glial immunopositivity at the site of compression. Immunopositivity to the TUNEL antibody was seen in neuronal nuclei throughout the grey matter in segments C2 (N2), C6 (N7), C8 (N8). There was also immunopositivity in the cytoplasm of neurons at these levels. TUNEL immunopositive neurons were found in the anterior horn of segments C4 (N3) and within one anterior horn of C5 (N5).

CMAP Immunopositivity was seen in glia, neurons, the majority of axons both small and large, and in ependymal cells. The degree of background staining negates the specificity of this marker at the dilution used.

Amy-33 amyloid-beta Non-specific immunopositivity was seen at C4 (N3) and C5 (N5, N6). Neuronal cytoplasmic immunopositivity was found at C2 (N2), C5 (N4) and C6 (N7). There was no immunopositivity within glia or axons. At C8 (N8) there was neuronal intracytoplasmic immunopositivity.

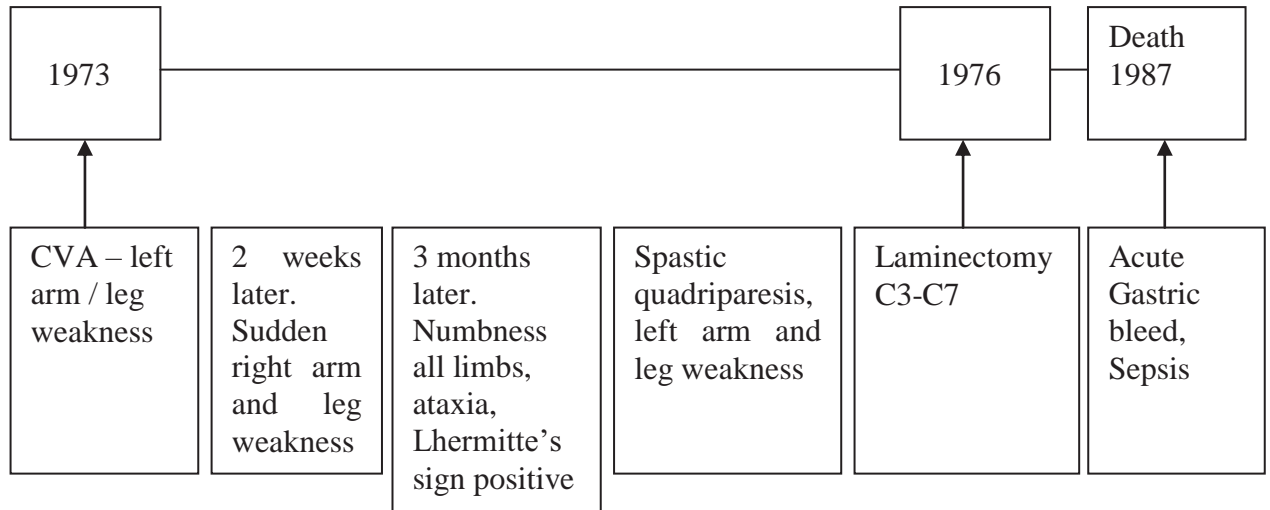
University of Melbourne amyloid-beta Negative.

DAKO amyloid-beta Negative.

AIF Above the site of compression at C2 (N2) there is occasional glial cytoplasmic immunoreactivity throughout the white matter. Immunopositive cytoplasmic staining was present in 5 AHCs on one side and 4 on the other. At the site of compression C5 (N4, 5) there is a greater number of immunopositive glia in the anterolateral cord and occasional immunopositive cells in the posterior columns. A significant number of immunopositive neurons are found in the preserved grey matter. At C6 (N7) there was glial immunoreactivity throughout the white matter greatest in the anterolateral cord. Neuronal cytoplasmic staining was present bilaterally. Rounded immunopositive profiles were rarely seen in the gracile fasciculi possibly axonal swellings but were non-specific. A similar pattern of staining was seen at C4 (N3) however there were fewer immunopositive glial profiles. At C8 (N8) cytoplasmic staining of glia is present throughout the

white matter. Rarely, immunopositive spheres possibly axonal swellings but non-specific were seen in the gracile fasciculus unilaterally. Neuronal immunopositivity is seen on both sides.

Timeline of clinical progression

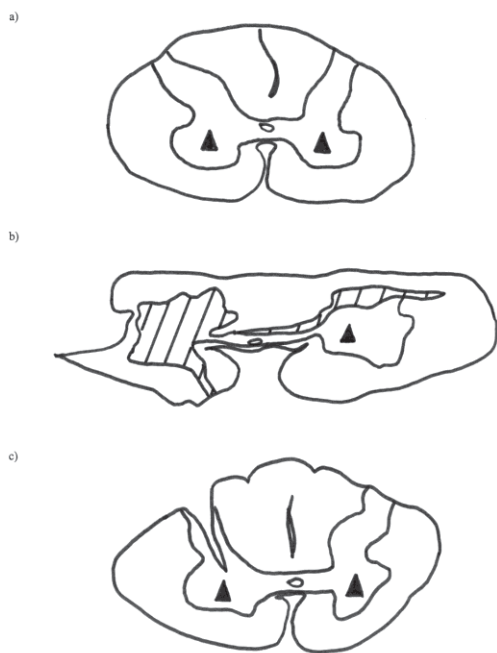


Spatial Distribution of Staining – Case 2

Case: 2
Amy-33

Levels:

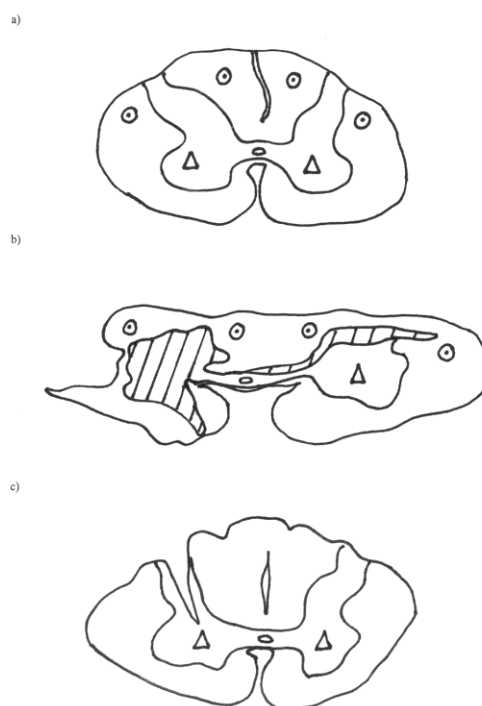
- a) Three levels above site - C2
- b) At the site of compression - C5
- c) Three levels below site - C8



Case: 2
Haematoxylin and eosin

Levels:

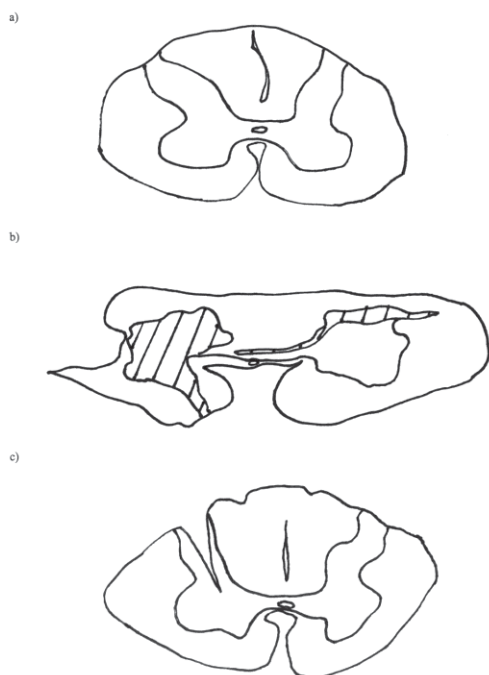
- a) Three levels above site - C2
- b) At the site of compression - C5
- c) Three levels below site - C8



Case: 2
APP

Levels:

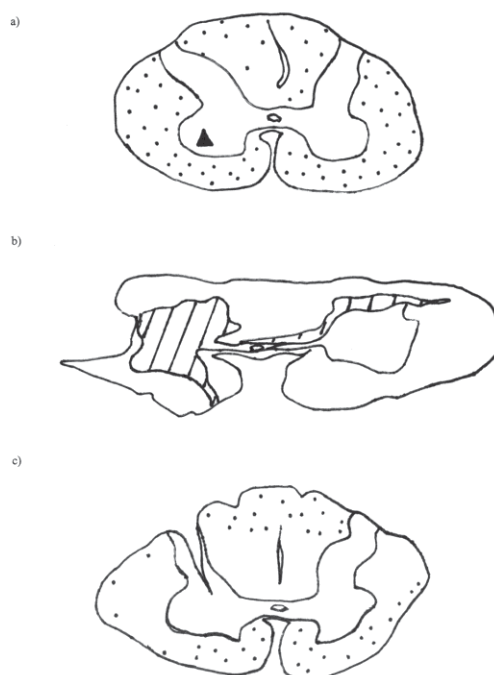
- a) Three levels above site - C2
- b) At the site of compression - C5
- c) Three levels below site - C8



Case: 2
DNA-PKcs

Levels:

- a) Three levels above site - C2
- b) At the site of compression - C5
- c) Three levels below site - C8



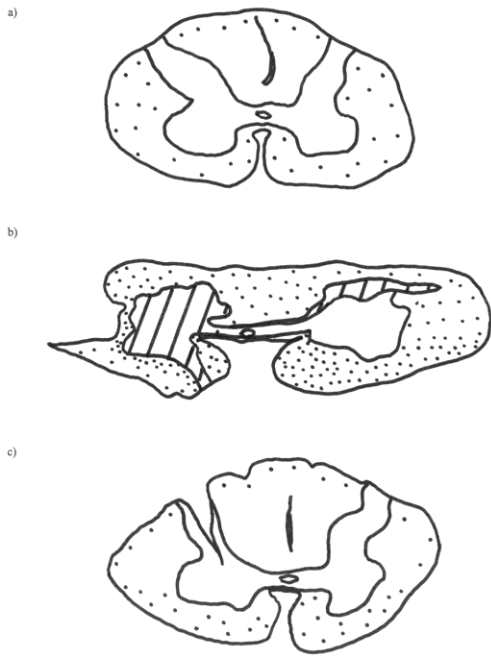
Spatial Distribution of Staining – Case 2

Case: 2

PARP

Levels:

- a) Three levels above site - C2
- b) At the site of compression - C5
- c) Three levels below site - C8

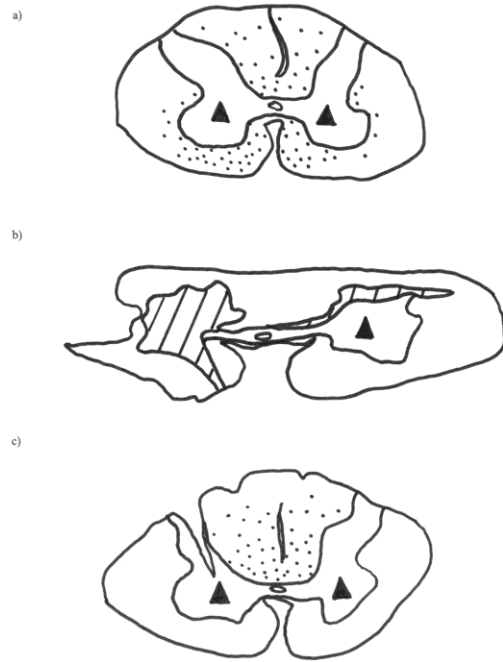


Case: 2

TUNEL

Levels:

- a) Three levels above site - C2
- b) At the site of compression - C5
- c) Three levels below site - C8

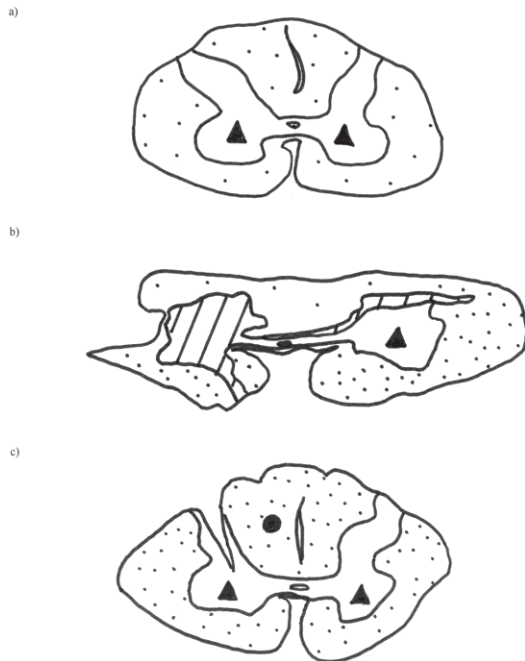


Case: 2

AIF 1

Levels:

- a) Three levels above site - C2
- b) At the site of compression - C5
- c) Three levels below site - C8



Summary of immunohistochemistry Case 2

Glia: DNA-PKcs, PARP, TUNEL, AIF, CMAP Axons: CMAP Neurons: TUNEL, AIF, DNA- PKcs, Amy-33, CMAP	C2	H&E: Posterolateral pallor, loss AHCs and glia Weil: pallor posterior columns
Glia: DNA-PKcs, PARP, TUNEL, AIF, CMAP Axons: CMAP Neurons: TUNEL, AIF, CMAP	C4	H&E: Posterolateral pallor, deformity, loss AHCs and glia, cystic cavitation LCST, lymphocytes, oedema, hyaline sclerosis Weil: pallor posterior columns
Glia: PARP, AIF, CMAP Axons: CMAP Neurons: TUNEL, AIF, Amy- 33, CMAP	C5	H&E: Distortion, Posterolateral pallor, loss AHCs and glia, cystic cavitation LCST, lymphocytes, oedema, hyaline sclerosis Weil: pallor posterior columns
Glia: PARP, TUNEL, AIF, CMAP Axons: CMAP Neurons: PARP, TUNEL, AIF, Amy-33, CMAP	C6	H&E: Distortion, Posterolateral pallor, loss AHCs, vacuolation, deformity Weil: pallor posterior columns
Glia: DNA-PKcs, PARP, TUNEL, CMAP Axons: CMAP Neurons: TUNEL, AIF, CMAP	C8	H&E: vacuolation, pallor, loss AHCs Weil: pallor

Conclusion Although the full clinical history is not known it is suggestive of ongoing cervical cord compression secondary to osteophytic spondylosis. The compression was sufficient to cause quadriparesis and sensory changes consistent with cervical myelopathy. Histologically, lymphocytic infiltration and necrosis also suggest the presence of chronic inflammation.

On histopathological examination of the spinal cord there was decreased Weil staining in the sensory tracts above, and motor tracts below the lesion indicating a demyelinating process or Wallerian degeneration of the axons in these regions. This finding correlated with an apparent loss of glia, possibly oligodendrocytes, in the posterolateral white matter. Examination was post-cervical laminectomy with dural scarring and subtotal necrosis of the cervical cord maximal at C5 level with secondary ascending and descending tract degeneration.

With each of the markers caspase-3, Bcl-2, Fas and caspase-9 there was occasional nonspecific cytoplasmic immunopositivity on the border of necrotic areas. At the site of compression, where necrosis was present, PARP and DNA-PKcs immunopositive glia were found on the border of

necrotic areas. This may have resulted from the tissue processing although there was minimal background immunopositivity in these regions. These profiles may alternatively represent foreign cells such as lymphocytes involved in the inflammatory process or they may indicate apoptotic glia within a 'penumbra' of relatively mild cytotoxic stress. Staining extended contiguously from the periphery of necrotic areas to the apparently normal neuropil.

TUNEL immunopositivity in neurons and glia was present above and below the site of compression. The reason for an absence of TUNEL staining at the site is unclear although it may be related to the loss of anterior horn cells shown using haematoxylin and eosin staining.

Amy-33 amyloid-beta immunopositivity was minimal and only present within the cytoplasm of anterior horn cells.

AIF immunopositivity was consistently present in glia and neurons. This staining was seen in profiles consistent with both oligodendrocytes and astrocytes and was without exception seen in the cytoplasm.

CASE 3

Clinical summary A 75 year-old male with ischaemic heart disease and atrial fibrillation who had died from cardiac failure. 22 years prior to death he underwent an anterior decompression and interbody fusion operation of C5-6 and C6-7 for cervical myelopathy. He had developed lumbar myelopathy and cauda equina compression. 12 years later he also underwent laminectomy of levels C3-6.

On autopsy, the vertebral column showed changes of severe osteoarthritis. There was severe degeneration of the intervertebral disc at C4-C5. An osteophytic protrusion measuring 8mm was present in the posterior spinal canal at this level. There was absence of the discs C5-6 and C6-7 and fusion of vertebral bodies. At C5-6 disc space there was an osteophytic protrusion and severe stenosis of the spinal canal to 6mm. Osteophytic lipping of several thoracic vertebrae was seen anteriorly as well as degeneration of thoracic discs and small protrusions posteriorly. The lumbar spine showed anterior osteophytic lipping and narrowing of the spinal canal. Anterior focal depression of the cord at C5, C6 and C7 existed as well as compression of C6 anterior nerve roots on the right side. The spinal cord was atrophic adjacent to the described osteophytic protrusions.

The microscopic examination revealed chronic denervation atrophy of left and right deltoid and vastus lateralis muscles. The C7 segment of spinal cord was deformed and showed loss of the normal architecture. Gliosis had replaced the posterior columns of the spinal cord. There was subtotal loss of anterior horn cells, particularly on the right side, and atrophy of the lateral columns on the right only. Degeneration of the descending motor tracts occurred below the lesion, and of the ascending sensory tracts above.

Pathology – brain

1. Old haemorrhagic infarction in the right parietal lobe.

Pathology – spine and spinal cord

1. Cervical myelopathy consistent with cervical spondylosis.

Haematoxylin and Eosin

Macroscopic findings On post-mortem examination there was a reportedly severe degeneration of the intervertebral disc separating C4 and C5 vertebral bodies with osteophytic protrusion (8mm) dorsally into the spinal canal. The intervertebral discs separating C5-6 and C6-7 were absent and the vertebral bodies fused. An osteophytic protrusion projected backwards into the spinal canal in

the proximate region where the C5-6 intervertebral disc would have been. The spinal canal showed severe narrowing at this point (AP diameter 6mm). Many of the thoracic discs showed evidence of degeneration with marked anterior osteophytic lipping and minor protrusions dorsally into the spinal canal. The lower lumbar spine showed severe anterior osteophytic lipping and the spinal canal was generally narrowed (spinal canal stenosis). External inspection of the spinal cord revealed a focal depression of the anterior spinal cord between C6 and C7 anterior nerve roots. The C6 anterior nerve roots on the right side were also compressed. A second compression was present on the anterior surface of the spinal cord between segments C5 and C6. The remainder of the spinal cord was externally normal. The anterior spinal artery was normal. Segmental sections of the spinal cord revealed artefactual laceration on the left side of the cord in the mid-cervical region and lumbosacral region. The right side of the spinal cord adjacent to the cervical osteophytic protrusions was atrophic.

Segment C3 (N12) is macroscopically normal. At segments C5 (N14, N15), C6 (N16) and C8 (N19) the spinal cord is divided, attributable to tissue processing. The spinal cord appears compressed at segment C7 (N17, N18). Segment T1 (N20) is macroscopically normal.

Left and right deltoid muscles showed severe chronic denervation atrophy.

Left and right vastus lateralis showed changes of denervation atrophy but less developed than in deltoids.

Microscopic findings Many corpora amylacea are present. At segments C3 (N12) there is a loss of anterior horn cells on one side and no other abnormalities. At C5 (N14, N15) there is compression and elongation of the grey matter associated with AHC loss. At C6 (N16) there is vacuolation within the ventral white matter and a paucity of glia in the lateral white matter. At C7 (N17, N18) there is loss of the normal architecture with subtotal destruction of the grey and white matter on one side with cystic cavitation and bilateral AHC loss. Gliosis was visible in the posterior column of section N18. There were no significant findings in segments C8 (N19) and T1 (N20).

Weil There was unilateral decreased staining of the lateral corticospinal tract below the lesion extending to C8 (N19) and of the posterior columns, particularly the gracile fasciculus, above the lesion consistent with Wallerian degeneration. Pallor of the gracile fasciculi was also seen at C3 (N12), C4 (N13), C5 (N14, N15), C6 (N16) and C7 (N17).

Immunohistochemical results

CASE 3 – Compression C4/5 and C5/6 – Immunological positivity (+) in glial, axonal or neuronal profiles:

Level	APP	Casp-3	DNA- PKcs	PARP	Bcl-2	Fas	Casp-9	TUNEL	Amy-33	CMAP	AIF
C3	-	-	+	+	-	-	-	+	+	+	+
C4	-	-	+	+	-	-	-	+	+	+	-
C5	-	-	+	+	-	-	-	+	+	+	+
C6	-	-	+	+	-	-	-	+	+	+	+
C7	-	-	+	+	-	-	-	+	+	+	+
C8	-	-	+	+	-	-	-	+	+	+	+
T1	-	-	+	+	-	-	-	+	+	+	+

* Shaded rows represent the site of compression

APP Negative for neurons, axons and glia.

Active caspase-3 Non-specific immunopositivity was present in cellular profiles on the edge of cystic cavities and extending into the neuropil at C7 (N18). There was no immunopositivity to the caspase-3 antibody within neurons or axons.

DNA-PKcs Nuclear immunopositivity within glial cells was found in the white matter of all segments. Positive glia were greater in number towards the periphery of the cord. Immunopositivity was present in the cytoplasm of mononuclear cells on the edge of cystic cavities and extending into the neuropil at C7 (N18). Rare immunopositive neuronal nuclei were seen in the anterior horn of C7 (N17) however this may be associated with cystic change in the area and artefactual immunopositivity. There was no immunopositivity to the DNA-PKcs antibody within axons.

PARP Nuclear glial immunopositivity to PARP antibody was found in the white matter of all segments. These cells appeared to have the morphology typical of oligodendrocytes. There was no immunopositivity within neurons or axons.

Bcl-2 There was no immunopositivity within neurons or axons. Cytoplasmic immunopositivity was rarely seen subpially glial profiles at C8 (N19) and T1 (N20).

FAS There was no immunopositivity within neurons or axons. Non-specific cytoplasmic immunopositivity was present in cellular profiles on the edge of cystic cavities and extending into the neuropil at C7 (N18).

Caspase-9 There was no immunopositivity within neurons or axons. Non-specific cytoplasmic immunopositivity was present in cellular profiles on the edge of cystic cavities and extending into the neuropil at C7 (N18).

TUNEL Neuronal nuclear immunopositivity for the TUNEL marker were found at C4 (N13) to C7 (N17) throughout the grey matter and in the anterior horn only in segment C3 (N12). Glial immunopositivity was seen throughout the white matter in segments C5-T1 (N14-N20) and in the posterior columns of segments C3 (N12) and C4 (N13).

CMAP Heterogeneous staining within all types of glia, neurons, ependymal cells and axons throughout the cord.

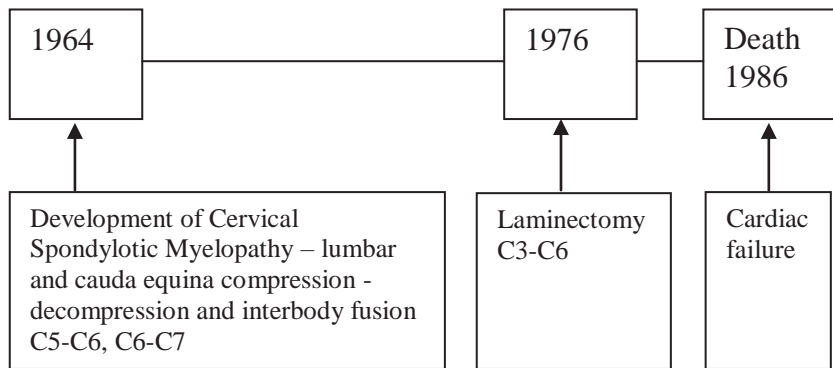
Amy-33 amyloid beta There is neuronal cytoplasmic and occasional glial immunoreactivity at C7, C8, T1 (N17, 18, N19, N20). At C3 (N12), C5 (N15), C6 (N16) there is neuronal cytoplasmic staining but otherwise negative. There are immunopositive axonal swellings at T1 (N20). At N18 there is immunopositivity in macrophages. Non-specific staining is seen at C4 (N13).

University of Melbourne amyloid-beta Negative.

DAKO amyloid-beta Negative.

AIF At C3 (N12), C6 (N16), C7 (N17) and T1 (N20) there is subpial immunoreactivity within the cytoplasm of glia. These cells showed morphology consistent with both oligodendrocytes and astrocytes. At C3, neuronal cytoplasmic immunopositivity is present in 7 neurons on one side and one anterior horn cell on the other. At the site of compression C6 (N16), and at C7 (N17), T1 (N20) there is cytoplasmic immunostaining in neurons bilaterally. There was no immunopositivity within axonal profiles. In section N18 of segment C7 immunopositivity was occasionally seen in glia where the white matter was preserved. No neuronal immunoreactivity occurred at this level likely due to necrosis of the grey matter. At C5 (N14, N15) occasional glial staining was seen in the subpial region. Neuronal immunopositivity was present in one anterior horn of section N14 and bilaterally at N15. In segment C4 (N13) neuronal cytoplasmic immunopositivity was visible. At C8 (N19) there was widespread glial, neuronal and axonal immunopositivity.

Timeline of clinical progression



Spatial Distribution of Staining – Case 3

Case: 3
Amy-33

Levels:

- a) Two levels above site - C3
- b) At the site of compression - C6
- c) Two levels below site - T1

a)



b)



c)



Case: 3
APP

Levels:

- a) Two levels above site - C3
- b) At the site of compression - C6
- c) Two levels below site - T1

a)



b)



c)



Case: 3
Haematoxylin and eosin

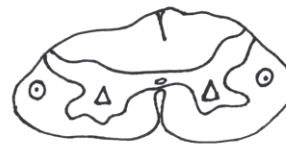
Levels:

- a) Two levels above site - C3
- b) At the site of compression - C6
- c) Two levels below site - T1

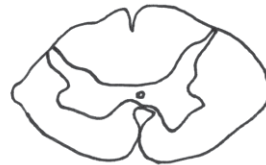
a)



b)



c)



Case: 3
DNA-PKcs

Levels:

- a) Two levels above site - C3
- b) At the site of compression - C6
- c) Two levels below site - T1

a)



b)



c)



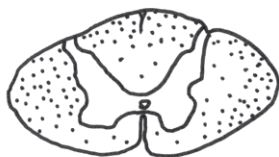
Spatial Distribution of Staining – Case 3

Case: 3
PARP

Levels:

- a) Two levels above site - C3
- b) At the site of compression - C6
- c) Two levels below site - T1

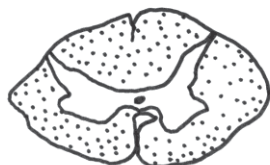
a)



b)



c)



Case: 3
TUNEL

Levels:

- a) Two levels above site - C3
- b) At the site of compression - C6
- c) Two levels below site - T1

a)



b)



c)



Case: 3
AIF 1

Levels:

- a) Two levels above site - C3
- b) At the site of compression - C6
- c) Two levels below site - T1

a)



b)



c)



Summary of immunohistochemistry Case 3

<p>Glia: DNA-PKcs, PARP, TUNEL, AIF, CMAP Axons: CMAP Neurons: TUNEL, AIF, CMAP, Amy-33</p>	C3	<p>H&E: loss AHCs Weil: pallor posterior columns</p>
<p>Glia: DNA-PKcs, PARP, TUNEL, CMAP Axons: CMAP Neurons: TUNEL, CMAP</p>	C4	<p>H&E: normal appearance Weil: pallor posterior columns</p>
<p>Glia: DNA-PKcs, PARP, TUNEL, AIF, CMAP Axons: CMAP Neurons: TUNEL, AIF, CMAP, Amy-33</p>	C5	<p>H&E: compression, loss AHCs Weil: pallor posterior columns</p>
<p>Glia: DNA-PKcs, PARP, TUNEL, AIF, CMAP Axons: CMAP Neurons: TUNEL, AIF, CMAP, Amy-33</p>	C6	<p>H&E: vacuolation Weil: pallor posterior columns</p>
<p>Glia: DNA-PKcs, PARP, TUNEL, AIF, Amy-33, CMAP Axons: CMAP Neurons: DNA-PKcs TUNEL AIF, Amy-33, CMAP</p>	C7	<p>H&E: Macroscopic distortion, cystic cavitation, AHC loss, gliosis Weil: pallor posterior columns</p>
<p>Glia: DNA-PKcs, PARP, AIF TUNEL, Amy-33, CMAP Axons: CMAP, AIF Neurons: Amy-33, CMAP, AIF</p>	C8	<p>H&E: normal appearance Weil: pallor LCST</p>
<p>Glia: DNA-PKcs, PARP, CMAP, Amy-33, TUNEL, AIF Axons: Amy-33, CMAP Neurons: AIF, Amy-33, CMAP</p>	T1	<p>H&E: normal appearance Weil: pallor LCST</p>

Conclusion Osteophytic stenosis of the cervical spinal canal resulted in chronic compressive myelopathy. An attempt at relieving this compression was twice undertaken. The success of each operation is unclear from the clinical summary although at autopsy the spinal cord was found to have a diameter of just 6mm and was atrophied. This may either indicate damage from the first compression or it may represent the development of a new stenosis and compressive myelopathy. The spinal cord segments below C7 (N19-N31) showed descending pyramidal tract degeneration (right greater than left) and ascending tract degeneration (loss of myelin staining posterior white

matter columns). The degenerative nature of compression is evident on Weil stain by a loss of myelin, anterior horn cell loss at several levels, gliosis and cystic cavitation. Furthermore, there was no evidence of axonal disruption on APP staining nor were there any axonal swellings on haematoxylin and eosin staining.

Glial immunopositivity was found using the markers of DNA damage, DNA-PKcs and PARP, across all segments. TUNEL positivity in glial nuclei was also seen above and below the compression however neuronal staining extending across several segments including the most severely affected regions. There were no significant findings for the Fas, Bcl-2, caspase-9 immunological markers. AIF immunopositivity was more common in the subpial region and was seen in profiles consistent with both oligodendrocytes and astrocytes. Staining in glia and neurons was only seen within the cytoplasm.

CASE 4

Clinical summary A 50 year-old male presenting with metastatic spinal cord compression secondary to oat cell carcinoma of the lung, progressing to paraplegia followed by death at 25 days. Other metastases were present in bone (right 4th rib) and liver. Examination of the spinal cord showed a single compression of the upper thoracic cord from a grey-white nodular tumour. The tumour involved the right vertebral body and paravertebral gutter. There was softening of the T2-T4 segments, most severe at T3. At the T3 spinal cord segment there was almost complete necrosis of the cord and infiltration by foamy macrophages, although there was no infiltration by tumour.

Pathology – brain

1. Normal brain.

Pathology – spine and spinal cord

1. Extradural tumour compression of upper thoracic spinal cord (T2-T4).
2. Complete spinal cord necrosis (compression) T2-T4.
3. Metastatic extradural undifferentiated small cell carcinoma.

Haematoxylin and Eosin

Macroscopic findings On post-mortem examination there was a grey-white nodular tumour compressing the upper thoracic spinal cord. Tumour involved the right paravertebral gutter and vertebrae. On opening the dura the T2-T4 spinal cord segments were softened maximal at the T3 segment where cross-section showed almost complete necrosis of the cord.

T2 (N1) appears macroscopically normal. At segment T3 (N2) there is pallor of the posterolateral white matter and this extends into the ventral white matter in section N3 (T3). The shape of T2 (N3) is not fully symmetrical but this does not necessarily represent compression. Segment T4 (N4) is fragmented throughout the cord, possibly artefact. T5 (N5) appears compressed on one side posterolaterally and is also fragmented.

Microscopic findings At segment T2 (N1) there is a mild loss of anterior horn cells, worse on one side. Occasional non-specific profiles are seen in the ventral white matter and may be axonal swellings. At T3 (N2) an invasion of macrophages is seen with sparing only of the ventral white matter. Vacuolation is throughout the cord. The vasculature is congested. There is a subtotal loss of anterior horn cells in N2 and total loss in section N3 (T3). There is complete necrosis of the grey and white matter of the spinal cord associated with numerous foamy macrophages. Small areas of

gliosis are seen. In regions where the white matter is preserved there are enlarged axons. At T4 (N4) the parenchyma is largely intact. Occasional foci of axonal swellings are seen throughout the cord and there is accompanying vacuolation. There is significant AHC loss. Within the central and posterior grey matter and deep posterior columns there is partial necrosis with macrophages and small areas of gliosis. At T5 (N5) there is a loss of AHCs. There is occasional vacuolation of the white matter which is worse in the lateral corticospinal tract corresponding to areas of axonal swellings and worse on one side.

The anterior and posterior nerve roots showed occasional axonal swellings, loss of myelin and vacuolation.

Weil There is a loss of myelin at the site of compression in areas of cystic change, axonal swellings and vacuolation however there is no apparent demyelination below the lesion.

Immunohistochemical results

CASE 4 – Immunological positivity (+) in glial, axonal or neuronal profiles:

Level	APP	Casp-3	DNA- PKcs	PARP	Bcl-2	Fas	Casp-9	TUNEL	Amy-33	CMAP	AIF
T2	+	+	-	+	-	-	-	+	+	+	+
T3	+	+	+	+	-	-	-	+	+	+	+
T4	+	+	+	+	-	-	-	+	+	+	+
T5	+	+	+	+	-	-	-	+	+	+	+

* Shaded rows represent the site of compression

APP Focal regions of axonal immunopositivity were seen in all sections, found in particular in the lateral and anterior corticospinal tracts and deep posterior columns. This was maximal at T3 (N2) to T4 (N4) and most severe in the area of the lateral corticospinal tract. APP axonal immunopositivity was occasionally found in the anterior and posterior nerve root however this was not apparent in all axonal swellings seen on haematoxylin and eosin staining. Cytoplasmic immunopositivity to glia was occasionally seen in sections T2 (N1) and T5 (N5).

Active caspase-3 At the site of compression and below many smaller and larger cellular profiles were observed suggestive of axons at T2 (N2), T4 (N4) and T5 (N5). These were greatest in number in regions of APP immunopositivity and axonal swellings. There were a greater number of

APP immunopositive large diameter axons than caspase-3, however the converse was true for small diameter immunopositive axons.

Cytoplasmic glial immunopositivity was seen in cellular profiles in the white matter at segments T2-T5 (N1, N3, N4, N5). Negative within neurons.

DNA-PKcs Occasional axonal swellings were immunopositive for DNA-PKcs at T3 (N2), T5 (N5), maximal at T4 (N4) in the lateral cord on both sides. Immunoreactive glial nuclei were seen occasionally throughout T5 (N5). Negative in neurons.

PARP In areas of white matter preservation PARP antibody was immunopositive in glial nuclei. PARP immunoreactivity is seen throughout the white matter at T2 (N1), T4 (N4) and T5 (N5) in the anterior cord only at T3 (N2). PARP immunopositive glia were rarely seen at T3 (N3) due to loss of tissue. The morphology of these cells was consistent was oligodendrocytes. PARP antibody was immunonegative for neurons.

Bcl-2 Negative.

Fas Negative.

Caspase-9 Negative.

TUNEL In areas of preserved white matter TUNEL was immunopositive in glial nuclei, in the anterolateral cord at T3 (N2), throughout T4 (N4) especially in the posterior columns, occasionally throughout the cord at T5 (N5) and maximally at T2 (N1) where staining was seen throughout the white matter, particularly in the posterior columns. TUNEL immunopositive macrophages were seen at T3 (N2) and T4 (N4). Negative for neurons and axons.

CMAP Many immunopositive glia, ependymal cells, neurons and axons were seen. This is combination with a strong background immunopositivity suggested the non-specificity of CMAP antibody at this dilution.

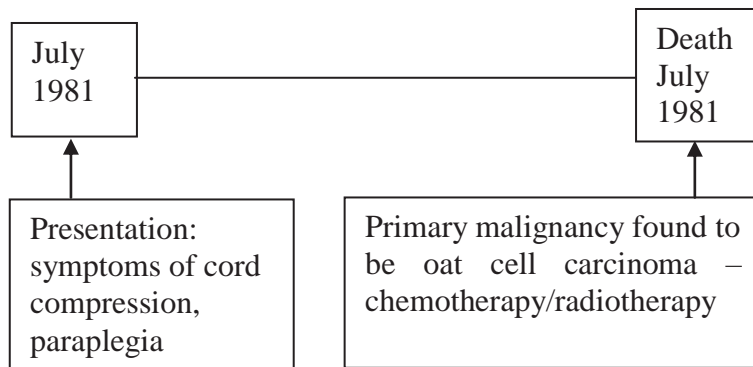
Amy-33 amyloid-beta Similar pattern of immunopositivity within axons to APP was seen using Amy-33 amyloid-beta antibody. However, there appeared to be a greater overall number of axons staining for Amy-33.

University of Melbourne amyloid-beta Negative.

DAKO amyloid-beta Negative.

AIF At T2 (N1, N2) there is neuronal and glial cytoplasmic staining in preserved regions and immunoreactivity in axonal swellings. At T3 (N3) immunopositive macrophages are seen throughout the necrosed cord. At T4 (N4) there was heterogeneous intracytoplasmic staining of glia and neurons, with axonal immunopositivity in normal and enlarged axons. At T5 (N5) there is neuronal and glial cytoplasmic staining throughout the cord and immunopositivity in axonal swellings.

Timeline of clinical progression



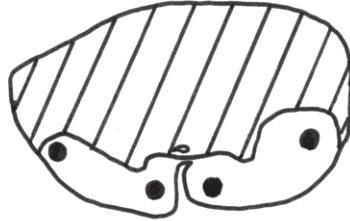
Spatial Distribution of Staining – Case 4

Case: 4
Amy-33

Levels:

- a) At the site of compression - T3
b) One level below site - T5

a)



b)

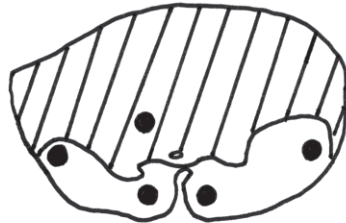


Case: 4
APP

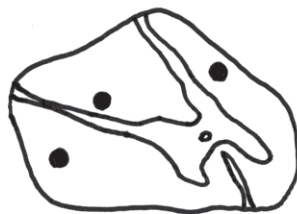
Levels:

- a) At the site of compression - T3
b) One level below site - T5

a)



b)

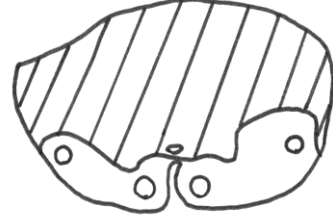


Case: 4
Haematoxylin and eosin

Levels:

- a) At the site of compression - T3
b) One level below site - T5

a)



b)



Case: 4
DNA-PKcs

Levels:

- a) At the site of compression - T3
b) One level below site - T5

a)



b)



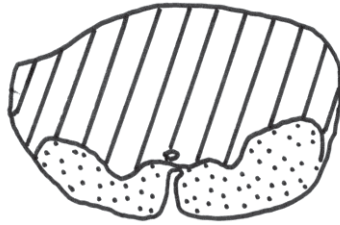
Spatial Distribution of Staining – Case 4

Case: 4
PARP

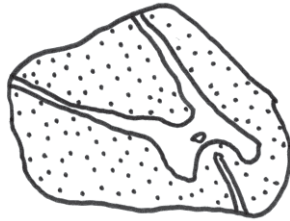
Levels:

- a) At the site of compression - T3
- b) One level below site - T5

a)



b)

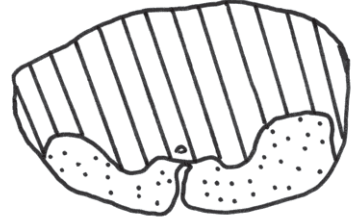


Case: 4
TUNEL

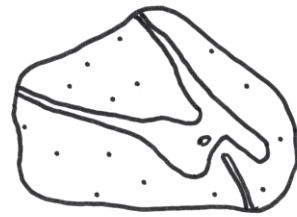
Levels:

- a) At the site of compression - T3
- b) One level below site - T5

a)



b)

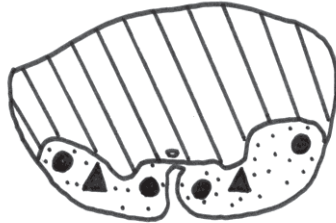


Case: 4
AIF 1

Levels:

- a) At the site of compression - T3
- b) One level below site - T5

a)



b)



Summary of immunohistochemical staining Case 4

<p>Glia: APP, PARP, TUNEL, caspase-3, AIF Axons: APP, caspase-3, Amy-33, caspase-3, AIF Neurons: AIF</p>	T2	<p>H&E: macroscopic asymmetry, AHC loss, tissue necrosis, vacuolation, congestion, gliosis Weil: patchy demyelination</p>
<p>Glia: PARP (rare), TUNEL, caspase-3 Axons: APP, DNA-PKcs, Amy-33 Neurons: Nil</p>	T3	<p>H&E: pallor.</p>
<p>Glia: PARP, TUNEL, caspase-3 Axons: APP, caspase-3, DNA-PKcs, Amy-33 Neurons: Nil</p>	T4	<p>H&E: Axonal swellings, AHC loss, tissue necrosis, gliosis Weil: patchy demyelination</p>
<p>Glia: APP, PARP, TUNEL, DNA-PKcs, AIF, caspase-3 Axons: APP, caspase-3, DNA-PKcs, Amy-33, AIF Neurons: AIF</p>	T5	<p>H&E: macroscopic asymmetry, AHC loss, vacuolation, axonal swellings</p>

Conclusion Malignant compressive myelopathy was greatest at the T3 segment although there was evidence on histopathological examination of injury to the T2 and T4 segments. This is reflected by the presence of tissue necrosis and patchy demyelination. APP positive axonal swellings are seen particularly in the anterior and lateral cord consistent with the patient's motor impairment. Caspase-3 and DNA-PKcs staining was present in axonal swellings suggesting a disruption of axonal transport and the accumulation of protein. Glial immunoreactivity using active caspase-3, DNA-PKcs, PARP and TUNEL antibodies suggests DNA-damage and potential caspase-dependent apoptotic processes. The presence of caspase-dependent apoptosis is not supported by caspase-9, Bcl-2 and Fas antibodies which were negative and therefore PARP, DNA-PKcs and TUNEL staining may represent non-apoptotic chromatinolysis. Amy-33 amyloid-beta antibody was positive in axonal swellings in a pattern similar to that of the APP antibody, supporting the hypothesis that amyloid-beta is a product of APP proteolysis. However, Amy-33 immunoreactivity was not found in the neuronal body, nor were alternative markers of amyloid-beta positive (DAKO and University of Melbourne antibodies). Therefore it is unlikely that amyloid-beta is a significant neurotoxic peptide in this case of malignant spinal cord compression.

CASE 5

Clinical summary A 75 year- old woman with disseminated malignant fibrous histiocytoma. This tumour metastasised to the vertebral column, resulting in an unstable crush fracture of T12 vertebra approximately 4 months before death. 1 month after the initial fracture the patient developed back pain and was immobilised for 8 weeks. Following this she experienced gradual development of paraparesis with incontinence until death. A myelogram showed a complete block at T12.

Stenosis of the dural sac was found adjacent to T12 vertebral body due to a plaque of hard, grey-white tissue. This tumour infiltrated into the dura mater, compressing the underlying conus medullaris and cauda equina. There was no evidence of tumour infiltration of the spinal cord. S1 segment and the conus medullaris showed patchy necrosis of white matter. This necrosis was greatest in the posterior columns of S1 segment.

Pathology – brain

1. Normal brain.

Pathology – spine and spinal cord

1. Multiple vertebral body metastases with pathological crush fracture of T12 vertebra.
2. Intradural metastatic tumour producing stenosis and compression of the underlying conus medullaris and cauda equina.
3. Compression myelopathy with patchy necrosis of the white matter, which in the S1 segment is most severe in the posterior white matter columns.

Haematoxylin and eosin

Macroscopic findings On post-mortem examination there was a crush fracture of T12 with almost complete necrosis and replacement of the vertebral body by grey-white tumour tissue. An irregular, firm, paraspinal tumour mass (60 x 50 x 20 mm) was present on both sides of the pathological crush fracture of T12. The anterior longitudinal ligament was still intact. There was no significant destruction of the spinal canal adjacent to the crush fracture. Multiple metastatic tumour deposits (5.0 to 20.0 mm) were present in other vertebral bodies (C7, T2, T7, T9 and L2).

The dural sac was stenosed in the lower thoracic region adjacent to the T12 vertebral body by a circumferential plaque of hard, grey-white tumour tissue that had infiltrated and expanded the dura mater. There was no tumour in macroscopic continuity between the vertebral body and the dura mater. This circumferential tumour stenosis (30 x 5 x 20 mm) compressed the underlying conus

medullaris and cauda equina nerve roots. The spinal cord was normal on section at multiple segmental levels.

Segment L5 (N12) is of normal macroscopic appearance. At S1 (N13) there is a mild distortion of the cord unilaterally in the posterolateral white matter and associated small cystic cavitation. The conus (N14) is of normal macroscopic appearance.

Microscopic findings Segment L5 (N12) appears normal except for the presence of multiple corpora amylacea which are spread throughout the cord. At S1 (N13) and the conus (N14, N15) cells with abundant cytoplasm suggestive of macrophages were seen. At S1 (N13) cystic cavitation was found in the posterior columns and extending partially into the posterior grey matter. The anterolateral white matter appeared relatively spared although there are early vacuolar changes. In addition, there were occasional rounded profiles with the appearance of axonal swellings.

Weil Macroscopically at L5 (N12) there is significant pallor of the posterior columns suggestive of a demyelinating process. This pallor is continued in S1 (N13) in addition to a generalised slight pallor of the cord. There is pallor in the posterolateral area of the conus at N14 and worsening to involve the entire conus at N15.

Immunohistochemical results

CASE 5 – Immunological positivity (+) in glial, axonal or neuronal profiles:

Level	APP	Casp-3	DNA- PKcs	PARP	Bcl-2	Fas	Casp-9	TUNEL	Amy-33	CMAP	AIF
L5	-	+	+	+	-	-	-	+	-	+	+
S1	+	+	+	+	-	-	-	+	+	+	+
conus	+	-	+	+	-	-	-	+	+	+	+

* Shaded rows represent the site of compression

APP L5 (N12) is immunonegative. At S1 (N13) there is a small focal region of axonal immunopositivity in the anterior corticospinal tract in axons of normal diameter. In the lateral regions there are scattered, rounded immunopositive profiles suggestive of axonal swellings or bulbs. There is a larger area of immunopositivity in the white matter surrounding both dorsal root entry zones (DREZ). These areas contain small and large diameter profiles, some likely to be axonal and some nucleated and more irregular with a morphology consistent with macrophages. A variable proportion of axonal swellings are immunonegative for APP marker. Occasional glial

immunopositivity is also seen and neuronal cytoplasmic positivity unilaterally. At the conus (N14) there is clear axonal immunopositivity of large and small diameter in the white matter surrounding the DREZ but no macrophages identifiable. Some non-specific immunopositivity is seen in the central grey matter and occasional glial and neuronal cytoplasmic staining. At the conus (N15) there are scattered immunopositive profiles consistent with glia as well as normal diameter and mildly enlarged diameter axonal profiles. Occasional neuronal cytoplasmic staining is present.

Active caspase-3 Cytoplasmic immunostaining was present in small cellular profiles with rounded nuclei. The staining was granular in appearance. These cells were found dispersed throughout the posterolateral white matter at L5 (N12) and less frequently through each region of the white matter at S1 (N13). At the conus (N14, N15) there was rare non-specific immunopositivity in the white matter. Negative for neurons and axons.

DNA-PKcs Occasional nuclear glial immunopositivity using DNA-PKcs marker was seen in the subpial white matter of segments L5 (N12), S1 (N13) and at the conus in N15 only. Negative for neurons. One large diameter immunopositive profile was seen at S1 (N13) which appears consistent with an axonal swelling or retraction bulb.

PARP Many glial nuclei with the morphology of oligodendrocytes were immunopositive using PARP in all regions of the white matter however numbers appeared fewer at L5 (N12) than at S1 and at the conus. Neuronal nuclear immunopositivity was seen in one anterior horn at S1 (N13) and in both anterior horns and one posterior horn at L5 (N12). Negative within axons.

Bcl-2 Negative.

Fas Negative.

Caspase-9 Negative.

TUNEL Nuclear and / or cytoplasmic immunopositivity was present in glia throughout the white matter at L5 (N12) and S1 (N13). Fewer immunopositive glial profiles were seen at the conus (N14, N15). Neuronal nuclear immunopositivity was seen in all regions of the grey matter at segment L5 (N12), and in the anterior horns and central grey matter at S1 (N13).

CMAP Axons of all sizes were immunopositive all segments. Ependymal and glial cytoplasmic immunopositivity was present in all sections. Immunopositive in neurons at the conus (N14, N15).

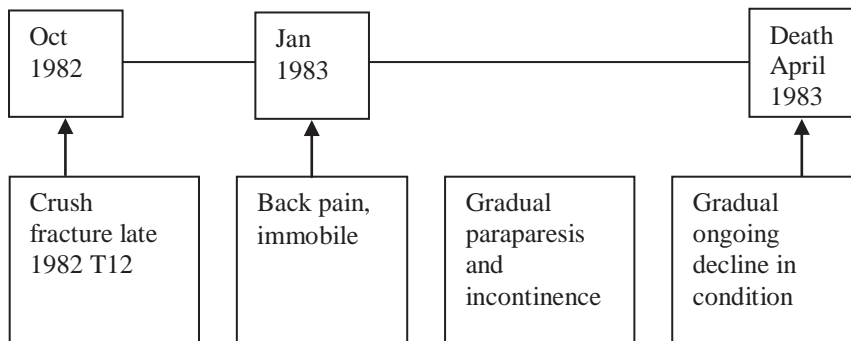
Amy-33 amyloid-beta Occasional, nonspecific immunopositivity in cellular profiles within white matter. Rare immunopositive neuronal cytoplasm at L5 (N12). At segment S1 (N13) and conus (N14, N15) axonal immunopositivity of small and large diameter axons is seen in areas surrounding the DREZ and in the anterior corticospinal tract and occasional glial profiles were immunopositive. Neuronal cytoplasmic staining is also present at S1 and particularly at the conus in greater numbers than at L5.

University of Melbourne amyloid-beta Negative.

Dako amyloid-beta Negative.

AIF At L5 (N12) there is neuronal and glial cytoplasmic immunopositivity throughout. At S1 (N13) there is glial and neuronal cytoplasmic staining throughout as well as axonal immunopositivity in normal and enlarged diameters axons. At the conus (N14, N15) there is neuronal and glial cytoplasmic immunopositivity throughout. No nuclear staining is seen.

Timeline of clinical progression

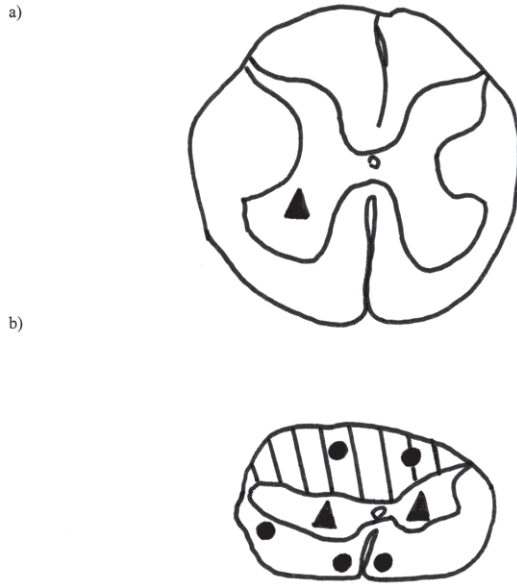


Spatial Distribution of Staining – Case 5

Case: 5
Amy-33

Levels:

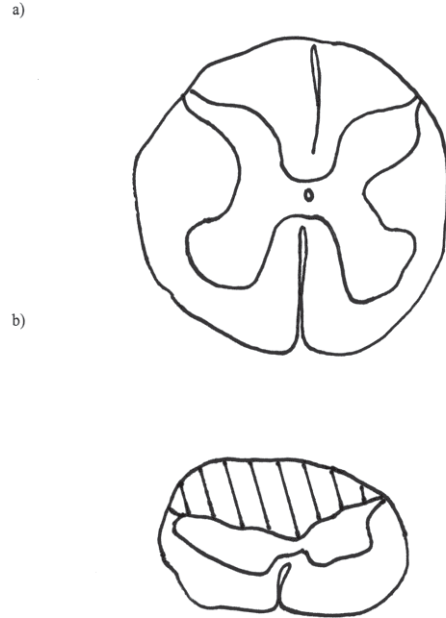
- a) One level above site - L5
- b) At the site of compression - Conus



Case: 5
Haematoxylin and eosin

Levels:

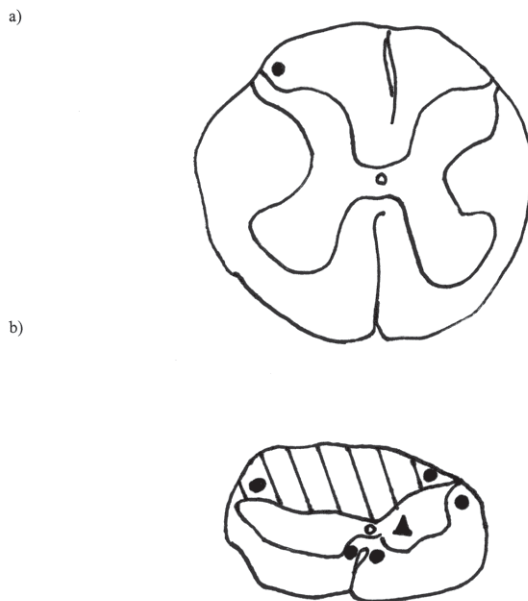
- a) One level above site - L5
- b) At the site of compression - Conus



Case: 5
APP

Levels:

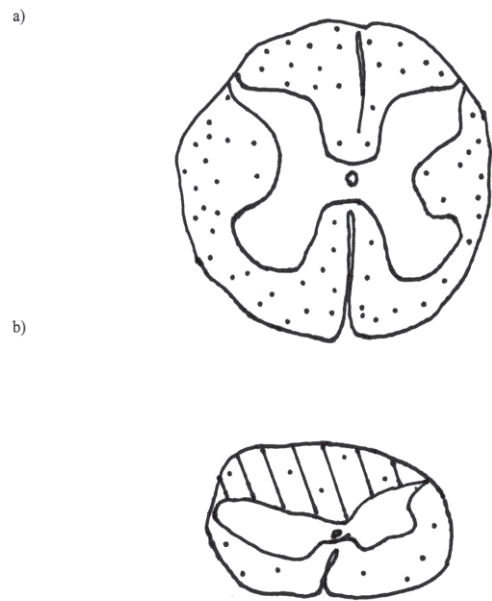
- a) One level above site - L5
- b) At the site of compression - Conus



Case: 5
DNA-PKcs

Levels:

- a) One level above site - L5
- b) At the site of compression - Conus

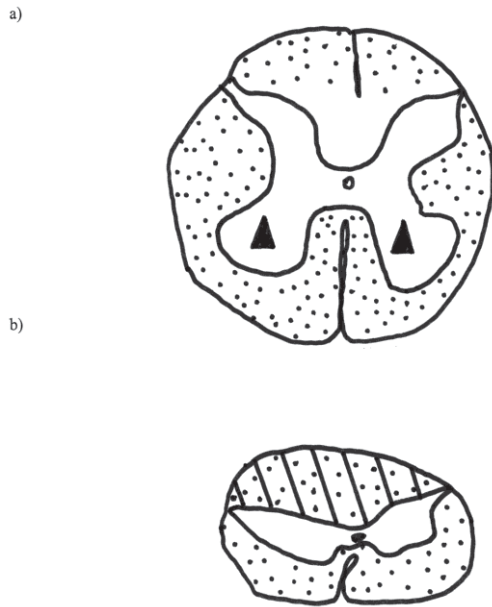


Spatial Distribution of Staining – Case 5

Case: 5
PARP

Levels:

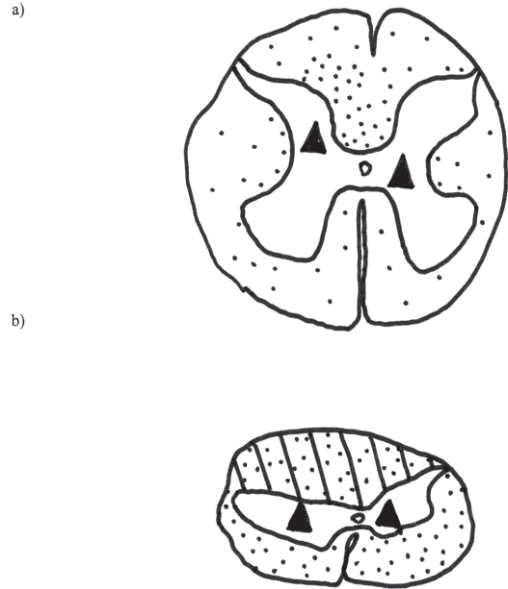
- a) One level above site - L5
- b) At the site of compression - Conus



Case: 5
TUNEL

Levels:

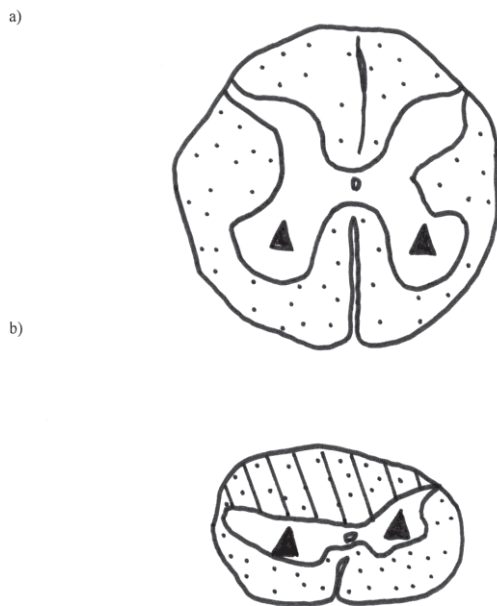
- a) One level above site - L5
- b) At the site of compression - Conus



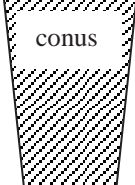
Case: 5
AIF 1

Levels:

- a) One level above site - L5
- b) At the site of compression - Conus



Summary of immunohistochemistry Case 5

<p>Glia: APP, caspase-3, DNA-PKcs, PARP, TUNEL, CMAP, AIF Axons: CMAP Neurons: TUNEL, PARP, Amy-33, AIF</p>	<p>L5</p>	<p>H & E: corpora amylacea. Weil: pallor within posterior columns</p>
<p>Glia: APP, caspase-3, DNA-PKcs, PARP, TUNEL, CMAP, AIF Axons: APP, DNA-PKcs, Amy-33, CMAP, AIF Neurons: APP, PARP, TUNEL, Amy-33, AIF</p>	<p>S1</p>	<p>H & E: corpora amylacea, macrophages, cystic change Weil: generalised pallor worse in posterior columns</p>
<p>Glia: APP, DNA-PKcs, PARP, TUNEL, AIF, CMAP Axons: APP, Amy-33, CMAP Neurons: APP, TUNEL, Amy-33, AIF, CMAP</p>	<p>conus</p> 	<p>H & E: corpora amylacea, macrophages Weil: generalised pallor worse in posterior columns</p>

Conclusion A 75 year old woman with intradural, extramedullary tumour compression of the conus medullaris and cauda equina. Pathological examination of the brain suggested no abnormality. The vertebral pathology includes acute injury from crush fracture at T12 and probable gradual onset, chronic compression from infiltrative histiocytoma neoplasm within the sub-dural space. In addition there was evidence of patchy necrosis and cellular damage secondary to compression at S1 segment just above the level of compression. Macrophages were seen in areas of cystic degeneration consistent with a chronic inflammatory process. Furthermore, the marker of acute apoptotic cell death, active caspase-3, was immunonegative. The small nature of these affected regions suggests a mild-moderate severity of compression.

APP axonal immunopositivity was found above the site of compression at S1 but where there was evidence also of cystic change. TUNEL and PARP immunostaining in glia and neurons also was maximal at this segment.

DNA-PKcs immunopositivity was found in fewer glia than PARP and was maximal at L5 and S1 segments. DNA-PKcs and PARP showed a subpial pattern of nuclear glial staining consistent with previous cases. PARP immunopositive glia maintained the morphology of oligodendrocytes, possible reflecting a subset of glia involved in the cell injury and remodelling process. TUNEL immunopositivity was maximal in the central cord. This may represent an ongoing pattern of DNA damage and subsequent cell death with remodelling in the peripheral white matter or more mildly affected regions.

CASE 6

Clinical summary A 79 year old man admitted from a rural centre with 6-week history of paresis of the right side, developing on the left side, with increasing pain (present for 6 months). There was an erosive lesion of C3-5 with cord compression and paralysis of the chest wall. No treatment was indicated due to severe chronic obstructive airways disease resulting in development of total right hemiplegia and left paresis.

There were features of chronic obstructive airways disease (emphysema, bronchitis – acute and chronic) with a left upper lobe scar carcinoma. No tumour was present within the liver, kidneys, adrenals or the prostate. There were extensive left-sided pleural plaques but no ferruginous bodies or tumours were located in these fibrotic regions.

Pathology – brain

1. Normal brain.

Pathology – spine and spinal cord

1. Cervical cord compression by extradural tumour C3 level. Extradural metastatic adenocarcinoma producing compressive cervical myelopathy.

Haematoxylin and Eosin

Macroscopic findings On post-mortem examination there was white tumour infiltration of the laminae and spinous process of C3 vertebra, but little involvement of the vertebral body. The tumour encircled the dura of the cord at this level and was larger on the right side. Cross sections showed that the main mass of tumour (25 x 20 x 20 mm) was present on the right side and had compressed and displaced the spinal cord to the opposite side of the dural sheath. The tumour had invaded the dura and this layer could not be macroscopically distinguished. The level of compression encompassed C2-C5 segments. The remainder of the spinal cord was macroscopically normal. Intradural invasion by a tumour is seen at segments C2-C5 (N20-N27). The tumour load is greater to one side. Asymmetry, assumed to be compression of the spinal cord is visible at C2-C6 (N19-N26).

Microscopic findings Adenocarcinoma is seen bordering but not invading the cord at segments C2-C5 (N20-N27). Occasional corpora amylacea were seen. There is mild vacuolation of the subpial region in section N27 of segment C2 and loss of anterior horn cells (AHCs) however this is more severe in section N26 (C2). At this level there are many axonal swellings and vacuolative

changes of the posterolateral cord on one side. There is also a loss of AHCs, worse on the same side. The grey matter appears compressed and there is morphological evidence of central chromatolysis of neurons. At C3-C5 there are similar changes and clear central chromatolysis is seen at C4 (N23) and C5 (N21). At section N20 (C5) the changes are less severe with smaller foci of axonal swellings and mild-moderate vacuolation of the white matter. There is a relative sparing of AHCs. At C6 (N19) and C7 (N18) there is mild vacuolation but no other significant changes except red cell change within occasional neurons.

Weil There is patchy demyelination of swollen axons in sections N20-N26 however there are no demyelination changes of motor and sensory tracts consistent with Wallerian degeneration.

Immunohistochemical results

CASE 6 – Immunological positivity (+) in glial, axonal or neuronal profiles:

Level	APP	Casp-3	DNA- PKcs	PARP	Bcl-2	Fas	Casp-9	TUNEL	Amy-33	CMAP	AIF
C2	+	+	-	+	-	-	-	+	+	+	+
C3	+	+	-	+	-	-	+	+	+	+	+
C4	+	+	+	+	-	-	-	+	+	+	+
C5	+	+	-	+	-	-	+	+	+	+	+
C6	+	-	-	+	-	-	-	+	+	+	+
C7	-	-	-	+	-	-	-	+	+	+	+

* Shaded rows represent the site of compression

APP Macroscopically visible axonal immunopositivity is seen in segments C2-C5 (N22-23, N25-26). In section N21 (C5) there is macroscopically visible foci in the anterior and lateral columns, the posterior and lateral columns at N24 (C3), and the lateral column only at N20 (C5). All other white matter columns of the above segments contained axonal immunopositivity which was not macroscopically visible. Axonal positivity occurred in the anterolateral region at N27 (C2) in many fewer axons than at the above levels. Non-specific, rare staining was found at C6 and C7 (N18-N19). Occasional glial cytoplasmic immunopositivity is present at C6 (N19). Negative in neurons.

Active caspase-3 Equivocal immunopositivity is present in axonal swellings at C2-C5 (N21-N26) and rarely there is convincing staining of axons. There was occasional non-specific staining within

the neuropil. Cytoplasmic immunopositivity is seen in unidentified cells of the white matter in C5 (N21, N22). Negative in neurons.

DNA-PKcs Equivocal immunopositivity is seen in glia and axons of segment C2-C5 (N20-N26). Occasional positive glial nuclei are seen at C4 (N23) in one posterior column and in the lateral subpial region. Rarely, positive axonal swellings are seen at C4 (N23) in the lateral cord on one side. Negative in neurons.

PARP Immunopositive glial nuclei are dispersed throughout the white matter of all segments and have the morphology suggestive of oligodendrocytes. Neuronal nucleoli are immunopositive in the anterior horn of segments C2-C5 (N20-N27) and in the posterior horn of segments C2-C4 (N23-N27). Negative in axons.

Bcl-2 Negative.

Fas Negative.

Caspase-9 Negative in glia and neurons. Equivocal immunostaining in axonal swellings except rarely immunopositive axons at C5 (N21) and C3 (N25).

TUNEL Glial nuclear immunopositivity was in all segments but maximal towards the centre of the cord. Greatest numbers of positive glia were found in section N26 (C2), the posterolateral cord at N18-23 (C4-C7) but particularly on one side of the cord at C3-C5 (N21-N23). Axonal immunopositivity in areas of greatest tissue disruption and axonal swellings such as C2 (N26). Neuronal immunopositivity is seen in anterior and posterior horns at C2, C4, C5, C6, C7 (N27, N23, N20, N19, N18) and in the anterior and posterior horn unilaterally in section N25 of C3.

CMAP Immunopositivity was seen in glia, the majority of axons both small and large, and in ependymal cells. The degree of background staining negates the specificity of this marker at the dilution used.

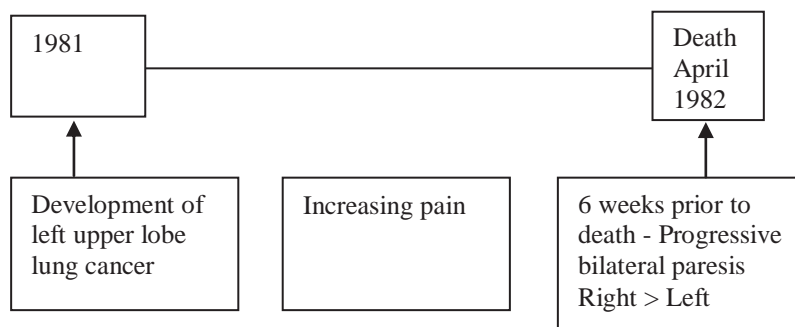
Amy-33 amyloid beta Immunopositivity in axonal swellings is seen in all segments in regions which were also immunopositive for APP. Amy-33 marker stained a greater number of small and large diameter axons than did the APP marker. Immunonegative axons were also present in these regions. Neuronal cytoplasmic immunopositivity was present at C2 (N26, N27), C4 (N23) and C5 (N21) and was equivocal in other segments. Negative in glia.

University of Melbourne amyloid beta At segment C2 (N26) there is equivocal staining within axonal swellings and one axon with convincing staining. However, the moderate level of background staining may account for this immunopositivity.

DAKO amyloid beta Negative at segment C2 (N26).

AIF At C2 (N26), C3 (N24, N25) and C4 (N23) there is axonal immunopositivity in focal regions throughout the white matter and scattered glial cytoplasmic immunopositivity. There is immunopositivity within the neuronal cytoplasm. At C5 (N20, N21, N22) a similar pattern of staining was seen however there were fewer numbers of immunopositive axons and glia. At C6 there is glial cytoplasmic immunopositivity, particularly in the subpial region and neuronal cytoplasmic staining. At C7 (N18) there is occasional glial, astrocytic and oligodendroglial, immunopositivity in the subpial region otherwise negative.

Timeline of clinical progression



Spatial Distribution of Staining – Case 6

Case: 6
Amy-33

Levels:

- a) At the site of compression - C4
b) Two levels below site - C7

a)



b)



Case: 6
APP

Levels:

- a) At the site of compression - C4
b) Two levels below site - C7

a)



b)



Case: 6
Haematoxylin and eosin

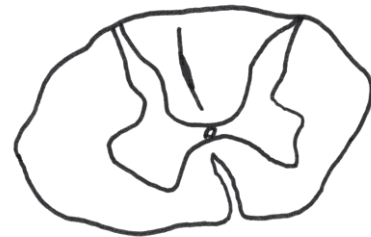
Levels:

- a) At the site of compression - C4
b) Two levels below site - C7

a)



b)



Case: 6
DNA-PKcs

Levels:

- a) At the site of compression - C4
b) Two levels below site - C7

a)



b)



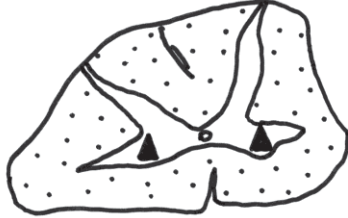
Spatial Distribution of Staining – Case 6

Case: 6
PARP

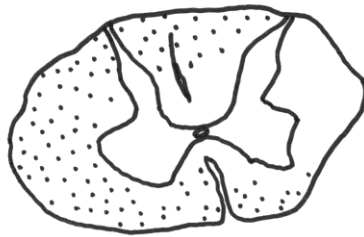
Levels:

- a) At the site of compression - C4
- b) Two levels below site - C7

a)



b)

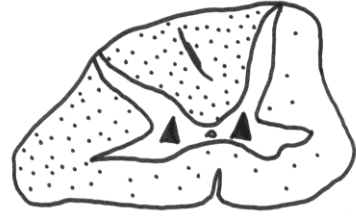


Case: 6
TUNEL

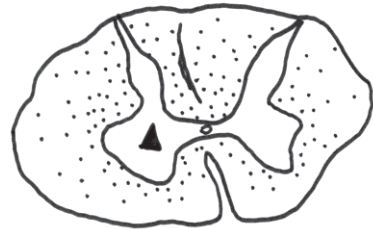
Levels:

- a) At the site of compression - C4
- b) Two levels below site - C7

a)



b)



Case: 6
AIF 1

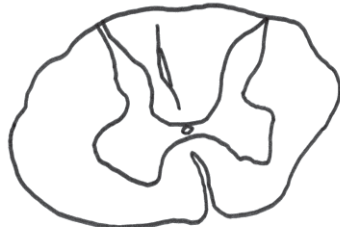
Levels:

- a) At the site of compression - C4
- b) Two levels below site - C7

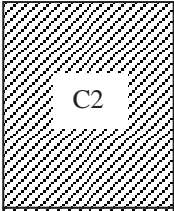
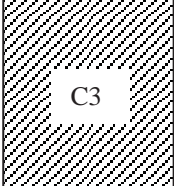
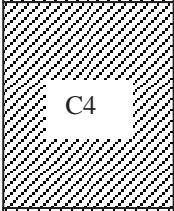
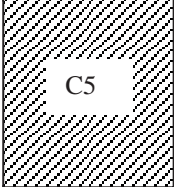
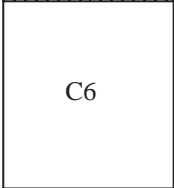
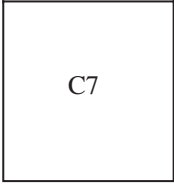
a)



b)



Summary of immunohistochemistry Case 6

<p>Glia: PARP, TUNEL (max), AIF, CMAP Axons: APP (max), Amy-33, AIF, caspase-3, CMAP Neurons: PARP (max), Amy-33, TUNEL, AIF</p>	 <p>C2</p>	<p>H&E: Tumour, vacuolation, axonal swellings, loss AHCs, central chromatolysis.</p>
<p>Glia: PARP, TUNEL (max), AIF, CMAP Axons: APP (max), caspase-9, AIF, Amy-33, caspase-3, CMAP Neurons: PARP (max), TUNEL, AIF</p>	 <p>C3</p>	<p>H&E: Tumour, vacuolation, axonal swellings, loss AHCs, central chromatolysis.</p>
<p>Glia: DNA-PKcs, PARP, AIF, TUNEL (max), CMAP Axons: APP (max), DNA-PKcs, AIF, Amy-33, caspase-3, CMAP Neurons: PARP (max), Amy-33, AIF, TUNEL</p>	 <p>C4</p>	<p>H&E: Tumour, vacuolation, axonal swellings, loss AHCs, central chromatolysis.</p>
<p>Glia: PARP, TUNEL (max), AIF, CMAP Axons: APP, caspase-9, Amy-33, caspase-3, CMAP, AIF Neurons: PARP, Amy-33, TUNEL</p>	 <p>C5</p>	<p>H&E: Tumour, vacuolation, axonal swellings, loss AHCs, central chromatolysis.</p>
<p>Glia: APP, PARP, TUNEL (max), CMAP, AIF Axons: Amy-33, CMAP Neurons: TUNEL, AIF</p>	 <p>C6</p>	<p>H&E: mild vacuolation, red cell change</p>
<p>Glia: PARP, TUNEL (max), AIF, CMAP Axons: Amy-33, CMAP Neurons: TUNEL</p>	 <p>C7</p>	<p>H&E: mild vacuolation, red cell change</p>

Conclusion Compression in this case was by an intradural, extramedullary tumour with the primary most likely lung carcinoma (poorly differentiated adenocarcinoma). A loss of anterior horn cells and axonal swellings at the site of compression suggest significant damage, and red cell change supports an ischaemic component. APP immunopositivity in axonal swellings was also maximal at the site of compression, suggesting significant axonal injury. TUNEL was maximal at the site in glia and PARP maximal at the site in neurons, suggesting DNA-damage. In support of this, DNA-PKcs was present in glia only at the site of compression. Amy-33 amyloid-beta antibody showed a similar pattern of staining to APP in axonal swellings but was surprisingly present in a greater number of axonal profiles. This was in contrast to staining using other antibodies to amyloid-beta which were negative and thus the Amy-33 antibody may be non-specific.

CASE 7

Clinical summary A 59 year-old man with a 2-month history of left lumbar back pain, sharp in nature which came on after manual labour and radiated to the flank. Investigations showed collapse of the T11 vertebral body and a T11 paraspinal mass metastasised from osteogenic sarcoma. 1 month later the patient experienced rapidly worsening paraparesis to almost complete paraplegia in 3 days. A course of chemotherapy was given. The patient died 6 days later of bronchopneumonia.

The T12 spinal cord segment showed slight anterior indentation. At L2 and L3 levels there was patchy necrosis in a posterolateral distribution with axonal swellings. The central grey matter showed oedema and there was anterior horn cell loss and acute ischaemic cell change of residual neurons. Oedema was found in the posterior columns of T10-T12.

Pathology – brain

1. Normal brain.

Pathology – spine and spinal cord

1. Subtotal pressure necrosis of lumbar spinal cord.

Haematoxylin and eosin

Macroscopic findings On post-mortem examination there was a paraspinal tumour mass 160 x 50 x 30 mm situated on the left side of T11 vertebra. Longitudinal section of the spine showed collapse of T11 body which had been destroyed by the tumour. The spinal cord was displaced posteriorly by the collapsed vertebra.

All segments are macroscopically normal except for L3 (N4) which shows cystic cavitation of the lateral white matter on one side.

Microscopic findings Many corpora amylacea are seen within the white matter. At T10 (N6) there is a loss of anterior horn cells but no other abnormalities. Segment T11 (N5) appears normal. At segment T12 (N1) there is one axonal swelling in the cuneate fasciculus on one side. At L1 (N2) there is one axonal swelling in the lateral white matter, loss of AHCs and vacuolation in the posterior columns. At L2 (N3) and L3 (N4) many axonal swellings are seen posterolaterally in focal regions. There is extensive patchy necrosis of the white matter in the lateral and posterior columns with the formation of numerous axonal retraction bulbs. The central grey matter is oedematous and scattered anterior horn cells show “acute ischaemic cell change”. There is

vacuolation throughout the white matter and cystic change laterally but no loss of AHCs. Central chromatolysis is seen in segments L2 (N3), L3 (N4) and T11 (N5). There is red cell change in the anterior horn at segment T10 (N6), T11 (N5) and L1 (N2) suggesting a possible ischaemic component.

Weil There was no pallor of Weil staining and no evidence of a demyelinating process.

Immunohistochemical results

CASE 7 – Immunological positivity (+) in glial, axonal or neuronal profiles:

Level	APP	Casp-3	DNA-PKcs	PARP	Bcl-2	Fas	Casp-9	TUNEL	Amy-33	CMAP	AIF
T10	+	-	+	+	-	-	-	+	+	+	+
T11	+	-	+	+	-	-	-	+	+	+	+
T12	+	-	+	+	-	-	-	+	+	+	+
L1	+	-	+	+	-	-	-	+	+	+	+
L2	+	+	+	+	-	-	-	+	+	+	+
L3	+	+	+	+	-	-	-	+	+	+	+

* Shaded rows represent the site of compression

APP Axonal immunopositivity was present throughout the white matter in a focal pattern at segments L1 (N2) - L3 (N4), and rarely in the posterolateral white matter at T11 (N5) and T12 (N1). Neuronal immunopositivity as found at segments T10 (N6), T11 (N5) and L3 (N4). Rare glial cytoplasmic staining at L1 (N2).

Active caspase-3 Axonal immunopositivity using caspase-3 antibody was occasionally present in the most severely damaged regions of the white matter at L2 (N3) and L3 (N4). Negative for neurons and glia.

DNA-PKcs Axonal immunopositivity using DNA-PKcs antibody was occasionally present in the most severely damaged regions of the white matter at L2 (N3) and L3 (N4). Immunopositivity to glial nuclei was seen across all segments. Negative for neurons.

PARP Immunopositivity to glial nuclei was seen across all segments. Neuronal immunopositivity was present within the posterior horn only at segments T10 (N6) on one side and both at T12 (N1),

within both anterior and posterior horns at L1 (N2) and T11 (N5), and anterior horn only at L3 (N4).

Bcl-2 Negative.

Fas Negative.

Caspase-9 Negative for glia and neurons. Rare equivocal immunopositivity seen within axons at L2 (N3) and L3 (N4) in the most severely damaged lateral regions of the white matter.

TUNEL Neuronal immunopositivity was found in all the posterior horn of all segments, in the anterior horn of T12 (N1) to L3 (N4), and in the central grey matter of T10 (N6) and L3 (N4). Glial nuclear immunopositivity was found across all segments and close to the grey matter. Immunopositive profiles suggestive of axonal swellings were seen but the morphology was equivocal.

CMAP All segments showed glial cytoplasmic and nuclear immunopositivity, however a sub-population were immunonegative that was difficult to distinguish morphologically. There is also staining within the majority of axons at all segments, including those which are apparently morphologically normal and in axonal swellings. A sub-population of axons were negative. There was a generalised, non-specific staining within the neuropil which may account for the above immunopositivity. Negative in neurons T10 (N6) and L1 (N2) to L3 (N4) but there was rare neuronal cytoplasmic immunopositivity at T11 (N5) and T12 (N1).

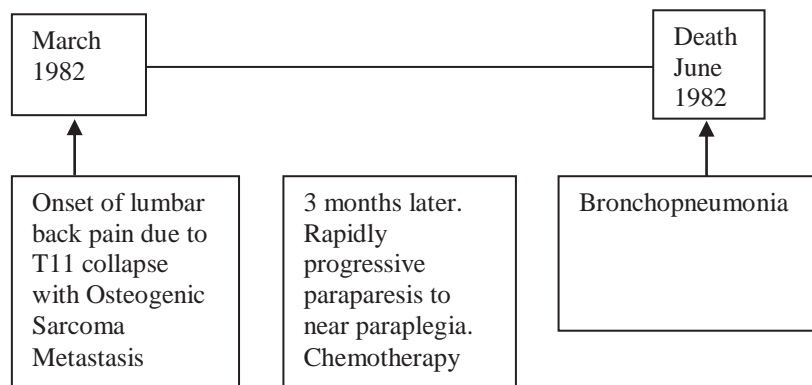
Amy-33 amyloid beta There was nuclear and cytoplasmic neuronal immunopositivity in the anterior horn at T10 (N6) and L2 (N3), neurons of anterior and lateral horn T11 (N5) and L3 (N4), anterior and posterior horn L1 (N2), and all regions of the grey matter at T12 (N1). There was occasional non-specific staining within the neuropil. At T12 (N1) non-specific rounded immunopositive profiles were seen in the white matter. At L3 (N4) and L2 (N3) there was axonal immunopositivity throughout the white matter in focal regions and this occurred in many axons of both small and large diameter. Few axons were immunonegative in the histologically abnormal regions. At L1 (N2) there was isolated axonal immunopositivity spread throughout the white matter but one focal region within the medial posterior white matter unilaterally. Occasional cytoplasmic glial immunopositive profiles were seen in all segments.

University of Melbourne amyloid-beta Immunopositivity was rarely seen in axonal swellings at segment L3 (N4). No other segments were stained.

DAKO amyloid-beta Negative at L3 (N4). No other segments were stained.

AIF In all segments there is glial and neuronal cytoplasmic immunopositivity in all areas of the white and grey matter respectively. Glial staining is present in both oligodendrocytes and astrocytes. Foci of axonal immunopositivity in normal and enlarged diameter axons are seen at L2-3 (N3, N4) in regions immunopositive for the APP antibody. Negative axonal profiles are also present.

Timeline of clinical progression



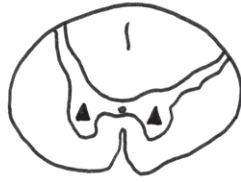
Spatial Distribution of Staining – Case 7

Case: 7
Amy-33

Levels:

- a) Two levels above site - T10
- b) At the site of compression - T12
- c) Two levels below site - L2

a)



b)



c)



Case: 7
Haematoxylin and eosin

Levels:

- a) Two levels above site - T10
- b) At the site of compression - T12
- c) Two levels below site - L2

a)



b)



c)

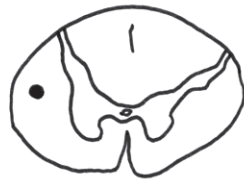


Case: 7
APP

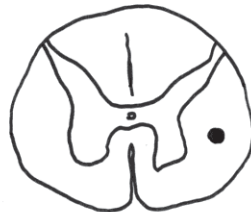
Levels:

- a) Two levels above site - T10
- b) At the site of compression - T12
- c) Two levels below site - L2

a)



b)



c)

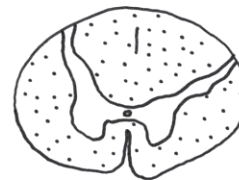


Case: 7
DNA-PKcs

Levels:

- a) Two levels above site - T10
- b) At the site of compression - T12
- c) Two levels below site - L2

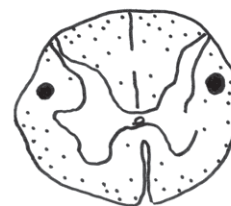
a)



b)



c)

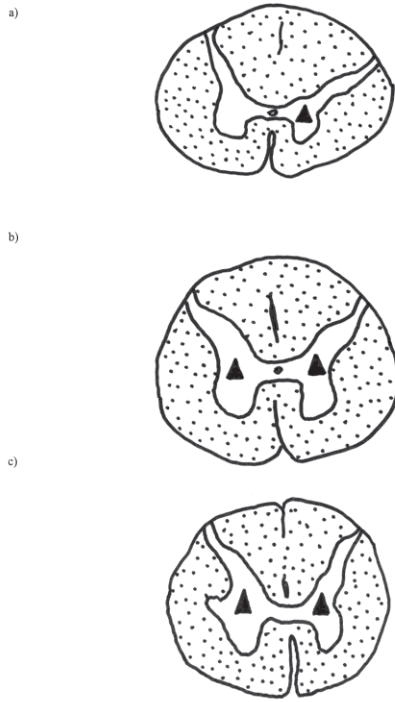


Spatial Distribution of Staining – Case 7

Case: 7
PARP

Levels:

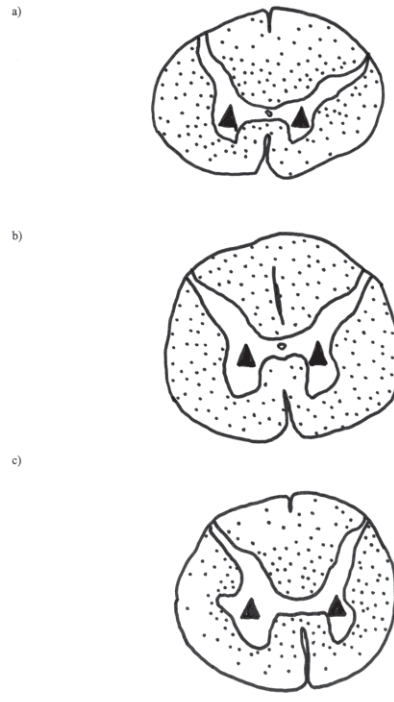
- a) Two levels above site - T10
- b) At the site of compression - T12
- c) Two levels below site - L2



Case: 7
TUNEL

Levels:

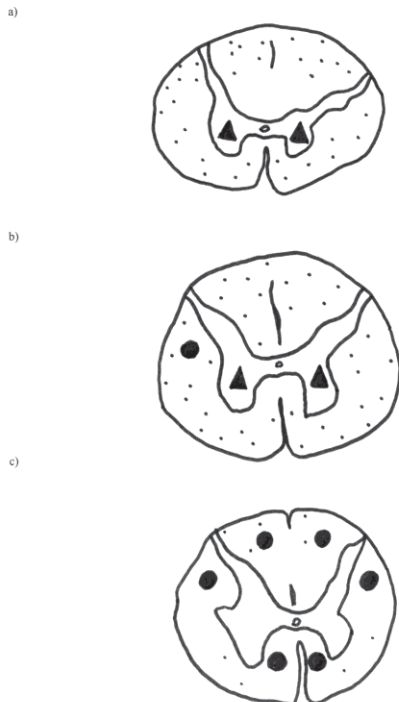
- a) Two levels above site - T10
- b) At the site of compression - T12
- c) Two levels below site - L2



Case: 7
AIF 1

Levels:

- a) Two levels above site - T10
- b) At the site of compression - T12
- c) Two levels below site - L2



Summary of immunohistochemistry Case 7

Glia: PARP, DNA-PKcs, TUNEL, Amy-33, CMAP, AIF Axons: CMAP Neurons: PARP, APP, TUNEL, Amy-33, AIF	T10	H&E: AHC loss, red cell change
Glia: PARP, DNA-PKcs, TUNEL, Amy-33, CMAP, AIF Axons: APP, CMAP Neurons: PARP, APP, TUNEL, Amy-33, CMAP, AIF	T11	H&E: Red cell change, central chromatolysis
Glia: PARP, DNA-PKcs, TUNEL, Amy-33, CMAP, AIF Axons: APP, CMAP Neurons: PARP, TUNEL, Amy-33, CMAP, AIF	T12	H&E: Axonal swellings
Glia: PARP, DNA-PKcs, APP, AIF, TUNEL, Amy-33, CMAP Axons: APP, Amy-33, CMAP Neurons: PARP, TUNEL, Amy-33, AIF	L1	H&E: Axonal swellings, loss of AHCs, red cell change
Glia: PARP, DNA-PKcs, TUNEL, Amy-33, CMAP, AIF Axons: DNA-PKcs, APP, caspase-3, Amy-33, CMAP, AIF Neurons: TUNEL, Amy-33, AIF	L2	H&E: Axonal swellings central chromatolysis, necrosis
Glia: PARP, DNA-PKcs, TUNEL, Amy-33, CMAP, AIF Axons: DNA-PKcs, APP, caspase-3, Amy-33, CMAP, AIF Neurons: PARP, APP, TUNEL, Amy-33, AIF	L3	H&E: Cystic necrosis, axonal swellings central chromatolysis, necrosis

Conclusion There is evidence on postmortem examination of compression of the spinal cord secondary to an extradural neoplasm with slight anterior indentation at T12 segment correlating to a collapsed T11 vertebra. In addition, the severity of changes found on histological examination, and the presence of red cell change in some neurons suggest a probable ischaemic component to the pathophysiology. It is likely that with the deterioration over 9 days and the necrotic and axonal injury changes on histology that this may be classified as a subacute event.

Immunohistochemical staining showed many APP positive axons and enlarged axons, either bulbs or swellings, at the site of injury. A subset of enlarged axons were also immunopositive for caspase-3 antibody which may represent the co-localisation of protein within the damaged axon

secondary to disrupted axonal transport. It is not known whether there is any molecular interaction between APP and caspase-3 at the site of accumulation. Many axons were immunopositive to the Amy-33 amyloid-beta but not to the DAKO or University of Melbourne amyloid beta antibodies. These axons were present in the same regions as those immunopositive to APP and thus the Amy-33 staining may be non-specific, staining only those axons which are APP positive. Alternatively it may indicate the break-down of APP into amyloid-beta peptides as originally suggested. The Amy-33 antibody immunolabels a smaller region on the amyloid-beta peptide than DAKO or UM antibodies which label the whole 4-42 amino acid amyloid beta peptide, and therefore there is the potential for cross-reaction with different antigens.

PARP and TUNEL immunopositivity to glia and axons was found, TUNEL within more medial glia and PARP in glia of the subpial region. Furthermore, PARP appeared to immunolabel a sub-population of glia with morphology similar to oligodendrocytes. Both markers were immunopositive in neurons at the site of the lesion and above. This result may indicate a separate process from the axonal pathology given that glia and neurons were immunonegative to caspase-3.

CASE 8

Clinical summary A 74 year-old male with increasing left-sided neck pain, reported 11 months prior to his death. He was admitted with a wedge fracture of T8 with 30% reduction in height centrally and anteriorly. Radiology of the cervical spine showed widespread degenerative change, facet joint degeneration, disc space narrowing, particularly in the inferior levels of the cervical spine. Osteophyte formation was also noted.

At autopsy, a right ventral dural plaque was observed at the level of C5 covering an area of 15mm in length and width by 2mm height. T4-T6 levels were indurated. Histology showed patchy leptomeningeal infiltration at C2-T12 levels by metastatic squamous cell carcinoma.

Pathology – brain

1. Swollen brain with cerebellar tonsillar necrosis.
2. Plaque jaune inferior frontal lobe.
3. Hypoxic / ischaemic encephalopathy with pseudolaminar cortical accentuation.
4. Raised intracranial pressure with cerebellar tonsillar necrosis.
5. Incidental Lewy body disease.
6. Old plaque jaune left inferior frontal lobe.

Pathology – spine and spinal cord

1. Extramedullary subdural mass of abnormal tissue of the left ventral proximal cord.
2. Intramedullary nodule of plaque tissue at T9-T10.
3. Fibrous dural plaque at C5 level.
4. Induration and pallor of the cord at T4-T6 levels.
5. Meningeal carcinomatosis (squamous cell carcinoma) involving predominantly the spinal cord including multifocal intramedullary spinal cord extension.

Haematoxylin and Eosin

Macroscopic findings On post-mortem examination there was an extramedullary subdural mass over the ventral surface of haemorrhagic and yellow tissue measuring 75 x 20 mm extending from the proximal margin. In addition there was a right ventral dural plaque at the level of C5 composed of fibrous white tissue extending over an area of 15 mm in diameter and up to 2 mm in height. The cord at the level of T4 to T6 appeared externally to have an indurated and white appearance which may be artefact. At the level of T9 to T10 there was a pale intramedullary nodule 4 mm in diameter.

Asymmetry and distortion of the cord is evident in all sections. In segments C4, C5, C6 and C8 (N35-N38) the cord appears compressed.

Microscopic findings C2-C8 cervical spinal cord segments (N32-N37): there is patchy leptomeningeal infiltration by metastatic squamous cell carcinoma including subdural infiltration and tumour infiltration of the dura mater. A multitude of corpora amylacea are seen dispersed throughout the cord but greatest in number around vessels. At C3 (N34) tumour is seen to infiltrate the posterior columns and extending into the posterior sulcus. Vacuolation and axonal swellings are visible throughout the white matter and neuronal red cell change. At C4 (N35) there is mild to moderate vacuolation of the white matter. At C5, C6, C8 (N37) occasional axonal swellings and vacuolation can be seen in the subpial region. The grey matter appears elongated or compressed at C6, C5.

T1-T12 thoracic spinal cord segments (N40-N52): patchy leptomeningeal and subdural infiltration by metastatic squamous cell carcinoma. Intraparenchymal cord invasion in segments N42, N48, N49, N50 with destruction of half of the spinal cord. There is tumour bordering cord segment T2 (N41) and moderate vacuolation with occasional axonal swellings. At T3 (N42) invasive tumour is seen within the entire posterior and part of the lateral cord in addition to vacuolation and foci of axonal swellings. There is extensive loss of grey matter replaced by the tumour. Segments T9 (N48) and T10 (N50) show posterolateral tumour invasion. At T7 (N46), T8 (N47), T9 (N48), T10 (N50) and T12 (N52) vacuolation and occasional axonal swellings are present throughout the white matter. At T11 (N51) mild vacuolation only is present, nil other significant. At L5 (N57) tumour is seen invading into the posterior white matter. There are vacuolative changes and occasional axonal swellings throughout the white matter. There is anterior horn cell loss at C3, C4 (N35), T2, T3, T7, T8, T10.

Weil Occasional pallor seen on Weil stain appears due to either to vacuolative changes, invasive tumour or corpora amylacea within the white matter. There is no evidence on microscopic analysis of demyelination of axons associated with Wallerian degeneration.

Immunohistochemical results

CASE 8 – Immunological positivity (+) in glial, axonal or neuronal profiles:

Level	APP	Casp-3	DNA- PKcs	PARP	Bcl-2	Fas	Casp-9	TUNEL	Amy-33	CMAP	AIF
C3	+	-	+	+	+	-	-	+	+	+	+
C4	+	+	+	+	-	-	-	-	+	+	+
C5	+	+	+	+	+	-	-	-	+	+	+
C6	+	+	+	+	+	-	-	-	+	+	+
C7	+	+	+	-	-	-	-	-	+	+	+
C8	+	+	+	-	-	-	-	-	+	+	+
T2	+	+	+	+	-	-	-	-	+	+	+
T3	+	+	+	+	-	-	-	-	+	+	+
T7	+	+	+	+	-	-	-	-	+	+	+
T8	+	+	+	+	-	-	-	-	+	+	+
T9	+	+	-	+	-	-	-	-	+	+	+
T10	+	+	+	+	-	-	-	-	+	+	+
T11	+	+	+	+	-	-	-	-	+	+	+
T12	+	+	+	+	-	-	-	+	+	+	+
L5	+	-	-	+	-	-	-	-	+	+	+

* Shaded rows represent the site of compression

APP Cytoplasmic neuronal staining is seen in all segments. Immunonegative in glia. Segment C3 (N34) shows focal areas of axonal immunopositivity in small and large diameter axons. These regions include the deep posterior columns and subpial anterolateral white matter. C4 (N35) and C5 (N36) segments have rarely present immunopositive axonal swellings. C6 (N37) was immunonegative. At C8 (N38) there are occasional positive large axons. At T2 (N41) focal regions of axonal staining occur in the lateral corticospinal tracts and dorsal root entry zone unilaterally. There are also occasional positive axons dispersed throughout the white matter. At level T7 (N46) there are again isolated positive axons but in addition one focus of staining in the gracile fasciculus unilaterally. At T8 (N47) immunopositive axonal swellings are rarely seen in the white matter. At T9 (N48) and T10 (N50) positive axons are dispersed throughout the white matter but greater in number along the border of the invasive tumour and in the anterior corticospinal tracts especially on one side. At T11 (N51) and T12 (N52) there is again a foci of staining in the anterior corticospinal tract but otherwise axonal immunopositivity is rarely seen. At L5 (N57) occasional axonal positivity was present in the anterior corticospinal tracts.

Active caspase-3 At T3 there was immunopositivity in axonal swellings in regions also immunopositive for APP. Fewer axons were immunopositive at T2 (N41). Equivocal neuronal cytoplasmic immunopositivity was found in segments T7-T8 (N46, N47) and T10-T12 (N50-N52) however this may also be accounted for by the background staining.

DNA-PKcs Equivocal neuronal immunopositivity was seen in T10-T12 (N50-N52). In these neurons the presence of both cytoplasmic and nuclear staining may indicate a non-specific reaction. However, one unequivocally immunopositive neuronal nucleus was seen at T12 (N52) and at segment T2 (N41) several nuclei were positive in the anterior horn on one side. Neurons were immunoreactive in the posterior horn and central grey at T7 (N46). At C8 (N38) immunopositive neuronal nuclei were seen in the anterior horn. A proportion of axonal swellings were immunopositive in segment T3 (N42) especially within the anterior white matter. Glial nuclear immunopositivity was present in the subpial region at C3-C6 (N34-N37), occasionally in the subpial and grey matter at C8 (N38) and T9 (N48) and may be non-specific due to its location at the edge of the tissue. At C8 (N38), T2 (N41), T7-T8 (N46-N47) and T10-T12 (N50-N52) the staining is more homogeneous. T3 (N42) and L5 (N57) are immunonegative within glia.

PARP Glial nuclei were immunopositive in all segments dispersed throughout the white matter. The morphology was suggestive of oligodendrocytes. Many equivocally staining glia were also seen. Neuronal nuclei and prominent nucleoli were immunopositive in neurons of all segments except T2-T3 (N41-N42). Immunopositive neurons were unilateral at T7 (N46). The PARP marker did not show any positive staining in axons.

Bcl-2 Equivocal glial staining in the subpial region. Immunopositive glial cell in white matter at C3 (N34), C5 (N36), C6 (N37). Negative in axons and neurons.

Fas Equivocal glial staining in subpial region. Rare equivocal staining in axons. Negative in neurons.

Caspase-9 Equivocal glial and rare axonal staining subpial region. Negative in neurons.

TUNEL One immunopositive neuronal nucleus was seen at T12 (N52) and at C3 (N34) otherwise the TUNEL marker was immunonegative in neurons. Non-specific immunopositivity in white matter bordering the tumour at T9 (N48) and T10 (N50) and there was glial immunoreactivity found in the central grey and surrounding white matter unilaterally at T12 (N52). Negative in axons.

CMAP Immunopositivity was seen in glia, neurons, the majority of axons both small and large, and in ependymal cells. The degree of background staining negates the specificity of this marker at the dilution used.

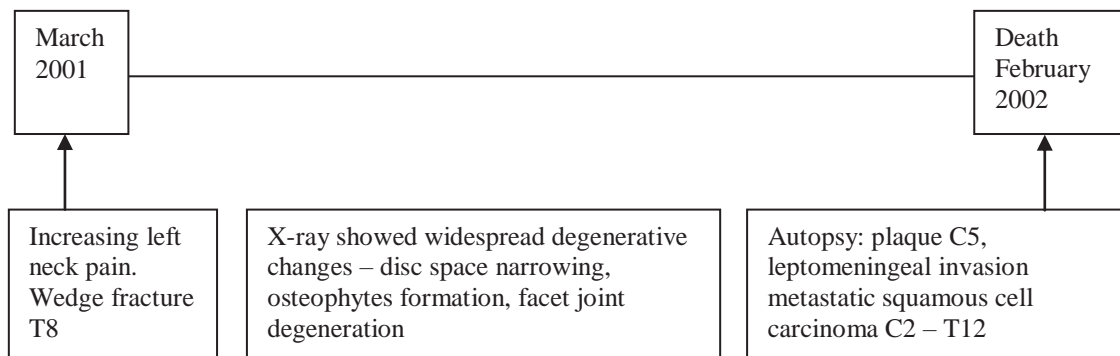
Amy-33 amyloid beta Immunopositivity in axonal swellings is seen in all segments in regions which were also immunopositive for APP. Amy-33 marker stained a greater number of small and large diameter axons than did the APP marker. Immunonegative axons were also present in these regions although these were rare. Cytoplasmic and occasionally nuclear immunopositivity was seen within neurons in all segments which were stained using Amy-33 amyloid-beta antibody.

University of Melbourne amyloid beta Negative.

DAKO amyloid beta Negative.

AIF In all segments many glia showed granular immunopositivity within the cytosol. There was also neuronal and ependymal cytoplasmic staining in all segments. There was no immunopositivity within axonal profiles.

Timeline of clinical progression

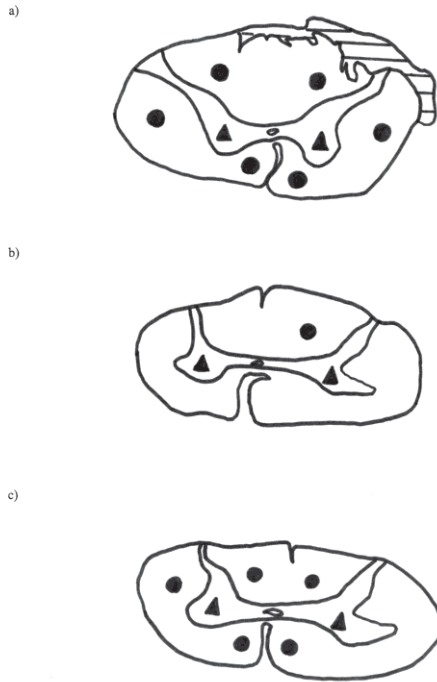


Spatial Distribution of Staining – Case 8

Case: 8a (first compression at C5)
Amy-33

Levels:

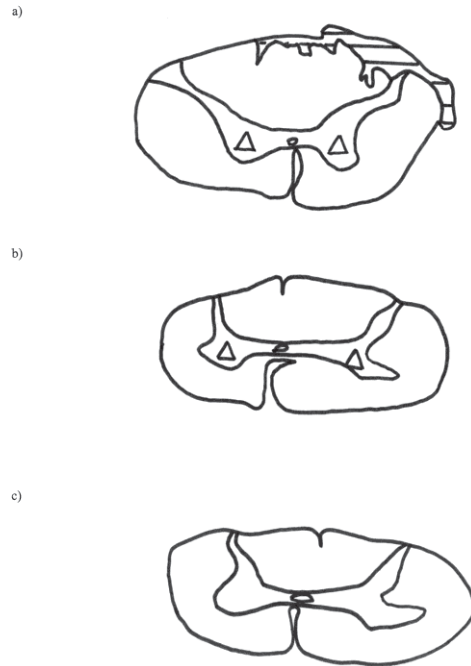
- a) Two levels above site - C3
- b) At the site of compression - C5
- c) Three levels below site - C8



Case: 8a (first compression at C5)
Haematoxylin and eosin

Levels:

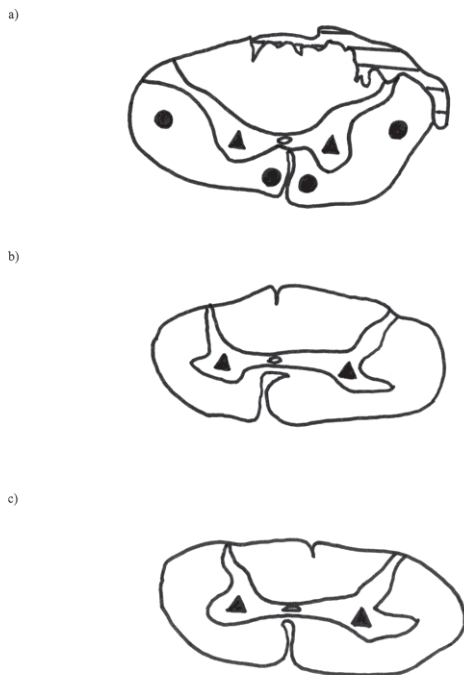
- a) Two levels above site - C3
- b) At the site of compression - C5
- c) Three levels below site - C8



Case: 8a (first compression at C5)
APP

Levels:

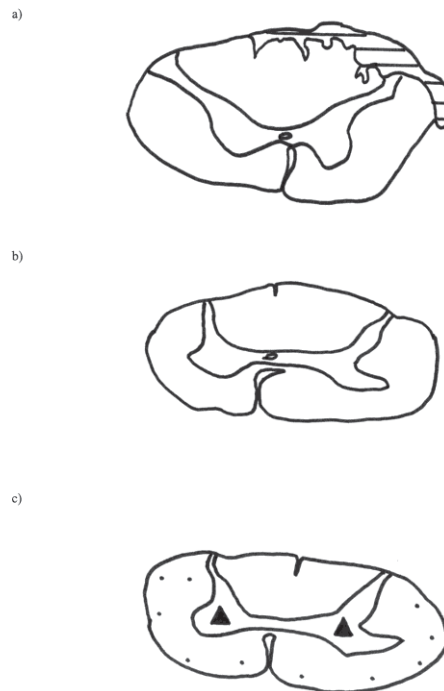
- a) Two levels above site - C3
- b) At the site of compression - C5
- c) Three levels below site - C8



Case: 8a (first compression at C5)
DNA-PKcs

Levels:

- a) Two levels above site - C3
- b) At the site of compression - C5
- c) Three levels below site - C8

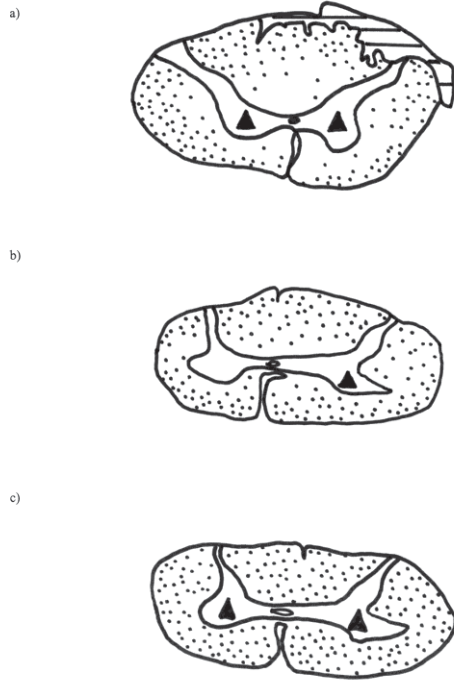


Spatial Distribution of Staining – Case 8

Case: 8a (first compression at C5)
PARP

Levels:

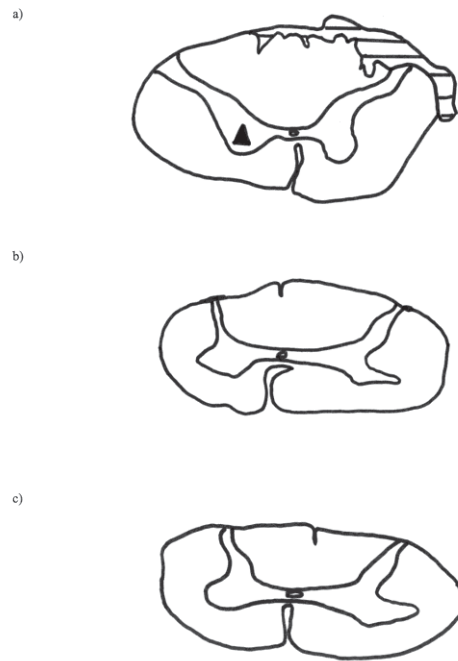
- a) Two levels above site - C3
- b) At the site of compression - C5
- c) Three levels below site - C8



Case: 8a (first compression at C5)
TUNEL

Levels:

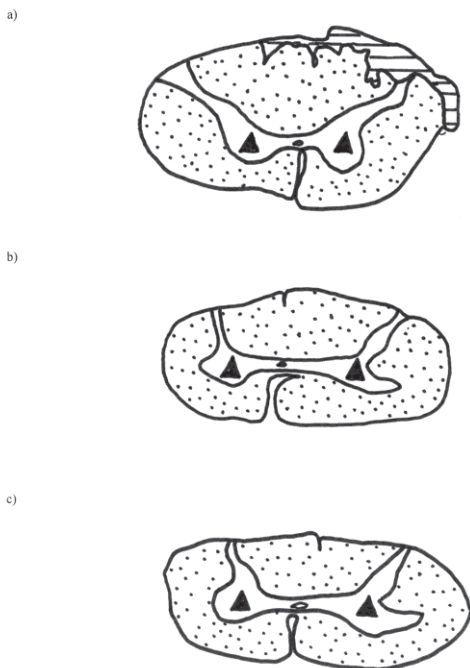
- a) Two levels above site - C3
- b) At the site of compression - C5
- c) Three levels below site - C8



Case: 8a (first compression at C5)
AIF 1

Levels:

- a) Two levels above site - C3
- b) At the site of compression - C5
- c) Three levels below site - C8

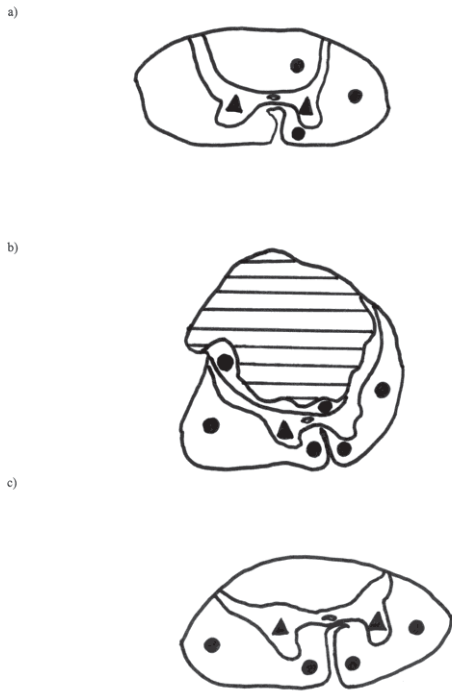


Spatial Distribution of Staining – Case 8

Case: 8b (second compression at T9-T10)
Amy-33

Levels:

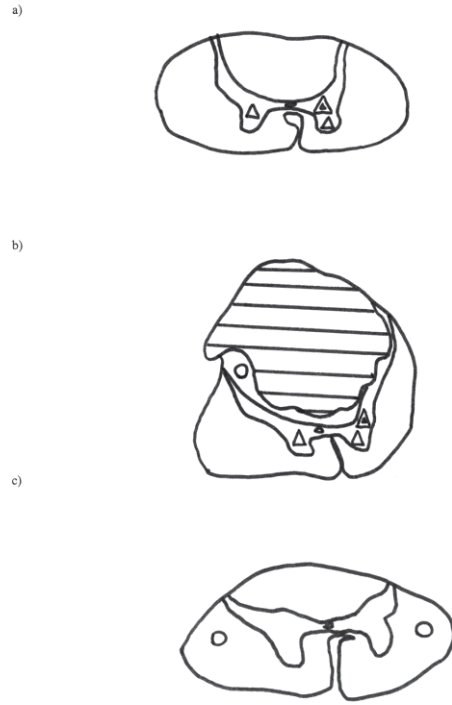
- a) Two levels above site - T7
- b) At the site of compression - T9
- c) Two levels below site - T12



Case: 8b (second compression at T9-T10)
Haematoxylin and eosin

Levels:

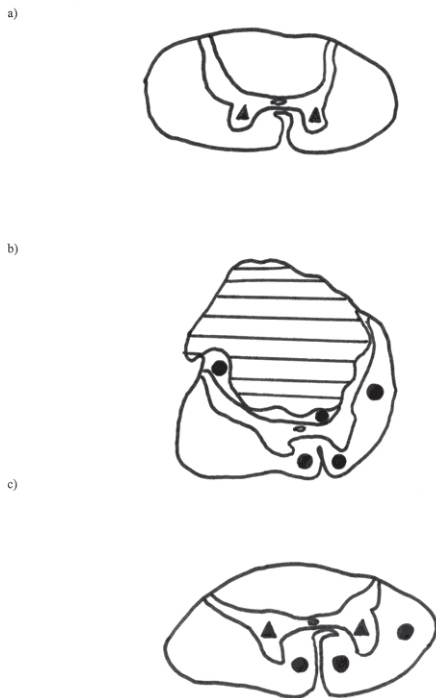
- a) Two levels above site - T7
- b) At the site of compression - T9
- c) Two levels below site - T12



Case: 8b (second compression at T9-T10)
APP

Levels:

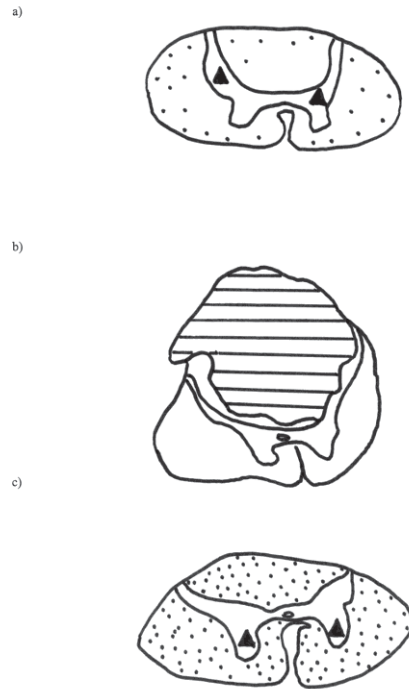
- a) Two levels above site - T7
- b) At the site of compression - T9
- c) Two levels below site - T12



Case: 8b (second compression at T9-T10)
DNA-PKcs

Levels:

- a) Two levels above site - T7
- b) At the site of compression - T9
- c) Two levels below site - T12



Spatial Distribution of Staining – Case 8

Case: 8b (second compression at T9-T10)
PARP

Levels:

- a) Two levels above site - T7
- b) At the site of compression - T9
- c) Two levels below site - T12

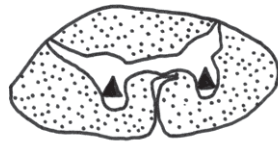
a)



b)



c)

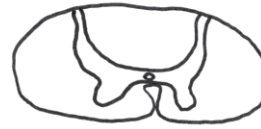


Case: 8b (second compression at T9-T10)
TUNEL

Levels:

- a) Two levels above site - T7
- b) At the site of compression - T9
- c) Two levels below site - T12

a)



b)



c)



Case: 8b (second compression at T9-T10)
AIF 1

Levels:

- a) Two levels above site - T7
- b) At the site of compression - T9
- c) Two levels below site - T12

a)



b)



c)



Summary of immunohistochemistry Case 8

<p>Glia: PARP, Bcl-2, CMAP, AIF Axons: APP, Amy-33, CMAP Neurons: APP, PARP, Amy-33, TUNEL, CMAP, AIF</p>	<p>C3</p>	<p>H&E: vacuolation, axonal swellings, red cell change</p>
<p>Glia: PARP, CMAP, AIF Axons: APP, Amy-33, CMAP Neurons: APP, PARP, Amy-33, CMAP, AIF</p>	<p>C4</p>	<p>H&E: Mild to moderate vacuolation</p>
<p>Glia: PARP, Bcl-2, CMAP, AIF Axons: APP, Amy-33, CMAP Neurons: APP, PARP, AIF Amy-33, CMAP</p>	<p>C5</p>	<p>H&E: Occasional axonal swellings and vacuolation, compression grey matter</p>
<p>Glia: PARP, Bcl-2, CMAP, AIF Axons: CMAP Neurons: APP, PARP, Amy-33, CMAP, AIF</p>	<p>C6</p>	<p>H&E: Occasional axonal swellings and vacuolation, compression grey matter</p>
<p>Glia: DNA-PKcs(rare) PARP, CMAP, AIF Axons: APP, Amy-33, CMAP Neurons: APP, PARP Amy-33, DNA-PKcs, CMAP</p>	<p>C8</p>	<p>H&E: Occasional axonal swellings and vacuolation</p>
<p>Glia: DNA-PKcs (rare), PARP, CMAP, AIF Axons: APP, Amy-33, CMAP Neurons: APP, DNA-PKcs, CMAP, AIF</p>	<p>T2</p>	<p>H&E: vacuolation, axonal swellings</p>
<p>Glia: PARP, CMAP, AIF Axons: DNA-PKcs, Amy-33, CMAP Neurons: APP, CMAP, AIF</p>	<p>T3</p>	<p>H&E: vacuolation, axonal swellings, loss of grey matter</p>

Glia: DNA-PKcs, PARP, CMAP, AIF Axons: APP, Amy-33, CMAP Neurons: APP, PARP, Amy-33, DNA-PKcs, CMAP, AIF	T7	H&E: vacuolation, axonal swellings
Glia: DNA-PKcs (rare), PARP, AIF, CMAP Axons: APP, Amy-33, CMAP Neurons: APP, PARP, Amy-33, CMAP, AIF	T8	H&E: vacuolation, axonal swellings
Glia: PARP, CMAP, AIF Axons: APP (max), Amy-33, CMAP Neurons: APP, PARP, Amy-33, CMAP, AIF	T9	H&E: vacuolation, axonal swellings
Glia: DNA-PKcs, PARP, CMAP, AIF Axons: APP (max), Amy-33, CMAP Neurons: APP, PARP, CMAP Amy-33, AIF	T10	H&E: vacuolation, axonal swellings
Glia: DNA-PKcs (rare), PARP, AIF, CMAP Axons: APP, Amy-33, CMAP Neurons: APP, PARP Amy-33, AIF, CMAP	T11	H&E: mild vacuolation only
Glia: DNA-PKcs (rare), PARP, AIF, TUNEL, CMAP Axons: APP, Amy-33, CMAP Neurons: APP, DNA-PKcs, PARP, TUNEL (rare), Amy-33, CMAP, AIF	T12	H&E: vacuolation, axonal swellings
Glia: PARP, CMAP, AIF Axons: APP, Amy-33, CMAP Neurons: APP, PARP, CMAP, AIF	L5	H&E: vacuolation, axonal swellings

Conclusion A 74 year old male with known metastatic squamous cell carcinoma and spinal cord intramedullary invasion. Two separate sites of malignant compression were present, one in the cervical and one in the thoracic cord. There was sensory impairment but no reported motor impairment and this was consistent with histopathological findings which found tumour infiltration into the posterior columns at both sites. There was evidence of ischaemic damage as there was neuronal red cell change. There was widespread immunopositivity to PARP antibody, being present at, above and below both sites of compression in glia and neurons. DNA-PKcs and TUNEL were rarely present in glia, suggesting that DNA-damage may be minimal and PARP immunopositivity may alternatively represent DNA-repair processes and cell-remodelling. APP and amy-33 antibody staining was seen in axonal swellings at, above and below. Other antibodies to amyloid-beta were negative. AIF was heterogeneously positive in glia and neurons.

CASE 9

Clinical summary A 24 year- old male who presented with right arm pain and paraesthesia. The onset of symptoms was 8 months before death. Investigations showed an extrasosseous Ewing's tumour of the right humerus. Chemotherapy and radiotherapy resulted in some improvement however he re-presented 4 months later with increasing right arm pain. He developed pneumonia followed by flaccid quadriparesis, associated with a cord lesion at segments C2-C5. A second course of radiotherapy was commenced, with slight neurological improvement in the upper limbs. Shortly afterwards, he suffered a massive gastrointestinal haemorrhage, endoscopy showing a bleeding duodenal ulcer.

On autopsy, no evidence of tumour could be found within the spinal canal following radiotherapy, however there were signs of left-sided compression of the cord at C5-C6. C2-C5 showed subtotal loss of ganglion cells. There were axonal swellings in the white matter of C5-C6, and some in the right lateral column at C4. C5-C6 segments showed marked oedema, demyelination of axons, and loss of anterior horn cells. The most severe white matter damage was in the right lateral white matter subpially.

Pathology – brain

1. Normal brain.

Pathology – spine and spinal cord

1. Macroscopically normal spinal cord.
2. The microscopic features are those of a compressive myelopathy at C5-C6 spinal cord levels.

Haematoxylin and Eosin

Macroscopic findings Segment C8 (N1) appeared macroscopically normal except for an artefactual splitting of the lateral white matter on one side. At C5-C7 (N2-N6) part of the lateral cord was missing from section likely due to the tissue processing technique. At C5 (N4) and C7 (N2) there was apparent cystic change in the lateral white matter on one side. Segments C4 (N7) and C3 (N8) were macroscopically normal.

Microscopic findings At C8 (N1), C7 (N2), C6 (N3), C5 (N4, N6), C4 (N7) and C3 (N8) there is a loss of anterior horn cells (AHC). At C8 (N1) and C6 (N3) there is occasional microvacuolar change and rarely axonal swellings are seen in the lateral white matter. At C7 (N2) more advanced

vacuolation is seen. Axonal swellings or bulbs are present occasionally in the anterior white matter and throughout the posterolateral white matter. A large region of cystic cavitation is found in the lateral spinothalamic tract and a second region in the lateral corticospinal tract on the same side. At C5 (N4, N6) there is a similar pattern of vacuolar changes and axonal swellings and at C7 with the lateral white matter severely affected on one side and in addition there is a further small region of cystic cavitation in the opposite lateral corticospinal tract. At C5 (N5) there is a large cystic region in the cuneate fasciculus on one side and macrophages are present. At segment C4 (N7) less severe changes are noted with only occasional axonal swellings present in the lateral corticospinal tract and contralateral spinothalamic tract. There are no cystic cavities at this level. At C3 (N8) there is mild vacuolation of the white matter.

Weil Macroscopically there is a generalised pallor of the cord at C8 (N1) and C7 (N2) most severe in the posterior columns. At the levels of compression, C6 (N3) and C5 (N4), there is involvement of both the posterior columns and subpial lateral white matter. At C5 (N5, N6) there is clear pallor of lateral corticospinal tract as well as posterior columns. A minimal decrease in staining is seen at C4 (N7) in the cuneate fasciculi. C3 (N8) is normal on Weil staining. Histologically a proportion of the pallor found on Weil staining could be accounted for by vacuolation of the white matter however in the lateral and posterior white matter distinct areas of demyelination were evident at C4, C5 and C7 (N2, N4, N5, N7).

Immunohistochemical results

CASE 9 – Immunological positivity (+) in glial, axonal or neuronal profiles:

Level	APP	Casp-3	DNA- PKcs	PARP	Bcl-2	Fas	Casp-9	TUNEL	Amy-33	CMAP	AIF
C3	+	+	-	+	+	+	+	+	+	+	+
C4	+	+	+	+	-	+	+	+	+	+	+
C5	+	+	+	+	+	+	+	+	+	+	+
C6	+	+	+	+	+	+	+	+	+	+	+
C8	+	+	+	+	-	+	+	+	+	+	+
T2	+	+	+	+	-	+	+	+	+	+	+
T3	+	+	+	+	-	+	+	+	+	+	+
T7	+	+	+	+	-	+	+	+	+	+	+
T8	+	+	+	+	-	+	+	+	+	+	+
T9	+	+	-	+	-	+	+	+	+	+	+
T10	+	+	+	+	-	+	+	+	+	+	+
T11	+	+	+	+	-	+	+	+	+	+	+
T12	+	+	+	+	-	+	+	+	+	+	+
L5	+	+	-	+	-	+	+	+	+	+	+

APP Immunopositive axonal swellings / bulbs and axonal profiles of normal diameter were seen in the white matter of all segments. These profiles were dispersed throughout the white matter including the anterior corticospinal tracts and deep posterior columns but were greatest in number in the lateral corticospinal tracts tending towards the subpial regions. Immunopositivity was greatest at the level of C5 (N4-N6). Occasionally the morphology of such profiles was indistinct from glial nuclei. Neuronal cytoplasmic immunopositivity was seen in one neuron at C5 (N5).

Active caspase-3 Occasional cytoplasmic immunopositive staining was found in unidentified cells within the white matter in all segments. Occasional immunopositive axonal swellings or bulbs were seen in all areas of the white matter at C7 (N2) and C5 (N4, N5, N6) and in the lateral white matter only at C6 (N3). Fewer immunopositive axons were found at segments C4 (N7) and C3 (N8). Negative in neurons.

DNA-PKcs At C5-C7 (N2-N4) immunopositive glial nuclei were present in all areas of the white matter but in highest numbers around the subpial rim. Sections N5 and N6 of C5 level, and C8 (N1) were immunonegative within glia. Positive glia were rarely present at C4 (N7). At C3 (N8)

immunopositive glia were again seen dispersed through the white matter, greatest in number subpially, and many with a morphology resembling microglia. Axonal immunopositivity was rarely seen at C4 (N7) to C7 (N2) but more commonly at C5 (N4). Negative in neurons.

PARP Glial nuclear immunopositivity was occasionally found in segments C3-C5 (N4-N8) in subpial regions but a cell type could not be determined based on morphology alone. PARP immunopositivity was rarely seen in axonal swellings of the lateral white matter on one side only at C5 (N4-N6) and C4 (N7). Negative in neurons.

Bcl-2 Rare non-specific staining was seen at C7 (N2) and C5 (N4). Equivocal axonal immunopositivity was rarely seen at C5 (N4). Negative in neurons.

Fas Equivocal immunopositivity was found occasionally in axonal swellings at C4-C6 (N3, N4, N6, N7). Negative in glia, neurons.

Caspase-9 Equivocal axonal immunopositivity segments C4, C5 and C7 (N2 and N4-N7). Negative in neurons and glia.

TUNEL Many neuronal nuclei were immunopositive using the TUNEL marker in all areas of the grey matter in all segments. Many glial nuclei were also immunopositive in anterior, posterior and lateral regions in all segments. Numbers of positive glia were greatest towards the central cord. Immunostaining was greatest in terms of neuronal and glial numbers at C5 (N5 and N6). In addition there were large immunopositive axonal profiles axonal.

CMAP Occasional neuronal immunopositivity was found. A subtotal number of axons both normal and larger size were positive with few immunonegative profiles. A subset of glia were also immunopositive. Given the high level of background staining in these sections the specificity of this marker at the current dilution is in question.

Amy-33 amyloid beta At C3 (N8) many neurons showed immunopositivity within the cytoplasm. Rarely, positive glia were viewed within the white matter. Occasional smaller immunopositive profiles, possibly axons were found in the white matter particularly in the posterior columns. At C4 (N7) there was again neuronal cytoplasmic positivity. A greater number of small and large diameter axonal profiles were seen throughout the white matter but especially in the posterolateral regions. Focal areas of immunostaining were clearly visible in both lateral corticospinal tracts, one side larger than the other. Occasional glia were immunopositive. At C5 (N4, N5) similar staining was seen except a larger region overall was affected. There was a mixture of immunopositive and

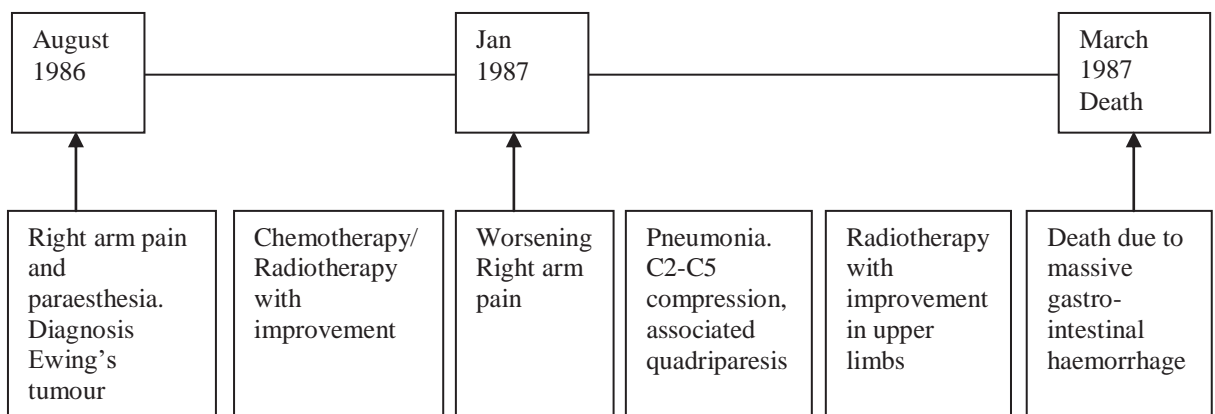
immunonegative axonal swellings. At C6 (N3) equivocal staining was seen within neurons. There were scattered small and sometimes larger positive axonal profiles in the white matter, again in greater number within the lateral corticospinal tracts. At C7 (N2) axonal immunopositivity was increased in number with focal regions of staining visible in the lateral spinothalamic tract on one side, both lateral corticospinal tracts, and both gracile fasciculi. Only occasional neuronal immunopositivity occurred. At C8 (N1) there was occasional neuronal staining and axonal immunopositivity in axons of variable diameter.

University of Melbourne amyloid beta Equivocal immunopositivity within axons and glia at C5 (N5, N6) however the degree of background staining negates the specificity of this marker.

DAKO amyloid beta Negative.

AIF At C3 and C8 (N1, N8) there is oligodendroglial and astrocytic immunopositivity throughout the cord and neuronal cytoplasmic immunopositivity. At C4, C5, C7 (N2, N4, N5, N6, N7) there is glial and neuronal staining as well as immunopositivity in axonal swellings and macrophages in all regions of the cord. Axons of normal and enlarged diameter are immunopositive and interspersed between negative axonal swellings. At C6 (N3) there is glial and neuronal immunopositivity and rare axonal swellings immunopositive in the lateral white matter.

Timeline of clinical progression



Spatial Distribution of Staining – Case 9

Case: 9
Amy-33

Levels:

- a) Two levels above site - C3
- b) At the site of compression - C5
- c) Two levels below site - C8

a)



b)



c)



Case: 9
Haematoxylin and eosin

Levels:

- a) Two levels above site - C3
- b) At the site of compression - C5
- c) Two levels below site - C8

a)



b)



c)

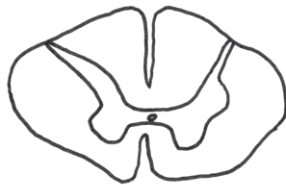


Case: 9
APP

Levels:

- a) Two levels above site - C3
- b) At the site of compression - C5
- c) Two levels below site - C8

a)



b)



c)

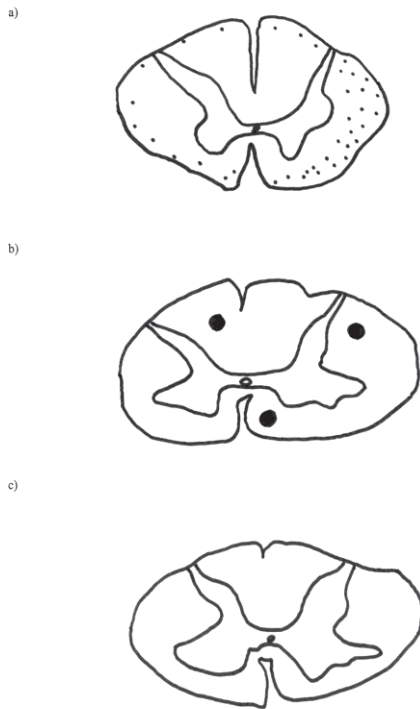


Spatial Distribution of Staining – Case 9

Case: 9
DNA-PKcs

Levels:

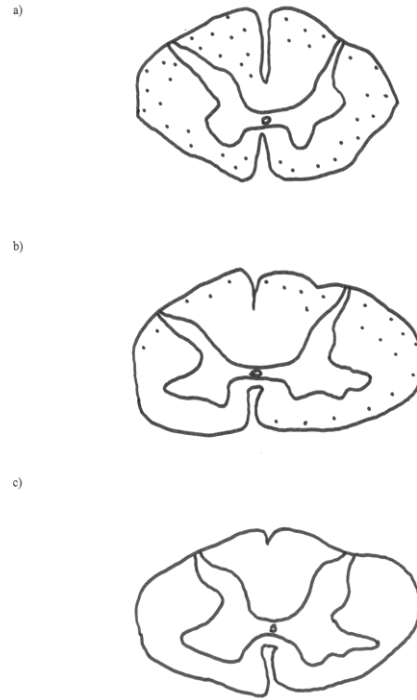
- a) Two levels above site - C3
- b) At the site of compression - C5
- c) Two levels below site - C8



Case: 9
PARP

Levels:

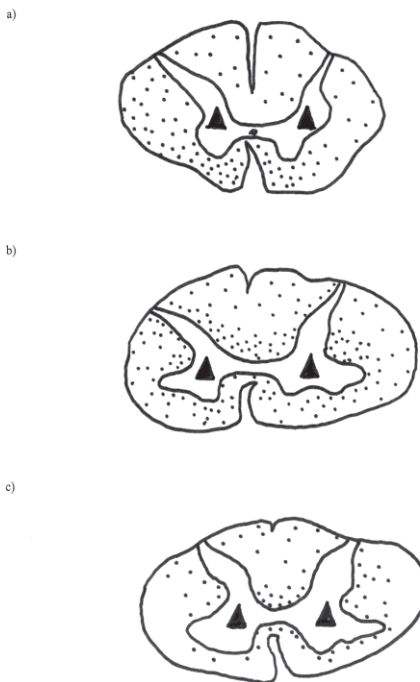
- a) Two levels above site - C3
- b) At the site of compression - C5
- c) Two levels below site - C8



Case: 9
TUNEL

Levels:

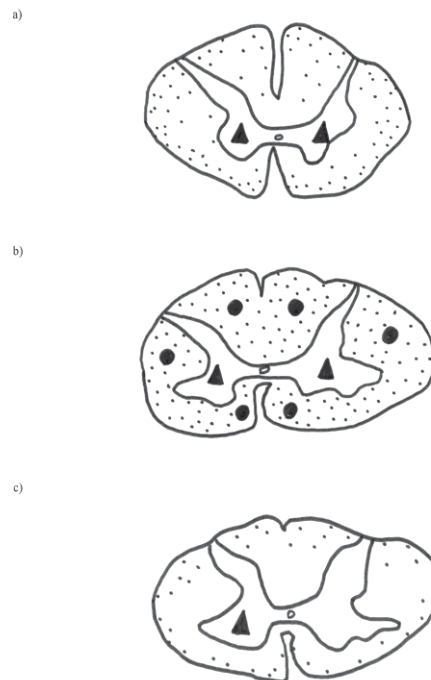
- a) Two levels above site - C3
- b) At the site of compression - C5
- c) Two levels below site - C8



Case: 9
AIF 1

Levels:

- a) Two levels above site - C3
- b) At the site of compression - C5
- c) Two levels below site - C8



Summary of immunohistochemistry Case 9

<p>Glia: TUNEL, DNA-PKcs, PARP, AIF, CMAP Axons: APP (minimal), Amy-33, CMAP, Caspase-3 Neurons: TUNEL, Amy-33, CMAP, AIF</p>	C3	<p>H & E: AHC loss, mild vacuolation Cord diameter: AP 6.5 Lat 10.5mm</p>
<p>Glia: TUNEL, DNA-PKcs, PARP, AIF, CMAP Axons: APP, Amy-33, Caspase-3, AIF, DNA-PKcs, PARP, CMAP Neurons: TUNEL, Amy-33, CMAP, AIF</p>	C4	<p>H & E: AHC loss, axonal swellings Weil: lateral white matter Cord diameter: AP 7 Lat 12mm</p>
<p>Glia: TUNEL (max), DNA-PKcs, AIF, PARP, CMAP Axons: APP (max), Amy-33 (max), Caspase-3, DNA-PKcs (max), PARP, CMAP, AIF Neurons: APP, TUNEL (max), Amy33, AIF, CMAP</p>	C5	<p>H & E: AHC loss, axonal swellings, cystic necrosis Weil: posterolateral white matter Cord diameter: AP 7 Lat 13mm</p>
<p>Glia: TUNEL, DNA-PKcs, PARP, CMAP, AIF Axons: APP, Amy-33, Caspase-3, AIF, DNA-PKcs, CMAP Neurons: TUNEL, CMAP, AIF</p>	C6	<p>H & E: AHC loss, vacuolation, axonal swellings Cord diameter: AP 7 Lat 13mm</p>
<p>Glia: TUNEL, DNA-PKcs, CMAP, AIF Axons: APP, Amy-33, Caspase-3, AIF, DNA-PKcs, CMAP Neurons: TUNEL, Amy-33, CMAP, AIF</p>	C7	<p>H & E: AHC loss, vacuolation (max), axonal swellings, cystic necrosis Weil: posterolateral white matter Cord diameter: AP 7 Lat 13mm</p>
<p>Glia: TUNEL, CMAP, AIF Axons: APP, Amy-33, CMAP Neurons: TUNEL, Amy-33, CMAP, AIF</p>	C8	<p>H & E: AHC loss, vacuolation, axonal swellings Cord diameter: AP 8 Lat 14mm</p>

Conclusion A 24 year-old male with spinal cord compression secondary to extrasosseous Ewing's tumour invasion. It is not clear from clinical reports whether the lesion was intra- or extra-dural. Histopathological analysis did not show any intramedullary invasion of the spinal cord. The tumour initially surrounded C2-C5 segments however post-radiotherapy the tumour apparently affected only the C5-C6 level.

CASE 10

Clinical summary A 72 year-old male with metastatic prostatic carcinoma of the vertebral column, compressing the cervical spinal cord and resulting in incomplete quadriplegia. Obstructive chronic pyelonephritis and right-sided ureteric obstruction caused progressive renal insufficiency and renal failure was the cause of death.

There was absence of the intervertebral discs and fusion of C4, 5, 6, 7 vertebral bodies. The architecture of these vertebrae was replaced by grey/white tissue. Stenosis of the spinal canal existed at the level of the odontoid process and C3 vertebral body.

There was compression cervical myelopathy at C8 and C2-C3 segments. At the level of C2 there was recent focal congestion of blood vessels and haemorrhage into one anterior horn. Loss of anterior horn cells was found at C3, C4, C5, C6, C7 and C8. There were intradural metastatic deposits of tumour.

Pathology – brain

1. Old lobular infarction left cerebellum.

Pathology – spine and spinal cord

1. Compression cervical myelopathy.
2. Metastatic prostatic carcinoma of the vertebral column.

Haematoxylin and Eosin

Macroscopic findings On post-mortem examination there were areas of A-P compression deformity present at C2-C3 and C8. Segmental levels C3 (N17) to C6 (N20), and C8 (N22) to T3 (N25) were macroscopically distorted on haematoxylin and eosin staining. There was mild unilateral distortion of the spinal cord at segments C2 (N16) and C7 (N21), which may either represent artefact or pathological compression.

Microscopic findings Many corpora amylacea are seen throughout the cord. In segment C2 (N16) there is a small area of haemorrhage towards the posterior grey matter. This segment is otherwise normal. Segment C3 (N17) shows loss of anterior horn cells. Central chromatolysis was seen in neurons of segments C4 (N18), C5 (N19) and C7 (N21) characterised by cell swelling and peripheral displacement of the Nissl substance and nucleus. There is a loss of anterior horn cells at C4-C8. At C6 (N20) and C8 (N22) there is a small region of haemorrhage and cystic change in the

grey matter unilaterally. C7 (N21) appears normal. At C8 (N22), T1 (N23), T2 (N24) there is the impression of anterior horn cell loss. T3 (N25) appears normal.

Weil Mild pallor is observed macroscopically on Weil staining in the posterior column in segments T2 (N24) and T3 (N25). On microscopic analysis there appeared to be normal myelination of axons however the posterior columns contained fewer axons than would normally be found, possibly accounting for the pallor on macroscopic examination.

Immunohistochemical results

CASE 10 – Immunological positivity (+) in glial, axonal or neuronal profiles:

Level	APP	Casp-3	DNA- PKcs	PARP	Bcl-2	Fas	Casp-9	TUNEL	Amy-33	CMAP	AIF
C2	-	+	+	+	-	-	-	+	+	+	+
C3	-	+	+	+	+	-	-	+	+	+	+
C4	-	+	+	+	-	-	-	+	+	+	+
C5	-	+	+	+	+	-	-	+	+	+	+
C6	-	+	+	+	+	-	-	+	+	+	+
C7	-	+	+	+	-	-	-	+	+	+	+
C8	+	+	+	+	+	-	-	+	+	+	+
T1	-	+	+	+	-	-	-	+	+	+	+
T2	-	+	+	+	-	-	-	+	+	+	+
T3	-	+	+	+	-	-	-	+	+	+	+

APP Immunonegative for glia and neurons. Non-specific immunopositivity is seen in spherical profiles at segments C2 and C3 (N16-17). Two immunopositive axonal profiles are seen in the gracile fasciculus and one in the contralateral cuneate fasciculus at C8 (N22). There were no other significant findings.

Active caspase-3 Immunonegative for glia, neurons and axons.

DNA-PKcs One immunoreactive neuronal nucleus was seen in the posterior horn at C8 (N22). Immunopositive glial nuclear profiles were recognised throughout the white matter of all segments. Possible isolated immunopositive axonal profiles in segments in lateral corticospinal tract of C6 (N20) and posterior column of T1 (N23).

PARP Immunonegative for neurons, axons. Many immunopositive glial nuclear profiles with the morphology of oligodendrocytes (oval) were recognised throughout the white matter of all segments.

Bcl-2 Immunonegative for neurons and axons. Immunopositivity for the nuclear membrane of cells within the neuropil, likely to be glia according to profile and size, were seen at segments C3 (N17), C5 (N19), C6 (N20) and C8 (N22).

Fas Immunonegative for neurons, glia and axons.

Caspase-9 Immunonegative for neurons glia and axons.

TUNEL Nuclear immunopositivity in neurons was found bilaterally in the posterior horn at segment C2 (N16). Positive neurons were seen in both anterior and posterior horns of segments C3-C8 (N17-N22) and T2, T3 (N24-N25). Neurons of the central grey matter were also present at C2, C3, C5, C8, T2 and T3 (N16, N17, N19, N22, N24, N25 respectively). Segment T1 (N23) was immunonegative for neurons. Glial nuclear immunopositivity was present scattered throughout the white matter in all segments studied but was maximal at C3 (N17) and T3 (N25). Immunonegative for axons.

CMAP From C2 (N16) to T1 (N23) approximately 50% of glial nuclei immunopositive using CMAP. Immunopositivity in ependymal cell nuclei and occasional small axonal profiles. Fewer immunopositive glia are seen at T2 (N24) but otherwise there is a similar pattern of axonal and ependymal staining. The increased level of background staining indicates that immunopositivity may be non-specific. Immunonegative in neurons.

Amy-33 amyloid beta

C2 (N16) and C3 (N17): Occasional equivocal immunopositivity within the cytoplasm of neurons. Non-specific immunopositivity within rounded profiles occasionally present in the white matter.

C4 (N18): Immunopositivity in the AHC cytoplasm. Distinct focus of axonal immunopositivity in the spinothalamic tract unilaterally. This region is not present using the APP immunomarker at the same level.

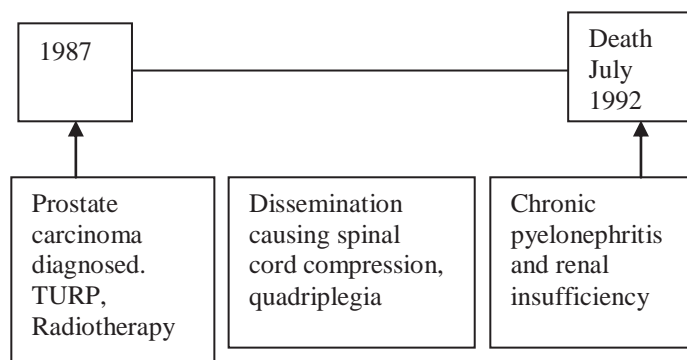
C5 to T2 (N19 to N24): Occasional immunopositivity in the AHC cytoplasm, greater numbers unilaterally from C7 to T2. Rounded profiles are seen scattered occasionally throughout the white matter, mostly posterior and lateral from C6 to T1. Some non-specific profiles in white and grey matter at T1 and T2.

University of Melbourne amyloid-beta Negative.

DAKO amyloid-beta Negative.

AIF Occasional immunoreactivity was found in the cytoplasm of oligodendrocytes and astrocytes in all segments. Neuronal immunostaining was also present in large numbers bilaterally. Immunopositivity was present in the cytoplasm of ependymal cells. There was no immunopositivity within axonal profiles.

Timeline of clinical progression



Spatial Distribution of Staining – Case 10

Case: 10
Amy-33

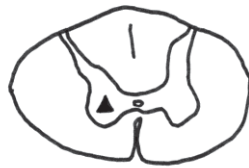
Levels:

- a) Two levels above site - C6
- b) At the site of compression - C8
- c) Two levels below site - T2

a)



b)



c)

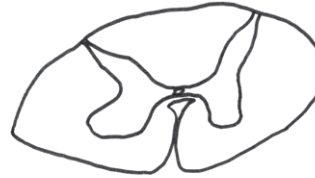


Case: 10
Haematoxylin and eosin

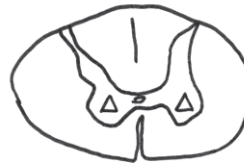
Levels:

- a) Two levels above site - C6
- b) At the site of compression - C8
- c) Two levels below site - T2

a)



b)



c)



Case: 10
APP

Levels:

- a) Two levels above site - C6
- b) At the site of compression - C8
- c) Two levels below site - T2

a)



b)



c)

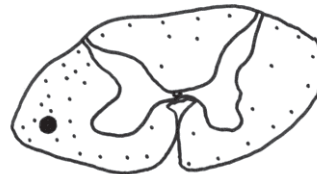


Case: 10
DNA-PKcs

Levels:

- a) Two levels above site - C6
- b) At the site of compression - C8
- c) Two levels below site - T2

a)



b)



c)



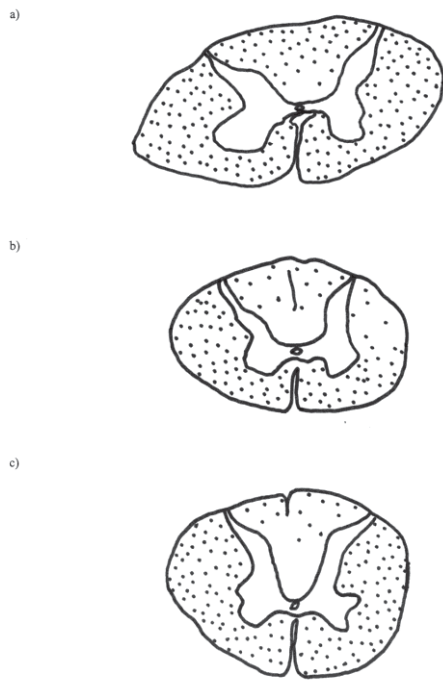
Spatial Distribution of Staining – Case 10

Case: 10

PARP

Levels:

- a) Two levels above site - C6
- b) At the site of compression - C8
- c) Two levels below site - T2

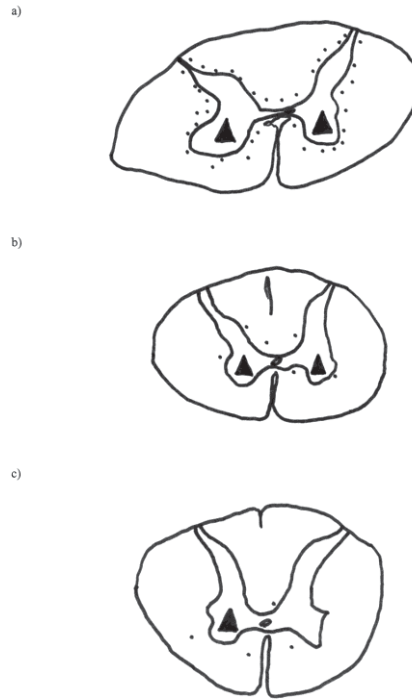


Case: 10

TUNEL

Levels:

- a) Two levels above site - C6
- b) At the site of compression - C8
- c) Two levels below site - T2

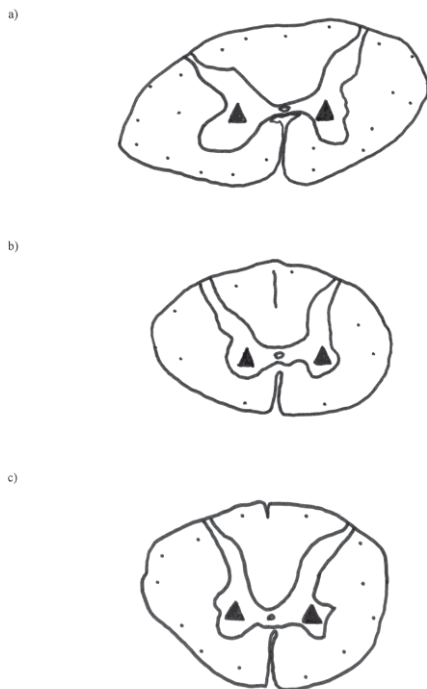


Case: 10


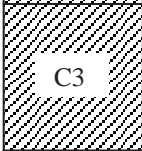

AIF 1

Levels:

- a) Two levels above site - C6
- b) At the site of compression - C8
- c) Two levels below site - T2



Summary of immunohistochemistry Case 10

<p>Glia: PARP, DNA-PKcs, TUNEL, CMAP, AIF Axons: Nil Neurons: TUNEL (Posterior), AIF, Amy-33</p>	 <p>C2</p>	<p>H & E: Corpora amylacea, small haemorrhage posterior column</p>
<p>Glia: PARP, DNA-PKcs, CMAP, Bcl-2, AIF, TUNEL (Max) Axons: Nil Neurons: TUNEL, Amy-33, AIF</p>	 <p>C3</p>	<p>H & E: Corpora amylacea, anterior horn cell loss</p>
<p>Glia: PARP, DNA-PKcs, TUNEL, CMAP, AIF Axons: Amy-33 Neurons: TUNEL, Amy-33, AIF</p>	<p>C4</p>	<p>H & E: Corpora amylacea, central chromatolysis, anterior horn cell loss</p>
<p>Glia: PARP, DNA-PKcs, TUNEL, CMAP, AIF, Bcl-2 Axons: Nil Neurons: TUNEL, Amy-33, AIF</p>	<p>C5</p>	<p>H & E: Corpora amylacea, central chromatolysis, anterior horn cell loss</p>
<p>Glia: PARP, DNA-PKcs, TUNEL, CMAP, AIF, Bcl-2 Axons: DNA-PKcs (Lateral), Amy-33, CMAP Neurons: TUNEL, Amy-33, AIF</p>	<p>C6</p>	<p>H & E: Corpora amylacea, haemorrhage and cystic change in grey matter, anterior horn cell loss</p>
<p>Glia: PARP, DNA-PKcs, TUNEL, CMAP, AIF Axons: Amy-33, CMAP Neurons: TUNEL, Amy-33, AIF</p>	<p>C7</p>	<p>H & E: Corpora amylacea, anterior horn cell loss</p>
<p>Glia: PARP, DNA-PKcs, TUNEL, CMAP, AIF, Bcl-2 Axons: APP (Post Column), CMAP Neurons: TUNEL, DNA-PKcs, Amy-33, AIF</p>	 <p>C8</p>	<p>H & E: Corpora amylacea, haemorrhage and cystic change in grey matter, anterior horn cell loss</p>
<p>Glia: PARP, DNA-PKcs, TUNEL, CMAP, AIF Axons: DNA-PKcs (Posterior), CMAP Neurons: Amy-33, AIF</p>	<p>T1</p>	<p>H & E: Corpora amylacea, anterior horn cell loss</p>
<p>Glia: PARP, DNA-PKcs, TUNEL, CMAP, AIF Axons: Nil Neurons: TUNEL (Ant/Post Horns), Amy-33, AIF</p>	<p>T2</p>	<p>H & E: Corpora amylacea, anterior horn cell loss Weil: Pallor posterior column</p>
<p>Glia: PARP, DNA-PKcs, TUNEL (Max), CMAP, AIF Axons: Nil Neurons: TUNEL (Ant/Post Horns), Amy-33, AIF</p>	<p>T3</p>	<p>H & E: Corpora amylacea Weil: Pallor posterior column</p>

Conclusion A 72 year-old man with intradural metastatic deposits from prostate carcinoma. The presence of numerous vertebral metastases was confirmed on autopsy. Pathological examination of the brain showed an old lobular infarction of the cerebellum but no acute abnormality. There was development of compression myelopathy at the C2-C3 and C8 segments. Prostate carcinoma was diagnosed 5 years prior to death however the duration of compression onto the spinal cord is not known.

The histological changes on haematoxylin and eosin staining were overall quite mild but indicative of some degree of cellular damage. Central chromatolysis of neurons was seen indicating damage of the axon and myelin sheath likely due to tumour compression of the anterior nerve roots. Such changes typically occur after 24-48 hours following injury and are thought either to represent an attempt at increased protein production in response to injury or a back-up of cytoskeletal elements normally found within the axon but which accumulate with disruption to axonal transport (McIlwain and Hoke, 2005). There were no neuronal changes suggestive of an ischaemic process. There was pallor of the posterior columns on Weil staining below the site of compression which was unusual given that the motor tracts are typically vulnerable to demyelination below the lesion. This may suggest that there is further unrecognised pathology at lower levels. A focal region of haemorrhage was present at C6 and C8. The increased cellularity surrounding this area indicated a true pathological basis rather than artefact.

DNA-PKcs and PARP showed a subpial pattern of nuclear glial staining consistent with previous cases. PARP immunopositive glia maintained the morphology of oligodendrocytes, suggesting a potential predisposition of such cells either to injury and remodelling or indicative of the repair following axonal damage and demyelination. TUNEL immunopositivity was maximal in the central cord. This may represent an ongoing pattern of DNA damage and subsequent cell death with remodelling in the peripheral white matter or more mildly affected regions.

There was no clear axonal immunopositivity using the marker APP, which suggests the maintenance of axonal transport. A focal area of immunopositivity within small diameter axons was seen at C4 using Amy-33 amyloid-beta antibody, marking one of the products of APP proteolysis, amyloid-beta. However, both the DAKO and University of Melbourne antibodies to amyloid beta were immunonegative and thus the true result is uncertain.

CASE 11

Clinical summary A 73 year-old female cyclist involved in a motor vehicle accident. The spinal cord was injured at C1-C2 segments with cord haemorrhage secondary to C2 vertebra fracture/dislocation. Quadriplegia developed from spinal level C1. Patient died 5 hours following the initial trauma.

Pathology – brain

1. Patchy subarachnoid haemorrhage only.
2. No histopathological evidence to suggest dementia.

Pathology – spine and spinal cord

1. Extensive haemorrhagic necrosis at levels C1-2 of the spinal cord.

Haematoxylin and Eosin

Macroscopic findings On post-mortem examination the proximal margin of the spinal cord showed extensive disruption. Subdural haemorrhage extended from the proximal margin for a distance of 20 mm. On sectioning there was extensive intraparenchymal haemorrhage extending from the C2-C1 segments to the proximal margin (C1).

Very mild asymmetry of the cord is evident at segments C4 (N19) and C3 (N20). Eosinophilic staining is seen in the grey matter at the level of compression in segments C1-2 at N22, N23 and to a lesser extent section N24.

Microscopic findings Corpora amylacea are present. A gradual reduction in severity of histopathological changes is noted for sections N22-24 at segment C1-2. Significant regions of haemorrhage, severe vacuolation, and axonal swellings are seen throughout the cord at C1-2 (N24). In addition there is reactive astrocytosis throughout the cord. There is a subtotal loss of anterior horn cells at this level. At section N23 (C1-2) changes are less severe with vacuolation and axonal swellings located towards the periphery. There is central haemorrhage, loss of AHCs and occasional red cell change in preserved neurons. Foci of cellularity, likely polymorphonuclear cells and lymphocytes, are found within the haemorrhagic area. At section N22 (C1-2) there is only mild vacuolation of the subpial white matter, and occasional axonal swellings greatest in number in the lateral cord unilaterally. On the opposite side of the cord there is haemorrhage within the grey matter. There is loss of AHCs. At C2 (N21) there is a loss of AHCs and occasional vacuolation. At C3 (N20) and C4 (N19) there are greater numbers of AHCs and occasional vacuolation.

Weil There is mild macroscopic pallor of the posterior columns in segments C2-C4 (N21-N19) however on microscopic examination this was found to be due to vacuolation not demyelination.

Immunohistochemical results

CASE 11 – Trauma series – Immunological positivity (+) in glial, axonal or neuronal profiles:

Level	APP	Casp-3	DNA- PKcs	PARP	Bcl-2	Fas	Casp-9	TUNEL	Amy-33	CMAP	AIF
C1-2	+	-	+	-	-	-	-	-	+	+	+
C2	+	-	+	-	-	-	-	-	+	+	+
C3	-	-	-	-	-	-	-	+	+	+	+
C4	+	-	-	-	-	-	-	+	+	+	+

* Shaded rows represent the site of compression

APP Small regions of axonal immunopositivity were seen in the lateral corticospinal tract, and rare staining in the posterior column and lateral spinothalamic tract, at C4 (N19). There were axons of normal and, less commonly, enlarged diameter. C3 (N20) was immunonegative in axons. At C2 (N21) small foci were again seen in the lateral white matter and rarely immunopositive axons in other regions. At C1-2 (N22) greater numbers of immunopositive axons were present in the lateral and anterior corticospinal tracts and lateral spinothalamic tracts, particularly on one side. These areas included small and less commonly swollen axons. A similar pattern of staining was seen in sections N23 and N24 (C1-2) but involving many more axons, particularly at N23, and also the posterior columns. There was dendritic immunopositivity in one neuron at C4 (N19). Immunonegative in glia.

Active caspase-3 Immunopositivity was seen in small, spherical structures of the subpial white matter at C1-2 (N23, N24) however this may be due to tissue disruption or background staining. Immunonegative in axons and neurons.

DNA-PKcs Occasional glial cytoplasmic immunopositivity at C1-2 (N23, N24), C2 (N21) which appears consistent with microglia or glial processes and rarely at C4 (N19), maximal staining in section N24 (C1-2). Immunonegative in axons, equivocal staining in neurons at C2 (N21) and C4 (N19).

PARP Occasional glial nuclear immunopositivity using PARP at C1-2 (N24) particularly in the anterior white matter. The morphology of these cells is consistent with oligodendrocytes. In section

N23 (C1-2) there is similar glial staining but these profiles are homogeneously dispersed throughout the white matter. In section N22 (C1-2) there is a similar pattern however fewer glia are truly immunopositive as the majority are equivocal staining. Many immunopositive glia, a morphology consistent with oligodendrocytes, are seen throughout the white matter at C2, C3 and C4 (N19-N21). Immunopositive neuronal nucleoli were rarely seen in the anterior horn at C2 and C3 (N19, N20). Immunonegative in axons.

Bcl-2 Nuclear membrane immunopositivity was seen rarely at segments C3, C4 (N20-N21), section N24 of C1-2, and more often at N22 (C1-2). At N23 (C1-2) greater numbers of these cells occur in hypercellular areas of haemorrhage with lymphocytes. Immunonegative in neurons and axons.

Fas Immunonegative in glia, axons and neurons.

Caspase-9 Negative in glia, neurons and axons.

TUNEL Immunopositive glial nuclei are dispersed throughout the white matter at C4 (N19). Immunopositive glia were seen at C3 (N20) maximal in the posterior columns. There were immunopositive neuronal nuclei present in segment C4 (N19). Neurons were only rarely immunopositive at C3 (N20), the majority were equivocal in staining. Immunopositive cells rarely seen in section N23 (C1-2) of uncertain identity. All other segments immunonegative.

CMAP Immunopositivity was seen in glia, the majority of axons both small and large, and in ependymal cells. The degree of background staining negates the specificity of this marker at the dilution used.

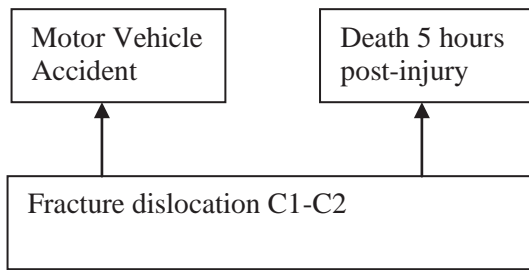
Amy-33 amyloid beta Immunopositive axonal profiles, small and large, in regions matching that of APP staining were found in C4 (N19). These axons were greater in number than that seen using the APP marker. In many neurons, especially AHCs, cytoplasmic immunopositivity was seen.

University of Melbourne amyloid beta Negative.

DAKO amyloid beta Negative.

AIF Many immunopositive corpora amylacea are seen. Neuronal immunopositivity in the cytoplasmic region was seen in all sections. In all segments there were immunopositive glia throughout the white matter, with staining of the cytoplasm only. Immunopositivity was present in scattered small and normal diameter axonal profiles within the white matter.

Timeline of clinical progression



Spatial Distribution of Staining – Case 11

Case: 11
Amy-33

Levels:

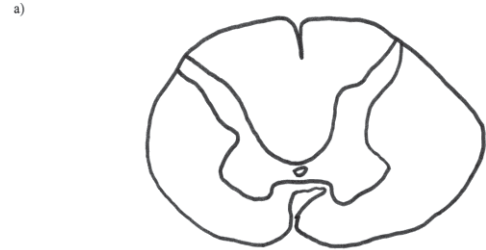
- a) At the site of compression - C2
- b) Two levels below site - C4



Case: 11
Haematoxylin and eosin

Levels:

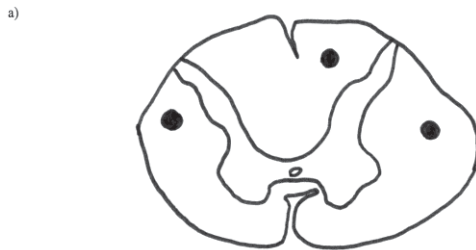
- a) At the site of compression - C2
- b) Two levels below site - C4



Case: 11
APP

Levels:

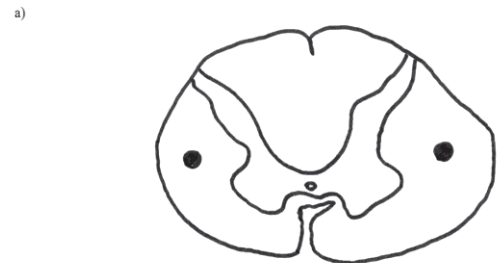
- a) At the site of compression - C2
- b) Two levels below site - C4



Case: 11
DNA-PKcs

Levels:

- a) At the site of compression - C2
- b) Two levels below site - C4

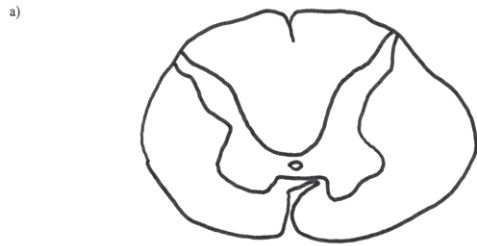


Spatial Distribution of Staining – Case 11

Case: 11
PARP

Levels:

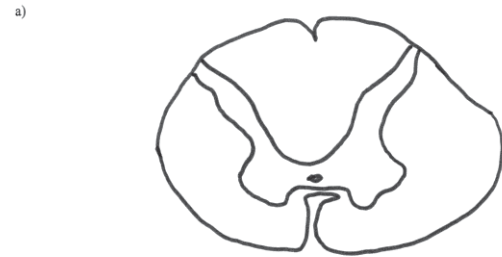
- a) At the site of compression - C2
- b) Two levels below site - C4



Case: 11
TUNEL

Levels:

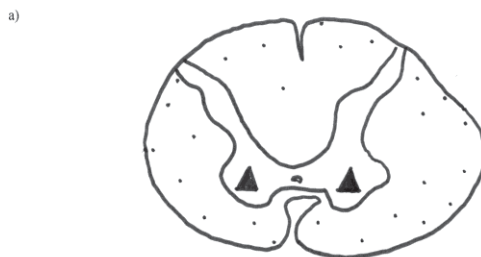
- a) At the site of compression - C2
- b) Two levels below site - C4




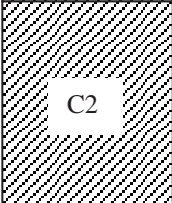
Case: 11
AIF 1

Levels:

- a) At the site of compression - C2
- b) Two levels below site - C4



Summary of immunohistochemistry Case 11

<p>Glia: DNA-PKcs (maximal), AIF, CMAP, PARP Axons: APP (maximal), AIF, Amy-33, CMAP Neurons: Amy-33, AIF</p>	 <p>C1-2</p>	<p>H&E: haemorrhage and hypercellularity, vacuolation, axonal swellings, AHC loss, gliosis, red cell change Weil: pallor : vacuolation</p>
<p>Glia: DNA-PKcs, AIF, CMAP, PARP Axons: APP, Amy-33, AIF, CMAP Neurons: Amy-33, AIF, PARP</p>	 <p>C2</p>	<p>H&E: Occasional vacuolation, loss of AHCs Weil: pallor : vacuolation</p>
<p>Glia: TUNEL, AIF, CMAP, PARP Axons: Amy-33, AIF, CMAP Neurons: TUNEL (rare), AIF, Amy-33, PARP</p>	<p>C3</p>	<p>H&E: Vacuolation, loss of AHCs Weil: pallor : vacuolation</p>
<p>Glia: TUNEL, AIF, CMAP, PARP Axons: APP, Amy-33, AIF, CMAP Neurons: APP (rare), Amy-33, TUNEL (max), AIF</p>	<p>C4</p>	<p>H&E: Vacuolation, loss of AHCs Weil: pallor : vacuolation</p>

Conclusion Survival in this case of traumatic fracture / dislocation was only 5 hours. Quadriplegia was suggestive of complete spinal cord injury. At the site of compression there were histopathological changes consistent with significant spinal cord damage and these changes lessened away from the site. Immunostaining using the APP antibody was accordingly maximal at the site, suggesting significant primary axonal injury. DNA-PKcs staining was also maximal at the site in keeping with DNA-damage. PARP glial staining was greatest in the anterior white matter at C1-2 and this may represent areas of DNA-damage and early repair. TUNEL immunopositivity in anterior horn cells and glia was found below the site of compression which may be explained by injury to motor tracts above. There was no positive staining using the active caspase-3 or caspase-9 antibodies, suggesting either an absence of caspase-dependent apoptotic processes or unsuitable time of survival for the occurrence of such processes. AIF was heterogeneously immunopositive at the site and below and did not correlate with the severity of histopathological changes. CMAP immunopositivity was heterogeneous and the specificity of this marker was questionable.

CASE 12

Case Summary A 48 year old male with a fracture/dislocation of C5-C6 vertebrae following a car rollover. He was quadriplegic at the C6 level. Haemorrhagic necrosis was found within spinal cord segments C5-T2. He died 1 day after injury from traumatic spinal cord and column injuries and cerebral oedema.

Pathology – brain

1. Recent infarction of right cerebellum and brain stem.
2. Traumatic right vertebral artery dissection.
3. Disruption of rostral brain stem by multiple secondary haemorrhages secondary to raised intracranial pressure in posterior fossa.

Pathology – spine and spinal cord

1. Post reduction C5/6 fracture dislocation.
2. Traumatic cervical myelopathy – haemorrhagic necrosis C7 segment of spinal cord.
3. Respirator brain with sloughing of necrotic cerebellar tonsils.

Haematoxylin and Eosin

Macroscopic findings On post-mortem examination there was a recent fracture through the intervertebral disc separating C5 and C6 vertebral bodies and extending obliquely downwards to involve the antero-superior half of the C6 vertebral body. Only remnants of the intervertebral disc and antero-superior half of C6 vertebral body were present. The posterior longitudinal ligaments were ruptured. The spinal canal was normal and not obstructed. The ligaments and soft tissues anterior to C5-6 were ruptured.

On opening the dural sac the spinal cord was found to be covered by fragments of necrotic cerebellar tissue maximal around the cervical cord. A transverse indentation was present at C7 segmental level. The pia mater was intact. Sections of the spinal cord showed almost total haemorrhagic necrosis of C7 segment with preservation only of a thin rim of peripheral subpial white matter. A core of haemorrhagic necrotic tissue dissected upwards in the right dorsal white matter column to C5 level and downwards to T2 level.

Tissue disruption is evident at C7 (N18). In section N19 (C7) the cord appears compressed into a near boomerang shape. Haemorrhage is seen macroscopically in both sections. At C5, C6, T1 and

T2 (N20, N21, N24, N25) there is an oval region of tissue disruption. Segments C3, C4 (N22, N23) and T3, T4 (N26, N27) appear macroscopically normal.

Microscopic findings A core of haemorrhagic necrotic tissue is present in the right dorsal white matter column descending down to T3 segmental level (N25) and ascending upwards to C5 segment (N21). Corpora amylacea are seen within the cord. At C7 (N18) there is severe necrosis and haemorrhage throughout. Many polymorphs are seen. Fewer numbers of neurons than normal are identifiable within the disrupted tissue. At section N19 of segment C7 the tissue is somewhat more preserved despite areas of haemorrhage, inflammation and vacuolation. In addition, many axonal swellings are found and there is a loss of anterior horn cells (AHCs). Most of the intrinsic blood vessels are patent but occasional small vessels show fibrous plugs.

At C6 (N20) there are less severe changes; that of mild vacuolation and occasional axonal swellings. The posterolateral white matter on one side is most affected. There is scattered haemorrhage and minor loss of AHCs with occasional red cell change. At C5 (N21) there is generalised vacuolation of the white matter and red cell change in neurons. At C4 (N22) there is vacuolation towards the cord periphery but no other significant changes. At C3 (N23) there is again mild peripheral vacuolation but in addition there are rare axonal swellings and AHC loss. At T1 (N24) there is a generalised vacuolation of the white matter, loss of AHCs, red cell change and a haemorrhagic region within the posterior column. At T2 (N25) the area of haemorrhage is smaller, there is subtotal loss of AHCs on one side, prominent red cell change and vacuolation. At T3 (N26) there is mild subpial vacuolation, loss of AHCs and red cell change. At T4 (N27) there is subtotal AHCs loss bilaterally, red cell change and vacuolation.

Weil There was no pallor on Weil stain and no evidence of demyelination.

Immunohistochemical results

CASE 12 – Trauma series – Immunological positivity (+) in glial, axonal or neuronal profiles:

Level	APP	Casp-3	DNA-PKcs	PARP	Bcl-2	Fas	Casp-9	TUNEL	Amy-33	CMAP	AIF
C3	-	-	-	+	-	-	-	-	-	+	+
C4	-	-	+	+	-	-	-	+	-	+	+
C5	-	-	-	+	-	-	-	-	+	+	+
C6	-	-	+	+	-	-	-	-	-	+	+
C7	-	-	-	+	-	-	-	-	+	+	+
T1	-	-	+	+	-	-	-	-	+	+	+
T2	-	-	+	+	-	-	-	+	-	+	+
T3	-	-	+	+	-	-	-	-	-	+	+
T4	-	-	+	+	-	-	-	+	-	+	+

* Shaded rows represent the site of compression

APP Axonal immunopositivity was seen at segments C3, C4 and C6 in the region surrounding an area of tissue necrosis (N19-23, N25). In these regions both small diameter axons and axonal swellings were seen. At C7 (N18) immunoreactive axonal swellings were rarely seen in the subpial region. There were immunopositive and occasional immunonegative axonal swellings. Equivocal immunostaining was seen in one neuron at T4 (N27) otherwise immunonegative. Negative in glia.

Active caspase-3 Non-specific immunopositivity was seen in the neuropil at C3 (N23) and C7 (N19). Equivocal immunopositivity in axonal swellings at C6, C7 (N19, N20). Negative in neurons.

DNA-PKcs Rare glial nuclear immunopositivity is seen in the subpial region at C6 (N20). There is occasional immunopositivity within axonal swellings and some equivocal staining of axonal swellings. At C5 (N21) there is equivocal glial immunostaining. At C4 (N22) there is rare glial nuclear immunopositivity in the white matter. C3 (N23), C8 (N19) and C7 (N18) are immunonegative. At T1 (N24) there is rare glial nuclear immunopositivity subpially. At T2 (N25), T3 (N26) and T4 (N27) there is rare glial nuclear immunopositivity in the white matter and equivocal staining within the neuropil. In addition at T4 (N27) there is equivocal staining within axonal swellings.

PARP Immunopositive glial nuclei were homogeneously spread throughout the cord in all segments. In addition there was cytoplasmic staining of unidentified cells which were consistent with macrophages in the white matter. The morphology was suggestive of oligodendrocytes. Immunopositive neuronal nucleoli were seen in the anterior and posterior horn at C6, C4 (N20, N22). Negative in axons.

Bcl-2 Negative in glia, neurons and axons.

Fas Equivocal immunopositivity in axonal swellings at C7, C6 (N19, N20). Negative in glia, neurons.

Caspase-9 Negative in glia, neurons and axons.

TUNEL Neuronal nuclear immunopositivity using TUNEL was rarely present in segments C4 (N22), T2 (N25) and T4 (N27). Negative in axons.

CMAP Immunopositivity was seen in glia, the majority of axons both small and large, and in ependymal cells. The degree of background staining negates the specificity of this marker at the dilution used.

Amy-33 amyloid beta Neuronal cytoplasmic immunoreactivity was seen at C5 (N21). At C7 (N19) there is immunopositivity in normal and enlarged axons throughout the white matter in the regions also immunopositive for APP, interspersed with immunonegative axonal swellings. Axonal immunoreactivity was also seen in this segment in the posterior white matter unilaterally. At T1 (N24) there was neuronal immunopositivity on both sides.

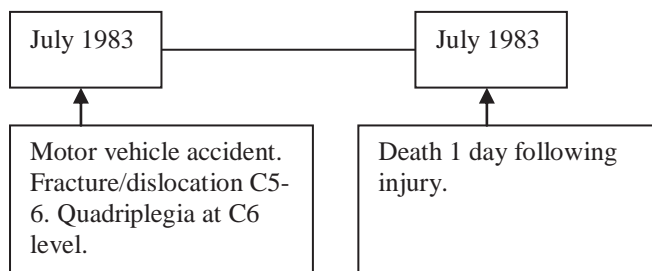
University of Melbourne amyloid beta Negative.

DAKO amyloid beta Negative.

AIF Above the site of compression at C3 (N23) immunopositive glia are occasionally found in all areas of the white matter. Neuronal cytoplasmic immunopositivity is found bilaterally. At C4 immunopositive glia are occasionally found within the white matter. Occasional neuronal cytoplasmic staining is found bilaterally. (N22) At C5 (N21) occasional immunopositive glia are present in the subpial region. Neuronal cytoplasmic staining is found bilaterally but greater numbers are present on one side. At C6 (N20) there is glial immunoreactivity throughout the white matter and neuronal immunoreactivity bilaterally. Staining was cytoplasmic. In the lateral white

matter foci of axonal swellings are seen and a proportion of medium to large axonal swellings are immunopositive for AIF. In section N18 of C7 there are regions of immunopositivity consistent with granular staining in dendritic processes but no distinct cellular profiles. In section N19 of segment C7 immunopositive axonal profiles are present throughout the white matter. These profiles range in size from normal sized axons to large axonal swellings. There is a subpopulation of negative axonal swellings. Occasional glial immunopositivity is seen in the glial cytoplasm. At T1 (N24) a similar pattern to C5 is seen where occasional immunopositive glia are present in the subpial region. Neuronal cytoplasmic staining is found bilaterally but greater numbers are present on one side. Immunopositive spheroids with a morphology consistent with corpora amylacea are seen. At T2 (N25) glial immunoreactivity is present in all regions except the deep white matter. Neurons and axons were immunonegative in this section. At T3 (N26) glial immunostaining is seen, greatest in number in the subpial region and excluding the deep white matter. Neuronal immunopositivity is found on both sides. At T4 (N27) immunopositive glia were occasionally seen in the subpial region otherwise the section was negative.

Timeline of clinical progression

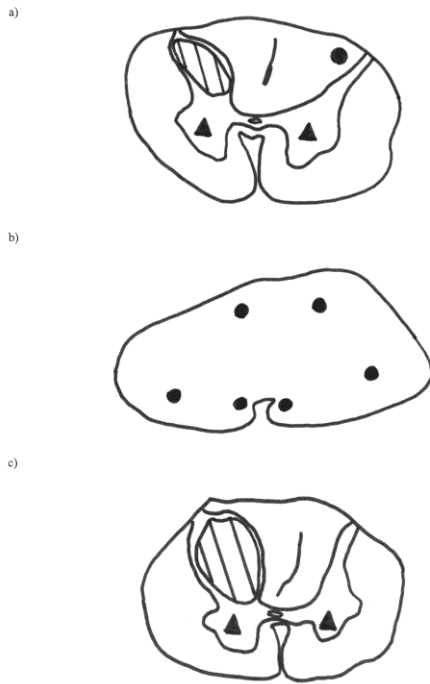


Spatial Distribution of Staining – Case 12

Case: 12
Amy-33

Levels:

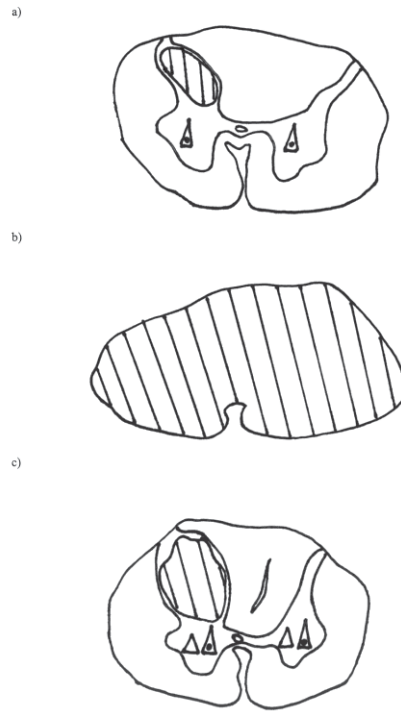
- a) Two levels above site - C5
- b) At the site of compression - C7
- c) Two levels below site - T1



Case: 12
Haematoxylin and eosin

Levels:

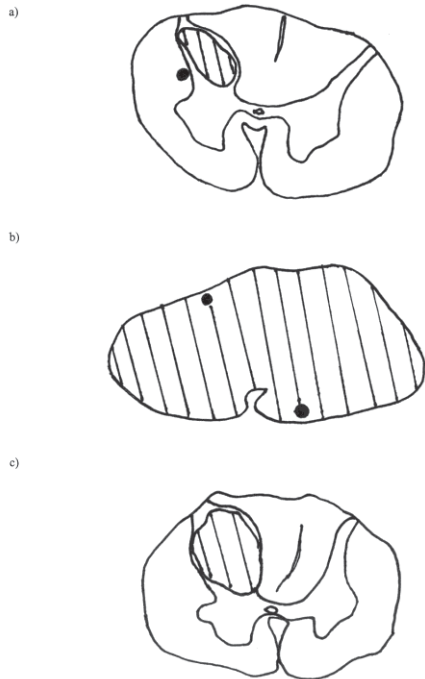
- a) Two levels above site - C5
- b) At the site of compression - C7
- c) Two levels below site - T1



Case: 12
APP

Levels:

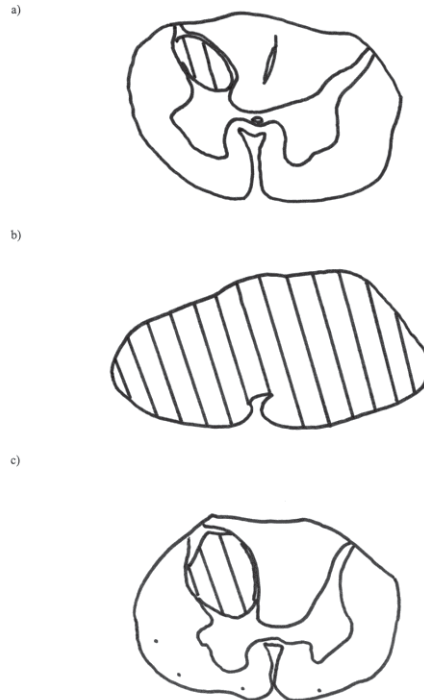
- a) Two levels above site - C5
- b) At the site of compression - C7
- c) Two levels below site - T1



Case: 12
DNA-PKcs

Levels:

- a) Two levels above site - C5
- b) At the site of compression - C7
- c) Two levels below site - T1

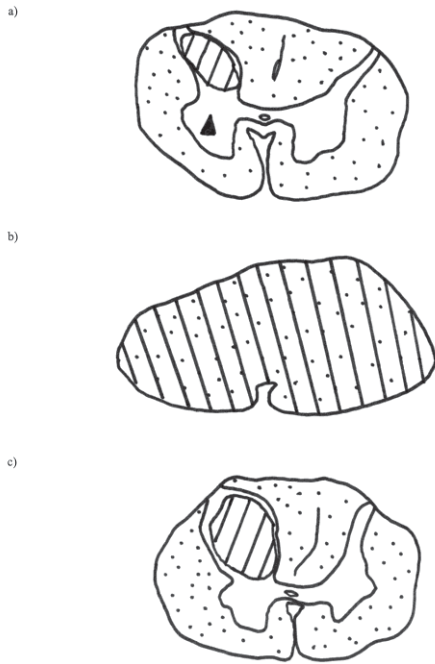


Spatial Distribution of Staining – Case 12

Case: 12
PARP

Levels:

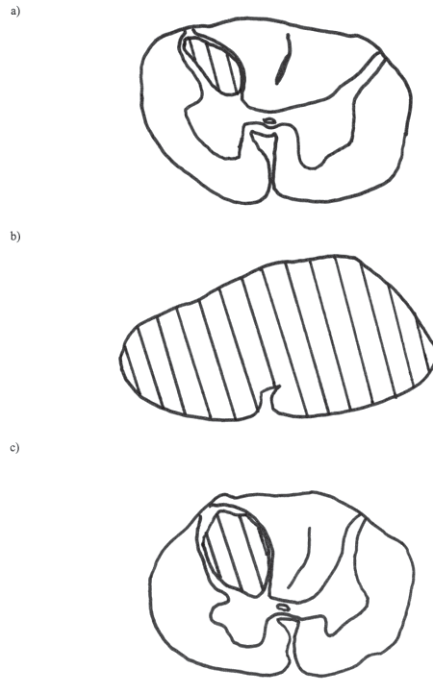
- a) Two levels above site - C5
- b) At the site of compression - C7
- c) Two levels below site - T1



Case: 12
TUNEL

Levels:

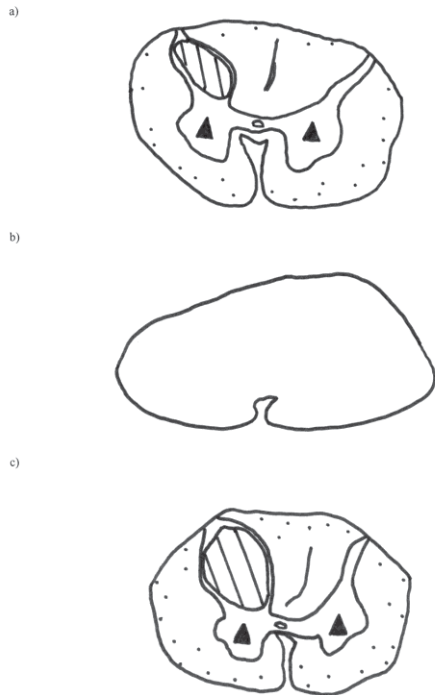
- a) Two levels above site - C5
- b) At the site of compression - C7
- c) Two levels below site - T1



Case: 12
AIF 1

Levels:

- a) Two levels above site - C5
- b) At the site of compression - C7
- c) Two levels below site - T1



Summary of immunohistochemistry Case 12

Glia: PARP, AIF, CMAP Axons: CMAP Neurons: AIF	C3	H&E: vacuolation, rarely axonal swellings, loss AHCs
Glia: DNA-PKcs (rare), PARP, AIF, CMAP Axons: CMAP Neurons: PARP, TUNEL (rare), AIF	C4	H&E: vacuolation
Glia: PARP, AIF, CMAP Axons: Amy-33, CMAP Neurons: AIF, Amy-33	C5	H&E: vacuolation and red cell change
Glia: DNA-PKcs (rare), PARP, AIF, CMAP Axons: DNA-PKcs, AIF, CMAP Neurons: PARP, AIF	C6	H&E: mild vacuolation, haemorrhage, axonal swellings, loss AHCs, occasional red cell change
Glia: PARP, AIF, CMAP Axons: AIF, CMAP Neurons: Nil	C7	H&E: Compression, haemorrhage, polymorphs. Necrosis, loss AHCs, axonal swellings
Glia: DNA-PKcs, PARP, AIF Axons: CMAP Neurons: AIF, Amy-33	T1	H&E: vacuolation, loss AHCs, red cell change, haemorrhage
Glia: DNA-PKcs (rare), PARP, AIF, CMAP Axons: CMAP Neurons: TUNEL (rare), AIF	T2	H&E: vacuolation, loss AHCs, red cell change, minor haemorrhage
Glia: DNA-PKcs (rare), PARP, AIF, CMAP Axons: CMAP Neurons: AIF	T3	H&E: mild vacuolation
Glia: DNA-PKcs (rare), PARP, AIF, CMAP Axons: CMAP Neurons: TUNEL (rare)	T4	H&E: vacuolation, loss AHCs, red cell change

Conclusion Severe haemorrhagic necrosis was present at the site of injury in similarity with other acute cases. There was no APP immunostaining in axons at the site of compression and this may represent a complete blockage of axonal transport. Furthermore, TUNEL staining was minimal towards the compression level and this may be due to the loss of neuronal and glial cells.

CASE 13

Clinical summary A 30 year-old man with past medical history of concussion following a head injury associated with an episode of loss of consciousness. There were no other known medical conditions, and no medications. He was involved in a motor vehicle accident - a single vehicle roll-over in which he was the driver. On review he was unconscious with a Glasgow coma score of 6/15. He was intubated at the scene and retrieved to the hospital. Episodes of bradycardia, hypotension and pulmonary oedema occurred during retrieval. Investigations performed included a CT head which revealed a traumatic subarachnoid haemorrhage, a cervical spine x-ray which revealed a step in the C4/C5 region and a CT chest which showed a left lung contusion and pulmonary oedema. Normal investigations included a CT abdomen / pelvis, CT of cervical spine of C7/T1, pelvic x-rays and lumbosacral spine x-rays. The patient's condition deteriorated over days with increasing intracranial pressure. A ventricular tachycardia / ventricular fibrillation arrest occurred resulting in death.

Cause of death

1. Closed head injury as a result of motor vehicle accident.

Other significant pathological findings:

2. Cervical spine fracture – C4/C5.
3. Pulmonary oedema and haemorrhage.
4. Sepsis.

Pathology – brain

1. Widespread subarachnoid haemorrhage.
2. Recent traumatic right basal ganglionic haemorrhage and adjacent ischaemic necrosis in disrupted perforator territory.
3. Scattered small petechial haemorrhages within the right central white matter.

Pathology – spine and spinal cord

1. Cervical spine fracture at level C4/C5 with C5/C6 segment affected.

Haematoxylin and Eosin

Macroscopic findings Haemorrhage in the region of the grey matter is suggested in segments C3, C4, C6 (N2, N3, N5) and especially at C5-6 (N9, N11). There is mild asymmetry at C6 (N5). At C5-6 (N11) the cord appears mildly compressed.

Microscopic findings At segment C3 (N2) there is generalised congestion of blood vessels, mild vacuolation, a loss of anterior horn cells (AHCs) and red cell change. In addition, there is a small focus of axonal swellings and polymorphs in the posterior column. At C4 (N3) the grey matter appears compressed. There is a region of haemorrhage and hypercellularity in the grey matter with rare axonal swellings. Red cell change is rarely present. The degree of congestion is lessened. At C5 (N4) there is a large region of haemorrhage within one side of the grey matter, AHC loss and central chromatolysis. The grey matter appears compressed. There is a focus of axonal swellings in both deep posterior columns. At C6 (N5) there is central chromatolysis, compression of the grey matter and AHC loss. At C5-6 (N9, 11) there is severe haemorrhage throughout and axonal swellings with cystic change. At C7 (N6) there is central chromatolysis, red cell change and loss of AHCs. Mild vacuolation of the subpial region is present. At C8 (N7) there is a loss of AHCs, a generalised loss of glia particularly in the subpial region and mild subpial vacuolation.

Weil At C5-6 (N9) there is distinct pallor of the cord. On microscopic analysis this appears to be due to many axonal swellings within the white matter, a proportion of which have an absence of Weil positivity around the rim suggestive of demyelination. There is no apparent Wallerian degeneration.

Immunohistochemical results

CASE 13 – Trauma series – Immunological positivity (+) in glial, axonal or neuronal profiles:

Level	APP	Casp-3	DNA- PKcs	PARP	Bcl-2	Fas	Casp-9	TUNEL	Amy-33	CMAP	AIF
C3	-	-	+	+	-	-	-	-	+	+	+
C4	+	-	-	+	-	-	-	-	+	+	+
C5	+	+	+	+	-	-	-	-	+	+	+
C6	+	+	+	+	-	-	-	-	+	+	+
C7	+	-	-	+	-	-	-	-	+	+	+
C8	-	-	-	+	-	-	-	+	+	+	+

* Shaded rows represent the site of compression

APP Axonal immunopositivity was seen in all segments except C8 (N7) and in C3 (N2) where there was equivocal staining. Axonal immunoreactivity was macroscopically visible at C6 (N5) and C5-6 (N9, N11). Positive normal and swollen axons were present as foci in the subpial region at C4 (N3). Axonal immunopositive swellings were also seen in the lateral subpial region on one side and in the deep posterior columns at C6 (N5). These axons were larger in diameter than at C4.

Occasional immunonegative axonal swellings were also noted. At C7 (N6) immunopositivity was only seen in the lateral subpial area on one side in mildly enlarged axons. Equivocal glial cytoplasmic staining was present in small numbers of glia. Equivocal staining was occasionally found in AHC nuclei and cytoplasm.

Active caspase-3 Non-specific immunopositivity was seen within the neuropil particularly in the subpial region. Immunopositive within axonal swellings at C5-6 (N9). Negative in neurons.

DNA-PKcs Segments C5-6 (N11) was immunonegative for glia. In section N9 of segment C5-6, at C6 (N5) and C3 (N2) there was widespread glial nuclear staining however the majority of immunopositive cells were polymorphic in profile. At C8 (N7) C7 (N6) and C4 (N3) there was equivocal glial immunopositivity. Negative within axons and neurons.

PARP Immunopositive glia were rarely present at C8 (N7). At C5-6 (N9) there was glial staining in the anterolateral cord. Immunopositive glial nuclei were dispersed throughout the white matter at segments C3, C4, C6 and C7 (N2, N3, N5, N6) maximal at C3-4. Negative within axons and neurons.

Bcl-2 Negative within glia, axons and neurons.

Fas Negative within glia and neurons. Equivocal staining within axonal swellings.

Caspase-9 Immunonegative within glia, neurons. Equivocal staining within axonal swellings.

TUNEL Immunopositive glial profiles were very rarely seen at C8 (N7), essentially negative. Negative within neurons, axons.

CMAP Immunopositivity was seen in glia, the majority of axons both small and large, and in ependymal cells. The degree of background staining negates the specificity of this marker at the dilution used.

Amy-33 amyloid beta Immunopositive axonal profiles, small and large, in regions matching that of APP staining were present. These axons were greater in number than that seen using the APP marker. Segment C8 (N7) is immunonegative for axons. Foci of axonal immunopositivity were seen in the subpial regions and deep posterior columns at segment (N11). At C5-6 (N9) positive axonal swellings extend throughout the entire posterolateral white matter, subpial anterior white matter and anterior corticospinal tract. At C7 (N6) there is a single focus of axonal

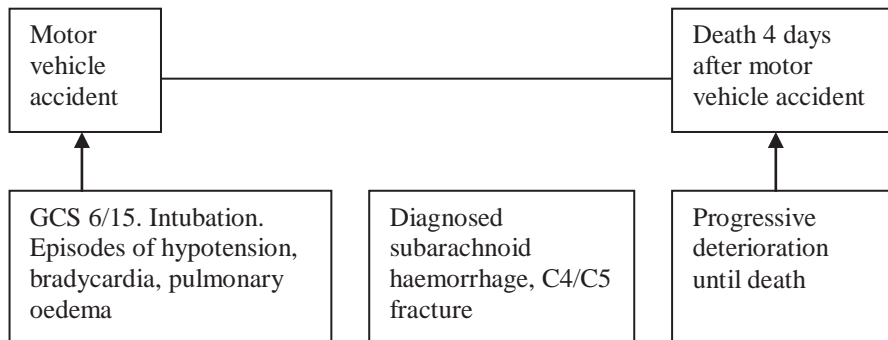
immunopositivity in the lateral subpial region on one side. These axons are mildly enlarged. Occasional small positive axonal profiles are seen scattered throughout the rest of the white matter. At C6 (N5) many normal diameter immunopositive axons are spread throughout the white matter, greater in number in the subpial area, as well as three large foci of axonal swellings: one in the lateral white matter; and two in the each of the deep posterior columns. There is associated vacuolation of tissue. At C4 (N3) similar changes are present but in fewer axons. At C3 (N2) there is a single focus of axonal swellings in the gracile fasciculus on one side with vacuolation. There was cytoplasmic immunopositivity of neurons at C3, C4, C5-6, C6, C7, C8 and T3 (N2, N3, N5, N6, N7, N11). In addition, many glia showed cytoplasmic immunopositivity using Amy-33 amyloid-beta antibody at C3, C4, C6, C7, C8 and T3 (N2, N3, N5, N6, N7, N11).

University of Melbourne amyloid beta Negative.

DAKO amyloid beta Negative.

AIF Glial cytoplasmic immunoreactivity is seen throughout the white matter at C3 (N2). Two neurons in one anterior horn and five on the other are immunopositive for AIF within the cytoplasm. At C4 (N3) glial cytoplasmic staining is seen in all areas of white matter. Neuronal cytoplasmic immunopositivity is present on both sides. There is no axonal immunostaining. At the site of compression in section N19 of segment C5-6 there is no glial or neuronal immunopositivity. Focal collections of immunopositive axonal swellings are seen in posterolateral white matter on both sides and in the anterior white matter unilaterally. These cellular profiles are the diameter of medium to large axonal swellings and may represent axonal retraction bulbs. However, in section N10 of segment C5-6 there is immunostaining within small or normal sized axons. Axonal immunopositivity is found throughout the white matter. In addition there is glial immunopositivity in the posterolateral white matter. There is a subpopulation of negative axonal swellings dispersed between those that are positive. In section N11 of C5-6 there is glial cytoplasmic immunoreactivity in all regions of the white matter. Axonal immunopositivity is seen in medium to large sized axons in the anterolateral white matter. There is no neuronal staining for AIF. At C6 (N5) glial cytoplasmic staining is seen in all areas of white matter. Neuronal cytoplasmic immunopositivity is present on both sides. Axonal immunopositivity in medium sized axonal swellings is occasionally seen in one lateral corticospinal tract. At C7 (N6) glial cytoplasmic staining is seen in all areas of white matter. Neuronal cytoplasmic immunopositivity is present on both sides. There is no axonal immunostaining. At C8 (N7) there are occasional glial immunopositive profiles and neuronal cytoplasmic immunopositivity bilaterally. At T1 (N8) glial cytoplasmic staining is seen in all areas of white matter. Neuronal cytoplasmic immunopositivity is present on both sides. There is no axonal immunostaining.

Timeline of clinical progression



Spatial Distribution of Staining – Case 13

Case: 13

Amy-33

Levels:

- a) Two levels above site - C3
- b) At the site of compression - C5-6
- c) Two levels below site - C8

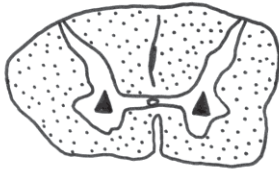
a)



b)



c)



Case: 13

Haematoxylin and eosin

Levels:

- a) Two levels above site - C3
- b) At the site of compression - C5-6
- c) Two levels below site - C8

a)



b)



c)



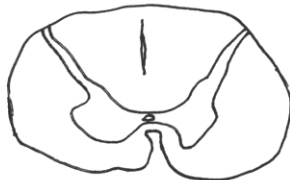
Case: 13

APP

Levels:

- a) Two levels above site - C3
- b) At the site of compression - C5-6
- c) Two levels below site - C8

a)



b)



c)



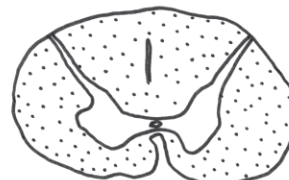
Case: 13

DNA-PKcs

Levels:

- a) Two levels above site - C3
- b) At the site of compression - C5-6
- c) Two levels below site - C8

a)



b)



c)



Spatial Distribution of Staining – Case 13

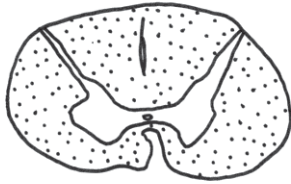
Case: 13

PARP

Levels:

- a) Two levels above site - C3
- b) At the site of compression - C5-6
- c) Two levels below site - C8

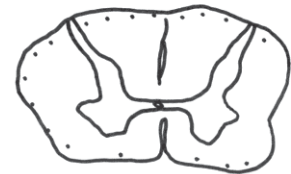
a)



b)



c)



Case: 13

TUNEL

Levels:

- a) Two levels above site - C3
- b) At the site of compression - C5-6
- c) Two levels below site - C8

a)



b)



c)



Case: 13

AIF 1

Levels:

- a) Two levels above site - C3
- b) At the site of compression - C5-6
- c) Two levels below site - C8

a)



b)



c)



Summary of immunohistochemistry Case 13

<p>Glia: DNA-PKcs, PARP, Amy-33, AIF, CMAP Axons: Amy-33, CMAP Neurons: Amy-33, AIF</p>	C3	<p>H&E: Congestion, vacuolation, AHC loss, red cell change, axonal swellings, polymorphs (rare) Weil: no evidence demyelination</p>
<p>Glia: PARP, Amy-33, AIF, CMAP Axons: APP, Amy-33, CMAP Neurons: Amy-33, AIF</p>	C4	<p>H&E: Compression grey matter, haemorrhage, hypercellularity, axonal swellings (rare), red cell change (rare), congestion (mild)</p>
<p>Glia: DNA-PKcs, PARP, AIF, CMAP Axons: APP (max), CMAP, AIF, Amy-33 (max), caspase-3 Neurons: Amy-33, AIF</p>	C5	<p>H&E: Compression grey matter, haemorrhage, AHC loss, central chromatolysis, axonal swellings Weil: demyelination surrounding axonal swellings</p>
<p>Glia: DNA-PKcs, PARP, Amy-33, AIF, CMAP Axons: APP (max), CMAP, AIF, Amy-33 (max), caspase-3 Neurons: Amy-33, AIF</p>	C6	<p>H&E: Central chromatolysis, haemorrhage within grey matter, AHC loss, haemorrhage, axonal swellings, cystic change Weil: demyelination surrounding axonal swellings</p>
<p>Glia: PARP, Amy-33, AIF, CMAP Axons: APP, Amy-33, CMAP Neurons: Amy-33, AIF</p>	C7	<p>H&E: Central chromatolysis, red cell change, vacuolation, loss AHCs</p>
<p>Glia: PARP (rare), TUNEL (rare), Amy-33, AIF, CMAP Axons: CMAP Neurons: Amy-33, AIF</p>	C8	<p>H&E: AHC loss, mild vacuolation subpially</p>

Conclusion Survival post-injury was short at 88 hours. Histopathological changes at the site of compression were severe with haemorrhagic necrosis, loss of anterior horn cells and axonal injury suggested by axonal swellings and supported by APP antibody reactivity maximal at the site of compression. APP immunopositivity also extended above and below the site indicating widespread axonal injury. PARP and DNA-PKcs immunopositive glia were found at the site suggesting DNA-damage however there was minimal TUNEL immunopositivity, perhaps due to insufficient injury time for the breakdown of DNA into 100-150 base pair segments. Caspase-3 antibody reactivity occurred in axonal swellings at the site of compression and this may be due to the accumulation of intracellular protein with disrupted axonal transport. At segment C5-6 (N9), the most severely affected level, there was no immunopositivity within neurons for Amy-33 amyloid beta however this may be attributed to the extent of tissue disruption and loss of cells. Furthermore, glia were negative at this level. AIF and CMAP staining was heterogeneous and in many cell types.

CASE 14

Clinical summary A 67 year-old male injured in a car roll-over accident resulting in fracture/dislocation of T7-T8 vertebrae. Haemorrhagic necrosis was found in spinal cord segments T6-T9. Paraplegia was present at the T6 spinal level. He died 6 days following injury.

Pathology – brain

1. Traumatic subarachnoid haemorrhage over the posterior half of the brain.
2. Scattered petechial haemorrhages of the corpus callosum and right dorsolateral brainstem.
3. Minimal bilateral gliding contusions.
4. Possible patchy ischaemic damage of cerebral cortex and central grey matter.

Pathology – spine and spinal cord

1. Central haemorrhagic necrosis of T6-7 spinal cord.
2. Traumatic haemorrhagic necrosis of T6-7 spinal cord.
3. Diffuse axonal injury.

Haematoxylin and Eosin

Macroscopic findings On post-mortem examination there was a complete transverse fracture of the odontoid process with the overlying ligaments being intact. There was no evidence of encroachment on the spinal canal. A fracture was present through the inter-vertebral disc separating C6 and C7 vertebral bodies with rupture of the anterior ligaments but no associated soft tissue haemorrhage. The spinal canal was not compressed by this lesion and the posterior ligaments were intact. There was a complex compression fracture involving T7 and T8 vertebral bodies with disruption of the intervertebral disc and a vertical fracture through the T7 vertebral body such that the anterior part of the vertebra was separate from the rest of the body. The T8 vertebra was compressed anteriorly with a fracture separating the anterior part of the body from the remainder of the vertebra apart from its attachment to the anterior ligaments. There was severe compression of the spinal canal at this level. The remainder of the vertebral column was macroscopically intact.

The dura mater was intact. On opening the dura mater the spinal cord was swollen and slightly discoloured at T6-7 segments. The overlying pia mater was intact. The anterior spinal artery was intact. Segmental sections through the level of cord compression at T6-7 showed recent haemorrhagic necrosis affecting the central part of the cord with only a thin rim of peripheral intact white matter, the white matter being better preserved on the left side of the cord. At the T5 level the necrotic tissue was only present as a central core (2 mm) at the base of the posterior columns. The

T4 segment was normal. Segmental sections of the cord above this level were normal apart from some irregular congestion of the central grey matter at the T2 level. The T8 spinal cord showed a small central core of necrotic tissue but the levels below this were macroscopically normal.

The cord appears narrow in diameter at T10 (N27). Necrosis is evident at T6, T7 and T10 (N25, 27, 28, 41, 42, 43, 44, 46). At segments N29 and N47 there is a cord of abnormal tissue which appears to be herniated spinal cord. The cord appears rounded or oval within normal limits.

Microscopic findings A core of herniated necrotic tissue was present. Corpora amylacea are seen within the cord. At N25 (T8) there are foci of axonal swellings in the white matter. Polymorphs are present in the tissue away from the haemorrhage and there is severe cystic necrosis. There is a loss of anterior horn cells with central chromatolysis. Occasional small areas of haemorrhage are seen. At T10 (N27) there is vacuolation and central chromatolysis. At T6 (N28) and T7 (N41-N43) haemorrhagic necrosis was evident. There were macrophages and polymorphic cells seen with subtotal destruction of the cord. In preserved regions there is vacuolation and axonal swellings. No neurons were present except in section N44 of segment T7 where there was central chromatolysis of neurons. In section N45 of segment T6 there was relative preservation of the white matter. Foci of axonal swellings were seen in the anterior and lateral corticospinal tracts. There was vacuolation of the peripheral white matter and loss of AHCs with central chromatolysis. At section N46 of T6 there were areas of axonal swellings and vacuolation. A loss of AHCs and central chromatolysis was noted. Rarely, polymorphs were seen to invade the tissues. There were small pockets of haemorrhage. At T5 (N29) there is a rare vacuolation subpially and mild AHC loss. In section N47 of T5 there is central chromatolysis. At T4 (N30) and T3 (N31) there is subpial vacuolation and AHC loss. In addition there is central chromatolysis at T3.

Weil There was no pallor on Weil staining and no evidence of a demyelinating process or Wallerian degeneration.

Immunohistochemical results

CASE 14 – Trauma series – Immunological positivity (+) in glial, axonal or neuronal profiles:

Level	APP	Casp-3	DNA- PKcs	PARP	Bcl-2	Fas	Casp-9	TUNEL	Amy-33	CMAP	AIF
T3	-	-	-	+	-	-	-	+	-	-	+
T4	-	-	+	+	-	-	-	+	+	-	+
T5	+	-	+	+	-	-	-	+	+	-	+
T6	+	-	+	+	+	-	-	+	+	-	+
T7	+	-	+	+	-	-	-	+	+	-	+
T8	+	-	+	+	-	+	-	+	+	-	+
T10	-	-	+	+	-	-	-	+	+	-	+

* Shaded rows represent the site of compression

APP Macroscopically visible immunopositive axonal swellings were seen in sections T5-T8 in posterior, lateral and anterior regions of the cord (N25, N44-47) and in the lateral column of section N43 (T7). At T7 (N43) there were also smaller areas of APP reactive axonal swellings. At T5 (N29) two small regions of immunopositive axons of normal diameter and equivocal immunopositivity were found in the lateral subpial area. T7 (N41, 42) and T6 (N28) also contained foci of immunopositivity within axons. Axonal immunoreactivity was rarely present at T10 (N27). T3 and T4 (N31, 30) were negative for APP.

Active caspase-3 Equivocal staining within cytoplasm of polymorphic cells and axonal swellings. This axonal staining was strongest at T8 (N25). Negative in neurons.

DNA-PKcs Immunopositive axonal swellings at T7 (N42, 44) and T8 (N25). Immunopositive glial nuclei are rarely present at segments T6 (N28), T4 (N30), and T8 (N25). Immunonegative for glia at T3 (N31). Immunopositive glial nuclei are found occasionally in the white matter at segment T10 (N27), T6 (N45, 46) and T5 (N29, 47) and are maximal at T5-T6. Glial immunopositivity is occasionally seen at T7 however there is a large degree of tissue disruption. Neuronal nuclear staining is visible at T5 and T7 (N44, N47). Neuronal cytoplasmic immunoreactivity is present unilaterally at T10 (N27). At T6 (N28) occasional immunopositive cells are seen with a morphology suggestive of phagocytes.

PARP Immunopositive glial nuclei with morphology consistent with oligodendrocytes are seen throughout the preserved cord in all segments. Negative in axons. Nuclear neuronal staining was seen in both anterior horns at T6 (N45).

Bcl-2 Immunonegative in glia. Equivocal staining within axonal swellings. One immunopositive neuronal nucleus was seen at T6 (N45).

Fas Equivocal staining was found in axonal swellings of the anterolateral subpial region of T8 (N25). Elsewhere, equivocal staining was seen at T6, T7 (N41-46) and T3 (N31). Negative in glia, neurons.

Caspase-9 Equivocal staining within axonal swellings. Negative in neurons and glia.

TUNEL Occasional glial nuclear immunopositivity was seen in all segments except T6 (N28) which showed non-specific staining. Neuronal nuclear staining was seen at T5 (N29).

CMAP Immunopositivity was seen in glia, the majority of axons both small and large, and in ependymal cells. The degree of background staining negates the specificity of this marker at the dilution used.

Amy-33 amyloid beta Immunopositive axonal profiles, small and large, in regions matching that of APP staining and in addition at T10 (N27) and T6 (N27) in normal size axons. A very large number of normal size axons were immunoreactive perhaps indicating the high severity of injury. These axons were greater in number than that seen using the APP marker and the areas involved included some immunonegative axons. In many neurons, especially AHCs, cytoplasmic immunopositivity was seen. At T4 (N30) there was neuronal cytoplasmic staining and immunopositivity in axons of normal diameter.

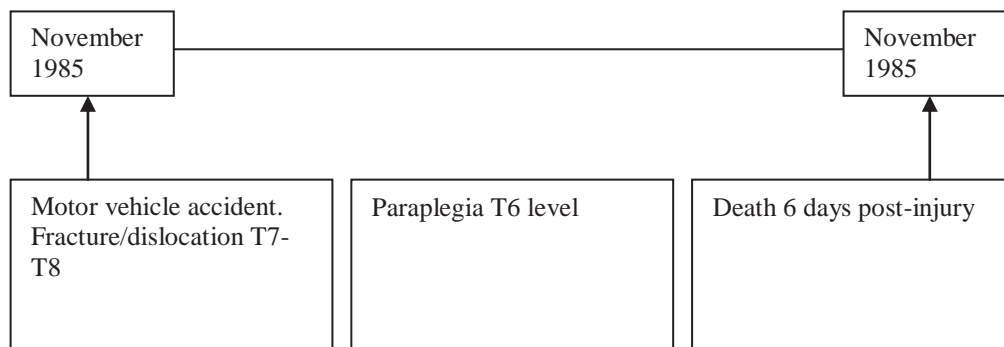
University of Melbourne amyloid beta Negative.

DAKO amyloid beta Negative.

AIF At T3 (N31) there is glial cytoplasmic staining throughout the white matter and equivocal immunostaining within neurons, but no axonal immunopositivity. At T4 (N30) glial cytoplasmic immunopositivity was present throughout the white matter. Neuronal immunopositivity was found in 3 anterior horn cells bilaterally. At T5 (N29) there is glial cytoplasmic staining throughout the white matter and neuronal immunopositivity bilaterally. In section N28 of segment T6

immunopositive glia are seen dispersed throughout the white matter in the regions unaffected by tissue necrosis. There were no immunopositive neurons seen at this level. Axonal immunopositivity was occasionally present unilaterally in the preserved anterior white matter. In section N46 of segment T6 axonal immunopositivity was present in all regions of white matter, greatest in the lateral corticospinal tract and gracile fasciculi. Glial cytoplasmic staining is seen throughout the white matter and neuronal immunopositivity in all regions of grey matter. In section N41 of segment T7 there is subtotal tissue necrosis but axonal and glial cytoplasmic immunopositivity in preserved subpial regions. At T7 (N47) glial cytoplasmic staining is present throughout the white matter and neuronal cytoplasmic staining throughout the grey. There was no axonal immunopositivity at this level. In section N42 of segment T7 many immunopositive axonal swellings are present in the preserved anterior white matter and fewer immunonegative axonal swellings. Occasional glial cytoplasmic staining is also seen. In section N44 of segment T7 axonal immunopositivity is present throughout the lateral and anterior white matter, focally within the lateral corticospinal and lateral spinothalamic tracts bilaterally, and anterior corticospinal tract unilaterally. Staining is present in axonal swellings and axons of normal diameter. Neuronal immunopositivity is seen in all regions of the grey matter. Glial cytoplasmic staining is also present in the anterolateral white matter and deep posterior columns. The same pattern of staining is present at T8 (N25) but axonal immunopositivity is maximal at this level. At T10 (N27) immunopositive glia and greater than 10 immunopositive neurons were seen bilaterally.

Timeline of clinical progression

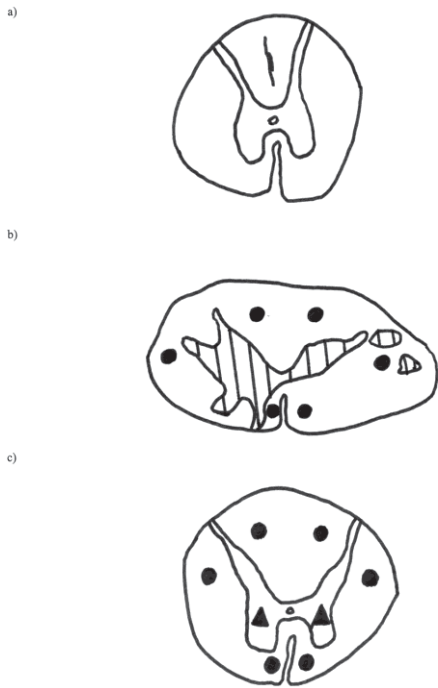


Spatial Distribution of Staining – Case 14

Case: 14
Amy-33

Sections:

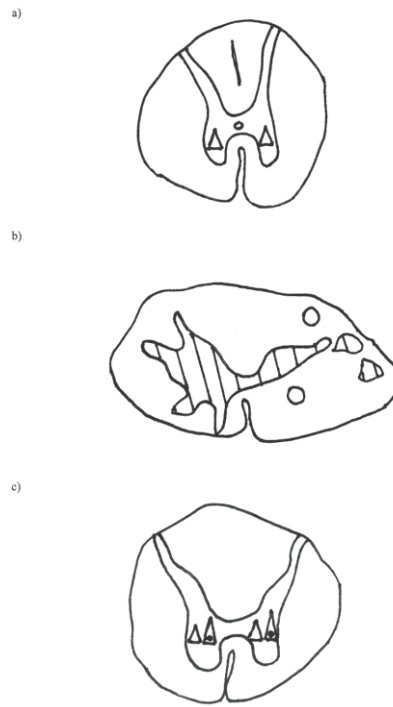
- a) Two levels above site - T4
- b) At the site of compression - T6
- c) Three levels below site - T10



Case: 14
Haematoxylin and eosin

Sections:

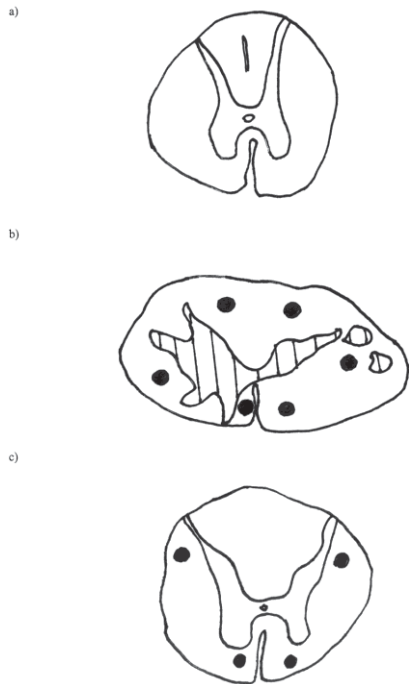
- a) Two levels above site - T4
- b) At the site of compression - T6
- c) Three levels below site - T10



Case: 14
APP

Sections:

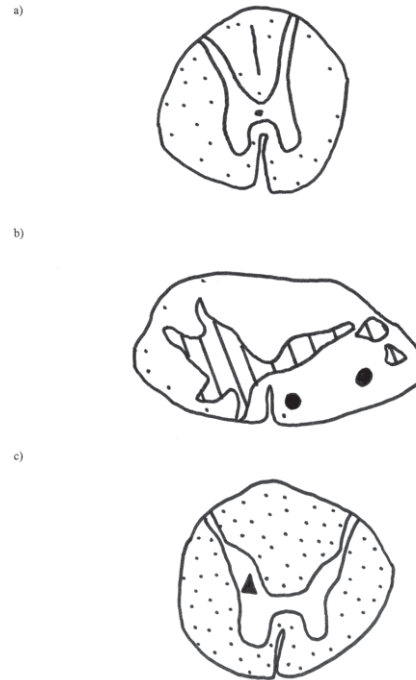
- a) Two levels above site - T4
- b) At the site of compression - T6
- c) Three levels below site - T10



Case: 14
DNA-PKcs

Sections:

- a) Two levels above site - T4
- b) At the site of compression - T6
- c) Three levels below site - T10



Spatial Distribution of Staining – Case 14

Case: 14
PARP

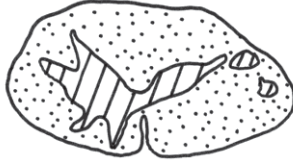
Sections:

- a) Two levels above site - T4
- b) At the site of compression - T6
- c) Three levels below site - T10

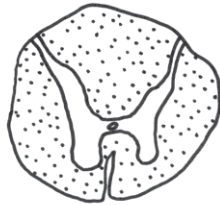
a)



b)



c)



Case: 14
TUNEL

Sections:

- a) Two levels above site - T4
- b) At the site of compression - T6
- c) Three levels below site - T10

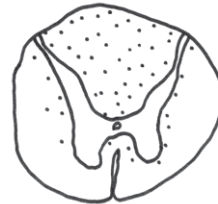
a)



b)



c)



Case: 14
AIF 1

Sections:

- a) Two levels above site - T4
- b) At the site of compression - T6
- c) Three levels below site - T10

a)



b)



c)



Summary of immunohistochemistry Case 14

<p>Glia: PARP, TUNEL, AIF, CMAP Axons: CMAP Neurons: AIF</p>	<p>T3</p>	<p>H&E: Subpial vacuolation, AHC loss, central chromatolysis</p>
<p>Glia: DNA-PKcs (rare), PARP, TUNEL, AIF, CMAP Axons: CMAP Neurons: AIF</p>	<p>T4</p>	<p>H&E: Subpial vacuolation, AHC loss</p>
<p>Glia: DNA-PKcs, PARP, TUNEL, AIF, CMAP Axons: APP (max), Amy-33, CMAP Neurons: DNA-PKcs, AIF</p>	<p>T5</p>	<p>H&E: Subpial vacuolation, mild AHC loss, central chromatolysis</p>
<p>Glia: DNA-PKcs, PARP, TUNEL, AIF, CMAP Axons: APP (max), Amy-33, DNA-PKcs, AIF, CMAP Neurons: PARP, Bcl-2 (rare), AIF</p>	<p>T6</p>	<p>H&E: Axonal swellings, vacuolation, polymorphic infiltrate, macrophages, haemorrhagic necrosis, loss AHCs</p>
<p>Glia: DNA-PKcs, PARP, TUNEL, AIF, CMAP Axons: APP (max), DNA-PKcs, Amy-33, AIF, CMAP Neurons: DNA-PKcs, AIF</p>	<p>T7</p>	<p>H&E: Axonal swellings, vacuolation, polymorphic infiltrate, macrophages, haemorrhagic necrosis, loss AHCs, central chromatolysis</p>
<p>Glia: DNA-PKcs (rare), PARP, TUNEL, AIF, CMAP Axons: APP (max), DNA-PKcs, Fas, Amy-33, AIF, CMAP Neurons: AIF</p>	<p>T8</p>	<p>H&E: Axonal swellings, polymorphic infiltrate, haemorrhagic necrosis, loss AHCs, central chromatolysis</p>
<p>Glia: DNA-PKcs, PARP, TUNEL, AIF, CMAP Axons: Amy-33, CMAP Neurons: DNA-PKcs, AIF</p>	<p>T10</p>	<p>H&E: Vacuolation, central chromatolysis</p>

Conclusion In variation to other cases, PARP immunopositivity was observed within neuronal nuclei instead of nucleoli at T6 (N45). Furthermore, at this level there was the only neuronal immunopositivity to the Bcl-2 marker within neuronal nuclei in the study. DNA-PKcs neuronal nuclear immunoreactivity was also a feature. These findings may therefore represent an immediate response by the cell to cytotoxic stressors with activation of Bcl-2 and potential DNA repair by the PARP enzyme and DNA-PKcs. It may indicate the occurrence of an apoptotic process of cell death whereby neuronal loss is the eventual outcome. PARP glial immunopositivity was frequently seen within cells resembling oligodendrocytes. AIF immunopositivity was present in glia and neurons of all segments. Axonal immunopositivity was also observed at T6, T7 and maximally at T8.

CASE 15

Clinical summary A 26 year-old male with a fracture/dislocation of T5-T6 vertebrae after falling from his motorbike. He was paraplegic at T5 spinal level. Haemorrhagic necrosis was found within spinal cord segments T3-T10. Patient died 18 days after injury from acute respiratory distress syndrome.

Pathology – brain

1. Scattered petechial haemorrhages in the central white matter of the cerebral hemispheres.
2. Microinfarction consistent with cerebral fat embolism.

Pathology – spine and spinal cord

1. Fracture dislocation of T5, T6 vertebral column.
2. Haemorrhagic necrosis of T6, T7 spinal cord with ascending herniation of necrotic tissue.

Haematoxylin and Eosin

Macroscopic findings On post-mortem examination there was an area of haemorrhagic necrosis present at the T7 segmental level with focal circumferential atrophy. The adjacent cord segments were swollen up to the T5 level and down to the T8/9 level. The cord was segmentally sectioned. There was haemorrhagic necrosis at the T7 level extending rostrally to T6. From T5 to T2 there was a central cord of necrosis in the base of the posterior white matter columns. The upper thoracic cord and cervical cord were normal. Both thoracic and lumbar sacral cords were macroscopically normal. Examination of the hemisected vertebral column revealed complete fracture dislocation of T5, T6 through the intervertebral disc.

There is asymmetry and distortion of the cord at T7 (N42, 43) more marked in section N42. The cord appears flattened at section N44 of T7. At T5 (N52) and T9 (N55) small areas of cystic cavitation are evident, increasing to involve the entire posterolateral cord on one side at section T8 (N54). There is pallor of the cord at T6 (N53) which may indicate generalised necrosis. At T4 (N50) and T3 (N51) there is a rounded area of pale tissue likely to be a herniation of necrotic tissue.

Microscopic findings At T7 (N42) there is generalised necrosis with small areas of haemorrhage. Macrophages and polymorphs are present in the remaining tissue. There is a complete loss of neurons. Similar changes are present in section N43 and N44 of T7 and T6 (N53) but more severe in nature with subtotal cystic necrosis. There is a loss of glia in preserved anterior and

posterolateral white matter. At C8 (N46) there is loss of AHCs, subtotal on one side and more minor loss on the other. There is mild vacuolation of the gracile fasciculus but no other changes. At T1 (N45) there is mild subpial vacuolation laterally with rare axonal swellings and AHC loss. At segment T2 (N49) there is AHC loss and central chromatolysis of lateral horn neurons. At T4 (N50) there is a subtotal loss of AHCs with central chromatolysis of anterior and lateral neurons. There are regions of vacuolation in the anterolateral subpial white matter with foci of axonal swellings. In addition, the deep posterior columns show severe cystic cavitation and macrophages. Occasional axonal swellings line this area. At T3 (N51) there is subtotal AHC loss with central chromatolysis of lateral neurons. Two small areas of vacuolation and axonal swellings are present in the lateral subpial white matter. There is a large cavity occupying the deep posterior columns and necrotic tissue. At N52 (T5) there is a subtotal loss of AHCs with central chromatolysis of anterior and lateral neurons. Severe cystic necrosis of the anterior, lateral and posterior white matter is seen extending from the subpial region inwards. In addition there is cystic involvement of the entire cuneate fasciculus bilaterally. Axonal swellings are present and macrophages are seen in the most severely affected regions. Similar changes are present at T8 (N54) however there is additional involvement of almost the entire posterolateral white matter on one side. At T9 (N55) the changes are the same as found in section N52. At T10 (N56) similar changes are again seen however there is relative preservation of one cuneate fasciculus. Numbers of glia were decreased at segment T7 (N44).

Weil Pallor in regions of necrosis due to tissue disruption. No apparent evidence of demyelination.

Immunohistochemical results

CASE 15 – Trauma series – Immunological positivity (+) in glial, axonal or neuronal profiles:

Level	APP	Casp-3	DNA- PKcs	PARP	Bcl-2	Fas	Casp-9	TUNEL	Amy-33	CMAP	AIF
C8	-	-	-	-	-	-	-	-	-	+	-
T1	-	-	+	+	-	-	-	+	+	+	+
T2	-	-	-	-	-	-	-	+	+	+	+
T3	+	-	-	+	-	-	-	+	+	+	+
T4	+	-	+	-	-	-	-	+	+	+	+
T5	+	-	-	+	-	-	-	+	+	+	+
T6	+	-	-	+	-	-	-	+	+	+	-
T7	+	-	-	+	-	-	-	+	+	+	-
T8	+	-	+	+	-	-	-	+	+	+	+
T9	+	-	+	+	-	-	-	+	+	+	+
T10	+	-	-	+	-	-	-	+	+	+	+

* Shaded rows represent the site of compression

APP A very small region of axonal immunoreactivity is present in the lateral white matter at section N42 and N44 (T7). There is severe tissue disruption at this level and thus the exact location of this staining is difficult to determine. A larger focus of axonal positivity is seen in section N43 (T7). Sections N46 (C8), N45 (T1) and N49 (T2) were immunonegative for APP. Foci of staining in axonal swellings was found in the subpial anterolateral white matter at T4 (N50). At T3 (N51) immunopositivity was confined to the lateral corticospinal tract on one side and rarely elsewhere in the lateral white matter. Axonal immunopositivity was macroscopically visible at T6 (N53) and was most commonly seen in the anterolateral cord. Numbers of positive axons were maximal at levels T5, T6, T8 and T9 and were found in regions of preserved white matter. Many equivocally immunostained axonal swellings were also seen. Occasional positive axons of normal as well as large diameter were present. At segment T10 (N56) immunoreactive axons were occasionally present however there was a focus of larger, positive axonal swellings in the lateral subpial region on one side. Negative in glia.

Active caspase-3 Negative in glia, axons and neurons. Equivocal cytoplasmic immunoreactivity was present in occasional binucleate or polymorphic cells within the white matter.

DNA-PKcs Rarely immunopositive in axonal swellings of the subpial white matter at T1 (N45), T4 (N50), T8 (N54) and T9 (N55). Non-specific immunoreactivity was seen at segment T6 (N53). All segments were negative in glia, neurons.

PARP Despite the severity of necrosis, PARP glial immunopositivity was only occasionally seen at T6 (N53), T7 (N44), T8 (N54) T9 (N55). At segments T1 (N45), T3 (N51), T5 (N52) and T10 (N56) staining was rarely present in glial cells. Negative in glia at T7 (N42, 43), T2 (N49) and T4 (N50). Negative in neurons and axons.

Bcl-2 Negative in glia, axons and neurons.

Fas Negative in glia, neurons. Rarely there was equivocal immunostaining in axonal swellings.

Caspase-9 Negative in glia, neurons. Rarely there was equivocal immunostaining in axonal swellings.

TUNEL Occasional glial immunoreactivity in areas of preserved white matter at T7 (N42-44). At T1 (N45) and T2 (N49) there is glial staining in the white and grey matter maximal towards the central cord. Neuronal immunopositivity is also seen in these segments. At T3 (N51) there was maximal glial immunoreactivity in grey and white matter and immunopositive neurons were present in anterior and posterior horns. At T4 (N50) glial immunoreactivity was found in the posterior columns, throughout the grey matter and surrounding central white matter. Five immunopositive anterior horn cells were seen on one side and three on the other. At T5 (N52) occasional glia consistent in appearance with microglia were immunopositive tending towards the central cord. At T6 (N53) rare glial positivity was seen in preserved tissue. At T8 (N54) immunopositive glia were present in the anterior white matter and anterolateral subpial region. At T9 (N55) scattered immunopositive glia were present in the white and grey matter. Two immunopositive anterior horn cells were seen on one side. Maximal glial immunopositivity was seen at segment T10 (N56) throughout grey and white matter. Immunopositive neurons were seen in all regions of grey matter. There was no immunopositivity within axons in any segment.

CMAP Immunopositivity was seen in glia, the majority of axons both small and large, and in ependymal cells. The degree of background staining negates the specificity of this marker at the dilution used.

Amy-33 amyloid beta Immunopositive axonal profiles, small and large, in regions matching that of APP staining were present. Foci of axonal immunopositivity were seen maximal in the subpial

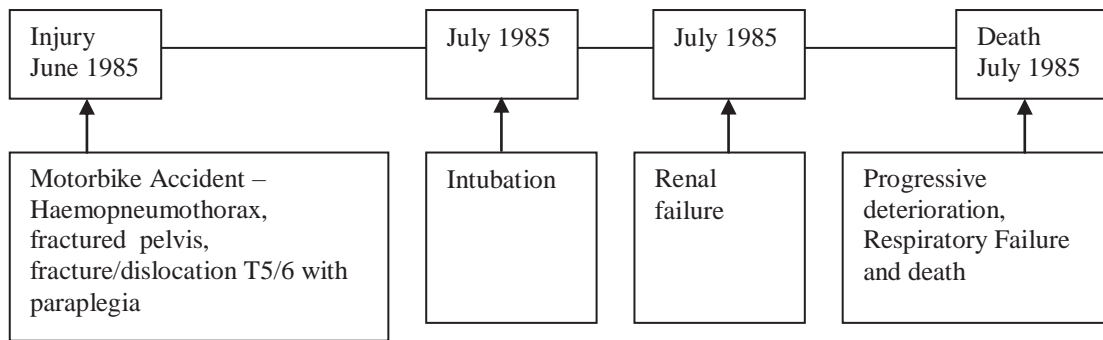
region and gracile fasciculi at T8 (N54), T9 (N55) and T10 (N56). Neuronal immunopositivity was seen at T9 (N55). At T6 (N53) there was intense immunopositive staining in groups of longitudinal and transverse axonal profiles throughout the necrotic cord excluding the preserved regions of white matter. At T5 (N52) axonal staining was seen in the lateral and anterior white matter maximal in the lateral and anterior corticospinal tracts. At T3 (N51) distinct foci of axonal immunoreactivity were found in the deep posterior columns and lateral corticospinal tract on one side. Immunopositive subpial foci in many small and some large axonal profiles were present at T4 (N50) in the anterior and lateral white matter only. Segment T2 (N49) was immunopositive within the cytoplasm of anterior horn cells. Immunopositive axonal profiles were rare at T1 (N45). At T7 (N42, 43) rare foci of longitudinal axonal immunopositive profiles were noted. Amy-33 immunopositive axons were greater in number than that seen using the APP marker.

University of Melbourne amyloid beta Negative.

DAKO amyloid beta Negative.

AIF At T1 (N45) and T2 (N49) there is glial cytoplasmic staining throughout the white matter and neuronal cytoplasmic immunopositivity in all regions of the grey matter. At T3 (N51) there are immunopositive swellings in the lateral corticospinal tract and lateral subpial white matter on one side. Immunopositive glia are present throughout the white matter and positive neurons throughout the grey. At T4 (N50) there are focal regions of axonal immunopositivity in the lateral white matter. Neuronal cytoplasmic staining is seen on both sides in all regions of the grey matter. Glial cytoplasmic immunopositivity is present in the subpial region anteriorly and dispersed throughout the rest of the white matter. There is a similar pattern of immunostaining at T9 (N55) however the numbers of immunopositive axonal profiles are greater. At T8 (N54) immunopositive axonal swellings are visible along the border of tissue necrosis in the region of the lateral corticospinal tract. Immunopositivity in neuronal cytoplasm and glial cytoplasm is also present bilaterally in preserved regions. At T10 (N56) a similar pattern of staining was seen however at this segment there was no necrosis and the axonal immunopositivity was present in the subpial lateral white matter on one side only. At T5 (N52) immunopositive axonal swellings were present in focal areas throughout the white matter. There was no neuronal immunopositivity in this segment. Glial cytoplasmic immunostaining was found in preserved white matter. There is no immunopositivity at T6 (N53). Subtotal tissue necrosis was present at T6 (N53) and T7 (N42-44) with staining only present in macrophages and immunonegative glia and neurons in small regions of preserved spinal cord. Negative axonal swellings were interspersed with immunopositive profiles. Immunopositivity was seen within tissue macrophages in areas of necrosis. The cytoplasm of ependymal cells was immunopositive.

Timeline of clinical progression



Spatial Distribution of Staining – Case 15

Case: 15
Amy-33

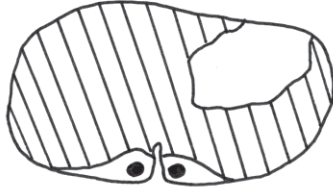
Sections:

- a) Two levels above site - T4
- b) At the site of compression - T6
- c) Two levels below site - T9

a)



b)



c)



Case: 15
Haematoxylin and eosin

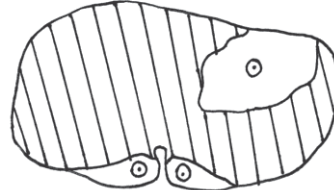
Sections:

- a) Two levels above site - T4
- b) At the site of compression - T6
- c) Two levels below site - T9

a)



b)



c)



Case: 15
APP

Sections:

- a) Two levels above site - T4
- b) At the site of compression - T6
- c) Two levels below site - T9

a)



b)



c)



Case: 15
DNA-PKcs

Sections:

- a) Two levels above site - T4
- b) At the site of compression - T6
- c) Two levels below site - T9

a)



b)



c)



Spatial Distribution of Staining – Case 15

Case: 15
PARP

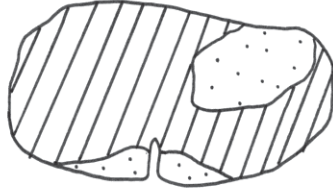
Sections:

- a) Two levels above site - T4
- b) At the site of compression - T6
- c) Two levels below site - T9

a)



b)



c)



Case: 15
TUNEL

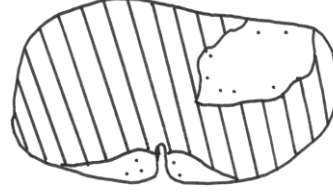
Sections:

- a) Two levels above site - T4
- b) At the site of compression - T6
- c) Two levels below site - T9

a)



b)



c)



Case: 15
AIF 1

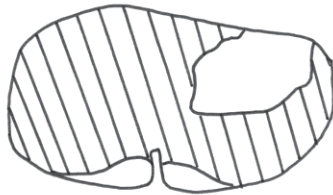
Sections:

- a) Two levels above site - T4
- b) At the site of compression - T6
- c) Two levels below site - T9

a)



b)



c)



Summary of immunohistochemistry Case 15

Glia: CMAP Axons: CMAP Neurons: Nil	C8	H&E: loss AHCs, mild vacuolation
Glia: PARP (rare) TUNEL, AIF, CMAP Axons: DNA-PKcs, Amy-33, CMAP Neurons: TUNEL, AIF	T1	H&E: loss AHCs, mild vacuolation, rare axonal swellings
Glia: PARP, TUNEL, AIF Axons: DNA-PKcs, APP, Amy-33 Neurons: TUNEL, AIF	T2	H&E: loss AHCs, central chromatolysis lateral horn
Glia: PARP (rare) TUNEL, AIF, CMAP Axons: APP, AIF, Amy-33, CMAP Neurons: TUNEL, AIF	T3	H&E: subtotal loss AHCs, central chromatolysis lateral horn, vacuolation, axonal swellings, cavitation
Glia: TUNEL, AIF, CMAP Axons: APP, DNA-PKcs, Amy-33, CMAP Neurons: TUNEL, AIF	T4	H&E: loss AHCs, central chromatolysis ant/lateral horn, vacuolation, axonal swellings, cystic cavitation, macrophages
Glia: PARP (rare) TUNEL, AIF, CMAP Axons: APP (max), AIF, Amy-33, CMAP Neurons: Nil	T5	H&E: severe cystic necrosis, loss AHCs, central chromatolysis ant/lateral horn, axonal swellings, macrophages
Glia: PARP, TUNEL, CMAP Axons: APP (max), Amy-33, CMAP Neurons: Nil	T6	H&E: pallor, asymmetry, necrosis, loss AHCs, macrophages, polymorphs, minor haemorrhage
Glia: PARP, TUNEL, CMAP Axons: APP, Amy-33, CMAP Neurons: Nil	T7	H&E: asymmetry, necrosis, loss AHCs, macrophages, polymorphs, minor haemorrhage, fewer glia
Glia: PARP, TUNEL, AIF, CMAP Axons: APP (max), DNA-PKcs, AIF, Amy-33, CMAP Neurons: AIF	T8	H&E: severe cystic necrosis (max), loss AHCs, central chromatolysis ant/lateral horn, axonal swellings, macrophages
Glia: PARP, TUNEL, AIF, CMAP Axons: APP (max), DNA-PKcs, AIF, Amy-33, CMAP Neurons: TUNEL, AIF, Amy-33	T9	H&E: severe cystic necrosis, loss AHCs, central chromatolysis ant/lateral horn, axonal swellings, macrophages
Glia: PARP (rare) TUNEL, AIF, CMAP Axons: APP, AIF, Amy-33, CMAP Neurons: TUNEL, AIF	T10	H&E: severe cystic necrosis, loss AHCs, central chromatolysis ant/lateral horn, axonal swellings, macrophages

Conclusion Necrosis was present in the 6 lower segments of this case from T5 to T10. In addition, neuronal damage was indicated by the presence of anterior horn cell loss in all segments and central chromatolysis in 7 of the 11 segments analysed. Axonal damage was indicated by APP immunopositivity in the lower 8 segments, often found in focal areas such as the lateral corticospinal tract. TUNEL and AIF positivity was present in neurons and glia in the majority of segments.

CASE 16

Clinical summary A 52 year-old male. Iatrogenic compression occurred during spinal surgery. Quadriplegia resulted from injury to the C3 spinal level. Cystic necrosis was found at C1-C4. Patient died 26 days after injury from bronchopneumonia and adult respiratory distress syndrome.

The patient had presented 20 days prior to operation with pain and weakness in both arms and legs. On examination of his central nervous system he was found to have reduced power in the left arm and left leg and somewhat reduced reflexes. Sensation appeared to be normal. He was then seen by the neurologists who diagnosed a post-viral demyelinating lesion high in the spinal cord above C5. A cervical myelogram was performed. CSF was clear and colourless and there appeared no obvious obstruction or lesions present. X-ray showed a congenital abnormality of C1-2 with non-union of the odontoid peg with pronounced anterior atlas subluxation. The assessment made at this time was that the odontoid peg lesion was long-standing but maybe producing cord signs. Over the next three days it was noted that his weakness, particularly in the right and left upper limbs, was becoming more pronounced and it was decided that he needed fusion of C1 and C2. He underwent this procedure which resulted in post-operative quadriplegia and hyper-reflexia. The operation was revised but there was no neurological improvement.

Operation:

This man, with an unstable subluxation of the dens consequent upon a congenital os odontoideum, had a Gallie fusion of C1 and C2. The operation terminated and he was then found to be quadriplegic. An urgent myelogram showed partial obstruction at C1-2. Myodil appeared to flow along the sides of the cord, but wires passing behind the arch of C1 to C2 appeared to be intruding into the canal. The position of fixation appeared satisfactory. There was an appearance of obstruction anterior to the cord where the Myodil stopped opposite of the spinal cord. He was returned to theatre, placed prone and the wound re-opened.

Second operation findings:

There was a wide space between the arch of C1 and the arch of C2 due to the developmental anomaly. The ligamentum flavum had been previously divided and on separating this it was possible to see two wires indenting the posterior aspect of the dural sac to a depth of at least 5 mm. On removing the wires the dural sac filled out and occupied the whole of the spinal canal. The sac now pulsated. A rubber catheter could be passed beneath the arch of C2 freely, but not beneath C1, because the ligamentum flavum and dura were adherent here. There appeared to be no further pressure on the sac. The surgeon explored either side, anterior to the nerve roots of C2 and there was no sign of an extra-dural haematoma. He did not therefore feel it necessary to open the dural

sac. The arches were then re-wired, placing the wire beneath C1 as previously, but now around the spine of C2. This appeared to give a satisfactory alignment and on inspecting the dural sac it still appeared to be under no tension and to pulsate. The wound was then closed in layers.

Comment:

The patient must be presumed to have had severe cord compression for about four hours. During this time the quadriplegia appeared to have become complete.

Post-mortem findings:

A laminectomy was carried out on the fixed vertebral column and skull base. X-rays had been taken of the removed specimen. A doubled wire anchored C1 and C2 vertebrae posteriorly over the back of the arches. It was looped in front of the posterior arch of C1 and beneath the spinous process of C2, with the free ends twisted together. There appeared to be a second wire around the first looped wire, twisted together probably to tighten the loop. When the posterior portion of the column was removed, the dura was exposed and found to be intact. The dura was opened and the spinal cord was exposed. The cord was found to be continuous and without transection. There was however, at the C2 level, an obvious point of narrowing in the spinal cord; rather like a "waist". The cord above and below was swollen. There was impressive softening of the cord at the level of the narrowed point and for several segments below. These appearances are consistent with mechanical compression of the spinal cord at that level, which could have resulted from anterior bulging of the posterior dura by pressure from the wire.

The sectioned column showed that the odontoid process was not joined to the anterior arch of C2 and there was a mobile segment behind the anterior arch of C1.

Pathology – brain

1. Normal brain.

Pathology – spine and spinal cord

1. Recent necrosis of upper cervical spinal cord extending macroscopically over C1-C5 segments and maximal at C2-C3 segments.

Haematoxylin and Eosin

Macroscopic findings There was an area of circumferential softening (12mm in length) involving the cord between segments C2 and C3. The remainder of the spinal cord appeared macroscopically normal. The anterior and posterior roots were normal. The dura mater and leptomeninges were

normal. The anterior spinal artery was patent and free of atheroma. Sections through the area of softening showed severe necrosis of the cord, most severe in the anterior half of the cord, with scattered small petechial haemorrhages mainly involving the central part of the cord. Sections above the area of softening showed that the lesion extended irregularly to the C1 level. Caudally the lesion reached to the C5 segment with a small focus of central necrosis extending over several segments in the right posterior horn.

There is pallor, disruption of the tissue and flattening of the cord at C3 (N13) and distal to the lesion at N18. There is occasional tissue damage at other levels but these appear artefactual. In section N15, proximal to the lesion, the cord appears mildly asymmetrical. Mild flattening of the posterior cord is seen in section N20 of segment C4. All other segments appear macroscopically normal.

Microscopic findings Corpora amylacea are seen. Proximal to the lesion (N15) subtotal tissue necrosis with areas of haemorrhage and macrophage infiltration are present with preservation of the anterior white matter and lateral subpial white matter. There is a complete loss of grey matter. Axonal swellings are seen in the lateral cord bilaterally however numbers are greater on one side. At C1 (N17) there is loss of AHCs particularly on one side and red cell change. On the opposite side there are occasional axonal swellings in the lateral white matter in addition to mild posterolateral vacuolation. Distal to the lesion in section N18 tissue necrosis is seen in the grey matter, lateral white matter on one side and posterior columns, with preservation of the anterior white matter, subpial posterior white matter and the majority of the lateral white matter. Anterior horn cells are rarely present. Occasional axonal swellings are visible in the lateral and posterior cord. At C3 (N19) there is bilateral loss of AHCs and red cell change on one side. Vacuolation and axonal swellings are seen throughout the lateral white matter on one side with mild vacuolation of the other. Vacuolation, occasional axonal swellings and cystic cavitation are seen in the posterior columns. At segment C3 (N13) there is subtotal necrosis of the cord and presence of macrophages. In section N20 of segment C4 the tissue parenchyma is intact. There is a mild loss of AHCs and central chromatolysis of one neuron. A small area of tissue necrosis is found in each posterior horn filled with macrophages. In the deep posterior column unilaterally there is a small region of cystic necrosis. Vacuolation and occasional axonal swellings occur in the lateral cord. In section N21 of C4 the regions of haemorrhagic necrosis in the posterior horn, and vacuolation in the lateral white matter, are enlarged. There is also vacuolation of the anterior and posterior white matter. There is a significant loss of AHCs and red cell change. In section N22 of C4 the white matter is relatively preserved, however the region of necrosis within one posterior horn remains enlarged. There is a loss of AHCs with red cell change and central chromatolysis a feature. Vacuolation of the anterior and lateral white matter is seen particularly on one side. At C5 (N23, N24) there is loss of AHCs

and red cell change bilaterally. Vacuolation is seen in the white matter and posterior horns. Rarely, axonal swellings are present in the posterior column in section N23. At C6 (N25) there is a mild loss of AHCs and vacuolation throughout the white matter and posterior horns. Segments C7 (N28) and L5 (N36) appear normal except for mild vacuolation of the posterior horns.

Weil Pallor suggestive of demyelination is present at C4 (N20-22) and C6 (N23-25) in the lateral corticospinal tract on one side and in the opposing lateral corticospinal tract in section N20 of C4.

Immunohistochemical results

CASE 16 – Trauma series – Immunological positivity (+) in glial, axonal or neuronal profiles:

Level	APP	Casp-3	DNA- PKcs	PARP	Bcl-2	Fas	Casp-9	TUNEL	Amy-33	CMAP	AIF
C1	+	-	-	+	-	-	-	+	+	+	+
C3	+	-	+	+	-	-	-	+	+	+	+
C4	+	-	+	+	-	-	-	+	+	+	+
C5	-	-	+	+	-	-	-	+	+	+	+
C6	-	-	+	+	-	-	-	+	+	+	+
C7	-	-	+	+	-	-	-	+	+	+	+
L5	-	-	-	+	-	-	-	+	+	+	+

* Shaded rows represent the site of compression

APP Axonal immunopositivity was seen near regions of cystic necrosis in addition to possible macrophage immunopositivity at C3 (N13), proximal and distal to the site of injury, and rarely at C1 (N17). Rare immunoreactivity was seen in spherical structures suggestive of axonal swellings at C4 (N20-22). No axonal immunoreactivity was present at C5 and C6 (N23-25) or at C7 (N28) and L5 (N36). Immunopositive profiles proximal (N15) and distal (N18) to the site of compression were occasionally difficult to distinguish as either glia or small axons. Negative in neurons.

Active caspase-3 Occasional cytoplasmic immunoreactivity was seen in the white matter at C3 (N13) in addition to rare positivity in axonal swellings. However, due to the disruption of the tissue this axonal staining may represent background staining. Equivocal cytoplasmic staining was rarely seen at C4 (N20, N22). Negative in neurons.

DNA-PKcs Immunonegative at C1 (N17). At C3 (N13) immunoreactivity within glial nuclei was seen however the high degree of background staining may account for this. Proximal to the lesion

(N15), distal to the lesion (N18) and at C3 (N19), C4 (N21, N22), C5 (N24), C6 (N25) and C7 (N28) there was occasional glial nuclear staining in the subpial area possibly due to tissue disruption. In addition there was equivocal cytoplasmic staining within macrophages in section N15. Negative at L5 (N36). Immunoreactivity occurred in axonal swellings at C3 (N19). Negative in neurons.

PARP Neuronal nucleoli were immunoreactive in the anterior horn of C5 and C6 (N23-25). Glial nuclear immunopositivity was found dispersed in the white matter at C3 (N13). Staining tended towards the subpial region proximal to the lesion (N15) and at C3 (N19), C4 (N20-N22), C5 (N23, 24), C6 (N25), C7 (N28) and L5 (N36). The morphology of cells was that of oligodendrocytes. PARP glial immunoreactivity was rarely seen in the lateral subpial region at C1 (N17). Negative in axons.

Bcl-2 Negative in glia, axons and neurons.

Fas Negative in glia and neurons. Rare, nonspecific immunostaining was seen at C3 (N13) in areas of hypercellularity. Equivocal immunoreactivity was seen in axonal swellings of the lateral white matter distal to the site (N18).

Caspase-9 At C3 (N13), proximal to the site (N15) and distal to the site (N18) rare cytoplasmic immunopositivity was seen in areas of hypercellularity. Negative in axons and neurons.

TUNEL Immunoreactivity was within the nuclei of macrophages and remaining glia at segment C3 (N13) and proximal to the site of compression in section N15. Many neuronal nuclei and glial nuclei were immunopositive in the central region of the cord at C1 (N17) and slightly fewer in number at C3 (N19). Fewer immunopositive glia again were seen in section N20 of segment C4 tending towards the central cord however immunoreactive neuronal numbers were maintained. In section N21 of C4 only rare neuronal immunopositivity was seen. However, in section N22 of C4 glial positivity was found throughout the cord and many neuronal nuclei were positive. At C5 (N23) immunopositive glia and neurons were found in the central cord but in section N24 of C5 there was no neuronal immunopositivity and rare glial immunopositivity. At segment C6 (N25) occasional neuronal and glial staining occurred towards the central cord. At C7 (N28) and at L5 (N36) many neurons and glia were immunoreactive throughout the cord. Immunopositive glial and neuronal nuclei were dispersed throughout the cord distal to the site (N18).

CMAP Immunopositivity was seen in glia, the majority of axons both small and large, and in ependymal cells. The degree of background staining negates the specificity of this marker at the dilution used.

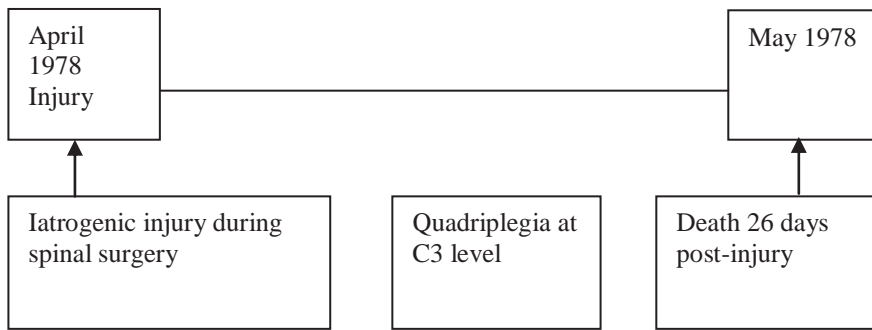
Amy-33 amyloid beta Immunopositive axonal profiles, small and large, in regions matching that of APP staining were present. These axons were greater in number than that seen using the APP marker. At C3 (N13) immunoreactivity was present in axons in preserved tissue. Proximal to the site of compression at N15 many immunoreactive axonal swellings are seen throughout the white matter but particularly in the lateral cord. At C1 (N17) there is neuronal cytoplasmic staining and occasional glial cytoplasmic staining. Distal to the site at N18 there is neuronal and occasional glial cytoplasmic staining as well as axonal reactivity in small and large diameter profiles particularly in the posterolateral cord. A similar pattern of staining is seen at C3 (N19). At C4 (N20 and N21) there is neuronal and occasional glial cytoplasmic staining as well as occasional axonal reactivity in small and large diameter profiles particularly in the posterolateral cord. At C4 (N22), C5 (N23, N24) and C6 (N25) there is neuronal cytoplasmic staining and occasional immunoreactivity in axons and axonal swellings. At C7 (N28) and L5 (N36) Amy-33 immunoreactivity was present in neuronal cytoplasm.

University of Melbourne amyloid beta Negative at segment distal to site of compression (N18).

DAKO amyloid beta Negative at segment distal to site of compression (N18).

AIF Proximal to the site of compression (N15) there is glial immunopositivity throughout the preserved white matter and immunopositive axonal swellings in the lateral region. At C1 (N17) immunopositive glia are scattered throughout the white matter and there is bilateral neuronal immunopositivity. Staining is cytoplasmic. At the site of compression, C3 (N19), a similar pattern of glial and neuronal staining is seen. In section N13 of segment C3 there are glia and occasional axonal swellings which are immunopositive in the preserved white matter. At C4 (N20-22) there is glial cytoplasmic immunoreactivity throughout the anterolateral white matter and in the subpial posterior white matter. Bilateral neuronal immunopositivity is present. At C5 (N23, N24) and C6 (N25) there is immunopositivity in glia throughout the anterior white matter and lateral white matter on one side, with immunopositivity found only in glia of the subpial region on the opposite side, and in the subpial region posteriorly. There is bilateral neuronal cytoplasmic staining. Immunopositive spheroids consistent with corpora amylacea are seen. Distal to the site of compression (N18) there is glial immunopositivity throughout the preserved white matter. At C7 (N28) and L5 (N36) there are occasional immunopositive glia in the subpial region and there is bilateral neuronal cytoplasmic immunopositivity.

Timeline of clinical progression

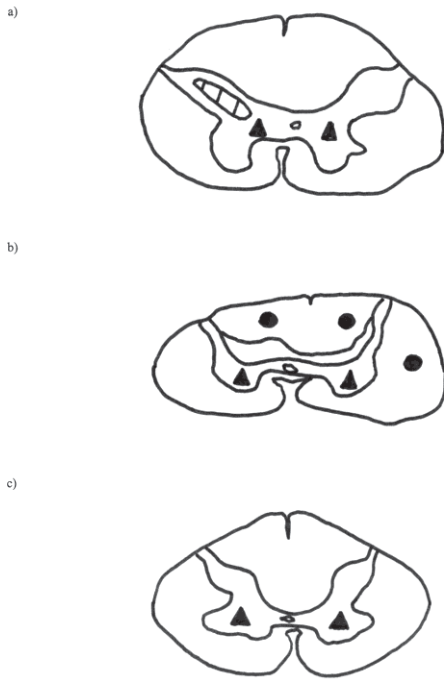


Spatial Distribution of Staining – Case 16

Case: 16
Amy-33

Sections:

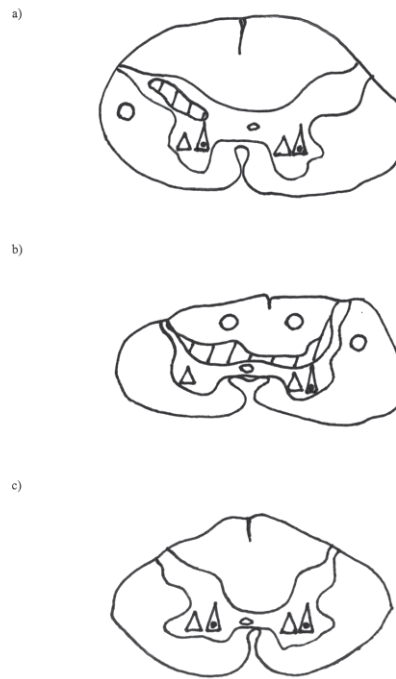
- a) Two levels above site - C1
- b) At the site of compression - C3
- c) Two levels below site - C5



Case: 16
Haematoxylin and eosin

Sections:

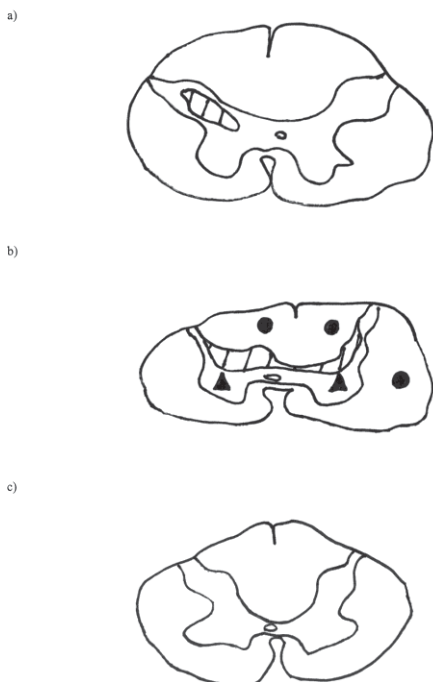
- a) Two levels above site - C1
- b) At the site of compression - C3
- c) Two levels below site - C5



Case: 16
APP

Sections:

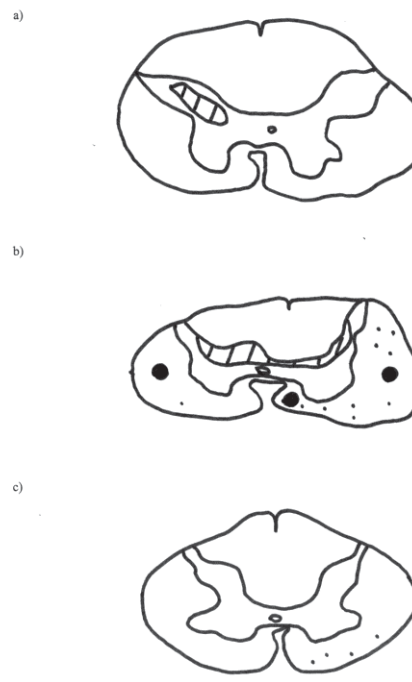
- a) Two levels above site - C1
- b) At the site of compression - C3
- c) Two levels below site - C5



Case: 16
DNA-PKcs

Sections:

- a) Two levels above site - C1
- b) At the site of compression - C3
- c) Two levels below site - C5

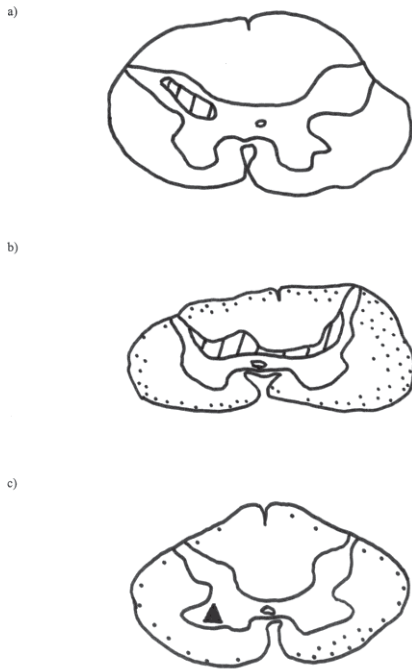


Spatial Distribution of Staining – Case 16

Case: 16
PARP

Sections:

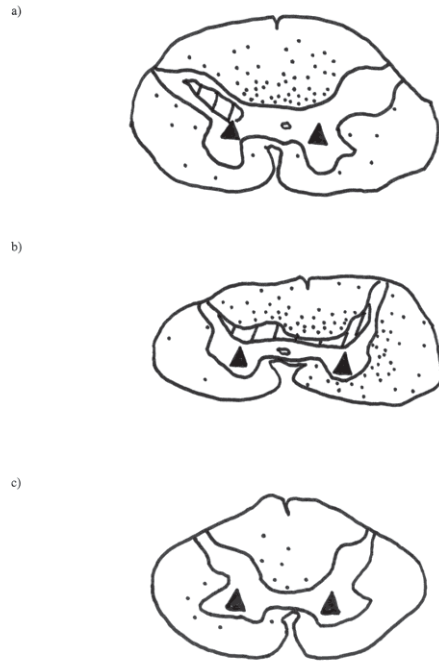
- a) Two levels above site - C1
- b) At the site of compression - C3
- c) Two levels below site - C5



Case: 16
TUNEL

Sections:

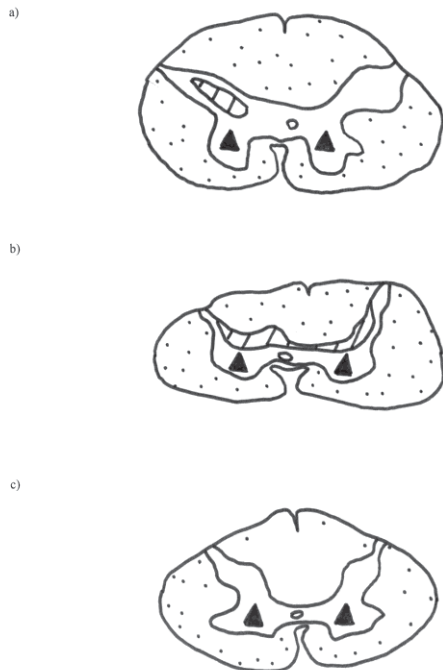
- a) Two levels above site - C1
- b) At the site of compression - C3
- c) Two levels below site - C5



Case: 16
AIF 1

Sections:

- a) Two levels above site - C1
- b) At the site of compression - C3
- c) Two levels below site - C5



Summary of immunohistochemistry Case 16

<p>Glia: PARP (rare), TUNEL, AIF, CMAP, Amy-33 Axons: APP, CMAP Neurons: TUNEL, AIF, Amy-33</p>	<p>C1</p>	<p>H&E: loss AHCs</p>
<p>Glia: DNA-PKcs, PARP, TUNEL, AIF, CMAP, Amy-33 Axons: APP, caspase-3 (rare), AIF, CMAP, Amy-33 Neurons: TUNEL, AIF, Amy-33</p>	<p>C3</p>	<p>H&E: subtotal necrosis, macrophages, axonal swellings, mild vacuolation</p>
<p>Glia: DNA-PKcs, PARP, Amy-33, AIF, CMAP, TUNEL (max) Axons: APP (rare), CMAP, Amy-33 Neurons: TUNEL (max), AIF, Amy-33</p>	<p>C4</p>	<p>H&E: loss AHCs, central chromatolysis, vacuolation Weil: pallor of lateral corticospinal tract</p>
<p>Glia: DNA-PKcs, PARP, CMAP, TUNEL, AIF Axons: CMAP, Amy-33 Neurons: PARP, TUNEL, AIF, Amy-33</p>	<p>C5</p>	<p>H&E: vacuolation</p>
<p>Glia: DNA-PKcs, PARP, CMAP, TUNEL, AIF Axons: CMAP, Amy-33 Neurons: PARP, TUNEL, AIF, Amy-33</p>	<p>C6</p>	<p>H&E: loss AHCs Weil: pallor of lateral corticospinal tract</p>
<p>Glia: DNA-PKcs, PARP, CMAP, TUNEL (max), AIF Axons: CMAP Neurons: TUNEL (max), AIF, Amy-33</p>	<p>C7</p>	<p>H&E: mild vacuolar changes</p>
<p>Glia: PARP, TUNEL (max), AIF, CMAP Axons: CMAP Neurons: TUNEL (max), AIF, Amy-33</p>	<p>L5</p>	<p>H&E: mild vacuolar changes</p>

Conclusion Almost complete cystic necrosis of the cervical cord at the C2-C3 segmental level.

There was necrosis involving the dorsal horns and the ventral part of the dorsal columns from C1 to C4-5.

CASE 17

Clinical summary A 72 year-old male was involved in a single vehicle rollover after he had apparently lost control on a dirt road. He was transferred to the Intensive Care Unit of a major hospital. His injuries included quadriplegia from a C7-T1 level with spinal shock, fractured right 4th and 5th ribs and minor lacerations to the scalp, left arm and right shin. His past medical history included an anterior myocardial infarct, coronary artery grafting twice and an aortic valve replacement. He was taking warfarin at the time of injury.

He underwent insertion of an AO locking plate for fixation of a C7-T1 fracture dislocation. Extubation was difficult post-operatively due to poor respiratory effort and he remained ventilated from this point on. His progress included repeated episodes of sepsis, mostly of respiratory origin, with pseudomonas, enterobacter and acinetobacter. He was treated symptomatically and his condition slowly improved with increased cardiovascular stability and resolution of the infection. He maintained good renal function, but persisting ventilatory problems necessitated long term partial ventilation. A CT scan suggested a persisting unstable oblique fracture below the area of fixation and thus skull traction was performed. He developed hyperpyrexia with marked hypotension, tachycardia and no urine output. Pseudomonas was cultured from the urine and sputum despite antibiotic therapy. The patient developed haematemesis and melaena and died.

Pathology – brain

1. Polymicrogyria.
2. Partial atresia of right cingulate gyrus, adjacent corpus callosum and compensatory diverticular outpouching of the right lateral ventricle.
3. Old lacunar infarct left caudate nucleus.

Pathology – spine and spinal cord

1. Fracture dislocation of C7-T1.
2. Severe compression necrosis of cervico-thoracic spinal cord maximal at C8-T1 levels.

Haematoxylin and Eosin

Macroscopic findings On post-mortem examination there was a complete fracture dislocation of C7/T1. The T1 vertebral body was displaced backwards and had completely occluded the spinal canal. The adjacent dural sac and spinal cord were severely crushed at this level. An oblique fracture line extended from the posterior part of the T7 vertebral body across the intervertebral disc

to join a crush fracture of the anterior T1 vertebral body. A metal plate was screwed into the anterior C7 vertebral body.

External inspection of the dural sac revealed a deep transverse groove corresponding to the C7-T1 fracture dislocation. The dura mater was densely adherent to the underlying crushed spinal cord which was represented by a meshwork of small cavities. The anterior spinal artery appeared patent. Compression necrosis of the spinal cord was most severe at C8-T1 levels but extended to involve the cervical cord to the C5 level and the thoracic cord to the T3 level.

Macroscopically visible distortion of the cord suggestive of compression in the antero-posterior plane is evident in segment C8 (N18, 20, 22). Distortion was present but less severe at T1 (N19). At C3, C4, T4 and T11 (N26, 27, 32, 34) there was mild narrowing of the lateral cord suggestive of compression or atrophy. Dura mater is present at C8 (N20), T1 (N19) and T11 (N34). A cavity is visible in the central cord at section N22 of the C8 segment and peripherally at section N20 of C8. At T1 there is a central syrinx in addition to apparent dilatation of the central canal. At C7 (N21, 23) two small cavities are seen in the lateral and anterior cord. The cord parenchyma appears fragmented at C5 (N25), C4 (N27) and T4 (N32) which may represent artefact. Pallor of the central cord is seen at C5. At T2 (N30) distinct pallor of one half of the cord is present suggestive of necrosis.

Microscopic findings Corpora amylacea are seen. At C3 (N26) there is vacuolation of the subpial white matter extending to cystic change in the lateral corticospinal tract worse on one side. Occasional axonal swellings are also seen. There is loss of anterior horn cells (AHC) and central chromatolysis. Similar changes occur at C4 (N27). At C5 (N25) there is compression of the grey matter, a loss of AHCs and central chromatolysis. There is cystic change in the posterolateral cord on one side which may be partly accounted for by artefact however macrophages are seen in this area. Vacuolation is found in the subpial region and less frequently throughout the cord. Axonal swellings are found in the lateral corticospinal tract bilaterally. At C7 (N21, 23) there is cystic necrosis throughout the grey matter extending into the posterolateral subpial region and many macrophages are seen. There is a large syrinx in the posterior white matter and subtotal loss of AHCs. At C8 there is severe cord compression or atrophy. Cystic necrosis is subtotal with the only preserved regions being the anterior subpial white matter. Many macrophages are present and there is a total loss of neurons with congestion of vessels. Two large syrinxes are found in the central cord in section N22 (C8). At T1 (N19) there are several large syrinxes occupying the cord and no neurons present. There is a generalised loss of glia. At T2 (N30) there is cystic necrosis and macrophages present in one half of the cord. No neurons are visible. There is also disruption of the subpial region on the relatively preserved side which may be artefact. At T3 (N31) there is subpial

vacuolation and loss of AHCs. At T4 (N32) there is mild vacuolation throughout the cord particularly in the lateral cord on one side. Occasional axonal swellings are seen. There is a loss of AHCs with rare central chromatolysis. Similar vacuolar changes and axonal swellings are present at T11 (N34). There is a mild loss of AHCs but no central chromatolysis. Glial processes and regions of mineralisation suggestive of dystrophic calcification lined the necrotic cavity. Foamy macrophages are seen from C2-T1.

Weil Pallor in regions of tissue necrosis but no evidence of Wallerian degeneration.

Immunohistochemical results

CASE 17 – Trauma series – Immunological positivity (+) in glial, axonal or neuronal profiles:

Level	APP	Casp-3	DNA- PKcs	PARP	Bcl-2	Fas	Casp-9	TUNEL	Amy-33	CMAP	AIF
C3	+	-	-	-	-	-	+	-	-	+	+
C4	+	-	-	+	-	-	-	-	-	+	+
C5	-	-	-	-	-	-	-	-	+	+	-
C7	+	-	-	-	-	-	-	-	+	+	+
C8	+	-	-	-	-	-	-	-	+	+	+
T1	-	-	-	-	-	-	-	-	-	+	+
T2	-	-	-	+	-	-	-	-	+	+	+
T3	+	-	-	-	-	-	-	-	+	+	+
T4	-	-	-	+	-	-	-	+	-	+	+
T11	-	-	-	+	-	-	-	+	-	+	+

* Shaded rows represent the site of compression

APP Non-specific immunostaining in segment C8 (N18). In segments C8 (N20) and C7 (N21, 23) occasional spherical immunoreactivity is seen lining the syrinx which may represent axonal profiles. At C3 (N26) there is rare immunoreactivity within axonal swellings of the lateral corticospinal tract on one side. At C4 (N27) rare immunoreactivity is seen in small spherical structures, probably axons. Scattered axonal immunoreactivity is seen at T2 (N30) in large diameter axons surrounding necrotic areas and normal-diameter axons in relatively preserved tissue. Immunopositive normal sized axons and occasionally swollen axons are rarely seen in the lateral corticospinal tract at T3 (N31) and in the anterior corticospinal tract unilaterally at T4 (N32). Negative in glia and neurons.

Active caspase-3 Non-specific immunoreactivity is seen in rounded profiles within the neuropil and may either be glial processes or small axons. Occasionally cellular profiles are immunopositive. Rarely, equivocal immunopositivity is present in axonal swellings. Negative in neurons.

DNA-PKcs Negative in glia, neurons and axons. Equivocal immunostaining is rarely seen in axonal swellings at C4 (N27).

PARP Glial nuclear immunoreactivity is occasionally present in the preserved white matter maximally at C4 (N27), C5 (N25) and C8 (N20, 22) and also found at T2 (N30). Immunopositive glia in the subpial region are less in number at T4 (N32). At T11 (N34) there are positive glial nuclei in the subpial region. These cells have morphology consistent with oligodendroglial cells. Negative in neurons, axons.

Bcl-2 Negative in glia, neurons and axons.

Fas Negative in glia, neurons and axons.

Caspase-9 Rare immunopositivity in spherical axonal profiles of lateral white matter at C3 (N26). One immunopositive cellular profile of unclear type was seen at T2 (N30). Occasional equivocal immunoreactivity at T2 (N30) in axonal swellings. Negative in neurons.

TUNEL Immunoreactivity within macrophages at C8 (N22) and T2 (N30). Many neuronal nuclei are immunoreactive at T4 (N32) and in astrocytes within the grey matter and glial nuclei within the posterior column. Similar structures are immunopositive within the anterior horn unilaterally at T11 (N34). Negative in axons.

CMAP Many immunopositive glia, ependymal cells, neurons and axons were seen. This combined with the degree of background staining negates the specificity of this marker at the dilution used.

Amy-33 amyloid beta At C8 (N20) there are immunoreactive rounded profiles consistent with axonal swellings lining the syrinx and are occasionally seen in the nerve roots. In section N22 of C8, small and large immunopositive axonal profiles were seen bordering the syrinx and throughout the white matter as well as macrophage immunopositivity. At C7 (N23) there was occasional cytoplasmic and nuclear immunoreactivity within glial profiles as well as staining in small and large axons and macrophages. At C7 (N21) small and large immunopositive axonal profiles were seen bordering the syrinx and throughout the white matter. In addition there was cytoplasmic

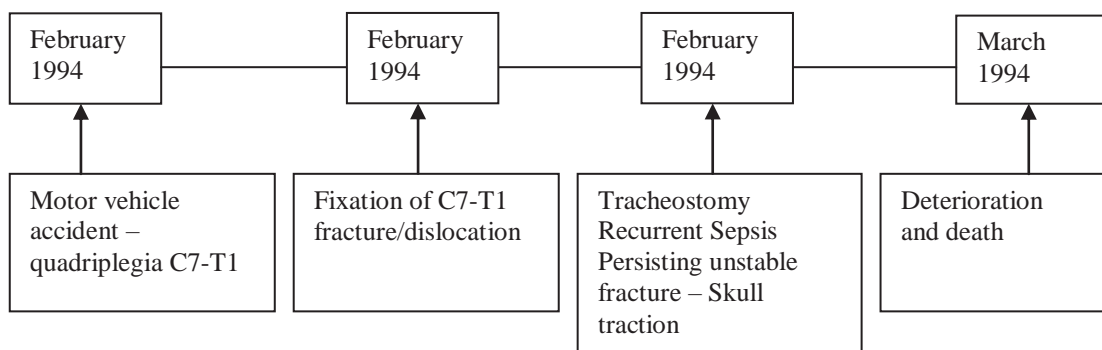
staining within neurons. At C5 (N25) glial cytoplasmic and neuronal cytoplasmic immunopositivity was seen. Immunopositive small axons were seen throughout the white matter and occasionally larger axons were present. A similar pattern was seen in segment T2 (N30) however greater numbers of immunopositive axonal swellings were present in the lateral corticospinal tract, especially on one side, than at C5. Small and large axons, glia with the morphology of oligodendrocytes, the cytoplasm of neurons and macrophages were immunoreactive at T3 (N31). A high degree of background staining was present in some areas likely due to parenchymal damage and necrosis. Negative at T1 (N19).

University of Melbourne amyloid beta Negative.

DAKO amyloid beta Negative.

AIF Neuronal, oligodendroglial and astrocytic cytoplasmic staining is seen at C3 (N26), C4 (N27), T11 (N34), T4 (N32) and T2 (N30). At C5 (N25) there are large numbers of immunopositive glia in all areas of white matter. Neuronal cytoplasmic staining is seen on both sides. At C7 (N21) glial immunostaining is present throughout the white matter and neuronal immunostaining in both anterior horns in the cytoplasm. Staining is also present within the macrophage cytoplasm. At C8 (N18, N20, N22) there is glial cytoplasmic staining in the preserved anterior white matter but no neuronal or axonal immunopositivity. At the site of compression, T1 (N19), immunopositive cell numbers are decreased, with rare glial immunopositivity only. At T2 (N30) there is extensive tissue necrosis and immunopositivity is present within macrophages. At T3 (N31) immunopositive glia are present in all areas of white matter. Neuronal cytoplasmic staining is seen on both sides. Negative in axons.

Timeline of clinical progression

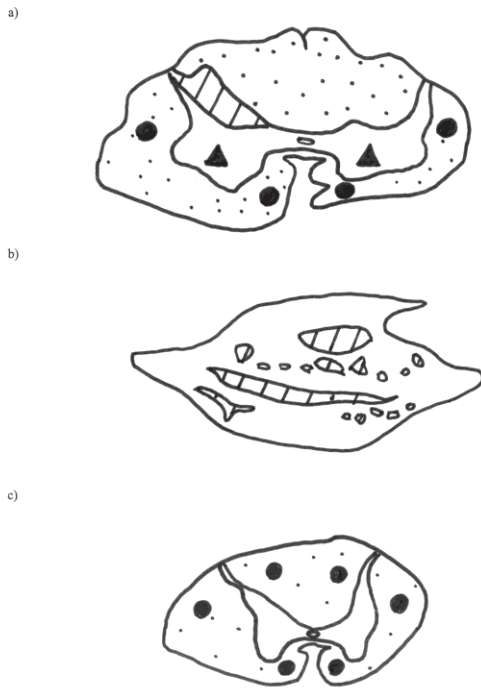


Spatial Distribution of Staining – Case 17

Case: 17
Amy-33

Sections:

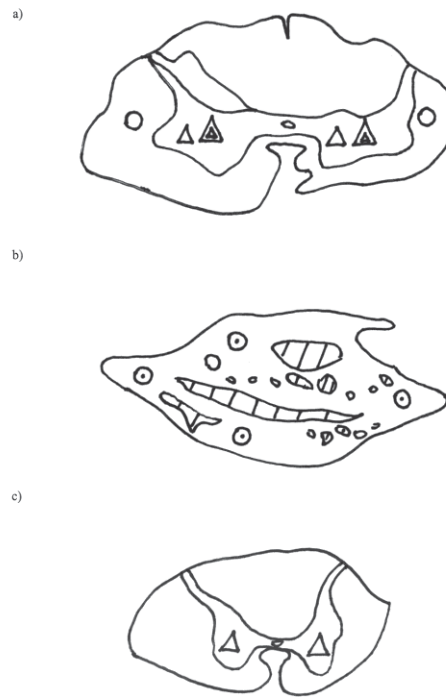
- a) Three levels above site - C5
- b) At the site of compression - T1
- c) Two levels below site - T3



Case: 17
Haematoxylin and eosin

Sections:

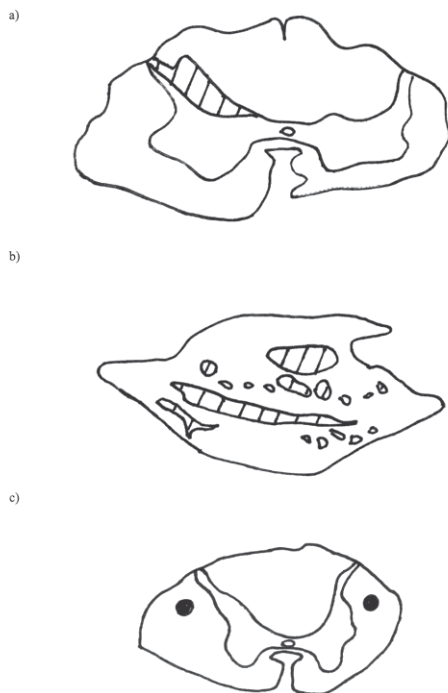
- a) Three levels above site - C5
- b) At the site of compression - T1
- c) Two levels below site - T3



Case: 17
APP

Sections:

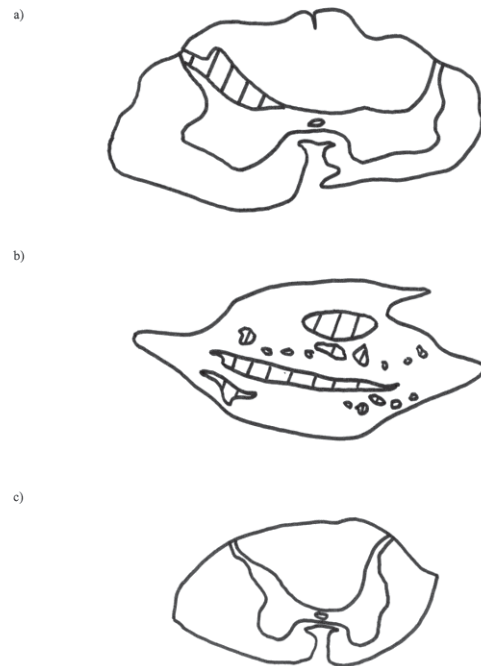
- a) Three levels above site - C5
- b) At the site of compression - T1
- c) Two levels below site - T3



Case: 17
DNA-PKcs

Sections:

- a) Three levels above site - C5
- b) At the site of compression - T1
- c) Two levels below site - T3

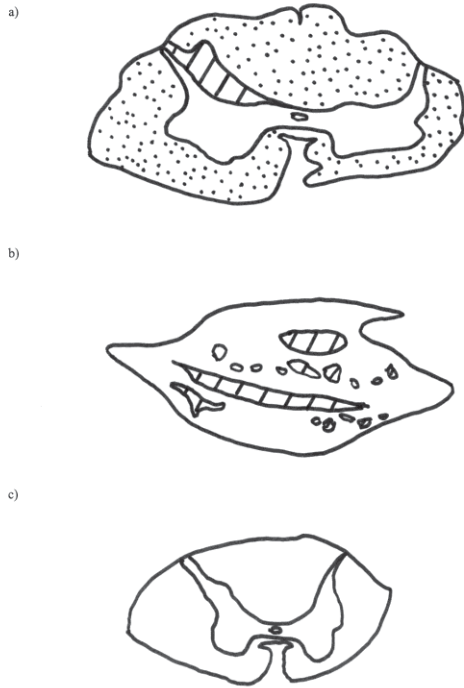


Spatial Distribution of Staining – Case 17

Case: 17
PARP

Sections:

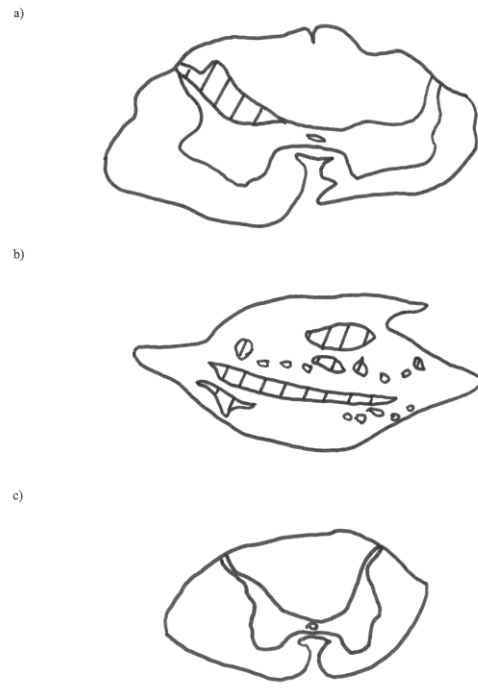
- a) Three levels above site - C5
- b) At the site of compression - T1
- c) Two levels below site - T3



Case: 17
TUNEL

Sections:

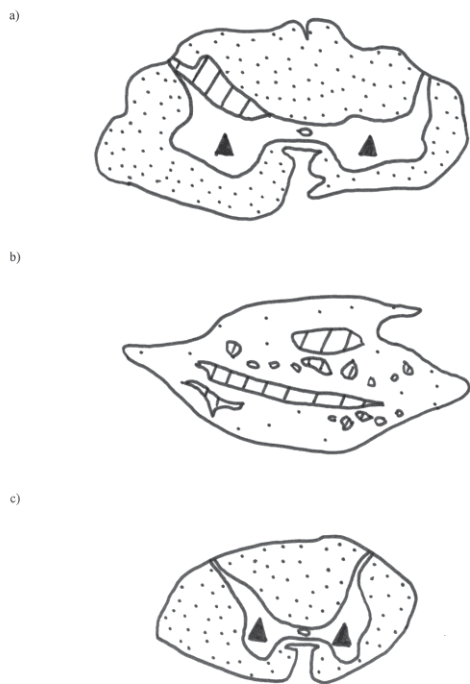
- a) Three levels above site - C5
- b) At the site of compression - T1
- c) Two levels below site - T3



Case: 17
AIF 1

Sections:

- a) Three levels above site - C5
- b) At the site of compression - T1
- c) Two levels below site - T3



Summary of immunohistochemistry Case 17

Glia: CMAP, AIF Axons: APP (rare), CMAP, Caspase-9 Neurons: CMAP, AIF	C3	H&E: vacuolation, cystic change, axonal swellings, loss AHCs, central chromatolysis, macrophages
Glia: PARP (max), CMAP, AIF Axons: APP (rare), CMAP Neurons: CMAP, AIF	C4	H&E: vacuolation, cystic change, axonal swellings, loss AHCs, central chromatolysis, macrophages
Glia: Amy-33, AIF, CMAP Axons: Amy-33, CMAP Neurons: Amy-33, AIF, CMAP	C5	H&E: compression grey matter, loss AHCs, vacuolation, cystic change, central chromatolysis, axonal swellings, macrophages
Glia: Amy-33, AIF, CMAP Axons: APP, Amy-33, CMAP Neurons: Amy-33, AIF, CMAP	C7	H&E: cystic necrosis, macrophages, loss AHCs, syrinx
Glia: AIF, CMAP Axons: APP, Amy-33, CMAP Neurons: CMAP	C8	H&E: grey matter compression / atrophy, cystic necrosis, macrophages, syrinx, loss neurons, congestion
Glia: AIF, CMAP Axons: CMAP Neurons: CMAP	T1	H&E: syrinx, loss neurons, macrophages
Glia: PARP, Amy-33, CMAP, AIF Axons: APP, Amy-33, CMAP Neurons: Amy-33, CMAP, AIF	T2	H&E: cystic necrosis, macrophages, loss neurons
Glia: AIF, CMAP, Amy-33 Axons: APP, Amy-33, CMAP Neurons: AIF, CMAP, Amy-33	T3	H&E: subpial vacuolation, loss AHCs
Glia: PARP, TUNEL, CMAP, AIF Axons: CMAP Neurons: TUNEL, CMAP, AIF	T4	H&E: vacuolation throughout, loss AHCs, central chromatolysis, axonal swellings
Glia: PARP, CMAP, AIF Axons: CMAP Neurons: TUNEL, CMAP, AIF	T11	H&E: vacuolation throughout, loss AHCs, axonal swellings

Conclusion Spinal cord compression was secondary to C7-T1 fracture-dislocation. There was widespread necrosis and penumbral immunoreactivity for apoptotic markers. This was supported by large numbers of immunopositive glia in all areas of white matter with occasional nuclear immunopositivity on both sides as well as cytoplasmic at C5 (N25). Staining was also present

within macrophages. At the site, C8 (N18, N20, N22), there was glial cytoplasmic staining using AIF in the preserved anterior white matter but no neuronal or axonal immunopositivity. TUNEL reactivity was present in neurons distant to the site of compression consistent with apoptosis. No significant axonal immunopositivity was found.

CASE 18

Clinical summary A 70 year-old female who died of pneumonia likely to have developed secondary to her immobility, chronic pain and inability to cough. Steroidal medication for asthma contributed to marked osteoporosis, eventually leading to instability of the spine, crush fracture at C7 and compressive myelopathy at C8-T1. This was surgically decompressed posteriorly but there was residual quadriparesis and patchy sensory loss. Cause of death was bronchopneumonia and debilitation secondary to thoracic cord compression.

The cord was compressed at C8, particularly on one side. There was haemorrhage in the posterior horn at C7 and congestion of blood vessels, worse in the anterior portion of the cord. The cord was greatly distorted with some necrosis and invasion by macrophages.

Demyelination was present in the sensory tracts above, and the motor tracts below the lesion. There was hyaline sclerosis of the blood vessels and many corpora amylacea were present, especially anteriorly closer to the midline.

Pathology – brain

1. Normal brain.

Pathology – spine and spinal cord

1. Compression myelopathy maximal C8-T1 levels.
2. Severe kyphoscoliosis of the vertebral column.
3. Crush fracture of C7 and L2 vertebrae.
4. Severe intravertebral disc degeneration with osteophyte formation.

Haematoxylin and Eosin

Macroscopic findings On post-mortem examination there was marked circumferential atrophy of C8-T1 cord segments. The anterior spinal artery was patent above the area of compression and only seen with difficulty below the site of compression. Segmental sections of the spinal cord revealed old necrosis of C8 and T1 segments. The remainder of the spinal cord was macroscopically normal. There was marked kyphosis at C7-T1 levels with the superior posterior aspect of the T1 vertebral body protruding into the vertebral canal with marked narrowing. The C7 vertebral body showed a wedge shaped crush fracture. There was severe disc degeneration of the cervical vertebral column associated with osteophyte formation. There was a marked scoliosis to the left of the lumbosacral spine. There was a crush fracture of L2 and anterior wedging of the L3 vertebral body. There was

severe disc degeneration of the lumbar spine with osteophyte formation maximal at L3-L4 and L5-S1 levels anteriorly and posteriorly with narrowing of the vertebral canal at L1-L2, L3-L4 and L5-S1.

All sections showed even eosinophilic staining with no loss of intensity. C6 (N4), C7 (N5), T2 (N11) and T3 (N12) were macroscopically normal. At the C8 segment (N6, N7) the cord was fragmented and mildly distorted indicating compression. Sections N8 and N9 were longitudinal. At the T1 segment (N10) there was mild asymmetry of the spinal cord. T2 (N11) and T3 (N12) appeared macroscopically normal.

Microscopic findings In segments C6 (N4) and C7 (N5) corpora amylacea are seen scattered throughout. There is some vacuolation present in the posterior nerve root and elongated separation of tissue within the white matter. This may be artefactual or it may indicate the friability of the tissue as a result of damage at lower levels. The cord is otherwise unremarkable at these segments.

At the level of compression, C8 (N6, N7) and C8/T1 (N8, N9) segments, there was diffuse cystic cavitation and disruption of tissue throughout the cord and engorgement of vessels with mild haemorrhage. There were occasional small areas of vacuolation. Polymorphonuclear cells, suggestive of neutrophils, were seen within vessels and occasionally within the tissue. There was significant anterior horn cell and glial cell loss. T1 (N10) and T2 (N11) segments showed mild subpial vacuolation and occasional parenchymal damage of the white matter which may be artefactual. At T3 (N12) there was a partial loss of AHCs unilaterally and mild vacuolation throughout the white matter.

Weil The spinal cord segments above C8 show Wallerian degeneration maximal in the posterior columns. Cord segment C8-T1 shows ill defined corticospinal tract degeneration. At T1 (N10) there is pallor of the posterolateral white matter suggesting demyelination. At T2 (N11) there is pallor of the anterior and lateral corticospinal tracts on one side.

Immunohistochemical results

CASE 18 – Trauma series – Compression C7 – Immunological positivity (+) in glial, axonal or neuronal profiles:

Level	APP	Casp-3	DNA- PKcs	PARP	Bcl-2	Fas	Casp-9	TUNEL	Amy-33	CMAP	AIF
C6	-	-	-	+	-	-	-	+	+	+	+
C7	+	-	-	+	-	-	-	+	+	+	+
C8	+	-	-	+	-	-	+	-	+	+	+
C8/T1	-	-	-	+	-	-	-	-	+	+	+
T1	+	-	-	+	-	-	-	-	+	+	+
T2	-	-	-	+	-	-	-	+	+	+	+
T3	+	-	-	+	-	-	-	+	+	+	+

* Shaded rows represent the site of compression

APP Well-defined areas of axonal immunopositivity were seen in C7 (N5), C8 (N6, N7) and T1 (N10). These immunopositive axons were of normal diameter and were evident in both longitudinal and transverse profiles. Regions of APP immunopositivity were macroscopically visible in these segments. Axonal positivity was rarely present within the lateral corticospinal tract at T3 (N12). Segment T2 (N11) was negative.

Active caspase-3 Negative for axons, glia and neurons. Occasional non-specific immunopositive profiles within the neuropil subpially at C6 (N4) and T3 (N12).

DNA –PKcs Negative for axons, glia and neurons.

PARP Many immunopositive glia with a morphology characteristic of oligodendrocytes were seen diffusely across the white matter in all segments. Neuronal nucleoli were rarely immunopositive in segments C6 (N4), C7 (N5) and T3 (N12). At T1 (N10), neuronal nuclei but not nucleoli were rarely immunopositive within the anterior horn. Negative for axons.

Bcl-2 Negative for axons, glia and neurons.

Fas Negative for axons, glia and neurons.

Caspase-9 Immunonegative for neurons and glia. Rare axonal immunopositivity at C8 (N6). Rare non-specific staining at C6 (N4).

TUNEL Immunonegative for neurons and axons. Immunopositive glia were occasionally found at segments C7 (N5), T2 (N11) and T3 (N12).

CMAP Many immunopositive glia were found in segments C6 (N4) - T3 (N12). Non-specific staining was seen which may represent either dendritic processes or axons. At T2 (N11) cytoplasmic immunopositivity was occasionally found within anterior horn cells.

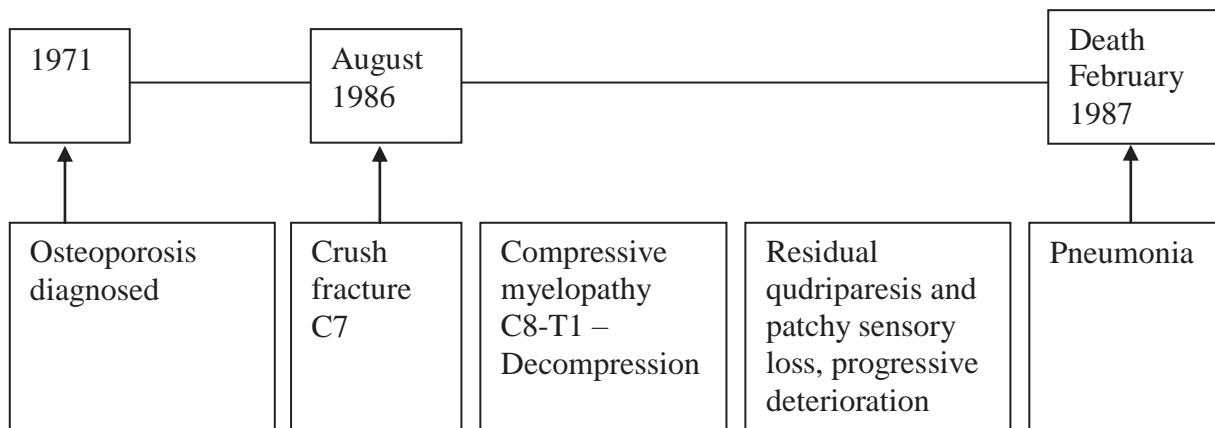
Amy-33 amyloid beta Immunopositive within the cytoplasm of anterior horn cells at C6 (N4) and also occasional glial cytoplasmic staining. At C7 (N5) and C8 (N6, N7) there was macroscopically visible axonal positivity throughout the white matter, maximal in the lateral and anterior corticospinal tracts. Axonal profiles were of normal diameter interspersed with occasional swollen axons and longitudinal profiles were also observed. Occasional cytoplasmic glial staining was seen at these segments but there were no immunopositive neurons. At C8/T1 (N8) there were macroscopically visible collections of axonal immunopositivity, occasional glia and immunopositive neurons. At T1 (N10) there were positive axons throughout the white matter but especially in the anterior and lateral corticospinal tracts. Cytoplasmic staining of anterior horn cells was found but glia were immunonegative. Greater numbers of immunopositive glia and their processes were present in segments T2 (N11) and T3 (N12) in addition to positive AHCs but there were only rarely positive axons at T2 and none in segment T3.

University of Melbourne amyloid-beta Negative.

DAKO amyloid-beta Negative.

AIF At C6 (N4) glial immunoreactivity was seen in all areas of white matter. This staining was cytoplasmic in nature and profiles were consistent with oligodendrocytes and astrocytes. Neuronal staining was found within the grey matter on both sides. At C7 (N5) there is glial and neuronal cytoplasmic immunopositivity in all regions but in greater numbers towards the central white matter. At C8 (N7, N8) and C8/T1 (N9) there is occasional cellular cytoplasmic staining of uncertain cell type however significant background staining is present. At C8 (N6) there is immunopositivity in normal and enlarged axons. At the site of compression T1 (N10) and below at T3 (N12) glial immunopositivity was greatly reduced to involve on the occasional glial cell. Neuronal immunostaining was present on both sides. At T2 (N11) there was glial cytoplasmic immunopositivity throughout the white matter and in neuronal cytoplasm bilaterally. There was no immunopositivity within axonal profiles.

Timeline of clinical progression

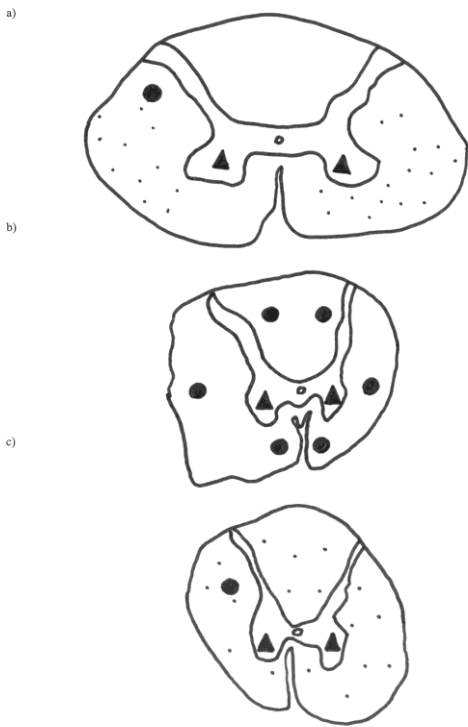


Spatial Distribution of Staining – Case 18

Case: 18
Amy-33

Sections:

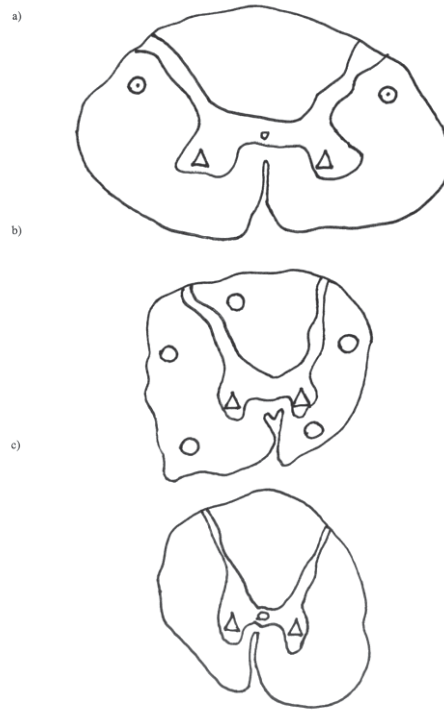
- a) Two levels above site - C6
- b) At the site of compression - T1
- c) Two levels below site - T3



Case: 18
Haematoxylin and eosin

Sections:

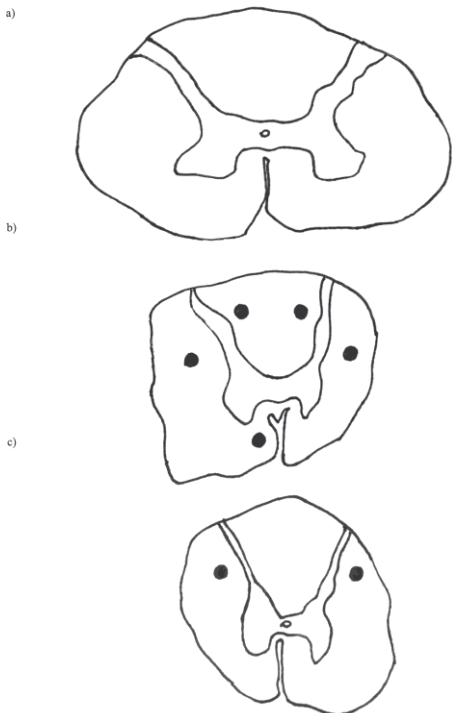
- a) Two levels above site - C6
- b) At the site of compression - T1
- c) Two levels below site - T3



Case: 18
APP

Sections:

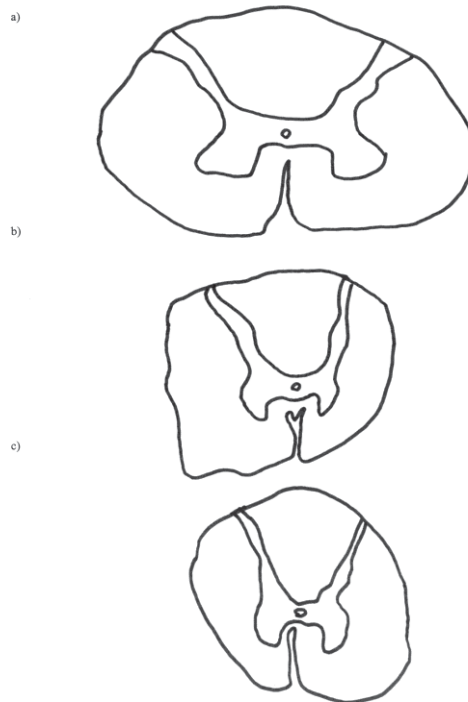
- a) Two levels above site - C6
- b) At the site of compression - T1
- c) Two levels below site - T3



Case: 18
DNA-PKcs

Sections:

- a) Two levels above site - C6
- b) At the site of compression - T1
- c) Two levels below site - T3

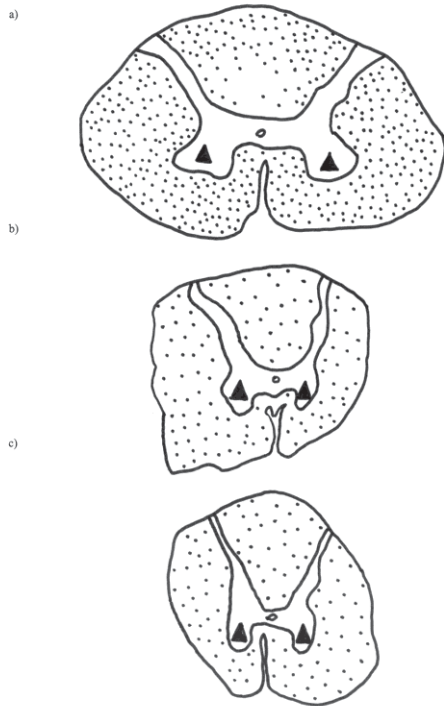


Spatial Distribution of Staining – Case 18

Case: 18
PARP

Sections:

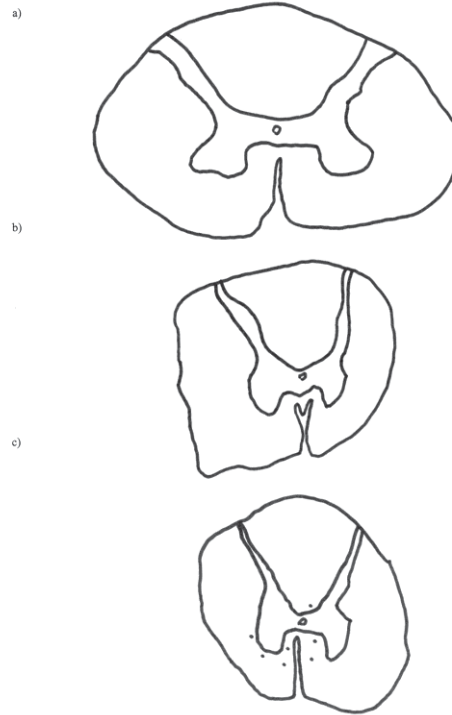
- a) Two levels above site - C6
- b) At the site of compression - T1
- c) Two levels below site - T3



Case: 18
TUNEL

Sections:

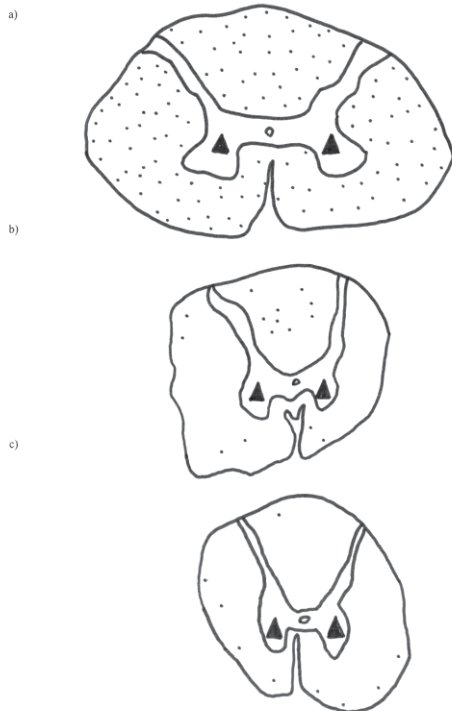
- a) Two levels above site - C6
- b) At the site of compression - T1
- c) Two levels below site - T3



Case: 18
AIF 1

Sections:

- a) Two levels above site - C6
- b) At the site of compression - T1
- c) Two levels below site - T3



Summary of immunohistochemistry Case 18

Glia: PARP, AIF Axons: Nil Neurons: PARP, AIF	C6	H&E: vacuolation
Glia: PARP, TUNEL, AIF Axons: APP Neurons: PARP, AIF	C7	H&E: vacuolation
Glia: PARP Axons: APP, caspase-9 (rare) Neurons: Nil	C8	H&E: macroscopic asymmetry, cystic change, congestion, haemorrhage, vacuolation, polymorphs, AHC/glial loss
Glia: PARP, AIF Axons: APP Neurons: PARP, AIF	T1	H&E: macroscopic asymmetry, cystic change, congestion, haemorrhage, vacuolation, polymorphs, AHC/glial loss Weil: pallor posterolateral white matter
Glia: PARP, TUNEL, AIF Axons: Nil Neurons: AIF	T2	H&E: subpial vacuolation Weil: Pallor of anterior and lateral corticospinal tract unilaterally
Glia: PARP, TUNEL, AIF Axons: APP (rare) Neurons: PARP, AIF	T3	H&E: partial loss AHCs, vacuolation

Conclusion The onset of spinal cord compression is most likely to be acute, secondary to the crush fracture of the C7 vertebral body. The survival time post-compression was 5 months. On haematoxylin and eosin staining there is evidence of a loss of anterior horn cells and of acute inflammation with the presence of polymorphonuclear cells and haemorrhage within the white matter. Ongoing cellular damage is indicated by the loss of myelin on Weil staining, paucity of glia and cystic cavitation of the spinal cord.

Axonal immunopositivity was seen using the marker APP in both longitudinal and transverse profiles which may suggest regenerating axons. Rarely these axons were also immunopositive for caspase-9, deemed to be an immunological marker of the mitochondrial apoptotic pathway. The pallor of Weil staining in motor tracts below and sensory tracts above the site of compression indicate Wallerian degeneration.

TUNEL immunopositivity within glia was seen above and below the lesion. This might be explained by a loss of glia at the site of compression however it is an unlikely reason as PARP glial immunopositivity was seen at all levels including the compressed level. Alternatively, such staining may represent either different stages of the apoptotic pathway or evidence of DNA damage characteristic of apoptosis due to other causes such as oncotic necrosis.

CASE 19

Clinical summary A 75 year-old male who died of an unknown cause. The patient had been a quadriplegic, level C6, for approximately 25 years following a gymnastic injury. The cause of death was undetermined.

Macroscopic examination showed an old healed fracture dislocation of the C7-T1 vertebrae, significant angulation of the spine and narrowing of the spinal canal at the level. The upper and lower limbs showed proximal and distal atrophy.

Pathology – brain

1. Normal brain.

Pathology – spine and spinal cord

1. Old fracture dislocation C7/T1.
2. Old traumatic necrosis of cervical spinal cord (C7-T1) with appropriate ascending and descending tract degeneration.
3. Post traumatic syringomyelia (descending to T5 level and ascending to C6 level).

Haematoxylin and Eosin

Macroscopic findings Examination of the hemisected vertebral column showed an old healed fracture dislocation of the C7-T1 vertebrae with a marked angulation deformity at that level with severe narrowing of the spinal canal. The remainder of the vertebral bodies were normal.

On post-mortem examination there was marked wasting of the spinal cord at C7-T1 segments. The anterior spinal artery was normal. Segmental section of the spinal cord revealed almost complete necrosis at C7 through T1 levels, maximal at the C8 segmental level with secondary dense leptomenigeal adhesions. An ascending traumatic syrinx (3 x 2 x 5 mm) extended rostrally in the left side of the cord to the C6 level. A descending traumatic syrinx (10 x 5 x 70 mm) extended below the level of the lesion to the T5 segmental level. Symmetrical atrophy of the posterior white matter columns was present rostral to the area of old traumatic necrosis and caudally there was symmetrical corticospinal tract degeneration in the anterolateral white matter columns.

At C8 (N8), T2 (N10) and T4 (N12) there is a generalised pallor of the cord and structural features are difficult to distinguish.

Microscopic findings At C8 (N8) there is a syrinx throughout the central cord extending to the lateral region on one side. No neurons are visible in the grey matter and there is a subtotal loss of glia. C8 and T1 show dystrophic calcification. At T2 and T4 (N10, 12) no glia are visible. These features account for the extreme pallor of the cord on haematoxylin and eosin staining. On immunological staining, neuronal profiles were identified in all sections however the number of anterior horn cells was abnormally low at T7 (N15) below the syrinx.

Weil At C8, T2 and T4 there is subtotal loss of myelin in all regions of the white matter.

Immunohistochemical results

CASE 19 – Syringomyelia series – Immunological positivity (+) in glial, axonal or neuronal profiles:

Level	APP	Casp-3	DNA- PKcs	PARP	Bcl-2	Fas	Casp-9	TUNEL	Amy-33	CMAP	AIF
C8	-	-	+	+	-	-	-	-	-	+	+
T2	-	-	+	+	-	-	-	-	+	+	+
T4	+	-	+	+	-	-	-	+	-	+	+
T7	-	-	-	+	-	-	-	-	+	+	+

* Shaded rows represent the site of compression

APP Immunopositive neuronal cytoplasm is present at T2 (N10) and in one neuron at T4 (N12). Negative in glia, axons. Negative at T7 (N15).

Active caspase-3 Negative in axons, neurons and glia. A significant amount of background staining was present in the subpial region.

DNA-PKcs Immunoreactive glial nuclei were seen throughout the cord in all segments. Immunopositive neuronal nuclei were seen unilaterally in C8 (N8) and T4 (N12). Negative in axons. Negative at T7 (N15).

PARP Immunopositive glial nuclei were seen in the remaining tissue of all segments. Negative in neurons, axons.

Bcl-2 Occasional immunoreactivity within the nuclear membrane in lymphocytic profiles. In addition there was occasional cytoplasmic staining at C8 of nonspecific cell type. Negative in neurons, axons. Negative at T7 (N15).

Fas Immunonegative for axons, glia and neurons.

Caspase-9 Negative in neurons, axons. Non-specific background staining in the subpial region.

TUNEL Rare nuclear immunoreactivity in the subpial region at T2 (N10). At T4 (N12) occasional nuclear immunoreactivity, likely to be glia, and rarely nuclear positivity in neurons.

CMAP Ependymal, glial, neuronal, macrophage and background staining was seen.

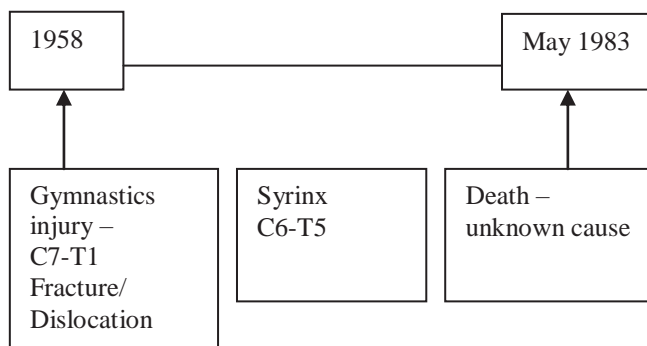
Amy-33 amyloid-beta Negative at C8 (N8) and T4 (N12). Neuronal cytoplasmic staining is present at T2 (N10). Non-specific staining is seen at T7 (N15).

University of Melbourne amyloid-beta Negative.

DAKO amyloid-beta Negative.

AIF Immunopositive in glial cytoplasm at T4 (N12). At C8 (N8), T2 (N10) and T7 (N15) there is neuronal and glial cytoplasmic staining.

Timeline of clinical progression



Spatial Distribution of Staining – Case 19

Case: 19
Amy-33

Sections:

Levels a) to c) contain syrinx

- a) One level above site of traumatic compression - C6
- b) At the level of traumatic compression - C8
- c) One level below site of traumatic compression - T2
- d) Level without syrinx - T7

a)



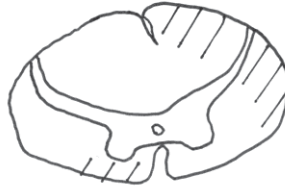
b)



c)



d)



Case: 19
APP

Sections:

Levels a) to c) contain syrinx

- a) One level above site of traumatic compression - C6
- b) At the level of traumatic compression - C8
- c) One level below site of traumatic compression - T2
- d) Level without syrinx - T7

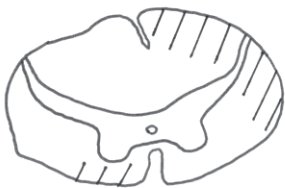
b)



c)



d)



Case: 19
Haematoxylin and eosin

Sections:

Levels a) to c) contain syrinx

- a) One level above site of traumatic compression - C6
- b) At the level of traumatic compression - C8
- c) One level below site of traumatic compression - T2
- d) Level without syrinx - T7

a)



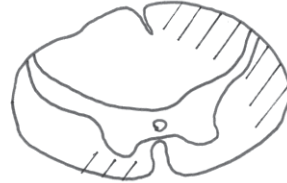
b)



c)



d)



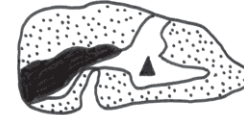
Case: 19
DNA-PKcs

Sections:

Levels a) to c) contain syrinx

- a) One level above site of traumatic compression - C6
- b) At the level of traumatic compression - C8
- c) One level below site of traumatic compression - T2
- d) Level without syrinx - T7

a)



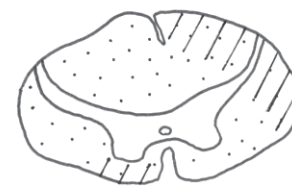
b)



c)



d)



Spatial Distribution of Staining – Case 19

Case: 19
PARP

Sections:

Levels a) to c) contain syrinx

- a) One level above site of traumatic compression - C6
- b) At the level of traumatic compression - C8
- c) One level below site of traumatic compression - T2
- d) Level without syrinx - T7

a)



b)



c)



d)



Case: 19
TUNEL

Sections:

Levels a) to c) contain syrinx

- a) One level above site of traumatic compression - C6
- b) At the level of traumatic compression - C8
- c) One level below site of traumatic compression - T2
- d) Level without syrinx - T7

a)



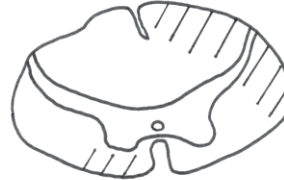
b)



c)



d)



Case: 19
AIF 1

Sections:

Levels a) to c) contain syrinx

- a) One level above site of traumatic compression - C6
- b) At the level of traumatic compression - C8
- c) One level below site of traumatic compression - T2
- d) Level without syrinx - T7

a)



b)



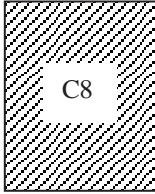
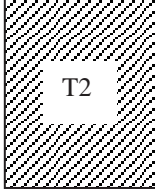
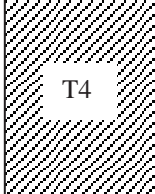
c)



d)



Summary of immunohistochemistry Case 19

<p>Glia: DNA-PKcs, PARP, AIF Axons: Nil Neurons: PARP, AIF</p>	 <p>C8</p>	<p>H&E: Syrinx, pallor, loss of glia, loss of AHCs Weil: pallor throughout cord</p>
<p>Glia: DNA-PKcs, PARP, AIF Axons: Nil Neurons: APP, Amy-33, AIF</p>	 <p>T2</p>	<p>H&E: Syrinx, pallor, loss of glia, loss of AHCs Weil: pallor throughout cord</p>
<p>Glia: DNA-PKcs, TUNEL, PARP Axons: Nil Neurons: APP, DNA-PKcs TUNEL</p>	 <p>T4</p>	<p>H&E: Syrinx, pallor, loss of glia, loss of AHCs Weil: pallor throughout cord</p>
<p>Glia: AIF, PARP Axons: Nil Neurons: AIF</p>	<p>T7</p>	<p>H&E: Severe tissue necrosis and neuronal loss Weil: pallor throughout cord</p>

Conclusion Syringomyelia was secondary to trauma and there was a long survival time following injury. There were no axonal swellings present and no APP axonal positivity was found. DNA-PKcs and TUNEL staining was predominantly within the central cord and may represent ongoing DNA damage, PARP immunopositivity may represent DNA repair.

CASE 20

Clinical summary A 55 year-old man with a past history of congestive heart failure resulting eventually in death. A syrinx of the spinal cord was found at autopsy.

The syrinx extended from C2-T12 and communicated with the subarachnoid space on the left at C4-C5, a developmental abnormality, incorporating the central canal and extending across segments C6-C8. There was anterior horn cell loss at these spinal cord segments.

The patient died in cardiac failure with a cardiopulmonary arrest despite inotropic support. No acute infarct was demonstrated. A focal acute prostatitis and pyelonephritis was evident. History of 7 years congestive heart failure resulting in numerous admissions, presumed to be secondary to ischaemic cardiomyopathy. Syringomyelia suspected to account for wasting of upper limbs.

Pathology – brain

1. Normal brain.

Pathology – spine and spinal cord

1. Syringomyelia (longitudinal extent C2-T12) communicating with the subarachnoid space at C4 and C5 levels on the left side. Developmental anomaly of the spinal cord.

Haematoxylin and Eosin

Macroscopic findings The cord is distorted and compressed in an antero-posterior plane. There is marked pallor of the cord.

Microscopic findings There is a syrinx in the central cord at all levels. In some segments this syrinx communicates with the subarachnoid space. Central syrinx is seen at C2 (N1). Loss of AHCs and glia at C3 (N2) with loss of glia in the anterior white matter and glial meshwork. At C4 (N3) there is a subtotal loss of glia, worse on either the anterior or posterior aspect of the cord (the structural morphology is difficult to recognise due to the distortion of the cord). At C7 (N6) the syrinx is lined by ependymal cells. There is preservation of the majority of glia with the exception of the lateral subpial region bilaterally. There is anterior horn cell loss and compression of the cord. At L2 (N21) below the syrinx there is normal appearing spinal cord.

Weil Pallor is seen in the gracile fasciculi at C2 (N1). At C3 (N2) and C4 (N3) both the gracile and

cuneate fasciculi show pallor suggestive of a loss of myelin. At C7 (N6) there is mild tissue disruption at the gracile fasciculus but no evidence of demyelination.

Immunohistochemical results

CASE 20 – Syringomyelia series – Immunological positivity (+) in glial, axonal or neuronal profiles:

Level	APP	Casp-3	DNA- PKcs	PARP	Bcl-2	Fas	Casp-9	TUNEL	Amy-33	CMAP	AIF
C2	-	-	+	+	-	-	-	+	-	+	+
C3	-	-	+	+	-	-	-	+	-	+	+
C4	-	-	+	+	-	-	-	+	-	+	+
C7	-	-	+	+	-	-	-	+	-	+	+
L2	+	-	+	+	-	-	-	+	+	+	+

* Shaded rows represent the site of compression

APP Non-specific immunoreactivity bordering the syrinx in all segments. Negative in glia. Neuronal cytoplasmic immunopositivity is present at L2 (N21).

Active caspase-3 Negative in axons, neurons and glia.

DNA-PKcs Immunoreactive in glia in all segments, particularly in the subpial region. In addition, neuronal cytoplasmic staining is seen in all segments. Negative in axons.

PARP Immunopositive glia are seen in all segments dispersed throughout the white matter, particularly in the subpial region. These immunopositive cells have a morphology typical of oligodendrocytes. One immunopositive prominent neuronal nucleolus is seen at C7 (N6). Many immunopositive neuronal nucleoli are seen at L2 (N21) and immunopositive glial nuclei are evident in the subpial region. Negative in axons.

Bcl-2 Immunoreactivity is rarely seen in the nuclear membrane of lymphocytes in all segments except L2 (N21). Negative in axons, neurons.

FAS Negative.

Caspase-9 Negative in glia, axons and neurons.

TUNEL Glial nuclear immunoreactivity throughout the white matter in all segments. Neuronal nuclei immunoreactive in all segments. Maximal staining at C2 and C3 (N1 and N2). Negative in axons.

CMAP Immunoreactivity was found in glial processes and nuclei in all sections. Neuronal cytoplasmic staining was seen at L2 (N21).

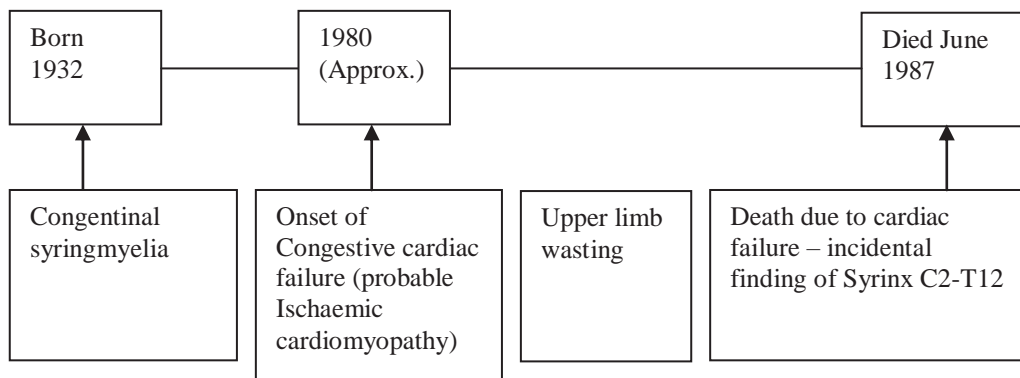
Amy-33 amyloid-beta Negative at all segments except L2 (N21) in which there is neuronal cytoplasmic staining.

University of Melbourne amyloid-beta Negative.

DAKO amyloid-beta Negative.

AIF Immunopositivity is seen in oligodendroglial, astrocytic and neuronal cytoplasm in all segments. There is also cytoplasmic staining in ependymal cells lining the syrinx.

Timeline of clinical progression



Spatial Distribution of Staining – Case 20

Case: 20
Amy-33

Sections:

- a) At the level of the syrinx - C3
- b) At the level of the syrinx - C7
- c) Level without syrinx - L2

a)



b)



c)

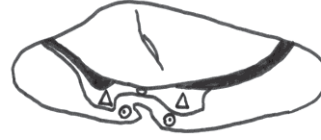


Case: 20
Haematoxylin and eosin

Sections:

- a) At the level of the syrinx - C3
- b) At the level of the syrinx - C7
- c) Level without syrinx - L2

a)



b)



c)



Case: 20
APP

Sections:

- a) At the level of the syrinx - C3
- b) At the level of the syrinx - C7
- c) Level without syrinx - L2

a)



b)



c)



Case: 20
AIF 1

Sections:

- a) At the level of the syrinx - C3
- b) At the level of the syrinx - C7
- c) Level without syrinx - L2

a)



b)



c)



Case: 20
TUNEL

Sections:

- a) At the level of the syrinx - C3
- b) At the level of the syrinx - C7
- c) Level without syrinx - L2

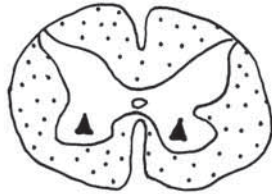
a)



b)



c)



Case: 20
PARP

Sections:

- a) At the level of the syrinx - C3
- b) At the level of the syrinx - C7
- c) Level without syrinx - L2

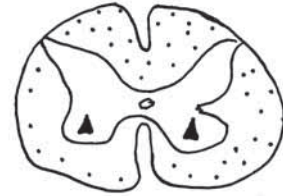
a)



b)



c)



Case: 20
DNA-PKcs

Sections:

- a) At the level of the syrinx - C3
- b) At the level of the syrinx - C7
- c) Level without syrinx - L2

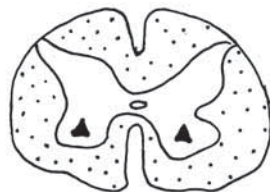
a)



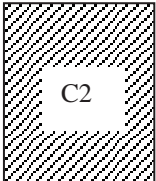
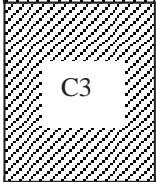
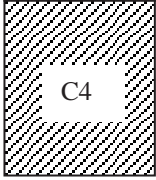
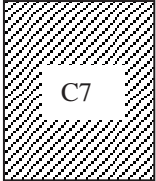
b)



c)



Summary of immunohistochemistry Case 20

<p>Glia: DNA-PKcs, PARP, AIF, TUNEL (max) Axons: Non-specific Neurons: DNA-PKcs, AIF, TUNEL (max)</p>	 <p>C2</p>	<p>H&E: distortion, pallor, subtotal loss glia, subtotal loss AHCs Weil: pallor of gracile fasculus</p>
<p>Glia: DNA-PKcs, PARP, AIF, TUNEL (max) Axons: Non-specific Neurons: DNA-PKcs, AIF, TUNEL (max)</p>	 <p>C3</p>	<p>H&E: distortion, pallor, loss of glia, loss of AHCs Weil: pallor of gracile and cuneate fasculi</p>
<p>Glia: DNA-PKcs, PARP, TUNEL, AIF Axons: Non-specific Neurons: DNA-PKcs, TUNEL, AIF</p>	 <p>C4</p>	<p>H&E: distortion, pallor, subtotal loss glia, subtotal loss AHCs Weil: pallor of gracile and cuneate fasculi</p>
<p>Glia: DNA-PKcs, PARP, TUNEL, AIF Axons: Non-specific Neurons: DNA-PKcs, PARP, AIF, TUNEL</p>	 <p>C7</p>	<p>H&E: distortion, pallor, loss of AHCs</p>
<p>Glia: DNA-PKcs, PARP, TUNEL Axons: Nil Neurons: APP, DNA-PKcs, PARP, TUNEL, Amy-33</p>	<p>L2</p>	<p>H&E: normal appearance</p>

Conclusion This patient had an extensive upper spinal cord syrinx extending from C2 to T12. There was associated loss of anterior horn cells and this correlated with findings of PARP, TUNEL and DNA-PKcs neuronal immunoreactivity. In addition there was pallor of the ascending tracts on Weil stain however there was no APP immunopositivity or axonal swellings to suggest axonal injury or a disruption of axonal transport. AIF immunopositivity was heterogeneous in nature.

CASE 21

Clinical summary A 74 year-old man with minor Arnold-Chiari malformation and associated syringomyelia. He died of cardiac failure. The syrinx had been decompressed surgically, although a residual syrinx was present following surgery from T1 to C2 segments. The patient's severe restrictive airways disease was attributed to neurological damage secondary to his long-standing syringomyelia.

The size of the syrinx was greatest at C2 in the right posterior column and macroscopically there was slight separation of the posterior columns in the midline. Extensive atrophy of the spinal cord was found distal to the site of decompression.

Histology showed a residual syrinx extending from C2 to L1 segment, with descending corticospinal tract degeneration below T6. Transverse syrinxes had formed at T12 and C7-T1. There was loss of anterior horn cells at these levels.

Pathology – brain

1. **Macroscopic findings** There was prominent cerebellar tonsillar protrusion and deep grooving of the cerebellar tonsils which extend down around the C1 cervical segment. The cerebellum was normal apart from cerebellar tonsillar protrusion (Arnold-Chiari malformation). **Conclusion** Arnold-chiari malformation (minor).

Pathology – spine and spinal cord

1. Evidence of operative decompression of syringomyelia.
2. Residual syrinx extending from C2 to L1.
3. Spinal cord caudal to site of operation shows extensive atrophy and degeneration.
4. Fibrosis leptomeninges of cauda equina.

Haematoxylin and Eosin

Macroscopic findings On post-mortem examination the dural sac showed fibrous scarring in the upper thoracic region. The spinal cord proximal and caudal to the scar tissue was abnormal with apparent separation of the dorsal white matter columns in the midline. There was arachnoid fibrosis of the lumbosacral and cauda equina regions and adhesions of the arachnoid to the dura mater with partial obliteration of the subdural space. The nerve roots of the cauda equina were matted together and could not be separated. Segmental sections of the spinal cord through the area of scarring revealed three cross sections of small silastic catheters in the midline region with extensive atrophy

and scarring of the adjacent spinal cord, more on the left side than on the right. A slit-like central syrinx, partially obliterated, extended from the upper end of the site of scarring to the C2 level. A metal clip was embedded in the dura mater on the dorsal surface adjacent to the region of maximal fibrosis. At the C2 level the syrinx was most evident in the region of the right dorsal white matter column. The spinal cord distal to the site of operation was atrophied down to the level of the lumbo-sacral enlargement. The cord appears narrowed in the antero-posterior plane. A macroscopically visible cavity is found in all segments.

Microscopic findings At the caudal scar there are few glia and no neurons present. At C4 (N29) there is a loss of anterior horn cells and a syrinx in the central cord. At C5 (N30) there is a loss of AHCs more severe on one side. A large syrinx occupies the central cord. At C6 (N31) there syrinx is smaller and lined partially by ependymal cells. There is a loss of AHCs but preservation of glia. Subtotal loss AHCs at T7 (N11) with atrophy of the posterior cord. In addition there is a small region of cystic change in the posterolateral cord on one side. At L4 (N20) and S2 (N23) there is red cell change but no other abnormality.

Weil There is pallor of the lateral corticospinal tract at L4 and S2 in association with atrophy of the white matter.

Immunohistochemical results

CASE 21 – Syringomyelia series – Immunological positivity (+) in glial, axonal or neuronal profiles:

Level	APP	Casp-3	DNA- PKcs	PARP	Bcl-2	Fas	Casp-9	TUNEL	Amy-33	CMAP	AIF
C6	+	-	+	+	-	-	-	+	+	+	+
T7	+	-	+	+	-	-	-	+	-	+	+
L4	+	-	-	+	-	-	-	+	+	+	+
S2	+	-	-	-	-	-	-	-	+	+	+

* Shaded rows represent the site of compression

APP Equivocal staining within neurons. Immunonegative in glia. Immunopositive in neuronal cytoplasm. Non-specific immunopositivity rarely present along the syrinx border.

Active caspase-3 There is rare cytoplasmic staining within cells of unknown origin. Immunonegative in axons and neurons.

DNA-PKcs Immunopositive glial nuclei are found at C6 and T7 (N31, N11). This staining is frequently found in cells near the anterior and posterior nerve roots. Immunopositivity is seen in the neuronal cytoplasm at C6 (N31). Negative in axons. No immunopositive staining is present at L4 and S2.

PARP Immunopositive glial nuclei are found throughout the cord in all segments except S2 (N23), particularly in the subpial region, however in fewer numbers than was found using the DNA-PKcs antibody. These immunopositive cells have the morphology of oligodendrocytes. Staining was found in cells of the anterior and posterior nerve roots. Negative in axons, neurons.

Bcl-2 Intracytoplasmic immunopositivity is seen at C6 (N31) lining the syrinx, suggestive of ependymal cells. There was no glial, neuronal or axonal immunoreactivity.

Fas Non-reactive.

Caspase-9 Rare cytoplasmic staining is seen in unidentified cells surrounding the syrinx. In addition there is rare, non-specific staining of spherical profiles in the white matter and nerve roots. Negative in neurons, glia and axons.

TUNEL Negative in axons. Negative within glia at T7 (N11). Glial and neuronal immunopositivity is seen at C6 (N31).

CMAP Heterogeneous staining was present in neurons, glia, axons and ependymal cells.

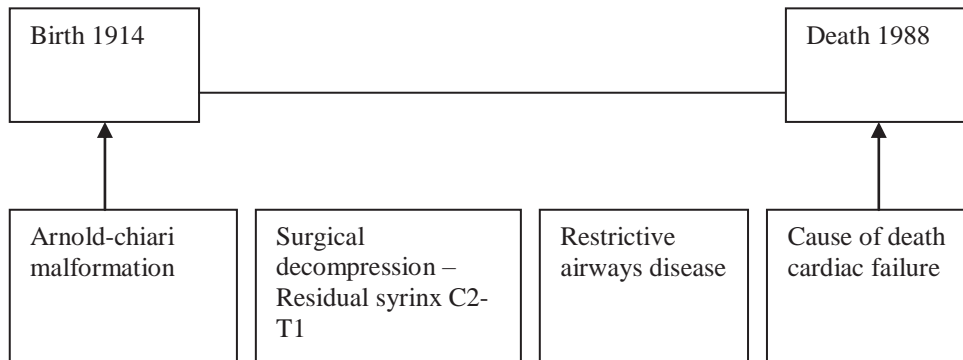
Amy-33 amyloid beta Negative in segment T7 (N11). Immunopositivity is seen in the neuronal cytoplasm at L4 (N20) as well as non-specific granular staining similar in appearance to neuritic plaques. There is neuronal cytoplasmic staining at C6 (N31). At S2 (N23) there is neuronal cytoplasmic staining.

University of Melbourne amyloid-beta Negative.

DAKO amyloid-beta Negative.

AIF There is immunopositivity within the cytoplasm of oligodendrocytes, astrocytes and neurons in all segments.

Timeline of clinical progression



Spatial Distribution of Staining – Case 21

Case: 21

Amy-33

Sections:

- a) At the level of the syrinx - C6
- b) At the level of the syrinx - T7
- b) Three levels below syrinx - L4

a)



b)



c)



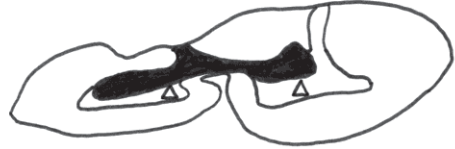
Case: 21

Haematoxylin and eosin

Sections:

- a) At the level of the syrinx - C6
- b) At the level of the syrinx - T7
- b) Three levels below syrinx - L4

a)



b)



c)



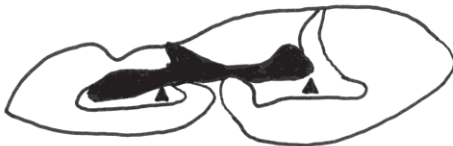
Case: 21

APP

Sections:

- a) At the level of the syrinx - C6
- b) At the level of the syrinx - T7
- b) Three levels below syrinx - L4

a)



b)



c)



Case: 21

DNA-PKcs

Sections:

- a) At the level of the syrinx - C6
- b) At the level of the syrinx - T7
- b) Three levels below syrinx - L4

a)



b)



c)



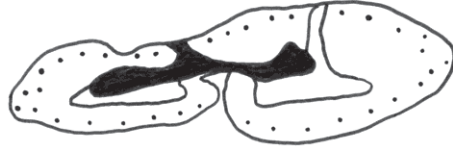
Spatial Distribution of Staining – Case 21

Case: 21
PARP

Sections:

- a) At the level of the syrinx - C6
- b) At the level of the syrinx - T7
- b) Three levels below syrinx - L4

a)



b)



c)

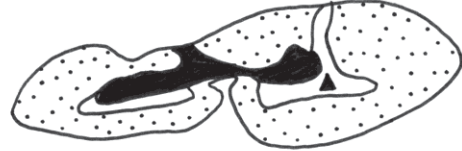


Case: 21
TUNEL

Sections:

- a) At the level of the syrinx - C6
- b) At the level of the syrinx - T7
- b) Three levels below syrinx - L4

a)



b)



c)



Case: 21
AIF 1

Sections:

- a) At the level of the syrinx - C6
- b) At the level of the syrinx - T7
- b) Three levels below syrinx - L4

a)



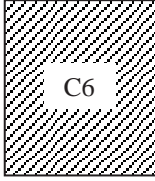
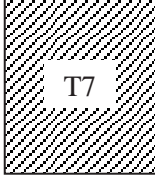
b)



c)



Summary of immunohistochemistry Case 21

<p>Glia: AIF, PARP, DNA-PKcs, TUNEL Axons: Nil Neurons: AIF, APP, DNA-PKcs, TUNEL, Amy-33</p>	 <p>C6</p>	<p>H&E: AHC loss, small syrinx</p>
<p>Glia: AIF, PARP, DNA-PKcs, TUNEL Axons: Nil Neurons: APP, AIF</p>	 <p>T7</p>	<p>H&E: AHC loss, syrinx</p>
<p>Glia: AIF, PARP Axons: Nil Neurons: APP, AIF, Amy-33</p>	<p>L4</p>	<p>H&E: Red cell change Weil: Pallor posterior columns suggesting demyelination</p>
<p>Glia: AIF Axons: Nil Neurons: APP, AIF, Amy-33</p>	<p>S2</p>	<p>H&E: red cell change Weil: Pallor posterior columns suggesting demyelination</p>

Conclusion APP antibody was negative and minimal axonal profiles suggestive of axonal swellings were seen. This evidence suggests that axonal damage was not a significant feature in the syringomyelia cases. The immunomarkers active caspase-3 and caspase-9, and antibodies to related proteins such as Bcl-2 were negative. In contrast, DNA-PKcs and TUNEL staining was present throughout many white matter tracts, predominantly within the central cord. PARP was immunopositive in glial nuclei within the white matter. AIF immunopositivity was seen in the majority of cells.